

749

PLANETARY EXPLORER LIQUID PROPULSION STUDY

N72-11702 (NASA-CR-123369) PLANETARY EXPLORER LIQUID
 PROPULSION STUDY Final Report, Jul. 1970 -
 Mar. 1971 F.X. McKeivitt, et al (Rocket
 Research Corp.) Jun. 1971 301 p CSCL 21H
 Unclas 08050

G3/27

F. X. McKeivitt, R. F. Eggers, C. W. Bolz, et al
 Rocket Research Corporation
 York Center
 Redmond, Washington 98052

June 1971
 Final Report for Period July 1970 - March 1971

Prepared for

GODDARD SPACE FLIGHT CENTER
 Glenn Dale Road
 Greenbelt, Maryland 20771

FACILITY FORM 602

N72-11702 (ACCESSION NUMBER)	(THRU)
301 (PAGES)	G3 (CODE)
CR-123369 (NASA CR OR TMX OR AD NUMBER)	27 (CATEGORY)

REPRODUCED BY
**NATIONAL TECHNICAL
 INFORMATION SERVICE**
 U. S. DEPARTMENT OF COMMERCE
 SPRINGFIELD, VA. 22161

335

1. Report No.	2. Government Accession No.	3. Recipient's Catalog No.
4. Title and Subtitle PLANETARY EXPLORER LIQUID PROPULSION STUDY	5. Report Date June 1971	6. Performing Organization Code
	8. Performing Organization Report No. RRC-71-R-249	
7. Author(s) F. X. McKeivitt, R.F. Eggers, C.W. Bolz. et al	10. Work Unit No.	
9. Performing Organization Name and Address Rocket Research Corporation York Center Redmond, Washington 98052	11. Contract or Grant No. NAS 5-11296	
	13. Type of Report and Period Covered Final Report July 1970-March 1971	
	14. Sponsoring Agency Code	
12. Sponsoring Agency Name and Address National Aeronautics and Space Administration Goddard Space Flight Center Glenn Dale Road Greenbelt, Maryland 20771		
15. Supplementary Notes		
16. Abstract <p>An analytical evaluation of several candidate monopropellant hydrazine propulsion system approaches is conducted in order to define the most suitable configuration for the combined velocity and attitude control system for the Planetary Explorer Spacecraft. Both orbiter and probe-type missions to the planet Venus are considered. The spacecraft concept is that of a Delta-launched spin-stabilized vehicle. Velocity control is obtained through preprogrammed pulse-mode firing of the thrusters in synchronism with the spacecraft spin rate. Configuration selection is found to be strongly influenced by the possible error torques induced by uncertainties in thruster operation and installation. The propulsion systems defined are based on maximum use of existing, qualified components. Ground support equipment requirements are defined and system development testing outlined.</p>		
17. Key Words (Selected by Author(s)) Planetary Explorer Hydrazine propulsion systems Attitude control Velocity control		18. Distribution Statement
19. Security Classif. (of this report) Unclassified	20. Security Classif. (of this page) Unclassified	

*For sale by the Clearinghouse for Federal Scientific and Technical Information, Springfield, Virginia 22151.

Page intentionally left blank

PRECEDING PAGE BLANK NOT FILMED

PREFACE

An analytical evaluation of several candidate monopropellant hydrazine propulsion system approaches is conducted in order to define the most suitable configuration for the combined velocity and attitude control system for the Planetary Explorer Spacecraft. Both orbiter and probe-type missions to the planet Venus are considered. The spacecraft concept is that of a Delta-launched spin-stabilized vehicle. Velocity control is obtained through preprogrammed pulse-mode firing of the thrusters in synchronism with the spacecraft spin rate. Configuration selection is found to be strongly influenced by the possible error torques induced by uncertainties in thruster operation and installation. The propulsion systems defined are based on maximum use of existing, qualified components. Ground support equipment requirements are defined and system development testing outlined.

Page intentionally left blank

TABLE OF CONTENTS

Section	Page
1.0 INTRODUCTION	1-1
1.1 Requirements	1-1
1.2 Configurations Studied	1-2
1.2.1 Thruster Arrangements	1-2
1.2.2 Feed System Configurations	1-8
2.0 VEHICLE DYNAMICS	2-1
2.1 Performance Analysis Formulae	2-2
2.1.1 Torque Arm Matrix	2-2
2.1.2 Attitude Control Torque, Arm Matrix T'	2-6
2.1.3 Spin Control Torque Arm Matrix T''	2-6
2.1.4 ΔV Motor Mean Torque Arm Matrices T and T'''	2-6
2.1.5 $\Delta V_{\max i}$ Computation Formulae	2-8
2.1.6 Calibration Coefficients and $\Delta V_{\max i}$ (cal)	2-8
2.1.7 Cross Coupling Factors and Effects	2-10
2.1.8 Impulsive Torque Produced Spin Axis Precession	2-11
2.2 Analysis Results	2-17
2.2.1 Maximum Allowed Velocity Corrections	2-17
2.2.2 Total Impulse and Usable Fuel Quantities	2-20
2.2.3 Nominal Attitude Control Maneuver Motion Details	2-20
2.2.4 Self-Induced and Cross Coupling Error Effects on Maneuver Precision and Total Fuel Requirements	2-35
2.2.5 ΔV Maneuver Directional Accuracy	2-39
2.2.6 Single Engine Failure Impact	2-42
2.2.7 Attitude and Spin Control Motor Mounting Configuration Flexibility	2-52
2.2.8 Vehicle Dynamics Study Conclusions and Configuration Selection	2-54
2.2.9 Sensitivity of Conclusions to Assumptions	2-56
2.3 Control Rates	2-57
2.3.1 Attitude/Spin Control	2-57
2.3.2 Velocity Control	2-66
3.0 RELIABILITY	3-1
3.1 Failure Mode/Redundancy Analysis	3-1
3.1.1 Effect of Thruster Location and Valve Type on System Failure Modes	3-1
3.1.2 Thruster Valve Combinations	3-4
3.1.3 Driver Circuit Redundancy	3-6
3.1.4 System Plumbing	3-8

TABLE OF CONTENTS (Continued)

Section	Page
3.1.5 Feed System Isolation Valve Configurations	3-9
3.1.6 Failure Mode/Effects Analysis	3-11
3.2 Reliability Analysis	3-12
3.2.1 Summary	3-12
3.2.2 Conclusions	3-13
3.2.3 Discussion	3-15
4.0 OPERATIONAL CONSIDERATIONS	4-1
4.1 Mission Profiles	4-1
4.1.1 Mission Sequence	4-1
4.1.2 Duty Cycles	4-1
4.1.3 Thrust/Pressure Profiles	4-5
4.1.4 Power Profiles	4-9
4.1.5 Instrumentation Recommendations	4-12
4.2 Command Logic	4-15
4.2.1 Ground Commanded Systems	4-15
4.2.2 Command System Employing Maximum On-Board Logic	4-18
4.2.3 Effect of Gimbaled Engine on Guidance Logic	4-19
4.3 Propellant Dumping	4-19
4.3.1 Retaining Excess Midcourse Propellant	4-19
4.3.2 Varying Fixing Sector Angle	4-20
4.3.3 Varying Orbit Injection Retromotor Parameters	4-20
4.3.4 Recommendations	4-24
4.4 Thermal Design Study	4-24
4.4.1 Hydrazine System Thermal Design Constraints	4-24
4.4.2 Hydrazine Propulsion Systems Design Limitations	4-25
4.4.3 Mission Thermal Restraints	4-25
4.4.4 Thruster Module Thermal Design Analysis	4-25
4.5 Plume Effects	4-44
4.5.1 Exhaust Contamination	4-44
4.5.2 Solar Array Nozzle Exhaust Plume Impingement Heating	4-45
4.6 Computer Model	4-48
5.0 SYSTEM DESCRIPTION	5-1
5.1 System Design and Integration	5-1
5.1.1 Propellant Tank Module	5-15
5.1.2 Valve Module	5-15

TABLE OF CONTENTS (Continued)

Section	Page
5.1.3	Radial Thruster 5-16
5.1.4	Gimbale Engine 5-16
5.1.5	Doublet Module 5-16
5.1.6	Electrical Harness 5-16
5.1.7	Assembly and Integration 5-18
5.2	Weight and Balance 5-33
5.2.1	Propellant Weight 5-33
5.2.2	Module Weights 5-34
5.2.3	System Weight and Balance 5-34
5.3	Component Description 5-40
5.3.1	5-lbf Rocket Engine Assembly 5-44
5.3.2	Thrust Chamber Valves 5-61
5.3.3	Isolation Valves 5-66
5.3.4	Propellant Line Filter 5-69
5.3.5	Propellant Tank 5-70
5.3.6	Instrumentation 5-71
5.3.7	Fill/Drain/Vent Valve 5-75
6.0	SYSTEM DEVELOPMENT 6-1
6.1	Development Test Plan 6-1
6.2	Acceptance Tests 6-1
6.2.1	Component Acceptance Tests 6-1
6.3	System Qualification 6-12
7.0	GROUND SUPPORT EQUIPMENT 7-1
7.1	GSE Requirements 7-1
7.2	Mechanical GSE 7-1
7.2.1	Physical and Schematic Description 7-1
7.2.2	Mechanical GSE Functional Description 7-8
7.2.3	Electrical GSE Design Description 7-22
8.0	SUMMARY AND CONCLUSIONS 8-1
8.1	Comparison of System Selection 8-1
8.1.1	Gimbale Engines – Configurations A and E 8-1
8.1.2	Tangential Doublets – Configuration C 8-1
8.1.3	Configuration D – Rectangle 8-3
8.1.4	Configuration B – Radial Pairs 8-4
8.1.5	Selected Configuration 8-4

TABLE OF CONTENTS (Concluded)

Section	Page
8.2 Limitations on System Operation	8-5
8.3 Future Work	8-6
9.0 NEW TECHNOLOGY	9-1

REFERENCES

APPENDIX A – Concept Survey

APPENDIX B – Failure Modes Analysis

APPENDIX C – Power Reduction Concepts

APPENDIX D – Dynamics Analysis – Formulae Derivations

LIST OF FIGURES

Figure	Page
1-1 System A – Gimbal Plus Fixed	1-3
1-2 System B – Radial Pairs	1-4
1-3 System C – Tangential Doublets	1-5
1-4 System D – Rectangle	1-6
1-5 System E – Alternate Gimbal	1-7
1-6 Feed System 1	1-10
1-7 Feed System 2	1-11
1-8 Feed System 3	1-12
2-1 Uncertainty Torque Matrix Coordinate System	2-3
2-2 Accumulated Lead/Lag Sector Command and Impulse Centroid Effects on X Axis Uncertainty Torque	2-5
2-3 (N + 1)ST Orbital Trajectory of the Spin Vector Tip	2-13
2-4 Mixed Motor Configuration B, C, D-1, and D-2	2-18
2-5 Mixed Motor Configuration F	2-18
2-6 Total Precession Angle and Coning Angle Data for Orbiter Midcourse ΔV	2-27
2-7 Total Precession Angle and Coning Angle Data for Orbiter Midcourse ΔV	2-28
2-8 Total Precession Angle and Coning Angle Data for Orbiter Periapsis Reduction (Beginning Maneuver)	2-29
2-9 Total Precession Angle and Coning Angle Data for Orbiter Periapsis Reduction (End Maneuver)	2-30
2-10 Total Precession Angle and Coning Angle Data for Probe Midcourse ΔV	2-31
2-11 Total Precession Angle and Coning Angle Data for Probe Midcourse ΔV	2-32
2-12 Total Precession Angle and Coning Angle Data for Late Mission ΔV	2-33
2-13 ΔV Maneuver Impulse Delivery Direction Error Cases	2-40
2-14 ΔV Impulse Delivery Direction Accuracy Data for Orbiter Midcourse ΔV	2-44
2-15 ΔV Impulse Delivery Direction Accuracy Data for Orbiter Midcourse ΔV	2-45
2-16 ΔV Impulse Delivery Direction Accuracy Data for Orbiter Periapsis Reduction (Beginning Maneuver)	2-46
2-17 ΔV Impulse Delivery Direction Accuracy Data for Orbiter Periapsis Reduction (End Maneuver)	2-47
2-18 ΔV Impulse Delivery Direction Accuracy Data for Probe Midcourse ΔV	2-48
2-19 ΔV Impulse Delivery Direction Accuracy Data for Probe Midcourse ΔV	2-49
2-20 ΔV Impulse Delivery Direction Accuracy Data for Probe Targeting Before Spin-Up	2-50
2-21 ΔV Impulse Delivery Direction Accuracy Data for Probe Late Mission ΔV Retargeting After Mini-Probe Release	2-51
2-22 Attitude and Spin Control Thruster Study	2-53
2-23 Precession Rate vs Resolution	2-58
2-24 Attitude Control – Orbiter Vehicle	2-59
2-25 Attitude Control – Probe Vehicle	2-60
2-26 Spin Rate of Change vs Thrust (One Thruster Pair)	2-63
2-27 Midcourse Maneuver Duration	2-67

LIST OF FIGURES (Continued)

Figure	Page
4-1	Effect of Tank Selection and Propellant Requirement on Blowdown Ratio 4-7
4-2	MR-50 Thrust/Pressure Profile 4-8
4-3	Typical Thrust/mission Profile – Probe (Configuration B) 4-10
4-4	Typical Thrust/mission Profile – Orbiter (Configuration B) 4-11
4-5	Instrumentation Recommendations 4-14
4-6	Command Logic Diagram 4-17
4-7	Regimes of Propellant Dumping Advantage 4-21
4-8	Orbit Maneuver Capability of Excess Midcourse Propellant 4-22
4-9	Effect of Firing Sector Angle on Midcourse and Dumping Parameters 4-23
4-10	Thruster Module – Worst-Case Orbit Heating and Shadow Environment (As Used in the Computer Simulation) 4-28
4-11	Planetary Explorer Thermal Analysis – Thermal Radiation A_E/A_S Values for Typical Module Surfaces (For Module Dimensions \ll Vehicle Dimensions) 4-32
4-12	Venus Orbit Solar Heating vs Shadow Cooling 4-34
4-13	External Thruster Module Design Allowable Geometry Factors and Paint Patterns 4-37
4-14	Thruster Assembly Mounting Detail (Typical) Showing Heat Conduction Paths 4-39
4-15	Candidate Tangential Thruster Module Thermal Network Schematic (One Half Shown) 4-40
4-16	Doublet Module Component Temperatures – Venus Mission (No Firing) 4-41
4-17	Post-Mounted Doublet Module – Valve Soakback Heating (Venus Insertion Maneuver – Spin Axis Sun-Line Angle = 45°) 4-42
4-18	Planetary Explorer Tangential Thruster Plume Heating of Adjacent Canted Solar Arrays Illustrating Impingement Flow Field 4-47
4-19	Propulsion Computer Model 4-49
5-1	Tank Module – Propulsion Subsystem Planetary Explorer 5-3
5-2	Valve Module, Planetary Explorer – Feed System 1 5-5
5-3	Valve Module – Planetary Explorer 5-7
5-4	5-lbf Reaction Engine Assembly 5-9
5-5	5-lbf Reactor – Gimbaleed 5-11
5-6	Doublet Module – Planetary Explorer 5-13
5-7	Gimbal Actuator Conceptual Design 5-17
5-8	Electrical Schematic – Planetary Explorer Propulsion Subsystem 5-19
5-9	Propulsion Subsystem – Planetary Explorer System A 5-21
5-10	Propulsion Subsystem – Planetary Explorer System B 5-23
5-11	Propulsion Subsystem – Planetary Explorer System C 5-25
5-12	Propulsion Subsystem – Planetary Explorer System D 5-29
5-13	Propulsion Subsystem Planetary Explorer System E 5-31
5-14	Average Specific Impulse MR-50 Thruster 5-35
5-15	MRM-50A 5-lbf Reaction Engine Modules 5-45

LIST OF FIGURES (Concluded)

Figure		Page
5-16	Qualification Test Plan REM-Mono MRM-50A	5-50
5-17	5-lbf Reaction Engine Assembly	5-57
5-18	Reaction Engine Assembly, MR-50A	5-59
5-19	Hydraulic Research Valve Schematic – Part Number 48000680	5-64
5-20	Qualified Configuration of Recommended Latching Valve Carleton Controls Corporation P/N 2217001-2	5-68
5-21	Transducer, Absolute Pressure	5-73
5-22	Fill Valve Assembly	5-77
6-1	Propellant Tank Assembly – Acceptance Tests	6-2
6-2	Filter Acceptance Test	6-4
6-3	Fill and Drain Valves – Acceptance Tests	6-5
6-4	Pressure Transducer – Acceptance Tests	6-6
6-5	Isolation (Latching) Valve – Acceptance Tests	6-7
6-6	Thruster Control Valve – Acceptance Tests	6-8
6-7	Catalyst Acceptance Flow Plan	6-9
6-8	Thruster Chamber Assembly – Acceptance Tests	6-10
6-9	Propulsion Subsystem – Final Assembly and Acceptance Tests	6-11
6-10	Subsystem Qualification Tests	6-13
7-1	Mechanical GSE Cart	7-3
7-2	Mechanical GSE Schematic	7-5
7-3	Mechanical GSE Control Panel	7-7
7-4	Mechanical GSE Schematic Evacuation/Vacuum Drying	7-9
7-5	Mechanical GSE Schematic Sample Bottle Evacuation	7-10
7-6	Mechanical GSE Schematic GSE N ₂ H ₄ Sample	7-11
7-7	Mechanical GSE Schematic N ₂ H ₂ Loading	7-13
7-8	Mechanical GSE Schematic Pressurizing/Proof Testing	7-14
7-9	Mechanical GSE Schematic VCPS N ₂ H ₄ Sample	7-15
7-10	Mechanical GSE Schematic N ₂ H ₄ Off-Loading	7-16
7-11	Mechanical GSE Schematic Venting	7-18
7-12	Mechanical GSE Schematic Draining	7-19
7-13	Mechanical GSE Schematic H ₂ O Loading	7-20
7-14	Mechanical GSE Schematic Alcohol Loading	7-21
7-15	Mechanical GSE Schematic Cold Trap Flushing	7-23
7-16	Mechanical GSE Schematic Catch Basin Drain and Purge	7-24
7-17	N ₂ H ₄ Transfer System	7-25
7-18	Electrical GSE	7-26
7-19	Electrical GSE Schematic	7-27

LIST OF TABLES

Table	Page
1-1	Spacecraft Mass Properties 1-2
2-1	Cross Coupling Factors Formulae 2-12
2-2	Maximum Allowed Uncorrected Midcourse Velocity Change Maneuvers for Orbiter 2-19
2-3	Maximum Allowed Uncorrected Midcourse Velocity Change Maneuvers for Probe 2-19
2-4	Late Mission Maximum Allowed Velocity Corrections for Orbiter and Probe 2-21
2-5	Orbiter ΔV_{\max} for Various Uncertainty Torque Contribution Combination Techniques and Values of $\Delta F/F$ 2-22
2-6	Probe ΔV_{\max} for Various Uncertainty Torque Contribution Combination Techniques and Values of $\Delta F/F$ 2-23
2-7	Orbiter Impulse and Fuel Quantity Data 2-24
2-8	Probe Impulse and Fuel Quantity Data 2-25
2-9	Orbiter Nominal Impulse, Fuel Weight, and I_{sp} Data 2-26
2-10	Probe Nominal Impulse, Fuel Weight, and I_{sp} Data 2-26
2-11	Attitude Maneuver Computation Results 2-34
2-12	Orbiter Torque Cross Coupling Factors 2-36
2-13	Probe Torque Cross Coupling Factors 2-37
2-14	Comparative Impulse and Fuel Data for Orbiter and Probe 2-38
2-15	Spacecraft Conditions for Total ΔV Direction Error Calculations 2-43
2-16	One Engine Out Effects on Configurations B and F 2-52
2-17	Attitude/Spin Control Performance Limits 2-62
2-18	Attitude/Spin Control Operating Parameters Orbiter/Probe Data 2-65
3-1	Effect of Valve Failure on System Function 3-2
3-2	Valve Concepts 3-5
3-3	Driver Circuit Redundancy Comparisons 3-7
3-4	Reliability Tabulation – Propulsion Subsystem 3-12
3-5	Pressurization/Propellant Subsystem 3-13
3-6	System Reliability Summary 3-13
3-7	Estimated Firing Data 3-14
3-8	Thruster Functional Modes 3-14
3-9	Propulsion Subsystem Failure Rate Data (Typical) 3-17
3-10	Failure Rate Data 3-20
4-1	Mission Sequence – Probe Vehicle 4-2
4-2	Mission Sequence – Orbiter Vehicle 4-3
4-3	First Midcourse Calibration and Stabilization 4-4
4-4	Nominal Duty Cycle Requirements 4-6
4-5	Thrust and Pressure Schedule 4-12
4-6	Propulsion System Power Consumption 4-13
4-7	Planetary Explorer Propulsion Instrumentation 4-15
4-8	Thermal Design Goals (Passive Thermal Control) 4-26

LIST OF TABLES (Concluded)

Table	Page
4-9 Idealized Worst-Case Thermal Environments	4-27
4-10 Candidate Thruster Module: Maximum Expected Temperature Uncertainties	4-43
5-1 Propellant Requirements—Orbiter Vehicle	5-33
5-2 Propellant Requirements—Probe Vehicle	5-34
5-3 Module Weight Summaries	5-36
5-4 Dry Weight Summaries	5-37
5-5 System Weight Summary	5-40
5-6 Propulsion Modules Mass Properties	5-41
5-7 Candidate System Mass Properties	5-41
5-8 MR-50A Rocket Engine Assembly Qualification Requirement Summary	5-46
5-9 Comparison of Qualification Test Requirements to Demonstrated Values	5-54
5-10 Candidate Thrust Chamber Valves (5-lbf Thrust), Planetary Explorer N ₂ H ₄ System	5-62
5-11 Environmental Capability, Recommended Thrust Chamber Valve	5-65
5-12 Candidate Isolation Valves (5-lbf Thrust System) Planetary Explorer N ₂ H ₄ System	5-67
5-13 Environmental Capability of Carleton Controls P/N 2217001-2 Latching Valve	5-69
5-14 Propellant Line Filter Characteristics	5-70
5-15 Propellant Tank Parameters	5-71
7-1 Mechanical GSE Functional Requirements	7-2
7-2 Electrical GSE Functional Requirements	7-2
8-1 Thruster Configurations – Summary Comparison	8-2

1.0 INTRODUCTION

This report presents the results of a study conducted for the Goddard Space Flight Center of the National Aeronautics and Space Administration on the definition of the propulsion system for the Planetary Explorer spacecraft. The basic concept is that of a Delta-launched, spin-stabilized vehicle designed for Venus exploration. A universal bus is to provide a vehicle for probe and orbiter missions and experiments. The propulsion system under study, a part of that bus, is to provide spin control, attitude control, and velocity control for each of the missions with a minimum of mission-dependent modification. Delta-launching and spin stabilization, while providing for overall low cost and simplicity, result in weight criticality and present some unique propulsion problems, notably those associated with open loop control during the large velocity corrections that must be provided for midcourse and orbital maneuvers and the relatively complex series of maneuvers associated with bus targeting and probe release. A description of the universal bus concept and some of the program philosophy and objectives are presented in the publication referenced below.*

1.1 REQUIREMENTS

The basic requirements to which the subsystem study was conducted are those contained in NASA-GSFC "Subsystem Specification No. S-723-P-10 Midcourse Correction, Orbital Maneuver, Attitude Control Spin (MICOMACS) Subsystem, Planetary Explorer Satellite," (Reference 1). This specification of original issue date May 7, 1969, was later updated to July 9, 1970, and modified by communication between GSFC and RRC. Important modifications not included in the referenced specification are as follows:

- Modifications to the original mission profile included postponement of the initial attitude orientation from immediately after despin and separation from the booster third stage to the time of first midcourse correction, some changes in the probe release sequence, and addition of a bus retargeting of the probe mission. The specific sequence of propulsion events used for the study is presented in paragraph 4.1 of this report.
- Attitude control primary and secondary (malfunction mode) must provide control torques in pure couples.
- The study will be directed at those concepts that make most effective use of existing qualified thrusters. Impulse accuracy requirements not currently attainable on this basis will be considered to be goals.
- The spacecraft-sunline attitude perpendicularity tolerance is increased from ± 3 to ± 6 degrees in the normal mode and from ± 4 to ± 7 degrees in the secondary mode.

Basic spacecraft mass properties for use in determining thruster locations and for the dynamic analyses were provided by GSFC. These are provided, for reference purposes, in Table 1-1.

*Planetary Explorer Summary Phase A Report and Universal Bus Description, December 1970, Goddard Space Flight Center, Greenbelt, Maryland

Table 1-1. SPACECRAFT MASS PROPERTIES

Mission	Configuration	Weight lbm	Center of Mass Inches(1)	Moment of Inertia Slug-ft ²	
				I _{spin}	I _{trans}
Venus 1975 Probe(2) Type II	Launch with delta	1,052	20.8	73	213
	Booms extended with delta	1,052	17.3	195	243
	Cruise	881	27.4	181	111
	Main probe separated	481	20.2	170	93
	All probes separated	252	16.2	48	28
Venus 1976 Orbiter(3) Type II	Launch with delta	916	9.10	51	142
	Booms extended with delta	916	9.32	75	153
	Cruise	745	19.44	68	53
	Orbit	468	21.36	65	44
	Fuel expended	372	19.80	56	39

(1) Center of mass is measured from PE/delta interface flange, station 647.31.

(2) Data based on 74.1 lbm of liquid fuel on board with moment of 171.17 lb-ft.

(3) Data based on 95.9 lbm of liquid fuel on board with moment of 220.00 lb-ft.

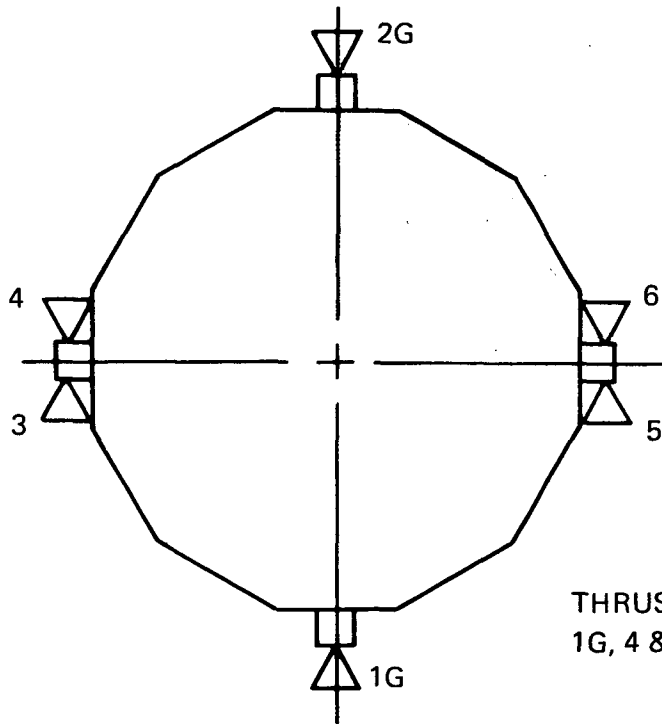
1.2 CONFIGURATIONS STUDIED

1.2.1 Thruster Arrangements

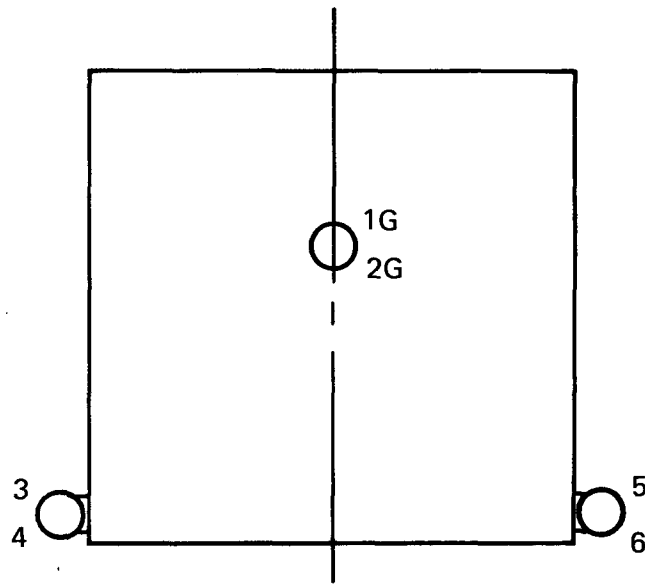
On the basis of a preliminary screening of candidate approaches (see Appendix A), five configurations were selected for detailed study and comparison. These configurations are illustrated in Figures 1-1 through 1-5. The particular thrusters that would be used for the various propulsive functions in both the primary and secondary modes are indicated. Some options exist as noted. The feed system branch grouping necessary to achieve the required redundancy and secondary mode operation is also noted on these figures.

1.2.1.1 System A—Gimbal

This system consists of a pair of one plane gimballed velocity control (ΔV) thrusters located on opposite sides of the spin axis in a plane near that of the center of gravity, Figure 1-1. Thruster gimbaling occurs in the longitudinal plane enabling, within the established tolerances, alignment of the thrust axis and the spacecraft center of gravity. Spin and despin for both planned spin rate profiles and for taking out main-thruster-induced spin perturbations is accomplished by a pair of

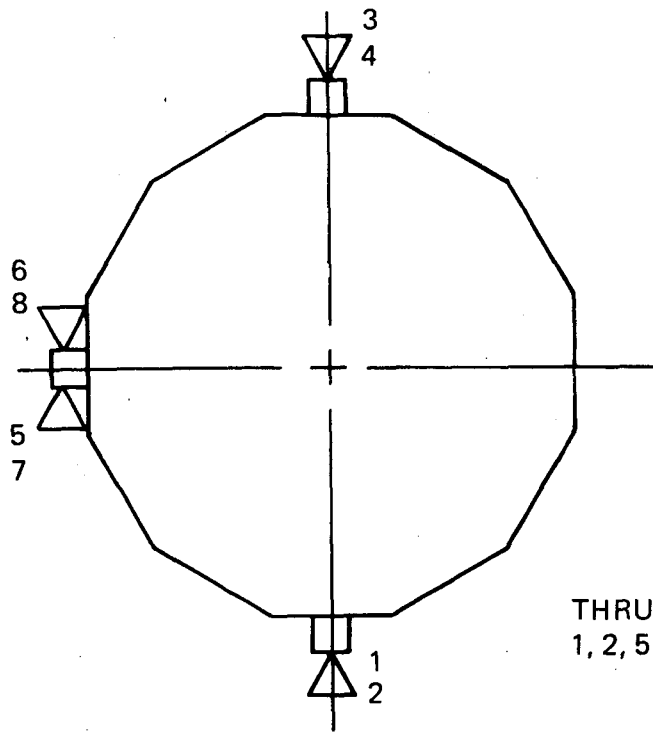


THRUSTER COUPLING –
1G, 4 & 6 AND 2G, 3 & 5

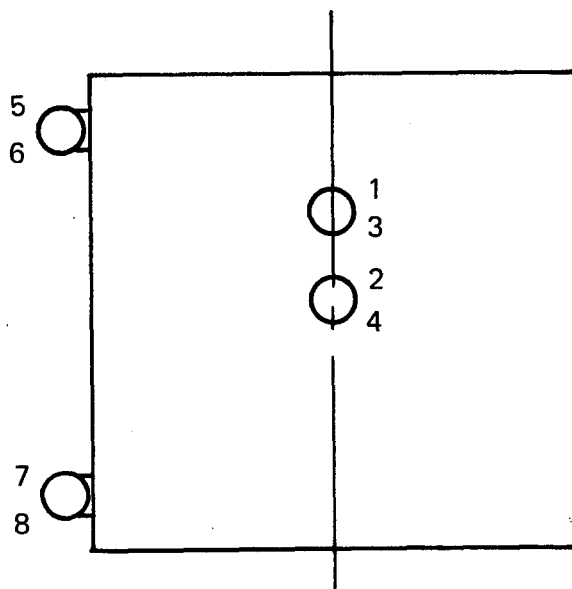


FUNCTION	PRIMARY	SECONDARY
ΔV	1G	2G
ACS	1G – 4 – 6	2G – 3 – 5 1G – 2G
+ SPIN	4 – 5	4; 5
- SPIN	3 – 6	3; 6

Figure 1-1. SYSTEM A – GIMBAL PLUS FIXED

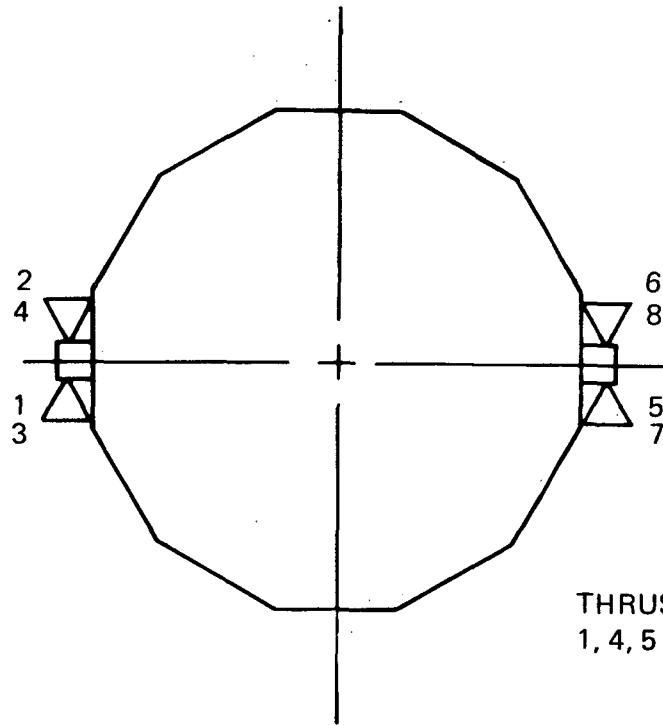


THRUSTER COUPLING –
1, 2, 5 & 8 AND 3, 4, 6 & 7

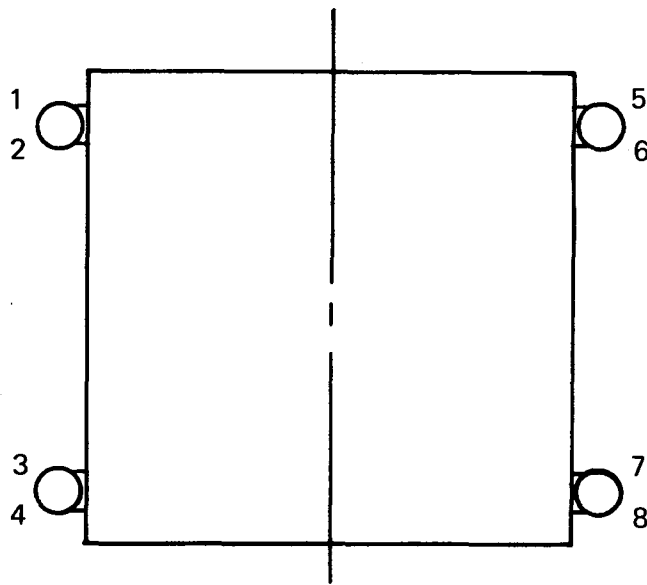


FUNCTION	PRIMARY	SECONDARY
ΔV	1 – 2	3 – 4
ACS	5 – 8	6 – 7
+ SPIN	6 – 8	8; 6
- SPIN	5 – 7	7; 5

Figure 1-2. SYSTEM B – RADIAL PAIRS

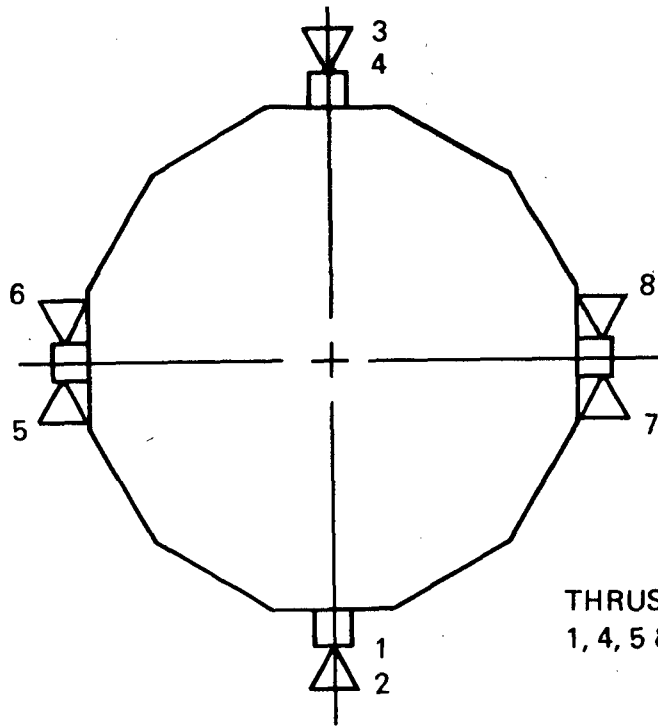


THRUSTER COUPLING –
1, 4, 5 & 8 AND 2, 3, 6 & 7

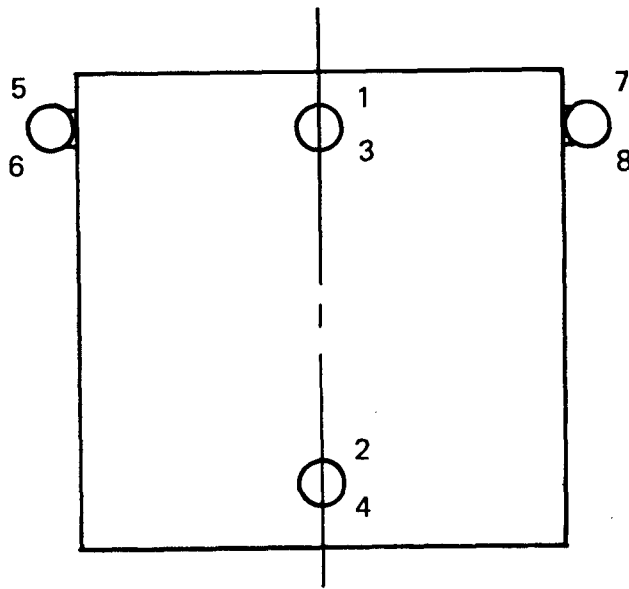


FUNCTION	PRIMARY	SECONDARY
ΔV	1 – 5 – 4 – 8	2 – 6 – 3 – 7
ACS	1 – 4	2 – 3; 5 – 8; 6 – 7
+ SPIN	2 – 5	4 – 7; 2; 5; 4; 7
- SPIN	1 – 6	3 – 8; 1; 6; 3; 8

Figure 1-3. SYSTEM C – TANGENTIAL DOUBLET

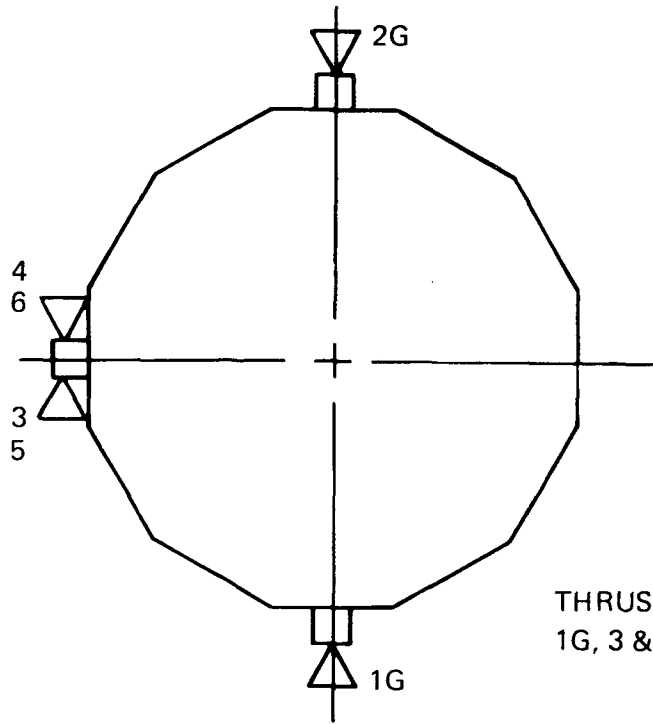


THRUSTER COUPLING –
1, 4, 5 & 6 AND 2, 3, 7 & 8

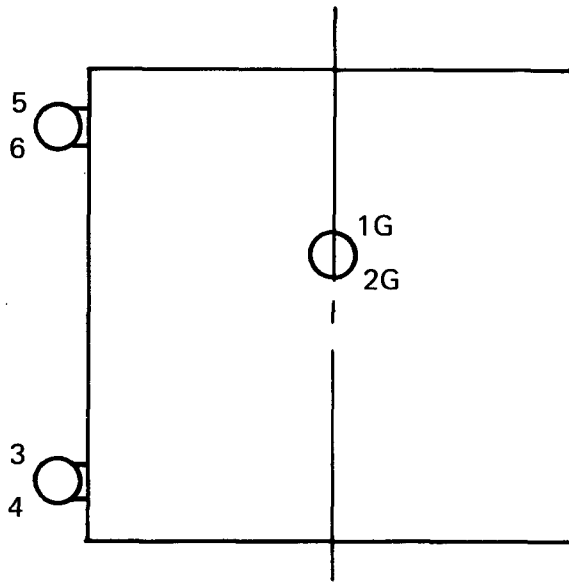


FUNCTION	PRIMARY		SECONDARY	
	D-1	D-2	D-1	D-2
AV	1-4	5-7	2-3	6-8
ACS	1-4	1-4	2-3	2-3
+SPIN	6-7	6-7	6; 7	6; 7
-SPIN	5-8	5-8	5; 8	5; 8

Figure 1-4. SYSTEM D – RECTANGLE



THRUSTER COUPLING -
1G, 3 & 6 AND 2G, 4 & 5



FUNCTION	PRIMARY	SECONDARY
ΔV	1G	2G
ACS	3 - 6	4 - 5
+ SPIN	6 - 4	4; 6
- SPIN	5 - 3	3; 5

Figure 1-5. SYSTEM E - ALTERNATE GIMBAL

tangentially mounted back-to-back thruster modules located in the aft section of the vehicle. These thruster pairs or doublets are mounted with thrust axis parallel to the main thrusters so as to enable a torque couple to be developed when used in conjunction with a main thruster for attitude control. The aft location maximizes the moment arm for this control function.

The two of the lower thrusters facing in the same direction and the upper gimbaled thruster facing in the opposite direction would each be manifolded together to a common isolation valve. This would enable the systems to provide all the required propulsive functions despite a failure necessitating closing one of the two isolation valves rendering one half the thruster inoperative. In this secondary mode, spin control would be degraded in that it would be accomplished by a single (noncouple) thruster.

1.2.1.2 System B—Radial Pairs

In this configuration velocity control is attained with a pair of radial thrusters located slightly above and below the axial limits of the center of gravity travel. Duty cycle of the upper and lower thrusters is varied to remove predictable disturbance torques of the spin axis. Another similarly disposed pair of thrusters is located 180 degrees opposed to provide the necessary redundancy.

Attitude and spin control functions are provided by a pair of side-mounted doublets located at the upper and lower extremities of the spacecraft. Moment arm for spin axis precessional control is maximized. The torque developed, although in a couple for both primary and secondary modes, is not in the plane of the spin axis. Therefore, spin control for both primary and secondary modes is produced by uncoupled thrusters.

Isolation valving would combine one velocity control engine pair with those thrusters producing spin axis precessional torque in each of the feed system branches. This configuration is illustrated in Figure 1-2.

1.2.1.3 System C—Tangential Doublets

This arrangement consists of four back-to-back thruster doublet modules mounted, with thrust axes parallel, at the extremities of the spacecraft (see Figure 1-3). Velocity control is provided by one of the two groups of four engines firing in the same direction. Duty cycle adjustment would be used to minimize disturbance torques. Attitude control could be provided by any of four torque couples while redundancy exists for both spin and despin.

Because of the fact that any of the engines may be used for any of the control modes (velocity, altitude, and spin control) with this configuration, some options exist with regard to thruster coupling. The obvious choice is grouping the sets of four engines all facing in the same direction, while seemingly best from the velocity control standpoint, separates all of the engine pairs providing attitude control couples. When only one of the feed system branches is open, attitude control must be performed by 180-degree phasing of the upper and lower thrusters. Evaluation of specific duty cycles indicates, however, that velocity control maneuvers will require this type of phasing because of the small fraction of the total impulse required of the lower engines (see paragraph 4.1.2.3).

Since the velocity control engines will be required to operate in this mode, there is no need to compromise the attitude control function by requiring this mode of operation unnecessarily. Consequently the recommended thruster manifolding scheme combines the upper two thrusters on one side (facing in the same direction) with the lower two thrusters on the opposite side. It should be noted that this arrangement separates all the spin control couples into opposite feed system branches. This is considered less serious since couples are not required for degraded mode spin control. Some of the candidate systems are, in fact, based on noncoupled spin control thrusters for primary mode operation.

1.2.1.4 System D—Rectangle

In this system two opposed tangential doublets are used in conjunction with radial thrusters at the upper and lower ends of the spacecraft to provide the required control forces, Figure 1-4. Either the radial (Configuration D-1) or the tangential (Configuration D-2) thrusters can be used for velocity control. Isolation valving would group one tangential module with one of the two radial engine pairs comprising an attitude control couple.

1.2.1.5 System E—Alternate Gimbal

This system combines the gimballed velocity control engine as in System A with the side mounted attitude/spin control doublet modules as used in System B. The greater moment arm for the attitude control couple should be more efficient than that of System A; spin control is, however, obtained with noncouples in the primary as well as the secondary mode. Isolation valving would combine each attitude control couple with one of the gimballed engines. This configuration is illustrated in Figure 1-5.

1.2.2 Feed System Configurations

In addition to the thruster arrangements described in the previous paragraphs, three feed system configurations provided by GSFC and shown schematically in Figures 1-6 through 1-8, were evaluated. A test valve is included in feed system 3 (Figure 1-8) to permit leak checking of the latching valves. Coupling of the most suitable feed system with the thruster arrangement permits definition of the complete propulsion subsystem.

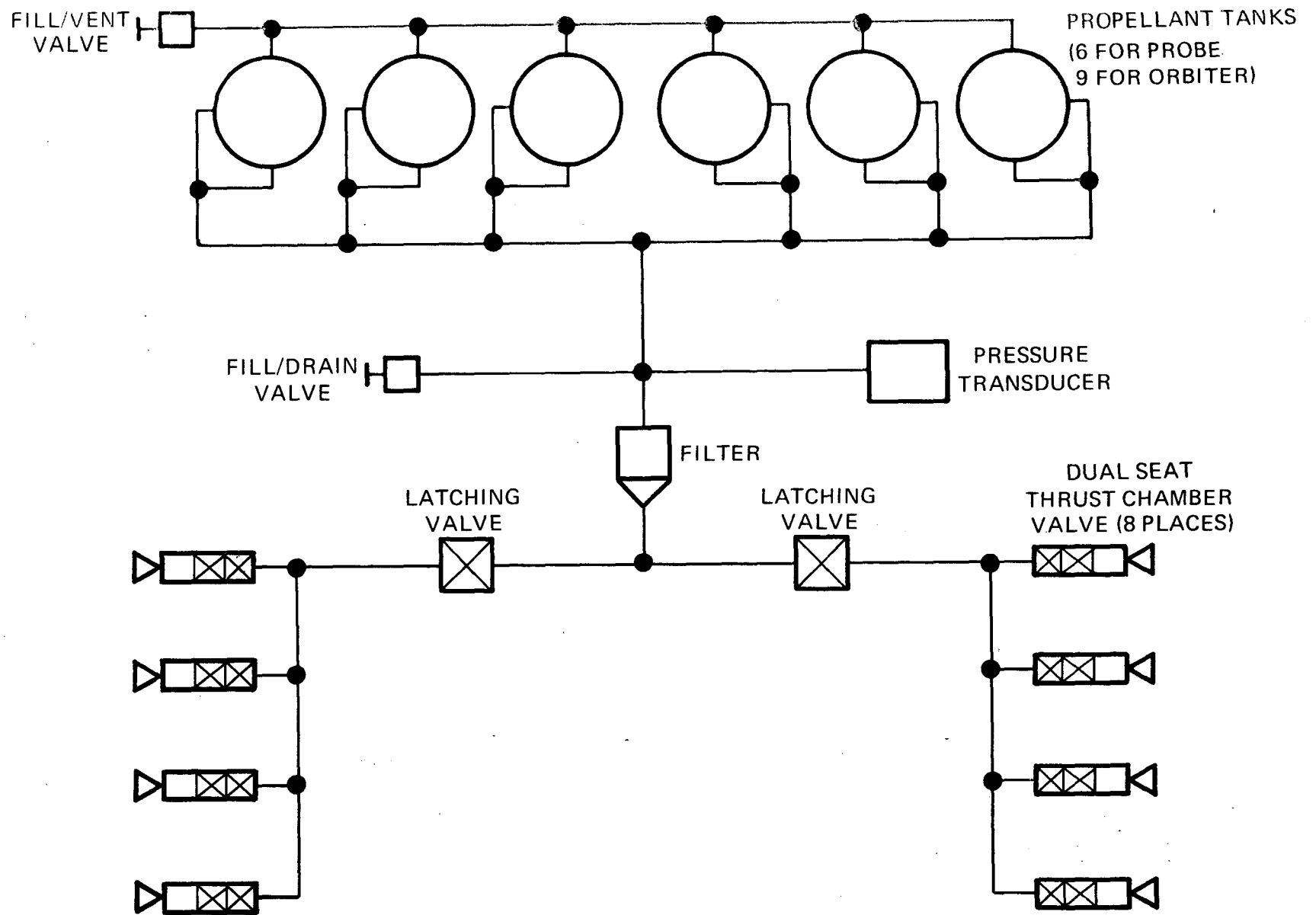


Figure 1-6. FEED SYSTEM 1

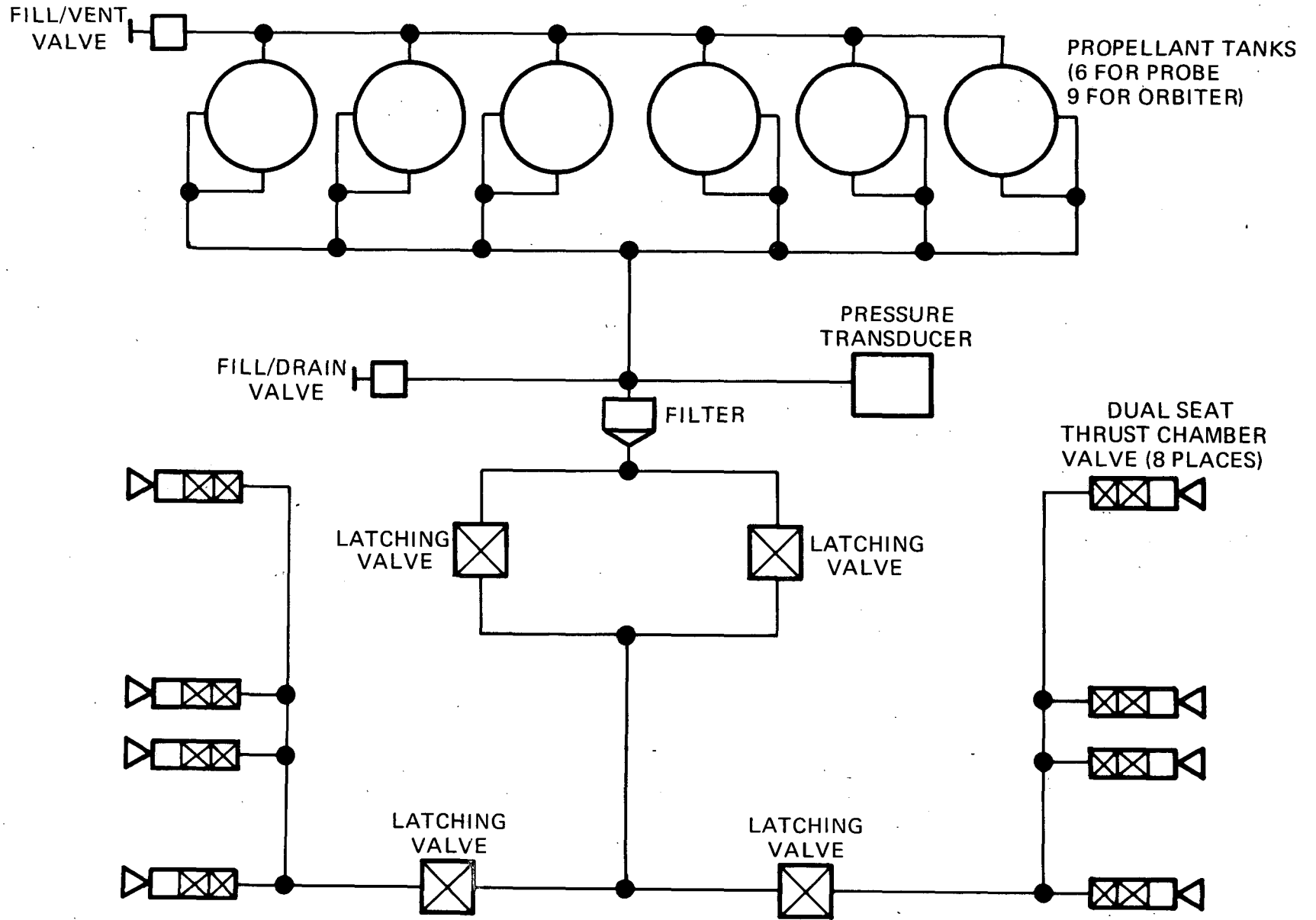


Figure 1-7. FEED SYSTEM 2

11039-96

1-12

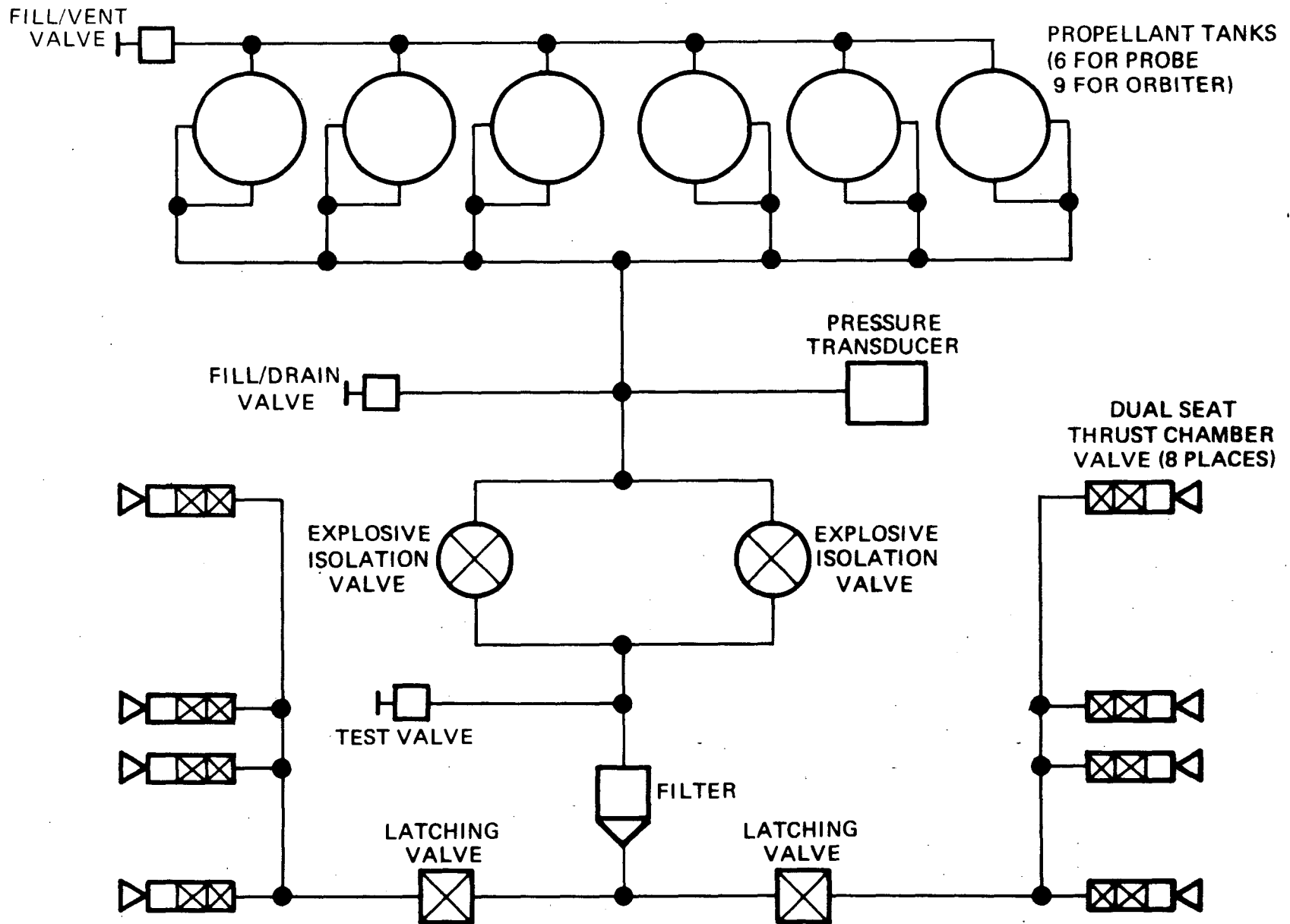


Figure 1-8. FEED SYSTEM 3

2.0 VEHICLE DYNAMICS

In order to identify the preferred rocket motor configuration from among the candidates, it was necessary to establish a set of selection criteria and to develop analytical formulae from which the necessary system performance information could be generated. The criteria defined are listed below:

- a. Configuration effect on maximum allowable uncorrected velocity maneuver in the light of the maximum allowed spin axis precession angles and spin rate change.
- b. Configuration effect on total impulse and propellant required. This includes torque arm length effects on required impulse (spin and attitude control) and impulse required to compensate for cross coupling uncertainty torque effects.
- c. Velocity, attitude, and spin rate correction maneuver accuracy.
- d. Engine-out effect on spacecraft stability during a preprogrammed velocity correction maneuver.
- e. Economy of thruster use, i.e., to minimize the number of motors required.

The limiting values employed in the application of the criteria stated above are as follows:

- a. Spin axis precession:
±6 degrees about X (thrust) axis for normal mode, ±7 degrees for degraded mode
±1 degree total about Y (transverse) axis
- b. Spin rate change:
±0.3 rpm for normal mode operation
±0.6 rpm to degraded operation
- c. Uncorrected single midcourse ΔV_{\max} :
108 m/sec (goal)
- d. Total fuel weight:
Minimize
- e. One-engine-out effect:
Noncatastrophic, mission not lost
- f. Correction accuracy goals:
Velocity control:
Large corrections: 2.5% (2 to 108 m/sec)
Small corrections: 5% (0.1 to 2 m/sec)
Attitude control:
0.2-degree resolution
Spin control:
0.1-rpm resolution
- g. Economy of thruster motors required:
Minimum number required.

The ± 1 -degree total precession limit about the Y axis was assumed on the basis of the requirement for delivering the required impulse to within 0.5 degree (average) of the desired direction.

Because of the immediately apparent critical effect of uncertainty torques on spin axis attitude change during velocity correction, the configurations were first evaluated relative to this effect. Next the criterion of single-engine-out criticality was examined. Finally, the systems were evaluated in the light of the other criteria. In all cases where absolute limits were not provided, systems which were quantitatively superior were preferred.

2.1 PERFORMANCE ANALYSIS FORMULAE

A brief description of the formulae employed in the evaluation is presented below.

2.1.1 Torque Arm Matrix

Assuming all motors perform within specification, the key element in determining the maximum allowed unmodified velocity change that can be accomplished in a single maneuver is the uncertainty torque arm matrix, which presents the various contributions to the disturbance torque arm about each axis. The matrix is simply derived by computing the cross product of the total radius arm vector, \vec{R} , which separates the actual motor and the center of gravity, with the total thrust vector of that motor, \vec{F} , and then subtracting the nominal or expected torque effects, $\vec{R}_O \times \vec{F}_O$ and the second order uncertainty effects, which involve the product of small uncertainty factors.

The uncertainty torque arm matrix is as follows (see Figure 2-1):

$$\begin{aligned}
 F_O \mathbf{T} &= (\vec{R} \times \vec{F}) - (\vec{R}_O \times \vec{F}_O) - (\text{second order effects}) \\
 &= F_O \begin{bmatrix} \hat{i} \left\{ (\tau_{\text{cent}} \Omega + a) Z_O + \delta Y_O - \delta Z_O \right\} \\ \hat{j} \left\{ (Z_1 - Z_2) + \left(\frac{\Delta F}{F} \right) Z_O - \delta X_O \right\} \\ \hat{k} \left\{ (-Y_1 + Y_2) - \left(\frac{\Delta F}{F} \right) Y_O + \delta X_O \right\} \end{bmatrix} \quad (2-1)
 \end{aligned}$$

Where:

- \mathbf{T} = Uncertainty torque arm matrix
- F_O = Nominal thrust level of one motor (directed along the minus X axis)
- $\hat{i}, \hat{j}, \hat{k}$ = Unit vectors along the X, Y, Z axes, respectively
- X_O, Y_O, Z_O = Nominal location of the motor with respect to the nominal center of gravity
- X_1, Y_1, Z_1 = Maximum coordinate values of the center of gravity uncertainty box relative to the nominal center of gravity (fixed)
- X_2, Y_2, Z_2 = Maximum coordinate values of the rocket motor uncertainty box relative to the nominal location of the motor (fixed)

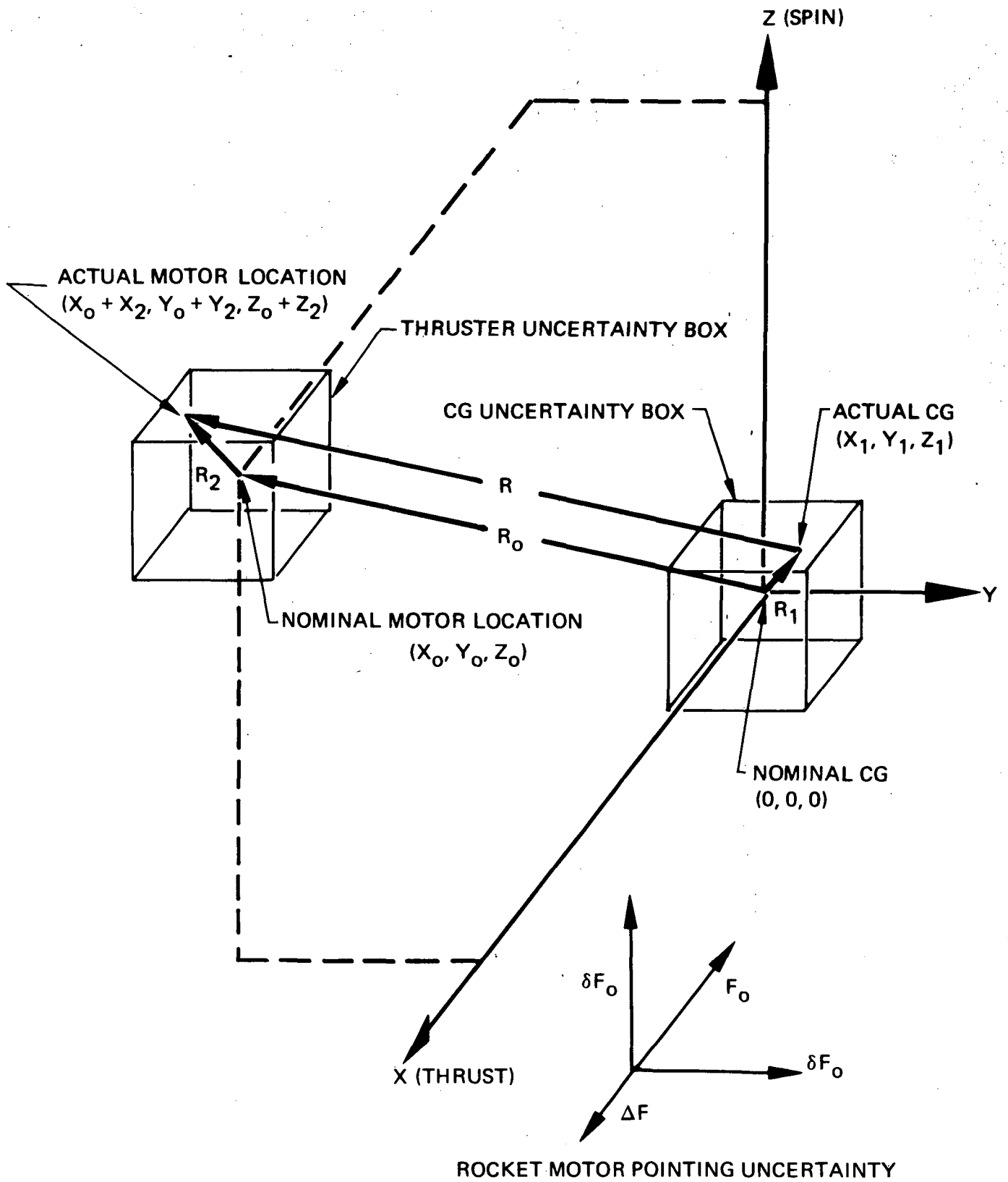


Figure 2-1. UNCERTAINTY TORQUE MATRIX COORDINATE SYSTEM

- δ = Rocket motor thrust vector pointing uncertainty (fixed)
- $\Delta F/F$ = Rocket motor thrust and impulse bit size uncertainty (time varying)
- τ_{cent} = Uncertainty in the time of delivery of the pulse centroid (time varying)
- Ω = Spacecraft rotation rate
- a = Motor firing command sector uncertainty (fixed)

The total thrust and radius arms are as follows:

$$\vec{F} = F_o \left\{ \hat{i} \left(-1 + \frac{\Delta F}{F} \right) + \hat{j}\delta + \hat{k}\delta \right\} + \text{time dependent effects } (\tau_{\text{cent}}, \Omega, a) \quad (2-2a)$$

$$\vec{R} = \hat{i} (X_o - X_1 + X_2) + \hat{j} (Y_o - Y_1 + Y_2) + \hat{k} (Z_o - Z_1 + Z_2) \quad (2-2b)$$

$$\vec{R}_o = \hat{i} X_o + \hat{j} Y_o + \hat{k} Z_o \quad (2-2c)$$

Equation 2-1 is derived in detail in Appendix D.

Several alternate forms of the T matrix are required to compute the values of $\Delta V_{\text{max } i}$ and C_i , the calibration factor, where:

$\Delta V_{\text{max } i}$ = Limitation on the maximum allowed uncorrected velocity change maneuver caused by uncertainty torques about the i th axis

C_i = Calibration factor for torques about the i th axis, which accounts for the possibility of compensating for the fixed contributions to the uncertainty torque.

2.1.1.1 X Axis Time Dependent Factor Derivation

When an upper and lower ΔV , attitude control, or spin rate adjustment motor fires, it produces an impulse bit with a centroid that is nominally on the X axis. However, because the time dependent operation of the rocket motor is not perfectly repeatable from pulse to pulse and because the commanded start and stop firing sectors of the upper and lower motors is not the same unless the upper and lower motors fire for the same length of time, a given motor or several motors will produce lead/lag centroid delivery with respect to nominal. The end result is a net torque about the X axis.

Figure 2-2 shows the effect of two motors firing. One motor is assumed to be placed above the center of gravity and the other is below it. The torque vector to the left of the X axis was produced by the motor above the center of gravity and the torque vector to the right by the motor below the center of gravity. If the impulse bit of both motors were delivered exactly along the X axis, the vectors would be antiparallel and would cancel. However, they cannot be expected to be truly antiparallel in all cases and, therefore, a net torque about X must be anticipated. For the worst case considered in Figure 2-2, the upper motor impulse was assumed to be delivered late by the maximum possible amount of time and the lower motor impulse delivered early.

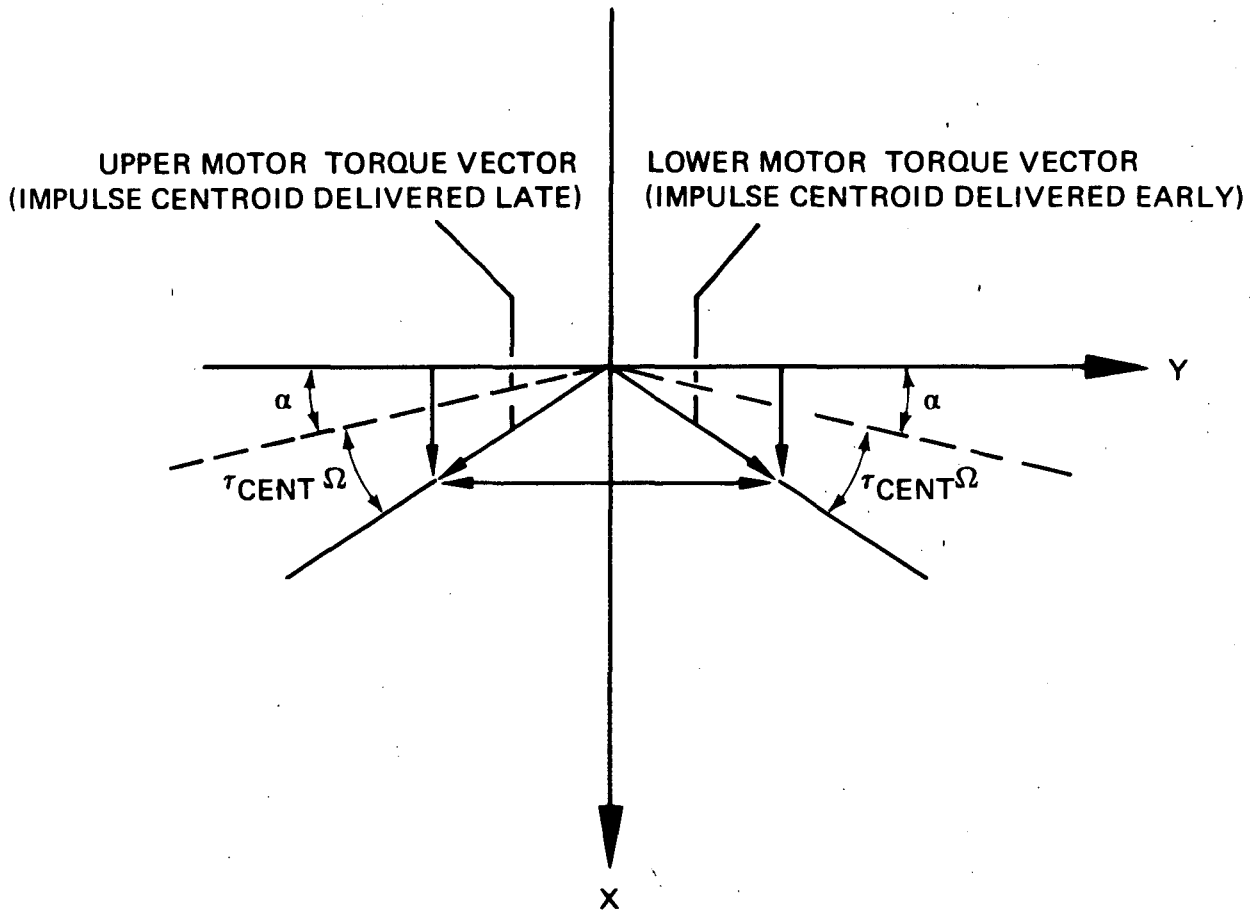


Figure 2-2. ACCUMULATED LEAD/LAG SECTOR COMMAND AND IMPULSE CENTROID EFFECTS ON X AXIS UNCERTAINTY TORQUE

The sector factor, a , is one-half a sector angle or 0.18 degrees. If the upper and lower motors fire together for the same period of time, the torque effect of this factor cancels.

For an individual motor the total maximum possible torque component along X is $Z_o(\tau_{cent}\Omega + a)$, which appears in the \mathbf{T} matrix.

2.1.2 Attitude Control Torque, Arm Matrix \mathbf{T}'

When attitude control motors fire simultaneously or 180 degrees out of phase, each motor fires the same length of time; i.e., each motor starts and stops in the same azimuth sector. The two (or more) motors must fire for the same period of time in order to produce the required attitude correction torque without producing a net velocity change or spin rate change. As a consequence, the factor, a , in the X axis portion of the uncertainty torque arm matrix is not included when dispersion torques produced during an attitude control maneuver are computed. The matrix \mathbf{T}' is therefore defined as follows:

$$\mathbf{T}' = \mathbf{T} - \begin{Bmatrix} \hat{i} a Z_o \\ 0 \\ 0 \end{Bmatrix} \quad (2-3)$$

2.1.3 Spin Control Torque Arm Matrix \mathbf{T}''

When one or several spin motors operate to change spacecraft spin rate, it is assumed that the motors fire in such a way that each portion of the impulse generated on one side of the spacecraft is matched by an equal amount of impulse delivered on the other side of the spacecraft as it rotates. The advantage of this operation mode is that the net torque, because of fixed uncertainty factors, is zero. The only net effect of fixed uncertainty factors is a small velocity change impulse along the Z axis. This will be discussed in paragraph 2.1.7, Cross Coupling Factors and Effects.

Another version of the original torque arm matrix is required to reflect the fixed uncertainty torque cancellation effect that can be achieved during spin change. The spin correction torque arm matrix is as follows:

$$\mathbf{T}'' = \begin{bmatrix} \hat{i} Z_o \tau_{cent} \Omega \\ \hat{j} \left(\frac{\Delta F}{F} \right) Z_o \\ \hat{k} \left(\frac{\Delta F}{F} \right) Y_o \end{bmatrix} \quad (2-4)$$

2.1.4 ΔV Motor Mean Torque Arm Matrices $\overline{\mathbf{T}}$ and $\overline{\mathbf{T}}'''$

The torque arm matrices required for evaluation of the disturbance torque effects, during ΔV maneuvers, are based on the \mathbf{T} matrix for two motors and on averaging effect factors that reflect the two simultaneous operating requirements for ΔV motors, which are given below:

- a. Delivery of total required ΔV
- b. Production of zero net nominal Y axis torque.

Two motors designated $F_O(U)$ and $F_O(L)$ will produce nominal ΔV impulse and zero net torque as follows:

$$\Delta V \text{ impulse: } F_O(U) t(U) + F_O(L) t(L) = I_O (\Delta V) \quad (2-5a)$$

$$\text{Zero torque: } F_O(U) t(U) Z_O(U) = F_O(L) t(L) Z_O(L) \quad (2-5b)$$

From the above two equations, it can be shown that the mean total torque arm matrix for two ΔV motors is:

$$\bar{\mathbf{T}} = \frac{\mathbf{T}(U) + \frac{Z_O(U)}{Z_O(L)} \mathbf{T}(L)}{1 + \frac{Z_O(U)}{Z_O(L)}} \quad (2-6)$$

Equation 2-6 is derived in detail in Appendix D.

If the thruster configuration has four motors, as in the case of Configuration C, the upper pair of motors may be taken together as one with regard to $Z_O(U)$ and the lower pair together as one with regard to $Z_O(L)$.

During a ΔV maneuver, the effect of time varying uncertainties cannot be cancelled, i.e., calibrated out, by the preprogrammed operation of the appropriate cancelling motor pairs, because time varying uncertainties are assumed not predictable. Fixed uncertainties, when quantitatively identified, are predictable and can be compensated within the limits of attitude direction and spin rate readout accuracy. As a consequence, it is useful to define a calibration factor, C_j for each axis.

In the determination of the calibration factor, it is necessary to use the $\bar{\mathbf{T}}'''$ matrix, which is the same as $\bar{\mathbf{T}}$ except that all fixed uncertainty factors are eliminated in each axis. Therefore, the matrix is defined, as follows:

$$\bar{\mathbf{T}}''' = \frac{\mathbf{T}'''(U) + \frac{Z_O(U)}{Z_O(L)} \mathbf{T}'''(L)}{1 + \frac{Z_O(U)}{Z_O(L)}} \quad (2-7)$$

Where:

$$\mathbf{T}''' = \begin{bmatrix} \hat{i} Z_O (\Omega \tau_{\text{cent}} + a) \\ \hat{j} \left(\frac{\Delta F}{F} \right) Z_O \\ \hat{k} \left(\frac{\Delta F}{F} \right) Z_O \end{bmatrix} \quad (2-8)$$

The sector control uncertainty factor, α , has been left in, though it is fixed, because an adjustment in ΔV motor firing schedule, after the calibration firing, to compensate for Y axis uncertainty torques can change the relative sector firing relationship that existed between the upper and lower ΔV motors during the calibration firing. Calibratable Y axis torques can be compensated by adjusting the firing duration of the upper and lower ΔV motors as indicated above. However, cancellation of calibratable disturbance torques about the X and Z axes requires operation of the appropriate attitude control (AC) and spin motors.

2.1.5 $\Delta V_{\max i}$ Computation Formulae

In Section 2.0, a limiting value of spin axis precession about the X or Y axis and spin rate change about the Z axis was specified. On the basis of elementary knowledge of the motion of a spinning body under the influence of impulsively applied torques, the degree of motion change about each axis under the influence of a specified torque can be computed. Below are given formulae for the computation of ΔV_{\max} for each axis.

$$\Delta V_{\max i} = (0.017453 \text{ rad/degree}) \Delta V M_z a_{ji} \frac{1}{I_o(\Delta V) \overline{T}_i} \quad (2-9a)$$

Where:

- i = X or Y = torque axis of interest
- j = Y or X = axis about which resulting precession occurs
- M_z = $I_z \Omega_z$ = Z axis angular momentum
- I_z = Z axis moment of inertia
- a_{ji} = Allowed maximum precession about the jth axis due to a torque about the ith axis
- ΔV = Velocity correction goal (meters/second)
- $I_o(\Delta V)$ = Total propulsive impulse from both upper and lower motors required to produce ΔV

For torques about the Z axis, the equation for maximum velocity becomes:

$$\Delta V_{\max z} = \Delta V \frac{\Delta \Omega_t I_z}{I_o(\Delta V) \overline{T}_z} \quad (2-9b)$$

The indicated total allowed change in Ω , $\Delta \Omega_t$, is 0.3 rpm for normal mode operation. Equations 2-9a and 2-9b are derived in detail in Appendix D.

2.1.6 Calibration Coefficients and $\Delta V_{\max i}$ (cal)

As previously stated, fixed contributions to the uncertainty torque arm matrix and its effects on precession and spin rate change during ΔV maneuvers can be observed and compensated. In practice the degree of measurement accuracy of spin axis precession or spin rate change produced by a preliminary calibration maneuver limits the degree of calibration achievable.

By use of definitions of \bar{T} and \bar{T}''' , previously described, it is possible to define the axis sensitive calibration factors as follows for X:

$$C_X = \frac{\theta_{pt} - 0.2 \text{ degree} - \theta_{pv}}{1 \text{ degree}} = \frac{\bar{T}_X - \bar{T}_X'''}{\bar{T}_X} - 0.2 \quad (2-10a)$$

Where:

- θ_{pt} = Total precession angle that could be produced
- θ_{pv} = Contribution to the total precession angle produced by variable uncertainty torques
- 0.2 degree = 2(0.10 degree) = twice maximum spin axis attitude measurement readout inaccuracy using SCADS
- 1 degree = Maximum allowed total precession about Y due to torques about X. This assumes that a total precession angle of 1 degree corresponds to a mean precession angle of 0.5 degree.

For Y:

$$C_Y = \frac{\theta_{pt} - 0.2 \text{ degree} - \theta_{pv}}{6 \text{ degrees}} = \frac{\bar{T}_Y - \bar{T}_Y'''}{\bar{T}_Y} - 0.03333 \quad (2-10b)$$

Where:

6 degrees = Maximum allowed precession about X due to torques about Y.

For Z:

$$C_Z = \frac{\Delta\Omega_t - 0.034 \text{ rpm} - \Delta\Omega_v}{0.3 \text{ rpm}} = \frac{\bar{T}_Z - \bar{T}_Z'''}{\bar{T}_Z} - 0.11333 \quad (2-10c)$$

Where:

0.034 rpm = 2 x 0.017 rpm = twice the maximum assumed readout uncertainty in spin rate measurement.

In general the calibrated ΔV_{\max} is related to the uncalibrated ΔV_{\max} as follows:

$$\Delta V_{\max} (\text{cal}) = \frac{\Delta V_{\max} (\text{uncal})}{1 - C_i}$$

A detailed derivation of the C_i is presented in Appendix D.

The calibration effect reflects the spacecraft controller's ability to observe and compensate for the nonvarying causes of thruster operation dispersion that contribute to the uncertainty torque. In general, the sum of the negative terms in the equations for the calibration factors will add to a number with a magnitude of less than unity so that the C_i factor is positive but smaller than unity. However, if the negative terms are great enough to cause the C_i factor to be negative, $1 - C_i$ will be positive and greater than unity. For such a condition, the calibration process would predict that $\Delta V_{\max}(\text{cal})$ is less than $\Delta V_{\max}(\text{uncal})$.

2.1.7 Cross Coupling Factors and Effects

Whenever a motor is fired to deliberately produce a velocity, attitude, or spin rate change, the contributions to the uncertainty torque arm matrix cause unwanted cross coupling torques or velocity changes, which must eventually be cancelled by operation of the appropriate motor system. This effect causes the total impulse that would nominally be loaded for velocity, attitude, or spin rate change to be increased according to the magnitude of the cross coupling effects.

In general the total velocity correction impulse and total attitude control or spin control torque impulse values can be computed from the nominal values, if the cross coupling factors are known. In particular, the three equations for $I_{\text{tot}}(\Delta V)$, $T_{\text{tot}}(\text{AC})$ and $T_{\text{tot}}(\text{spin})$ are as follows:

$$I_{\text{tot}}(\Delta V) = I_o(\Delta V) \left(1 + \frac{\Delta F}{F} \right) + T_o(\text{AC}) f_{\Delta V}(\text{AC}) + T_o(\text{spin}) f_{\Delta V}(\text{spin}) \quad (2-11)$$

$$T_{\text{tot}}(\text{AC}) = I_o(\Delta V) \sqrt{\overline{T}_X^2 + (1 - C_Y)^2 \overline{T}_Y^2} + T_o(\text{AC}) \left[1 + \sqrt{f_X^2(\text{AC}) + f_Y^2(\text{AC})} \right] + T_o(\text{spin}) \sqrt{f_X^2(\text{spin}) + f_Y^2(\text{spin})} \quad (2-12a)$$

$$T_{\text{tot}}(\text{spin}) = I_o(\Delta V) \overline{T}_Z + \overline{T}_o(\text{AC}) f_Z(\text{AC}) + T_o(\text{spin}) \left\{ 1 + f_Z(\text{spin}) \right\} \quad (2-12b)$$

Where:

$I_{\text{tot}}(\Delta V)$	=	Total impulse (lbf-sec) required for velocity change
$I_o(\Delta V)$	=	Nominal impulse calculated for ΔV
$T_{\text{tot}}(\text{AC})$	=	Total torque impulse (lbf-ft-sec) required for attitude control
$T_{\text{tot}}(\text{spin})$	=	Total torque impulse (lbf-ft-sec) for spin control
$T_o(\text{spin})$	=	Nominal spin torque impulse
$f_{x, y}(\text{AC, spin})$	=	Factor, which reflects attitude control or spin maneuver induced cross coupling torques about X or Y
$f_{\Delta V}(\text{AC, spin})$	=	Factor, which reflects attitude control or spin maneuver induced change in velocity
$f_Z(\text{AC, spin})$	=	Factor, which reflects attitude control or spin maneuver induced change in Z axis torque

The term, $(1-CY)$ is introduced in front of the Y component of the uncertainty torque matrix, \overline{T}_y , for velocity correction motor firing effects on attitude control to reflect the fact that the calibratable fraction of these torques can be compensated by adjusting the relative operating time of the upper and lower ΔV motors without requiring the attitude control motors to fire.

To compute the total impulse (lbf-sec) of all motors, the following equation is used:

$$I_{\text{tot}}(\text{all}) = I_{\text{tot}}(\Delta V) + \frac{2 T_{\text{tot}}(\text{AC})}{Z_o(\text{U}) + Z_o(\text{L})} + \frac{T_{\text{tot}}(\text{spin})}{Y_o} \quad (2-13)$$

A more detailed description of Equations 2-12 and 2-13 is given in Appendix D.

Formulae for the computation of the cross coupling factors employed in the equations above are presented in Table 2-1. It will be noted that the spaces set aside for the effect of ΔV or attitude control maneuvers on Z direction ΔV are left blank. The reason for this is that the contribution along Z is proportional to the pointing direction uncertainty, δ , which causes the Z axis contribution to ΔV to be much smaller than X axis contribution. Therefore, assuming that the Z and X axis contributions would be RSS (root sum square) combined in application, the Z axis effects were omitted. In the case of X directed ΔV produced during spin maneuvers, the fact that $(\Delta F/F)$ varies slowly with time was used to conclude that a net X axis directed ΔV would not be produced during a short spin rate change exercise.

2.1.8 Impulsive Torque Produced Spin Axis Precession

When a spinning body is perturbed by a torque applied about an axis normal to the spin axis, the attitude of the spin axis will decline away from its original direction in a predictable manner. The attitude of the Planetary Explorer Spacecraft is to be adjusted in this fashion.

At any time during such a maneuver the end of the spin axis will be observed to be moving in a circle corresponding to the coning motion of the axis. If the coning motion is completely undamped, the magnitude of the cone angle will be observed to cycle through upper and lower values as the torque motors continue to pulse. The accumulated precession angle of the spin axis follows the simple formula below:

$$\begin{aligned} \Delta\theta &= \frac{\text{torque impulse (lbf - ft - sec)}}{\text{spin axis angular momentum (slug - ft}^2\text{/sec)}} \\ &= \frac{\int [F(\text{U})t(\text{U})Z_o(\text{U}) + F(\text{L})t(\text{L})Z_o(\text{L}) dt]}{I_z \Omega_z} \end{aligned} \quad (2-14)$$

In order to generate a detailed prediction of the motion of the axis after each pulse, a computer program was developed. The key to the program is a description of the successive coning motion circles that reflect the fact that each torque pulse contributes (positively or negatively) to the total energy of the rotational motion.

Table 2-1. CROSS COUPLING FACTORS FORMULAE

Factor	About or Along	
	x or y	z
$f_{\Delta V} (\Delta V)$	$\Delta F/F$	
$f_{\Delta V} (AC)$	$2 \frac{\Delta F/F}{Z_o(U) + Z_o(L)}$	
$f_{\Delta V} (spin)$		δ/y
$f_{AC} (\Delta V)$	$\bar{T}_{x,y}$	
$f_{AC} (AC)$	$\frac{\sum_m T'_{x,y,m}}{\sum Z_{o,m}}$	
$f_{AC} (spin)$	$\frac{\sum T''_{x,y,m}}{\sum Y_{o,m}}$	
$f_{spin} (\Delta V)$		\bar{T}_z
$f_{spin} (AC)$		$\frac{\sum_m T'_{z,m}}{\sum Z_{o,m}}$
$f_{spin} (spin)$		$\frac{\sum_m T''_{z,m}}{\sum Y_{o,m}}$

A more detailed explanation of the above factor is given in Appendix D.

2.1.8.1 Detailed Analysis of Precession of Symmetrical Spinning Body

With regard to precession and declination of the spin axis, a rotating body exhibits four fundamental characteristics that determine the motion that will result from an applied torque. These characteristics are as follows:

- a. Spin axis moment of inertia
- b. Transverse axis moment of inertia
- c. Spin axis angular momentum
- d. Total angular momentum

Figure 2-3 shows the coning motion trajectory of the spin axis for the (n + 1)st circle that is produced by the combined effects of the residual motion of the nth circle and the incremental motion produced by a firing of the thruster pair at the junction of the transition of motion from

the n th to the $(n + 1)$ st circle. In this choice of the numbering sequence of precessive circles and torque impulse firings, the first circle produced is designated $n + 1 = 1$, i.e., $n = 0$. Motor firing numbers are the same as the original circles in which they occur. The first firing that occurs corresponds to $n = 0$, which is before any circles are generated.

When the n th motor firing occurs, the $(n + 1)$ st circle is produced. Conceptually, the nomenclature presented in Figure 2-3 is as follows:

- $\Delta\Omega_{txn}$ = Impulse firing induced change in the n th orbit's transverse rate of spin axis coning, which causes spin axis tip to move parallel to X.
- Ω_{txn} = Instantaneous value of the transverse rate of angular motion in the n th orbit that produces spin axis tip motion parallel to X simultaneously with torque impulse delivery.
- Ω_{tyn} = Instantaneous value of the transverse rate of angular motion in the n th orbit that produces spin axis tip motion parallel to Y simultaneously with torque impulse delivery.
- $\Omega_{t(n+1)}$ = Total transverse rate of angular motion in the $(n + 1)$ st orbit.
- \bar{A} = Angle between the +X axis and the vector connecting the origin of the coordinate system with the center of the $(n + 1)$ st circle.
- A_3 = Angle of rotation of the tip of the spin vector in the $(n + 1)$ st orbit between the n th and $(n + 1)$ st motor firing.
- $(A_3 + \bar{A} - \pi)$ = Angle between the +X axis and the vector between the center of the $(n + 1)$ st circle and the instantaneous location of the tip of the spin vector at the time of the $(n + 1)$ st motor firing.
- \bar{X}, \bar{Y} = Location of the center of the $(n + 1)$ st circle relative to the origin of the local coordinate system.

Computation of the various characteristics of the circle are made as shown in the sequence of equations below.

Starting with the n th orbit, the values of Ω_{txn} , Ω_{tyn} , and $\Delta\Omega_{txn}$ must be calculated as follows:

$$\Omega_{tyn} = \Omega_{tn} \cos (A_{3n} + \bar{A}_n - \pi) \quad (2-15a)$$

$$\Omega_{txn} = -\Omega_{tn} \sin (A_{3n} + \bar{A}_n - \pi) \quad (2-15b)$$

$$\Delta\Omega_{txn} = \frac{\int T_y dt}{I_t} \quad (2-16)$$

Where:

- T_y = Torque about the Y axis
- I_t = Transverse axis moment of inertia of the spacecraft

The total transverse angular motion of the body for the (n + 1)st orbit is computed as follows:

$$\Omega_{t(n+1)} = \sqrt{\Omega_{tyn}^2 + (\Omega_{txn} + \Delta\Omega_{txn})^2} \quad (2-17)$$

The transverse axis total angular momentum of the (n + 1)st orbit, $M_{t(n+1)}$ and the coning angle, B_{n+1} , are presented below:

$$M_{t(n+1)} = \Omega_{t(n+1)} I_t \quad (2-18)$$

$$B_{n+1} = \frac{M_{t(n+1)}}{M_z} \approx \frac{M_{B(n+1)}}{M_z} \quad (2-19)$$

Where:

M_z = Z axis angular momentum

$M_{B(n+1)}$ = Component of the transverse angular momentum projected onto the axis perpendicular to the total angular momentum vector.

The key angle, \bar{A}_{n+1} becomes:

$$\bar{A}_{n+1} = \pi/2 + \arctan \frac{\Omega_{tyn}}{\Omega_{txn} + \Delta\Omega_{txn}} \quad (2-20)$$

For small values of the ratio M_t/M_z , the rate of circular motion of the spin axis around the orbit circle is as follows:

$$\begin{aligned} \Omega_{pr(n+1)} &= \frac{\Omega_z I_z}{I_t} \left(1 + \frac{1}{2} \frac{M_{t(n+1)}^2}{M_z^2} \right) \\ &\approx \frac{\Omega_z I_z}{I_t} \quad (\text{fr } M_t^2 \ll M_z^2) \end{aligned} \quad (2-21)$$

In other words, the rate of precession around the cone is greater than the rate of spin axis rotation if $I_z > I_t$ and the rate of precession is essentially the same for all orbits. Computation of the angle $A_{3(n+1)}$ is accomplished as follows:

$$A_{3(n+1)} = \Omega_{pr} \tau_3 \quad (2-22)$$

$$\tau_3 = \frac{1}{\nu_3} = \frac{2\pi}{\Omega_z} \quad (2-23)$$

Where:

τ_3 = Period of rotation about the spin axis.

By definition M_B is the projection of M_t on the axis perpendicular to the total angular momentum vector, and therefore:

$$M_{B(n+1)} = M_z \sin B_{(n+1)} \simeq M_z B_{(n+1)} \quad (2-24)$$

Determination of the two independent angles of declination of the mean spin axis as time passes during the attitude control maneuver is accomplished by successive calculations of the values of X_n , \bar{X}_n , Y_n , and \bar{Y}_n and by summing them approximately to produce the basic parameter for computing a total declination angle.

Rotation angles about the X axis are termed C and rotating angles about the Y axis are termed D. The cumulative effects of precession and declination may be computed as follows, where $C_{cum(n+1)}$, $D_{cum(n+1)}$, denote the angular location of the center of the (n + 1)st orbit relative to the original position of the spin vector prior to the start of the attitude control maneuver:

$$\bar{C}_{cum(n+1)} = \bar{C}_{n+1} + \sum_0^n C_m \quad (2-25a)$$

$$\bar{D}_{cum(n+1)} = \bar{D}_{n+1} + \sum_0^n D_m \quad (2-25b)$$

Where:

$$\bar{C}_{n+1} = \frac{\bar{Y}_{n+1}}{M_z} \quad (2-26a)$$

$$\bar{D}_{n+1} = \frac{\bar{X}_{n+1}}{M_z} \quad (2-26b)$$

$$C_{n+1} = \frac{Y_{n+1}}{M_z} = \frac{\bar{Y}_{n+1} + \Delta Y_{n+1}}{M_z} \quad (2-27a)$$

$$D_{n+1} = \frac{X_{n+1}}{M_z} = \frac{\bar{X}_{n+1} + \Delta X_{n+1}}{M_z} \quad (2-27b)$$

and
$$\bar{Y}_{n+1} = M_{B(n+1)} \sin \bar{A}_{(n+1)} \quad (2-28a)$$

$$\bar{X}_{n+1} = M_{B(n+1)} \cos \bar{A}_{(n+1)} \quad (2-28b)$$

$$\Delta Y_{n+1} = M_{B(n+1)} \sin (A_{3n+1} + \bar{A}_{n+1} - \pi) \quad (2-29a)$$

$$\Delta X_{n+1} = M_{B(n+1)} \cos (A_{3n+1} + \bar{A}_{n+1} - \pi) \quad (2-29b)$$

The above equations can be readily solved in a successive fashion on a computer to produce the desired data. Computer printouts of considerable interest are \bar{C}_{cum} , \bar{D}_{cum} , and B, the coning angle.

2.2 ANALYSIS RESULTS

The formulae derived and presented in paragraph 2.1 provide many of the tools for evaluating the various spacecraft configurations proposed for consideration. The magnitude of the various error sources used in the analysis was as follows:

$\Delta F/F$	=	± 0.05	Y_1	=	± 0.030 inch = ± 0.0025 foot
δ	=	± 0.1 degree	Y_2	=	± 0.020 inch = ± 0.00167 foot
Z_1	=	± 0.060 inch = ± 0.005 foot	τ_{cent}	=	± 0.004 second
Z_2	=	± 0.020 inch = ± 0.00167 foot	α	=	0.18 degree

The points of motor location are extremely important in determining the ability of a particular system to accomplish the ΔV , attitude control, and spin control maneuvers in an efficient fashion. Figure 2-4 presents the four fixed-motor configurations, B, C, D-1, and D-2. The gimballed engine approach, which is appropriate to RRC Configurations A and E, is rejected as being incompatible with the pointing accuracy requirements for the spacecraft. The reason for this is the large probe vehicle center of gravity shift, which is caused by deployment of the main probe and miniprobe. In particular, a total center of gravity movement of 12 inches would require a gimballed engine to pivot through a total angle of about 26 degrees to remain lined up with the center of gravity under all circumstances. If the motor were positioned midway between the possible center of gravity location extremes, the motor would have to pivot 13 degrees, which exceeds the maximum allowed spin axis attitude declination of 6 degrees toward or away from the sun. Consequently, only configuration options containing fixed engines will be evaluated in this section. A fifth arrangement, designated F and shown in Figure 2-5, is defined as baseline with respect to performance only.

2.2.1 Maximum Allowed Velocity Corrections

Tables 2-2 and 2-3 present the ΔV_{max} calculation results for the orbiter and the probe during the midcourse regime of operation.

The uncal values are based on allowing a possible precession through the nominal allowable angles 6 degrees about the X-axis and 1 degree about the Y-axis; practically, however, these values should be reduced by 3.3% and 20% respectively (effectively limiting precession to 5.8 and 0.8 degrees) to allow for possible worst-case uncertainties in the initial and final vehicle measured attitude. Without this correction, the tabulated uncal values may sometimes exceed the cal values which take the attitude measurement uncertainty into account.

From the orbiter data it is clear that Configuration B is superior to others with the exception of F, which has the identical ΔV motor placement as B. For the probe, Configurations B and D-1 are nearly identical with respect to ΔV_{max} because the upper motors are placed very close to and the same distance above the mean center of gravity position.

The important aspect of ΔV motor placement in ΔV_{max} calculations is the distance of the motor from the center of gravity. In the B and F configurations for both orbiter and probe, one of the two motors is placed as near as possible to the extreme center of gravity location appropriate to either the midcourse correction ΔV or late mission ΔV maneuver in order to minimize the torque arm through which the large uncertainty torque factors can operate. For both the orbiter and probe,

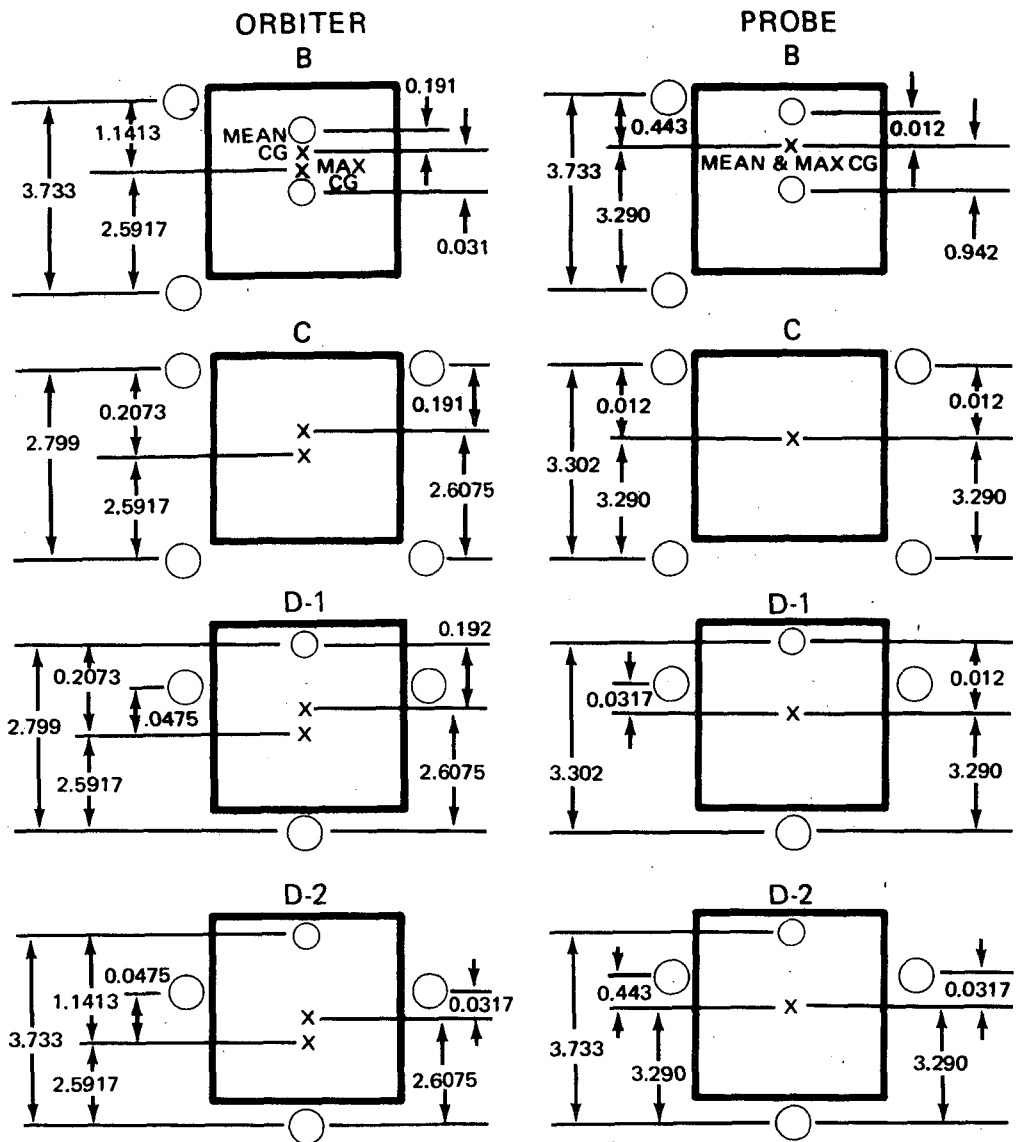


Figure 2-4. FIXED MOTOR CONFIGURATIONS B, C, D-1, AND D-2
(ALL DIMENSIONS ARE IN FEET)

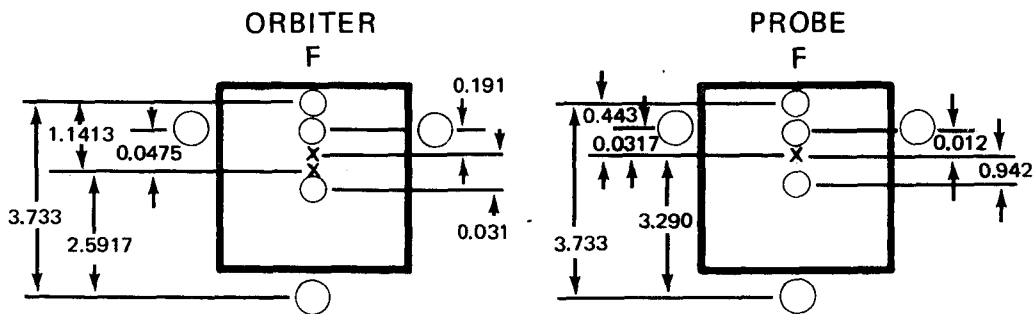


Figure 2-5. FIXED MOTOR CONFIGURATION F
(ALL DIMENSIONS ARE IN FEET)

Table 2-2. MAXIMUM ALLOWED UNCORRECTED MIDCOURSE VELOCITY CHANGE MANEUVERS FOR ORBITER
 $\Delta V_{\max}(\text{goal}) = 108 \text{ m/sec}$

Configuration	I_z	Ω_z	ΔV_{\max} Type	$\Delta V_{\max x}$ (m/sec)	$\Delta V_{\max y}$ (m/sec)	$\Delta V_{\max z}$ (m/sec)
B	68	15	Uncal	41.21	11.19	3.52
			Cal	39.49	47.44	31.03
C	68	15	Uncal	3.15	6.02	0.25
			Cal	5.00	7.92	0.23
D-1	68	15	Uncal	6.15	5.19	3.52
			Cal	5.89	7.83	31.03
D-2	68	15	Uncal	5.42	15.03	0.25
			Cal	16.41	42.60	0.23
F	68	15	Uncal	41.22	11.19	3.52
			Cal	39.49	47.44	31.03
B	68	60	Uncal	61.35	44.76	3.52
			Cal	53.73	189.77	31.03
C	68	60	Uncal	6.77	24.09	0.25
			Cal	7.58	31.67	0.23
D-1	68	60	Uncal	9.15	20.76	3.52
			Cal	8.01	31.30	31.03
D-2	68	60	Uncal	17.20	60.13	0.25
			Cal	33.72	170.42	0.23
F	68	60	Uncal	61.35	44.76	3.52
			Cal	53.73	189.76	31.03

Table 2-3. MAXIMUM ALLOWED UNCORRECTED MIDCOURSE VELOCITY CHANGE MANEUVERS FOR PROBE
 $\Delta V_{\max}(\text{goal}) = 108 \text{ m/sec}$

Configuration	I_z	Ω	ΔV_{\max} Type	$\Delta V_{\max x}$ (m/sec)	$\Delta V_{\max y}$ (m/sec)	$\Delta V_{\max z}$ (m/sec)
B	181	12	Uncal	188.36	22.70	7.92
			Cal	183.98	168.52	69.84
C	181	12	Uncal	10.87	33.73	0.56
			Cal	43.82	182.01	0.52
D-1	181	12	Uncal	186.67	22.68	7.92
			Cal	182.32	167.34	69.84
D-2	181	12	Uncal	10.01	26.95	0.56
			Cal	31.67	76.51	0.52
F	181	12	Uncal	188.36	22.70	7.92
			Cal	183.98	168.52	69.84
B	181	60	Uncal	310.80	113.51	7.92
			Cal	272.19	842.61	69.84
C	181	60	Uncal	48.59	168.66	0.56
			Cal	139.39	910.04	0.52
D-1	181	60	Uncal	308.01	113.41	7.92
			Cal	269.75	836.72	69.84
D-2	181	60	Uncal	38.92	134.74	0.56
			Cal	75.94	382.55	0.52
F	181	60	Uncal	310.81	113.51	7.92
			Cal	272.19	842.61	69.84

two ΔV motors are required, one immediately above the highest point of excursion of the center of gravity and one below the lowest point of excursion. Mounting of the lower motor closely to the lowest point of center of gravity excursion is particularly important for late probe mission velocity changes because the center of gravity will have moved downward away from the upper motor by that time. For the orbiter, the upper motor is closest to the center of gravity, during late mission orbit maneuvers, after the retromotor has been fired.

Because the ΔV motor arrangement of Configuration B was superior, the late mission velocity correction capabilities of the orbiter and probe were computed for B only. Table 2-4 presents the ΔV_{\max} calculation results.

Because $\Delta F/F$ can be a major contributor to the uncertainty torque arm matrix and the root-sum-square technique of combining independent error factors is a useful indicator of errors to be expected, ΔV_{\max} data based upon $\Delta F/F = 0.025$ and error calculations based upon the RSS method were generated. Tables 2-5 and 2-6 present ΔV_{\max} calculation results for orbiter and probe respectively.

In general, the RSS approach to error combination tends to suppress the additive effect of smaller magnitude contributors in a group of contributions, when compared to the linear combination technique. This effect is evident in some entries in the tables.

Another result that is noteworthy is the increased ratio of calibrated to uncalibrated ΔV_{\max} for axes in which $\Delta F/F$ appears as a part of a non-zero quantity, i.e., for cases in which the motor mounting torque arm through which $\Delta F/F$ acts is not zero.

2.2.2 Total Impulse and Usable Fuel Quantities

Another significant aspect of ΔV motor placement with respect to the center of gravity is the magnitude of cross coupling torques, which must eventually be cancelled. Table 2-7 presents nominal and total impulse and torque values for the orbiter without spinup to 60 rpm. Table 2-8 provides similar data for the probe without spinup to 60 rpm. Tables 2-9 and 2-10 present I_{sp} information based upon nominal data for the attitude control, velocity correction, and spin motors. These values of I_{sp} were used in conjunction with I_{tot} values to compute fuel weight.

Again, reviewing the data, it is clear that Configuration B is superior to other configurations except F in terms of the maximum allowed velocity correction and fuel consumption. Because of the requirement for 12 motors to accomplish the tasks performed by 8 motors on Configuration B, Configuration F is not preferred.

2.2.3 Nominal Attitude Control Maneuver Motion Details

When a nominal attitude control maneuver is performed, spin axis coning motion is superimposed on the average effect of spin axis declination. Figures 2-6 through 2-12 present both the linearly accumulated declination angle and the coning orbit effects. The salient features of the graphically presented data are shown in Table 2-11. Damping was neglected in all cases.

Table 2-4. LATE MISSION MAXIMUM ALLOWED VELOCITY CORRECTIONS FOR ORBITER AND PROBE

Configuration	I_z (slug ft ²)	Ω_z (rpm)	Mission Time	Fuel Condition	ΔV (Goal) per Firing (m/sec)	ΔV_{max} Type	$\Delta V_{max x}$ (m/sec)	$\Delta V_{max y}$ (m/sec)	$\Delta V_{max z}$ (m/sec)	Z Axis Coordinate	Displ/Feet
B Orbiter ↓	65	15	Orb man	No fuel used	12.2	Uncal Cal	167.19 160.18	19.50 162.03	5.35 47.23	Z ₀ (U) Z ₀ (L)	0.0105 0.2142
	62.65	15	Orb man	25 lb used	12.2	Uncal Cal	52.44 50.25	16.61 61.61	5.45 48.10	Z ₀ (U) Z ₀ (L)	0.0394 0.1853
	60.308	15	Orb man	50 lb used	12.2	Uncal Cal	35.58 34.09	15.14 43.16	5.56 49.07	Z ₀ (U) Z ₀ (L)	0.0718 0.1529
	58.431	15	Orb man	70 lb used	12.2	Uncal Cal	31.84 30.51	14.77 38.93	5.66 49.94	Z ₀ (U) Z ₀ (L)	0.1006 0.1241
	56.084	15	Orb man	95 lb used	12.2	Uncal Cal	34.48 33.04	15.41 42.02	5.80 51.14	Z ₀ (U) Z ₀ (L)	0.1409 0.0838
B Probe ↓	170	12	Post main probe release	No fuel used	5.0	Uncal Cal	17.54 17.13	14.09 19.87	13.61 120.05	Z ₀ (U) Z ₀ (L)	0.6145 0.3395
	170	12	Post main probe release	Maximum possible prior fuel used	5.0	Uncal Cal	24.17 23.61	18.24 27.31	15.63 137.9	Z ₀ (U) Z ₀ (L)	0.7085 0.2455
	48	85	Post main probe release	Maximum possible prior fuel used (thru 59 ft/sec ΔV)	18.0	Uncal Cal	151.49 130.94	133.21 621.60	7.19 63.48	Z ₀ (U) Z ₀ (L)	0.9302 0.0238

Table 2-5. ORBITER ΔV_{max} FOR VARIOUS UNCERTAINTY TORQUE CONTRIBUTION COMBINATION TECHNIQUES AND VALUES OF $\Delta F/F$

Mission Activity	Liquid Fuel Used	Spin Rate (rpm)	I_z (slug/ft ²)	ΔV_{max} About	ΔV_{max} Type	Linear (m/sec)		RSS (m/sec)	
						$\frac{\Delta F}{F} = .05$	$\frac{\Delta F}{F} = .025$	$\frac{\Delta F}{F} = .05$	$\frac{\Delta F}{F} = .025$
Cruise ↓	~zero	15	68	X	Uncal	41.22	41.22	63.61	63.61
					Cal	39.49	39.49	54.34	54.34
				Y	Uncal	11.19	12.45	19.97	21.75
					Cal	47.44	85.27	50.58	94.50
				Z	Uncal	3.52	3.52	5.78	5.78
					Cal	31.03	31.03	50.98	50.98
Beginning Orb Man ↓	~zero	15	65	X	Uncal	167.19	167.19	258.00	258.00
					Cal	160.18	160.18	220.42	220.42
				Y	Uncal	19.50	20.39	32.89	33.92
					Cal	162.03	258.65	182.63	311.17
				Z	Uncal	5.35	5.35	8.79	8.79
					Cal	47.24	47.24	77.60	77.60
End Orb Man ↓	95#	15	56.1	X	Uncal	34.48	34.48	53.21	53.21
					Cal	33.04	33.04	45.46	45.46
				Y	Uncal	15.41	18.50	28.78	34.42
					Cal	42.02	79.24	43.87	84.84
				Z	Uncal	5.80	5.80	9.52	9.52
					Cal	51.14	51.14	84.02	84.02

Table 2-6. PROBE ΔV_{\max} FOR VARIOUS UNCERTAINTY TORQUE CONTRIBUTION COMBINATION TECHNIQUES AND VALUES OF $\Delta F/F$

Mission Activity	Liquid Fuel Used	Spin Rate (rpm)	Iz (slug/ft ²)	ΔV_{\max} About	ΔV_{\max} Type	Linear (m/sec)		RSS (m/sec)	
						$\frac{\Delta F}{F} = .05$	$\frac{\Delta F}{F} = .025$	$\frac{\Delta F}{F} = .05$	$\frac{\Delta F}{F} = .025$
Cruise ↓	~zero	12	181	X	Uncal	188.36	188.36	302.25	302.25
					Cal	183.98	183.98	260.74	260.74
				Y	Uncal	22.70	23.91	37.58	39.31
					Cal	168.52	275.74	186.82	324.59
				Z	Uncal	7.92	7.92	13.00	13.00
					Cal	69.84	69.84	114.74	114.74
Post Main Probe Release ↓	~zero	12	170	X	Uncal	17.54	17.54	28.15	28.15
					Cal	17.13	17.13	24.28	24.28
				Y	Uncal	14.09	21.27	19.92	35.54
					Cal	19.87	39.15	20.15	40.14
				Z	Uncal	13.61	13.61	22.35	22.35
					Cal	120.05	120.05	197.22	197.22
Post Mini Probe Release ↓	Max Possible	85	48	X	Uncal	151.49	151.49	171.41	171.41
					Cal	130.94	130.94	142.98	142.98
				Y	Uncal	133.21	146.46	223.83	244.59
					Cal	621.60	1,102.72	663.37	1,226.17
				Z	Uncal	7.19	7.19	11.82	11.82
					Cal	63.48	63.48	104.29	104.29

Table 2-7. ORBITER IMPULSE AND FUEL QUANTITY DATA

	B		C		D-1		D-2		F	
	Dynamic Quantity	Fuel Mass (lbm)								
I_0 (ΔV) (lb-sec)	16,984		16,984		16,984		16,984		16,984	
I_{tot} (ΔV) (lb-sec)	17,902.1	82.22	17,924.93	82.323	17,924.93	82.322	17,902.1	82.22	17,902.1	82.22
T_0 (ac) (lb-ft-sec)	2,553.78									
T_{tot} (ac) (lb-ft-sec)	2,772.62		3,058.54		3,029.64		2,794.80		2,751.69	
I_{tot} (ac) (lb-sec)	1,485.46	9.1473	2,185.45	12.930	2,164.80	12.827	1,497.35	9.2014	1,474.25	9.0785
T_0 (spin) (lb-ft-sec)	604.84		604.84		604.84		604.84		604.84	
T_{tot} (spin) (lb-ft-sec)	926.93		2,778.71		785.60		2,581.69		781.94	
I_{tot} (spin) (lb-sec)	422.099	2.0094	1,265.35	6.024	357.74	1.703	1,175.63	5.5969	356.08	1.6952
Total usable fuel, lbm		93.377		101.277		96.853		97.019		92.994

Table 2-8. PROBE IMPULSE AND FUEL QUANTITY DATA

	B		C		D-1		D-2		F	
	Dynamic Quantity	Fuel Mass (lbm)								
$I_o (\Delta V)$	11,211.842									
$I_{tot} (\Delta V)$	11,820.112	54.054	11,826.17	54.081	11,826.17	54.081	11,820.112	54.054	11,820.112	54.054
$T_o (AC)$	1,732.2		1,732.2		1,732.2		1,732.2		1,732.2	
$T_{tot} (AC)$	1,912.66		1,936.24		1,849.67		1,893.40		1,848.28	
$I_{tot} (AC)$	1,024.73	5.9195	1,172.77	6.6745	1,120.33	6.393	1,014.41	5.851	990.23	5.721
$T_o (spin)$	1,605.358		1,605.358		1,605.358		1,605.358		1,605.358	
$T_{tot} (spin)$	1,881.12		3,083.01		1,738.75		2,959.528		1,782.778	
$I_{tot} (spin)$	856.612	3.9621	1,403.92	6.4936	812.27	3.757	1,347.690	6.234	811.829	3.755
Total usable fuel, lbm		63.9356		67.2491		64.231		66.139		63.53

Table 2-9. ORBITER NOMINAL IMPULSE, FUEL WEIGHT, AND I_{sp} DATA

Nominal AC Data			
Configuration	I_0 (ac) (lb-ft-sec)	Total Fuel (lb)	I_{sp}
B, D-2, F	1,368.22	8.392	163.04 ⁽¹⁾
C, D-1	1,824.782	10.729	170.08 ⁽¹⁾
Nominal Spin Data			
All	I_0 (spin)	Total Fuel	I_{sp}
	275.426	1.3112	210.05 ⁽¹⁾
Nominal ΔV Data			
All	I_0 (ΔV)	Fuel	I_{sp}
	16,984	78.00	217.74 ⁽¹⁾

Table 2-10. PROBE NOMINAL IMPULSE, FUEL WEIGHT, AND I_{sp} DATA

Nominal AC Data			
Configuration	I_0 (ac) (lb-ft-sec)	Fuel Mass (lbm)	I_s (lb-ft-sec/lbm)
B, D-2, F	928.047	5.343	173.70 ⁽¹⁾
C, D-1	1,048.23	5.960	175.86 ⁽¹⁾
Nominal ΔV Data			
All	I_0 (ΔV)	Total Fuel	I_{sp}
	11,211.842	51.272	218.674 ⁽¹⁾
Nominal Spin Data			
All	I_0 (spin)	Total Fuel	I_{sp}
	731.042	3.831	216.2 ⁽¹⁾

(1) I_{sp} data is weighted for the finite length of the impulse trains required and is derated by 2% to account for the firing direction efficiency of an 11% firing sector.

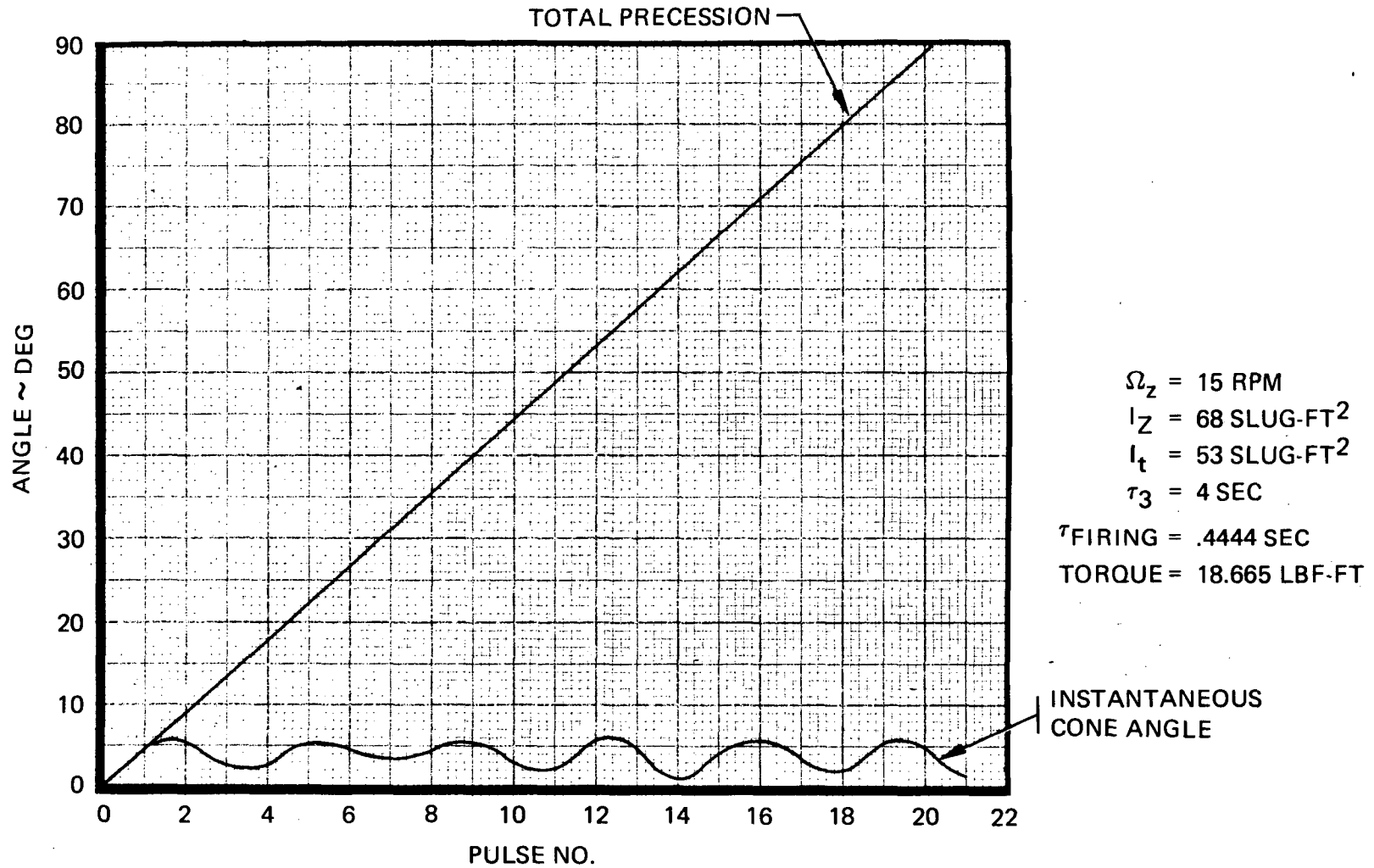


Figure 2-6. TOTAL PRECESSION ANGLE AND CONING ANGLE DATA FOR ORBITER MIDCOURSE ΔV

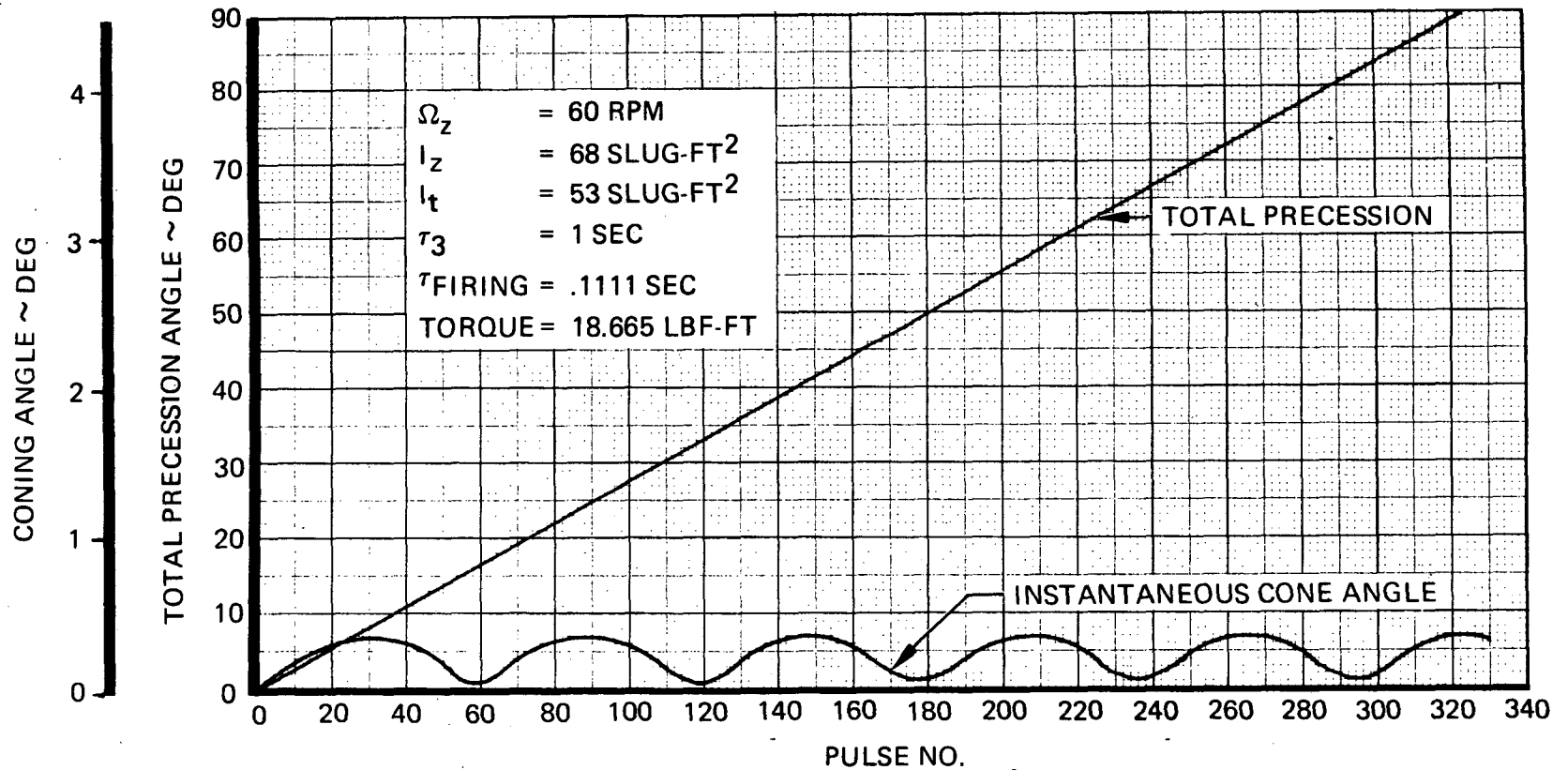


Figure 2-7. TOTAL PRECESSION ANGLE AND CONING ANGLE DATA FOR ORBITER MIDCOURSE ΔV

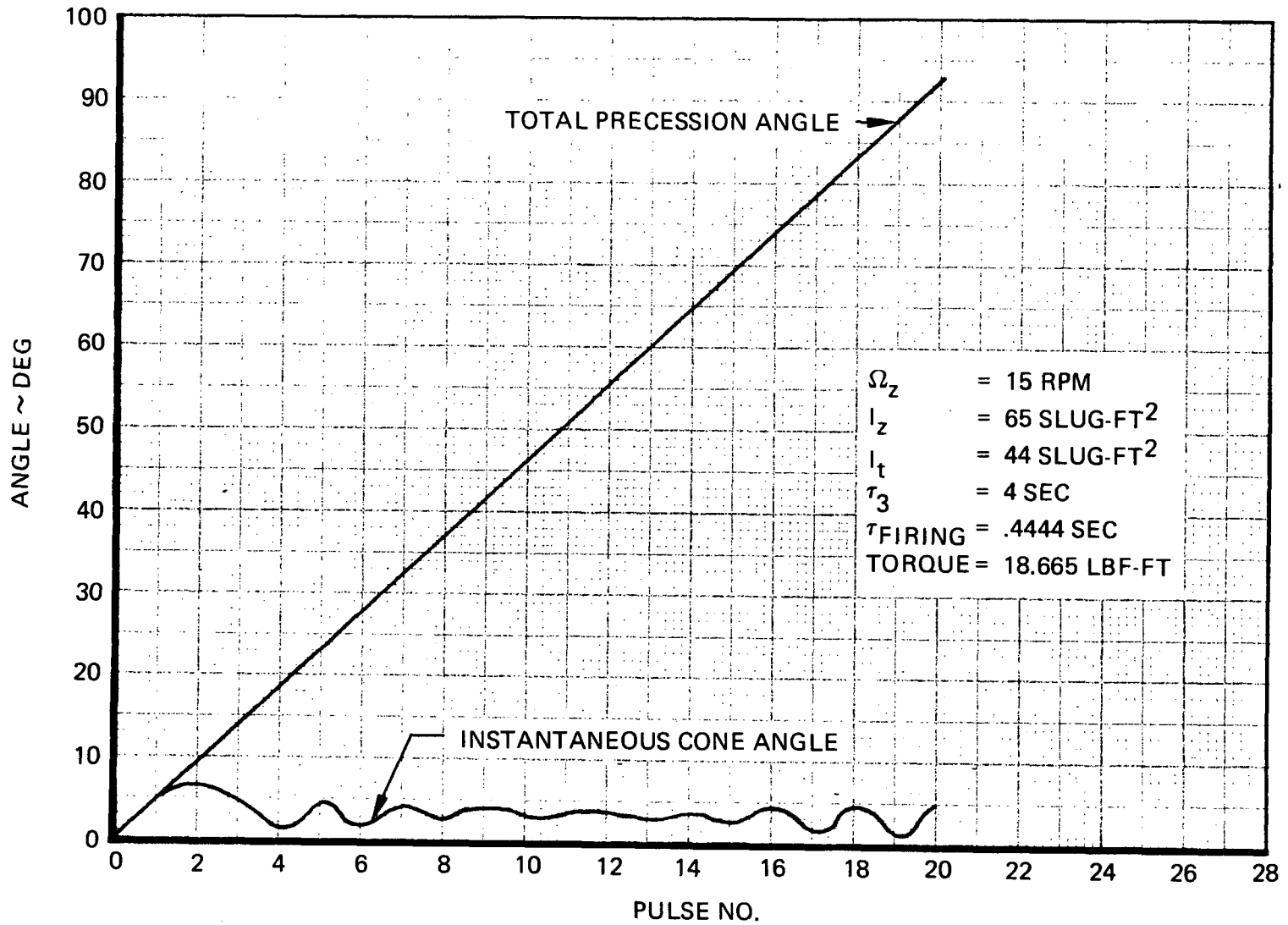


Figure 2-8. TOTAL PRECESSION ANGLE AND CONING ANGLE DATA FOR ORBITER PERIAPSIS REDUCTION (BEGINNING MANEUVER)

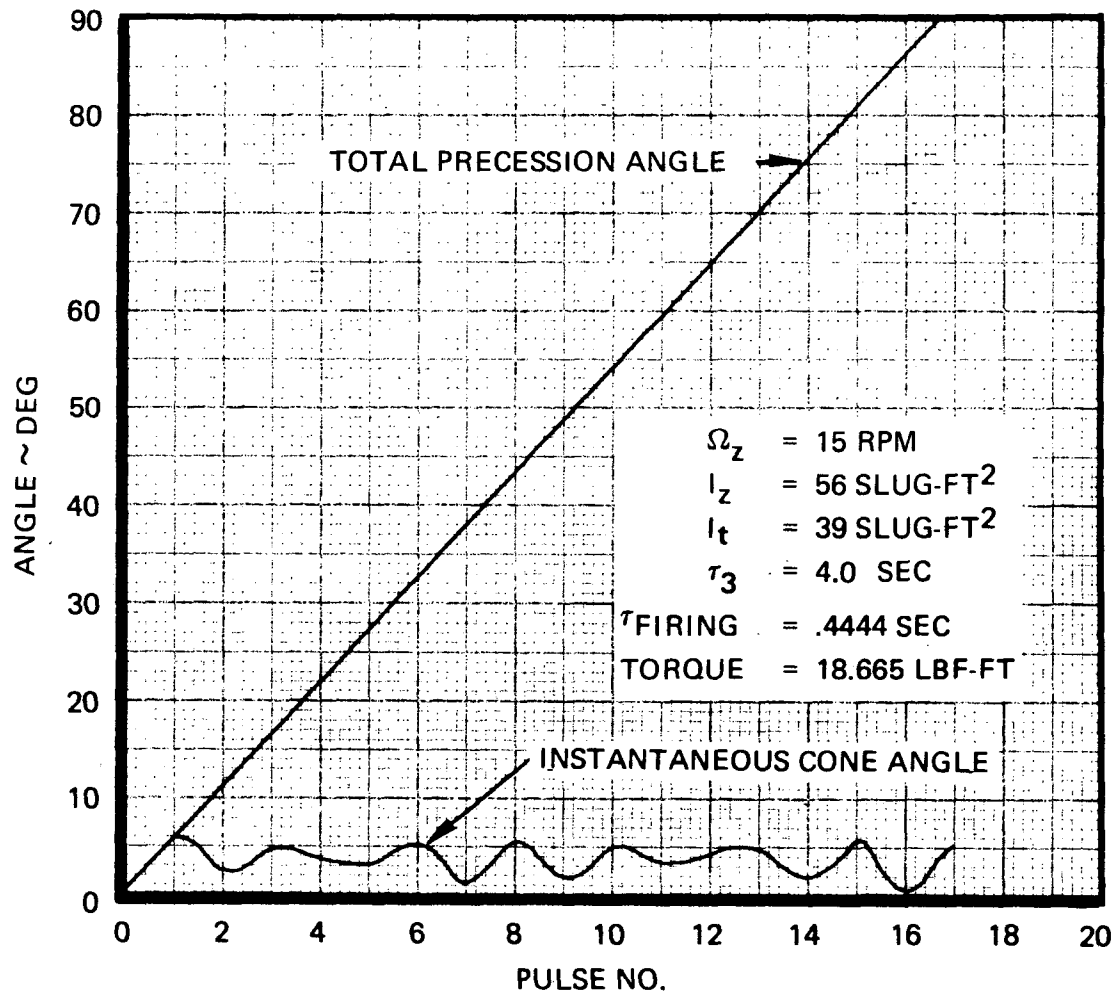


Figure 2-9. TOTAL PRECESSION ANGLE AND CONING ANGLE DATA FOR ORBITER PERIAPSIS REDUCTION (END MANEUVER)

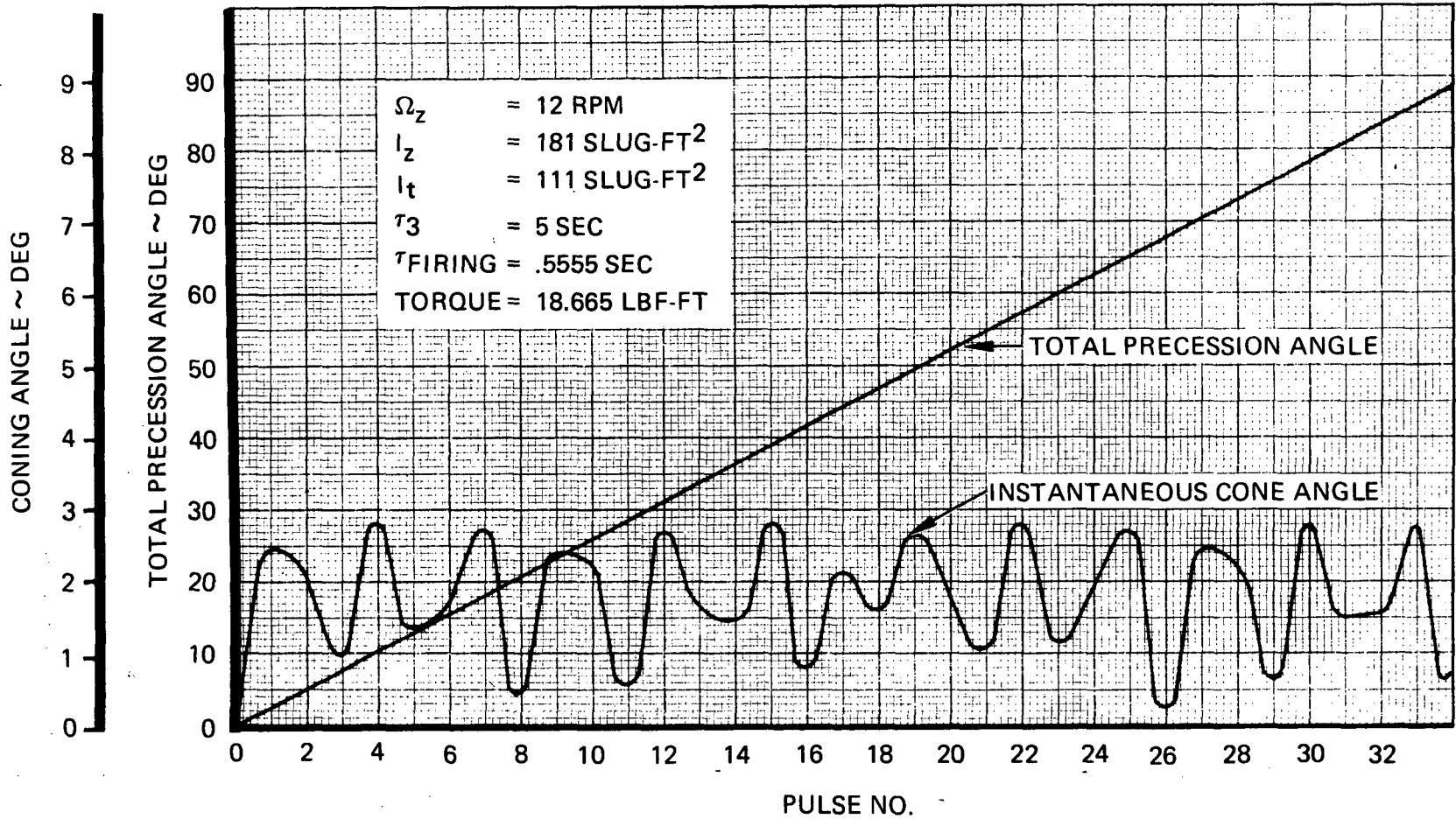


Figure 2-10. TOTAL PRECESSION ANGLE AND CONING ANGLE DATA FOR PROBE MIDCOURSE ΔV

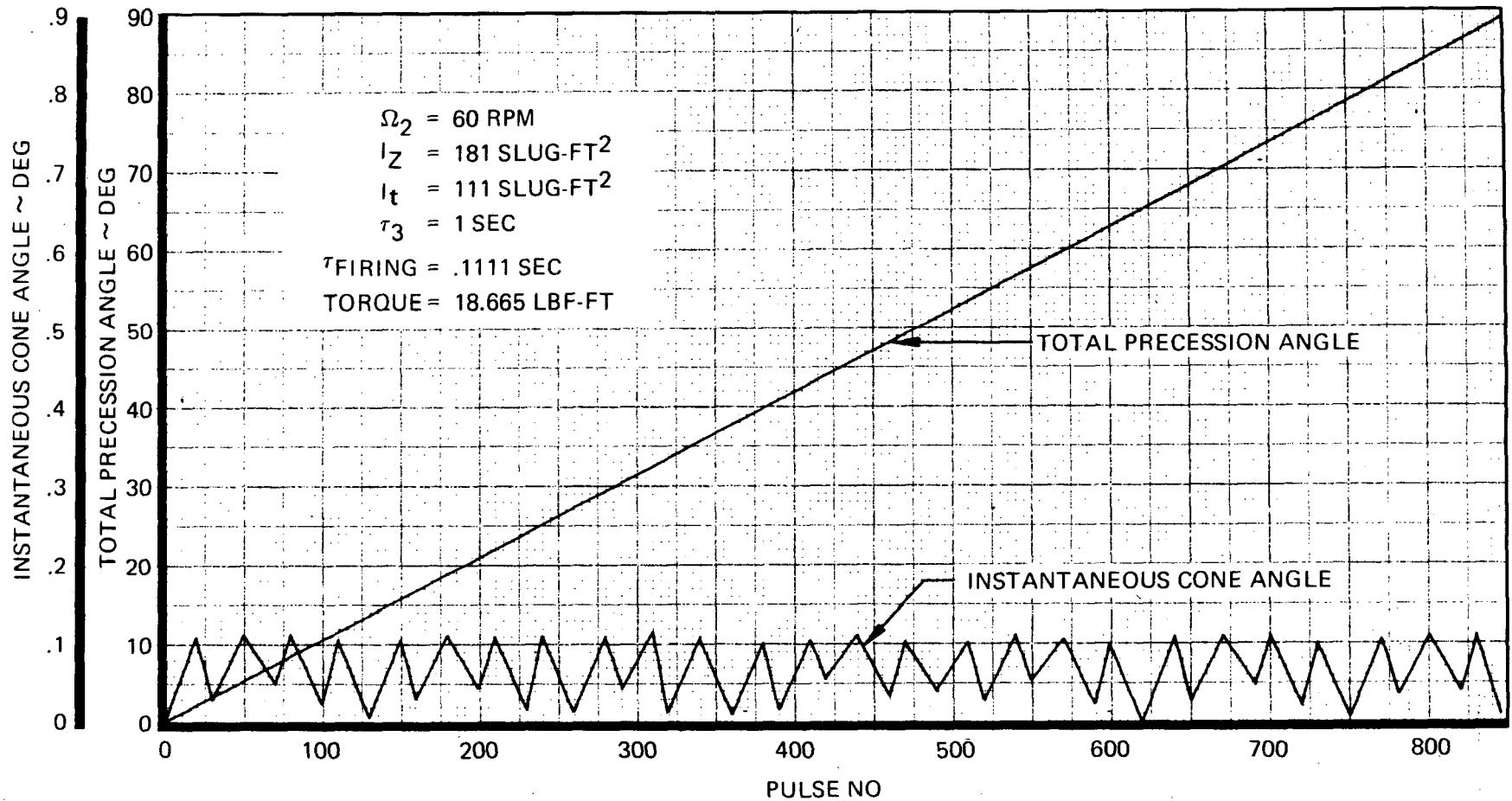


Figure 2-11. TOTAL PRECESSION ANGLE AND CONING ANGLE DATA FOR PROBE MIDCOURSE ΔV

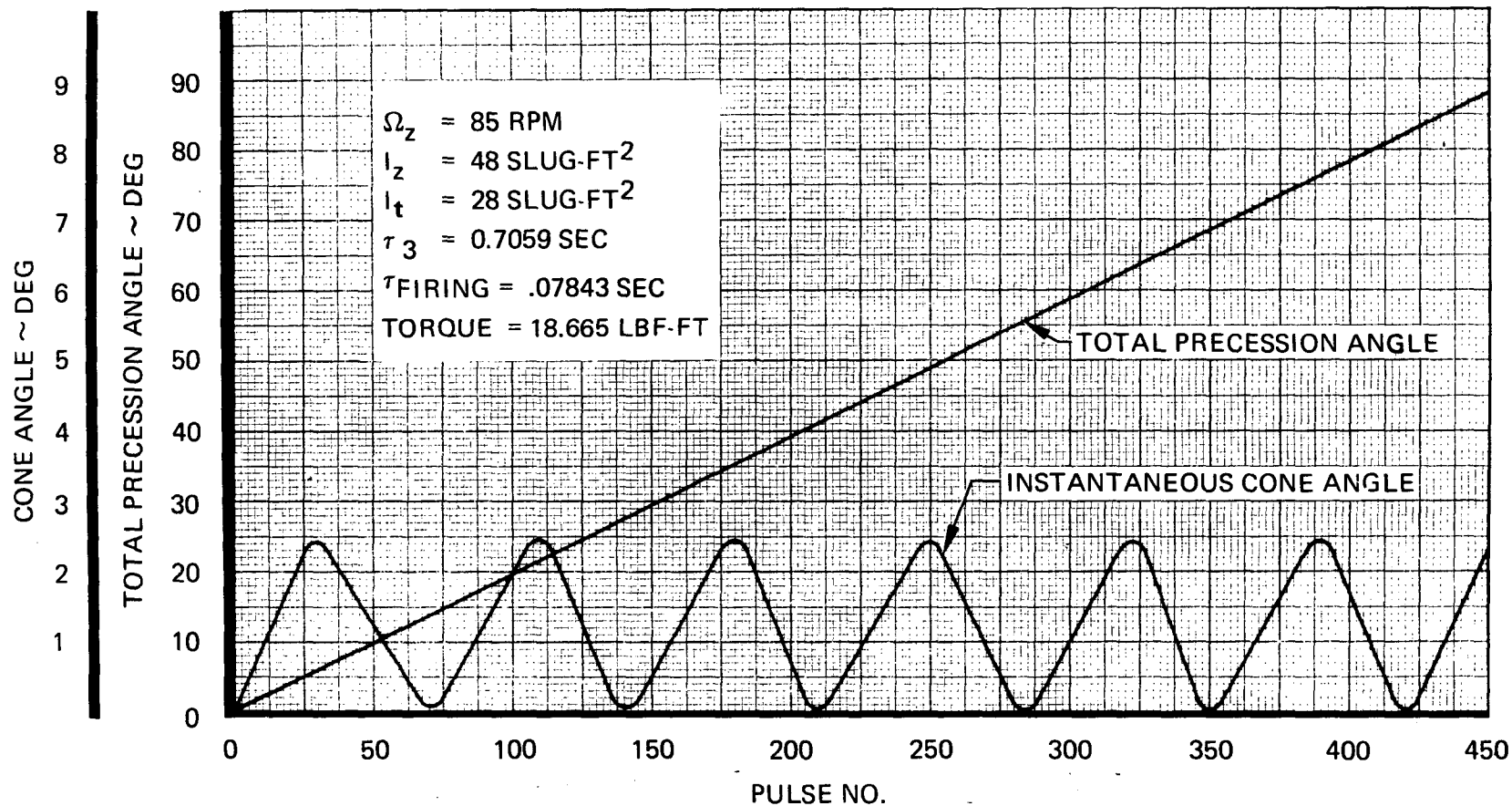


Figure 2-12. TOTAL PRECESSION ANGLE AND CONING ANGLE DATA FOR LATE MISSION ΔV

Table 2-11. ATTITUDE MANEUVER COMPUTATION RESULTS

Spacecraft	I_z (slug-ft ²)	I_t (slug-ft ²)	Ω_z (rpm)	τ_3 (sec)	τ_{firing} (sec)	Total Angle (deg)	No Pulses	Deg. per Pulse (deg)	Deg. per Second (deg)	Max. Con. Angle (deg)	Torque (lbf-ft)
Orbiter	68	53	15	4	0.4444	93.436	21	4.4493	1.1123	5.7	18.665
Orbiter	68	53	60	1	0.1111	91.768	330	0.27808	0.27808	0.36	18.665
Orbiter	65	44	15	4	0.4444	93.094	20	4.6547	1.1637	4.7	18.665
Orbiter	56	39	15	4	0.4444	91.847	17	5.4028	1.3507	5.5	18.665
Probe	181	111	12	5	0.5555	94.026	36	2.6118	0.5224	2.8	18.665
Probe	181	111	60	1	0.1111	90.892	870	0.10447	0.10447	0.11	18.665
Probe	48	28	85	0.7059	0.0784	90.303	460	0.19631	0.2781	0.25	18.665

2.2.4 Self-Induced and Cross Coupling Error Effects on Maneuver Precision and Total Fuel Requirements

When maneuvers of any type are performed, the uncertainty torque arm matrix effects on delivered velocity, attitude, or spin rate changes will manifest themselves as errors in the delivered maneuver. The magnitude of these errors will be proportional to the magnitude of the maneuver intended. This type of error or uncertainty is to be considered additive to the resolution uncertainty that results from minimum delivered impulse bit limitations on motor performance.

As previously discussed for spacecraft velocity changes, the time independent contributions to the uncertainty matrix can in principle be observed and compensated within the accuracy of attitude, ΔV , and spin rate change measurement. However, more than one calibration effort may be required over the entire mission because of the relatively gross movements of the center of gravity that accompany retrofiring for the orbiter and probe deployment for the probe vehicle.

Tables 2-12 and 2-13 present a summary of the cross coupling effect factors, the formulae for which were presented in paragraph 2.1.7. These factors were calculated for ΔV motors located relative to the mean midcourse center of gravity and for attitude control and spin control motors located with respect to the maximum midcourse maneuver center of gravity.

In evaluating the data in the tables with respect to errors inherent in any maneuver, the primary factors are the self-coupling ones, which are $f_{\Delta V}(\Delta V)$, $f_{ACX}(AC)$, $f_{ACY}(AC)$, and $f_{spin}(spin)$. As might be expected, these are essentially the same for all configurations. The only notable variations observed occur in the $f_{ACX}(AC)$ when the spacecraft Z axis spin rate is increased from the nominal cruise values of 12 or 15 rpm to 60 rpm.

Noting that all attitude control maneuvers in this study are assumed to be accomplished by the application of torque impulses about the Y axis, the factor $f_{ACX}(AC)$ is not a self-induced coupling in the sense that $f_{ACY}(AC)$ is. Examining the factors $f_{\Delta V}(\Delta V)$, $f_{ACY}(AC)$, and $f_{spin}(spin)$, the errors or uncertainties are all about 0.05. Inspection of the uncertainty torque arm matrix, \mathbf{T} , shows that the principle contributor to this is $(\Delta F/F)$. An engine system with an inherently reduced value of $(\Delta F/F)$ will therefore produce less maneuver magnitude proportional error.

The most important single measure of the overall effect of self-induced and cross coupling effects are the ratios $I_{tot}(\Delta V)/I_o(\Delta V)$, $T_{tot}(AC)/T_o(AC)$, and $T_{tot}(spin)/T_o(spin)$, which can be computed from the data of Tables 2-7 and 2-8. These ratios are presented in Table 2-14. Configurations B, F, and D-1 are generally superior to C and D-2, the principle reason being that ΔV is accomplished with tangentially operating motors in C and D-2, which cause a very large cross coupling of ΔV impulse into unwanted spin torque. Configuration D-1 is inferior to B and F because the ΔV motor closest to the center of gravity during the midcourse ΔV firing is only within 0.191 foot of the center of gravity, whereas for the B and F configurations, the closest motor is within 0.031 foot of the center of gravity for the orbiter. The D-1 configuration also suffers from having a short total torque arm for attitude control.

In the case of the probe, the D-1 configuration is very competitive with the B and F configurations for the midcourse and cruise portions of the mission. However, the D-1 probe configuration will

22

Table 2-12. ORBITER TORQUE CROSS COUPLING FACTORS

Configuration	Spin Rate (rpm)	$f_{\Delta V(\Delta V)}$	$f_{\Delta V(AC)}$	$f_{\Delta V(\text{spin})}$	$f_{AC_x(\Delta V)}$	$f_{AC_x(AC)}$	$f_{AC_x(\text{spin})}$	$f_{AC_y(\Delta V)}$	$f_{AC_y(AC)}$	$f_{AC_y(\text{spin})}$	$f_{\text{spin}(\Delta V)}$	$f_{\text{spin}(AC)}$	$f_{\text{spin}(\text{spin})}$
B	15	0.050	0.027	0.0008	0.0006	0.010	0.005	0.013	0.053	0.042	0.008	0.061	0.050
B	60	0.050	0.027	0.0008	0.002	0.029	0.021	0.013	0.053	0.042	0.008	0.061	0.050
C	15	0.050	0.036	0.0008	0.008	0.011	0.004	0.024	0.055	0.032	0.114	0.081	0.050
C	60	0.050	0.036	0.0008	0.015	0.030	0.016	0.024	0.055	0.032	0.114	0.081	0.050
D-1	15	0.050	0.036	0.0008	0.004	0.008	0.0001	0.028	0.058	0.001	0.008	0.006	0.050
D-1	60	0.050	0.036	0.0008	0.011	0.027	0.0005	0.028	0.058	0.001	0.008	0.006	0.050
D-2	15	0.050	0.027	0.0008	0.005	0.008	0.0001	0.010	0.056	0.001	0.114	0.004	0.050
D-2	60	0.050	0.027	0.0008	0.006	0.027	0.0005	0.010	0.056	0.001	0.114	0.004	0.050
F	15	0.050	0.027	0.0008	0.006	0.008	0.0001	0.013	0.056	0.001	0.008	0.004	0.050
F	60	0.050	0.027	0.0008	0.0016	0.027	0.0005	0.013	0.056	0.001	0.008	0.004	0.050

Table 2-13. PROBE TORQUE CROSS COUPLING FACTORS

Configuration	Spin Rate (rpm)	$f_{\Delta V(\Delta V)}$	$f_{\Delta V(AC)}$	$f_{\Delta V(\text{spin})}$	$f_{AC_x(\Delta V)}$	$f_{AC_x(AC)}$	$f_{AC_x(\text{spin})}$	$f_{AC_y(\Delta V)}$	$f_{AC_y(AC)}$	$f_{AC_y(\text{spin})}$	$f_{\text{spin}(\Delta V)}$	$f_{\text{spin}(AC)}$	$f_{\text{spin}(\text{spin})}$
B	12	0.050	0.027	0.0008	0.0002	0.009	0.004	0.012	0.054	0.042	0.008	0.061	0.050
B	60	0.050	0.027	0.0008	0.0007	0.029	0.021	0.012	0.054	0.042	0.008	0.061	0.050
C	12	0.050	0.030	0.0008	0.0041	0.009	0.004	0.008	0.054	0.038	0.114	0.069	0.050
C	60	0.050	0.030	0.0008	0.0046	0.029	0.019	0.008	0.054	0.038	0.114	0.069	0.050
D-1	12	0.050	0.030	0.0008	0.0002	0.0068	0.0000	0.0117	0.056	0.0007	0.008	0.005	0.050
D-1	60	0.050	0.030	0.0008	0.0007	0.0269	0.0004	0.0117	0.056	0.0007	0.008	0.005	0.050
D-2	12	0.050	0.027	0.0008	0.0044	0.0067	0.00007	0.010	0.056	0.0007	0.113	0.004	0.050
D-2	60	0.050	0.027	0.0008	0.0057	0.0269	0.0004	0.010	0.056	0.0007	0.113	0.004	0.050
F	12	0.050	0.027	0.0008	0.0002	0.0068	0.00007	0.0117	0.056	0.0007	0.008	0.004	0.050
F	60	0.050	0.027	0.0008	0.0007	0.027	0.0004	0.0117	0.056	0.0007	0.008	0.004	0.050

Table 2-14. COMPARATIVE IMPULSE AND FUEL DATA FOR ORBITER AND PROBE

	Spin Rate	$\frac{I_{tot}(\Delta V)}{I_0(AV)}$	$\frac{T_{tot}(AC)}{T_0(AC)}$	$\frac{T_{tot}(Spin)}{T_0(Spin)}$	ΔV Motor $Z_0(U)$ (feet)	ΔV Motor $Z_0(L)$ (feet)	AC Motor Total Torque Arm (ft)	ΔV_{tot} Fuel (lbm)	AC _{tot} Fuel (lbm)	Spin _{tot} Fuel (lbm)	Total Usable Fuel
ORBITER B	15	1.0540	1.0857	1.5325	0.191	.031	3.733	82.22	9.15	2.01	93.38
C	15	1.0554	1.1977	4.5941	0.191	2.608	2.799	82.32	12.93	6.02	101.28
D-1	15	1.0554	1.1863	1.2989	0.192	2.608	2.799	82.32	12.83	1.70	96.85
D-2	15	1.0540	1.0944	4.2684	0.317	2.608	3.733	82.22	9.20	5.60	97.02
F	15	1.0540	1.0775	1.2928	0.191	0.031	3.733	82.22	9.08	1.70	93.00
PROBE B	12	1.0543	1.1042	1.1718	0.012	0.942	3.733	54.05	5.92	3.96	63.94
C	12	1.0548	1.1178	1.9205	0.012	3.290	3.302	54.08	6.67	6.49	67.25
D-1	12	1.0548	1.0678	1.1111	0.012	3.290	3.302	54.08	6.39	3.76	64.23
D-2	12	1.0543	1.0931	1.8435	0.317	3.290	3.733	54.05	5.85	6.23	66.14
F	12	1.0543	1.0670	1.1105	0.12	0.942	3.733	54.05	5.72	3.76	63.53

suffer significantly in maximum allowable ΔV after the probes are released because of the large accompanying downward translation of the center of gravity. The D-1 probe configuration also suffers from a short attitude control torque arm.

From the point of view of fuel consumption, therefore, the B or F configurations are preferred.

2.2.5 ΔV Maneuver Directional Accuracy

When a spacecraft velocity correction is made, the average direction in which the impulse is delivered will be off nominal in accordance with the magnitude and algebraic sign of the following quantities:

1. $\epsilon =$ Accuracy of SCADS system measurement of spin axis orientation relative to reference stars
 $= \pm 0.1$ degree
2. $\delta =$ Thruster directional alignment uncertainty
 $= \pm 0.1$ degrees
3. $\alpha =$ Spacecraft azimuth sector minimum increment size effect on mean impulse centroid delivery direction
 $= \pm 0.18$ degree
4. $\tau =$ Impulse bit centroid delivery time uncertainty
 $= \pm 0.004$ second
5. $\Omega =$ Spacecraft Z axis spin rate as required
6. $\left(\frac{\Delta\theta}{\Delta V}\right)_X \left(\frac{\Delta V}{2}\right) =$ Mean precession angle about the Y axis produced by uncertainty torques about the X axis during a velocity correction maneuver.

Figure 2-13 shows the significant error producing quantities. The errors can be combined in a linear fashion, assuming all quantities have the same sign, or they may be combined in the root-sum-squares fashion, which assumed that all errors are random and independent. Considering these possibilities, several angle definitions can be made to suit the computation assumptions, as follows:

1. $\Delta\theta_Z(L) =$ Linearly summed contributions of Z axis attitude uncertainty
2. $\Delta\theta_\ell(L) =$ Linearly summed contributions of latitude attitude uncertainty
3. $\Delta\theta_{Z,\ell}(RSS) =$ Root-sum-square combined contributions of Z or lateral axis uncertainty
4. $\Delta\theta_{tot}(L,RSS) =$ Total (composite) Z and lateral axis uncertainties by linear or root-sum-square methods

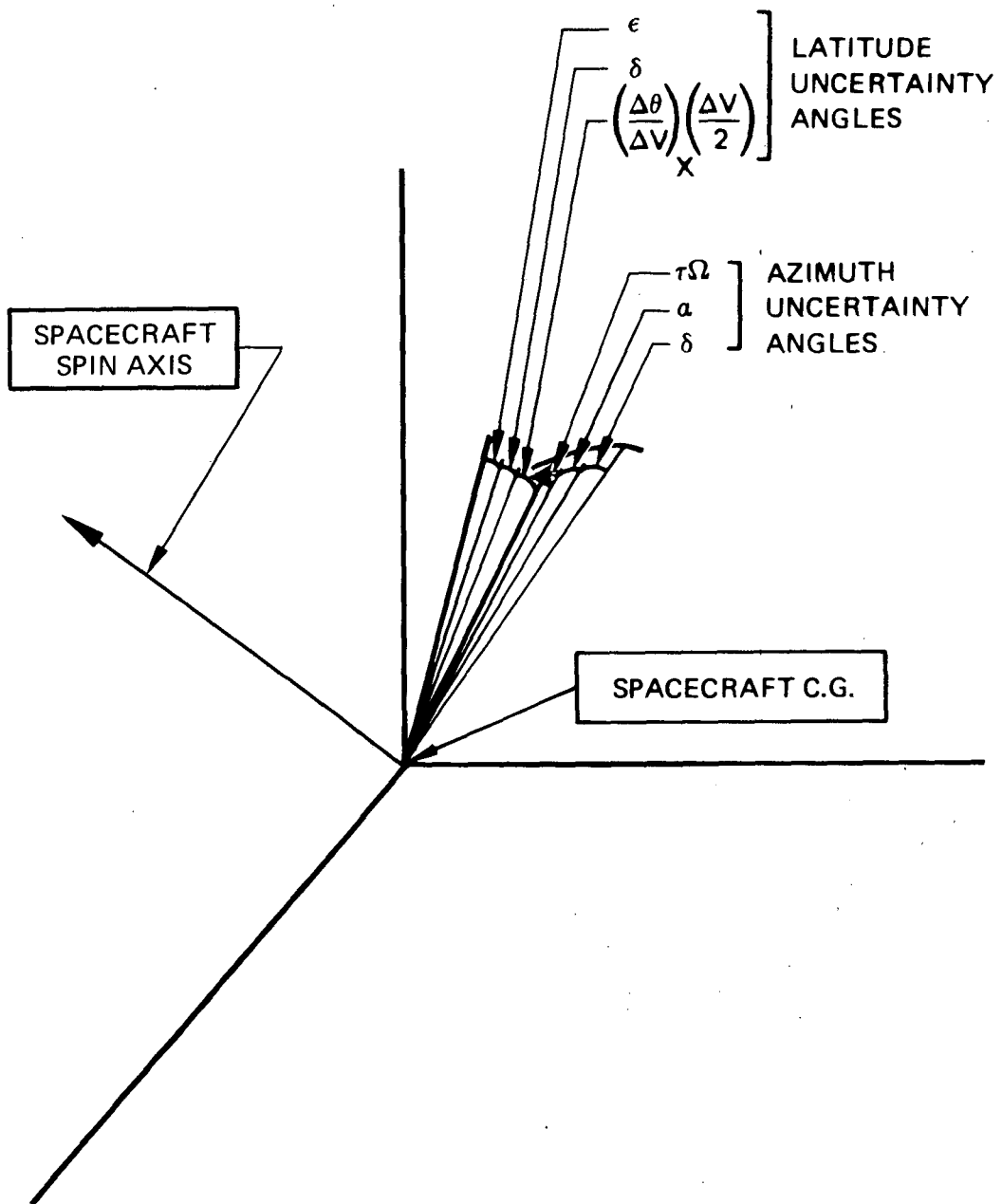


Figure 2-13. ΔV MANEUVER IMPULSE DELIVERY DIRECTION ERROR CASES

The detailed expressions for total velocity correction impulse angle dispersions are as follows:

$$\Delta\theta_{\text{tot}}(L) = \left[(\tau\Omega + \alpha + \delta)^2 + \left(\epsilon + \delta + \left(\frac{\Delta\theta}{\Delta V} \right)_X \left(\frac{\Delta V}{2} \right) \right)^2 \right]^{1/2} \quad (2-30)$$

$$\Delta\theta_{\text{tot}}(\text{RSS}) = \left[(\tau\Omega)^2 + \alpha^2 + \delta^2 + \epsilon^2 + \delta^2 + \left(\frac{\Delta\theta}{\Delta V} \right)_X^2 \left(\frac{\Delta V}{2} \right)^2 \right]^{1/2}$$

$$= \left[(\tau\Omega)^2 + \alpha^2 + 2\delta^2 + \epsilon^2 + \left(\frac{\Delta\theta}{\Delta V} \right)_X^2 \left(\frac{\Delta V}{2} \right)^2 \right]^{1/2}$$

The computation results presented below were restricted to spacecraft Configuration B. The computation of $(\Delta\theta/\Delta V)_X$ is accomplished in the same manner as in paragraph 2.1, where the ΔV_{max} equations were first introduced. In particular, the following results:

$$\left(\frac{\Delta\theta}{\Delta V} \right)_X = 187.98 \text{ M } \frac{\overline{\tau}_X}{I_Z \Omega_Z} \quad (2-31)$$

Where:

$$\left(\frac{\Delta\theta}{\Delta V} \right)_X = \text{Rate of angular displacement with } \Delta V \text{ delivery in units of degrees/meter/sec}$$

M = Spacecraft mass (slugs)

$\overline{\tau}_X$ = Mean uncertainty torque arm matrix for torques about the X axis (feet), see paragraph 2.1.4

I_Z = Z axis (spacecraft spin axis) moment of inertia (slug-ft²)

Ω_Z = Z axis rotation rate (radians/second).

The nature of the quantities which contribute to the total dispersion as time passes are as follows:

$\tau\Omega$: Variable, random, or steady

α : Fixed

δ : Fixed

ϵ : Variable, random

$\left(\frac{\Delta\theta}{\Delta V} \right)_X \left(\frac{\Delta V}{2} \right)$: Part 1. Variable, random, or steady
Part 2. Fixed (see $\overline{\tau}_X$ in paragraph 2.1).

Quantities described as time variable and random or steady are quantities that are assumed to vary with time in some unpredictable fashion during the mission. These quantities cannot be expected to be uniformly constant or random in value. They are expected to reproduce themselves during the delivery of between a few or a great many pulses, but the time at which a train of values will shift cannot be predicted.

From the spacecraft designer's point of view, the preferred technique of combining these uncertainties, i.e., either linearly summing or root-sum-squaring, is determined by the number of independent uncertainties to be considered and by their nature. Because most of the variables presented are either fixed or variable/steady, as discussed above, and because each angle is made up of only three contributions, it is recommended that the more conservative results of linear combination be employed ultimately. Calculation results are given below for both techniques.

Table 2-15 presents the input data for the results graphically presented in Figures 2-14 through 2-21 for activity numbers O-1, O-1A, O-2, O-6, P-1, P-1A, P-2, and P-4. Table 2-15 also includes a summary of the ΔV_{\max} data for allowed mean angle dispersions of 1 and 2 degrees.

From the data, it is clear that the spin axis stability that accompanies high spin rates, e.g, 60 rpm, produces the undesirable effect of angularly shifting the impulse bit centroid delivery direction either positively or negatively with respect to the nominal direction according to whether the bit is delivered before or after the nominal time of delivery.

2.2.6 Single Engine Failure Impact

The planned mode of ΔV delivery for the Planetary Explorer spacecraft is a series of motor pulses of predetermined length and firing schedule for each motor. If an engine assembly fails closed, its part of the required impulse will not be delivered, while the other engine continues to pulse through the preprogrammed number of cycles. Because no onboard attitude sensing and control equipment is planned, the spacecraft must not be allowed to tumble excessively in the event of a failure.

Because radially firing ΔV motors located above and below the center of gravity are preprogrammed to deliver zero net nominal torques about the Y axis, the effect of an engine-out failure in terms of total torque impulse delivered during the mission is the same for the upper and lower motors.

Referring to Equations 2-5a and 2-5b in paragraph 2.1.4, the total torque impulse that will be delivered is:

$$T_{(EF)} = \frac{Z_o(U) Z_o(L)}{Z_o(U) + Z_o(L)} I \quad (2-32)$$

Where:

I = Impulse to be delivered in one uninterrupted stream of pulses.

From the equation, it is clear that it is of paramount importance to have one motor near the center of gravity at the time the firing occurs. The equation is derived in Appendix D.

In the case of the C and D-2 configurations, the occurrence of one engine out will produce a spin rate change as well as an attitude change. Considering engine Configurations B and F, the spin axis attitude declination data for orbiter and probe are presented in Table 2-16.

Table 2-15. SPACECRAFT CONDITIONS FOR TOTAL ΔV DIRECTION ERROR CALCULATIONS

									Maximum Velocity Correction			
									Linear (m/sec)		RSS (m/sec)	
	Activity No	Activity	Ω_z (rpm)	M (slug)	I_z (slug-ft ²)	Fuel Condition (lbm)	Other Condition (lbm)	\bar{T}_x (feet)	1 ^o	2 ^o	1 ^o	2 ^o
Orbiter ↓	O-1	Cruise	15	23.158	68.000	~zero used	—	.00059583	47	140	74	161
	O-1A	Cruise	60	23.158	68.000	↓	—	.00160133	*	100	—	167
	O-2	640 ft/sec Orbit Man.	15	14.538	65.000	~zero used	-277.1 for retro	.00022361	190	577	301	650
	O-3	↓	15	13.761	62.650	~25 lb used		.00072585	60	177	94	205
	O-4	↓	15	12.984	60.308	~50 lb used		.00109145	40	121	64	139
	O-5	↓	15	12.362	58.431	~70 lb used		.00124121	36	108	57	124
	O-6	↓	15	11.585	56.084	~95 lb used		.00117389	39	117	62	135
Probe ↓	P-1	Cruise	12	27.387	181.000	~zero used	—	.00023477	247	650	350	740
	P-1A	Cruise	60	27.387	181.000	↓	—	.00071141	—	510	—	850
	P-2	16.4 ft/sec ΔV	12	14.961	170.000	~zero used	-399.7 (main probe)	.00433290	22	60	32	69
	P-3	16.4 ft/sec ΔV	12	13.021	170.000	62.4 used (max possible)		.0036125	30	83	45	95
	P-4	59 ft/sec ΔV (end condition)	85	7.989	48.000	69.5 used	-154.8 (mini-probe)	.00187933	—	—	—	—

*Blanks reflect the result that the dispersion was greater than the reference angle (1^o or 2^o) for $\Delta V = 0$; i.e., no impulse delivery.

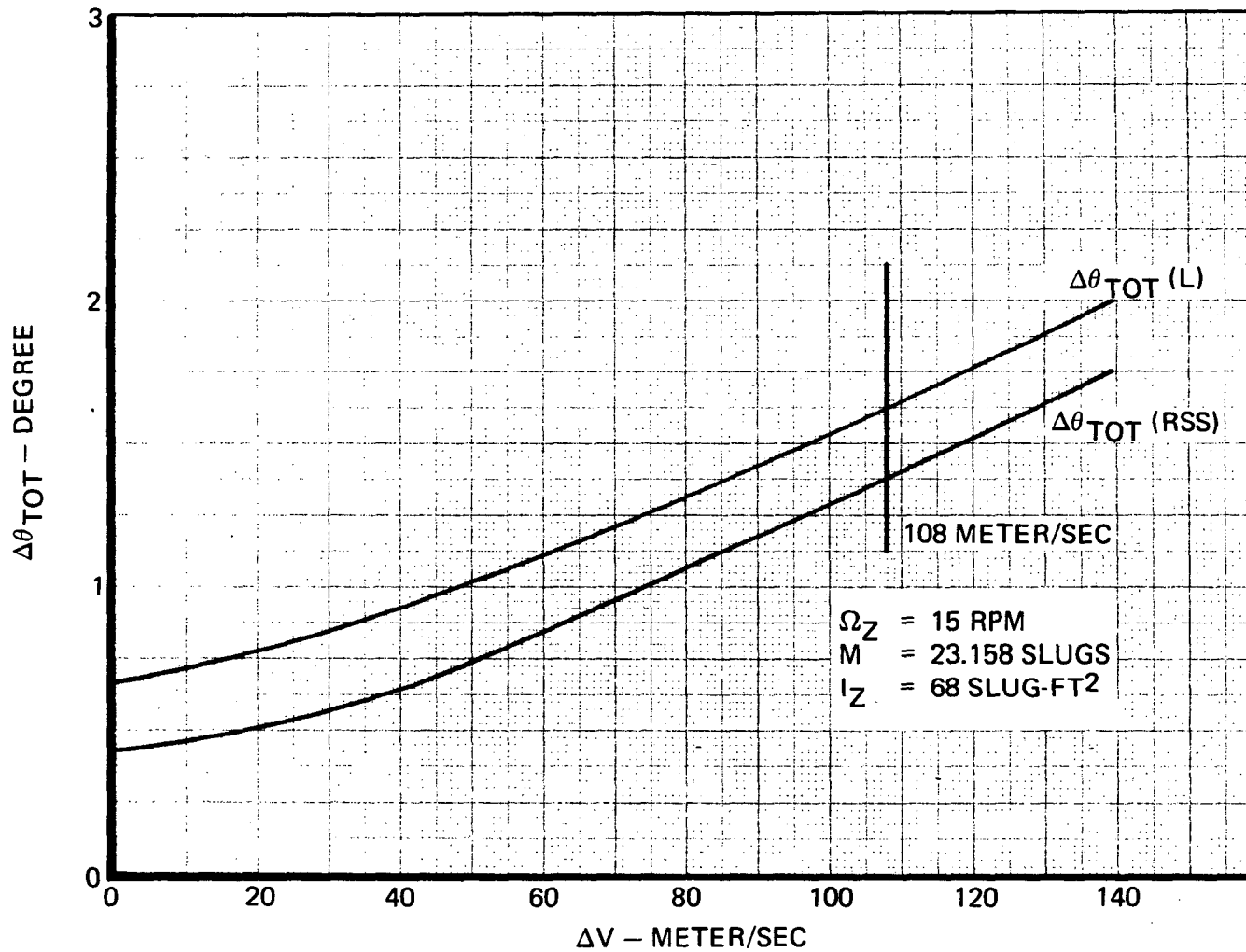


Figure 2-14. ΔV IMPULSE DELIVERY DIRECTION ACCURACY DATA FOR ORBITER MIDCOURSE ΔV

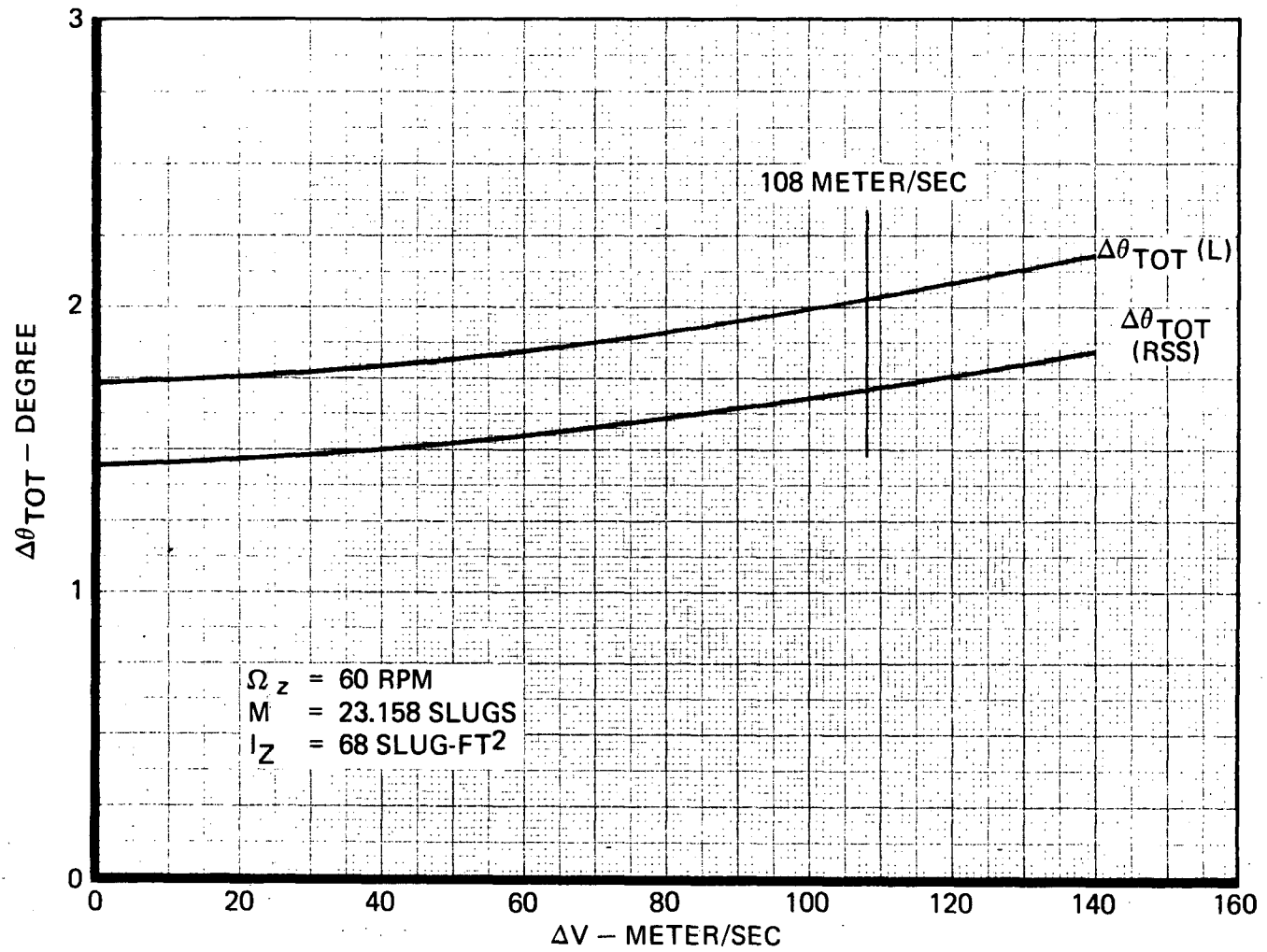


Figure 2-15. ΔV IMPULSE DIRECTION ACCURACY DATA FOR ORBITER MIDCOURSE ΔV

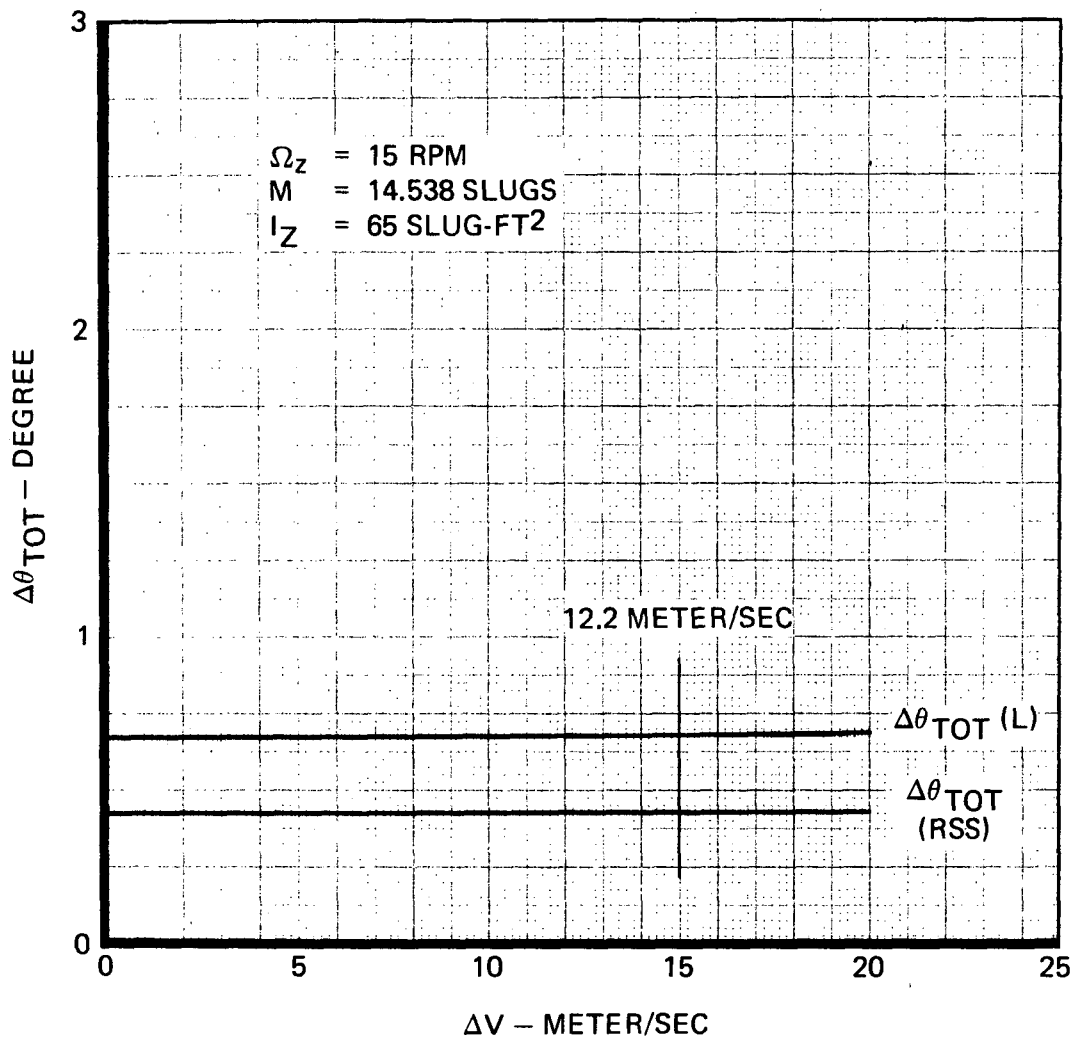


Figure 2-16. ΔV IMPULSE DELIVERY DIRECTION ACCURACY DATA FOR PERIAPSIS REDUCTION (BEGINNING MANEUVER)

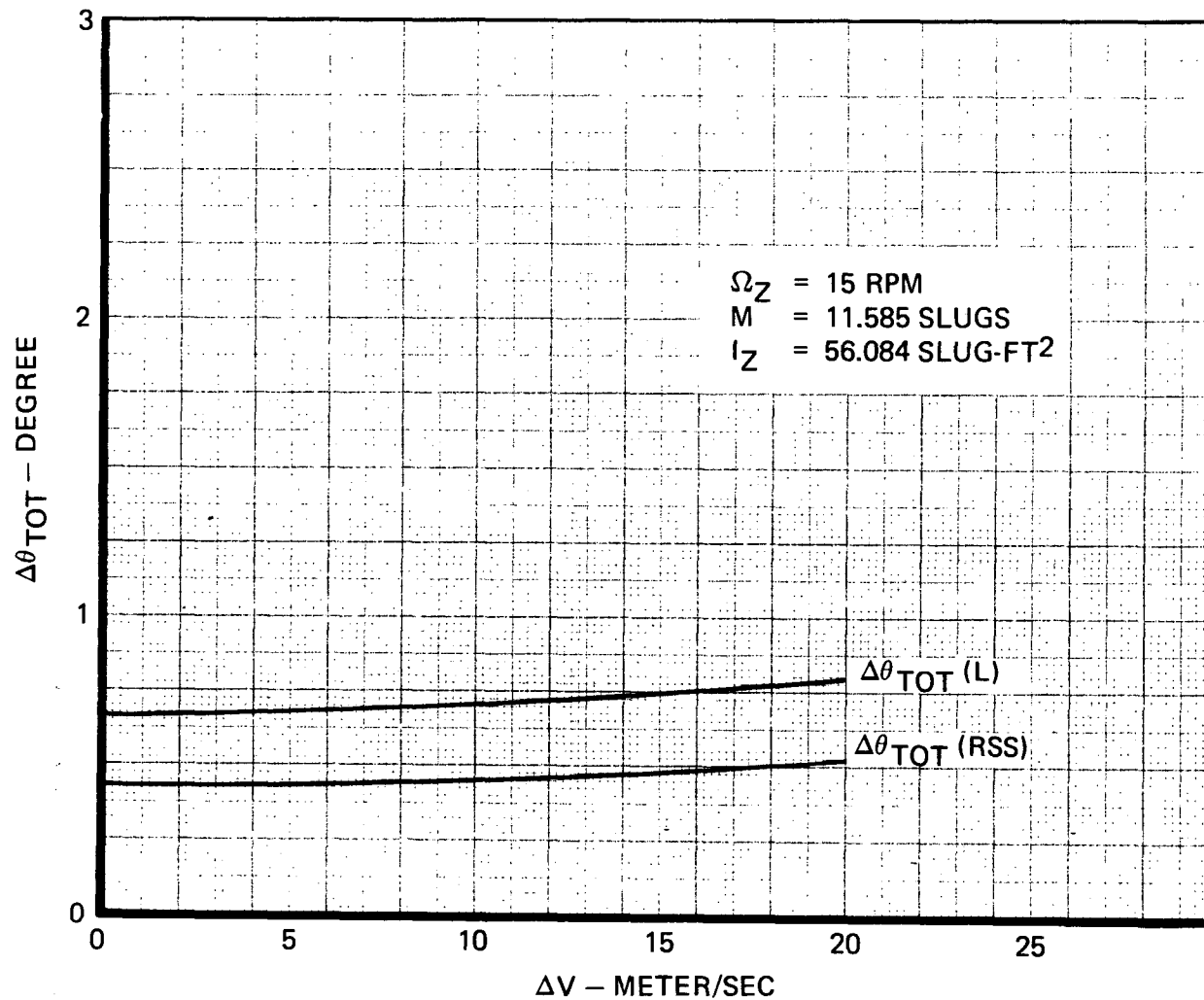


Figure 2-17. ΔV IMPULSE DELIVERY DIRECTION ACCURACY DATA
FOR ORBITER PERIAPSIS REDUCTION (END MANEUVER)

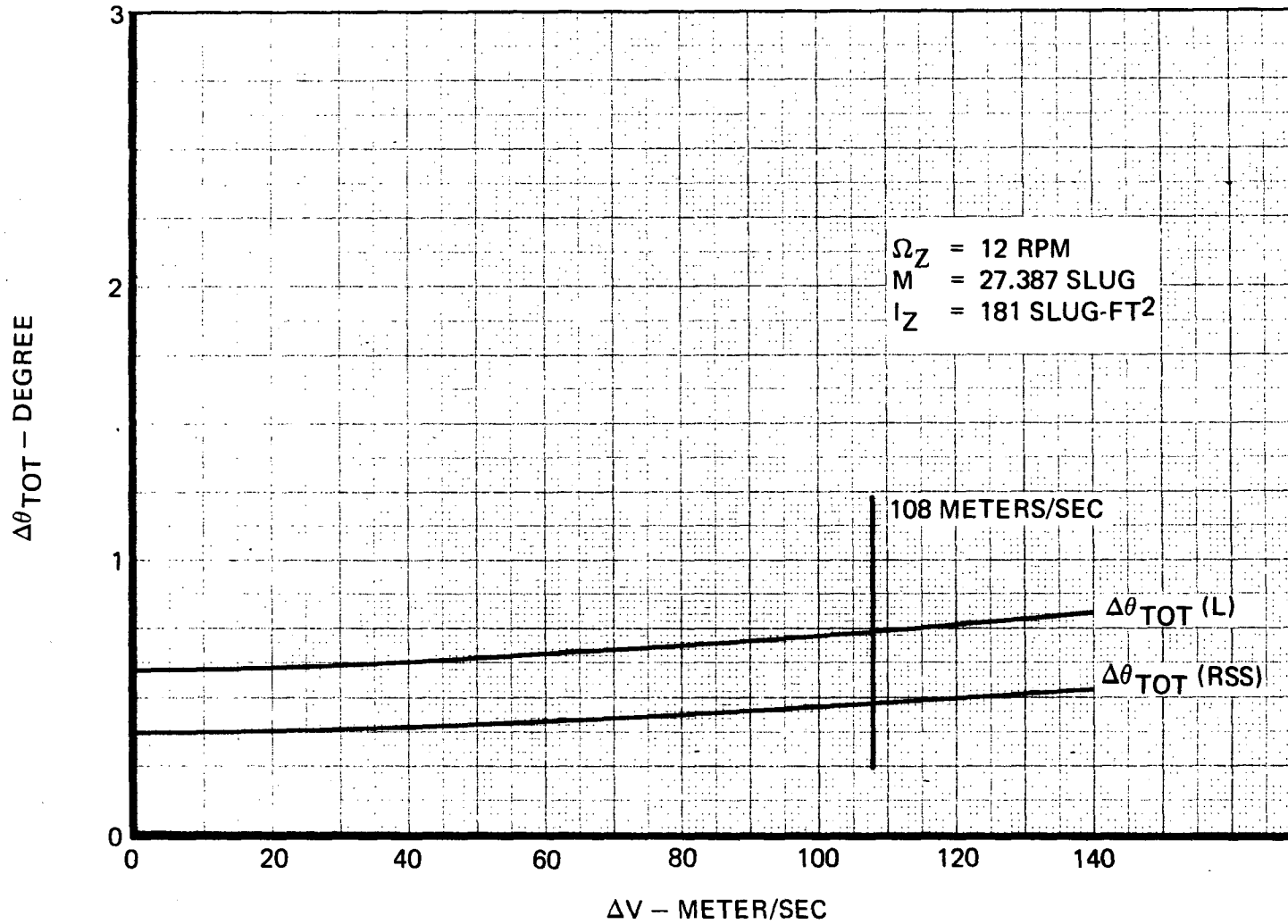


Figure 2-18. ΔV IMPULSE DELIVERY DIRECTION ACCURACY DATA FOR PROBE MIDCOURSE ΔV

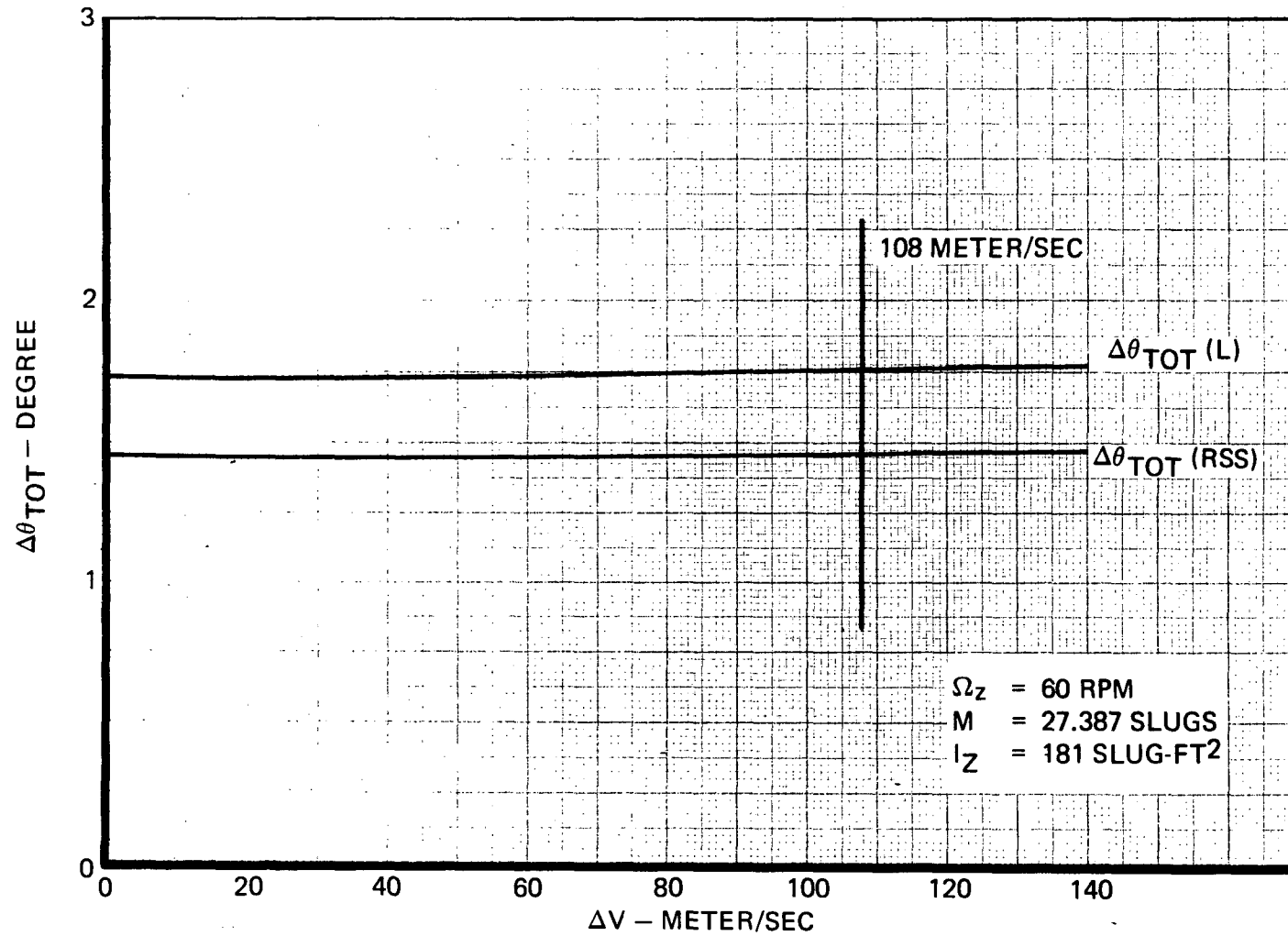


Figure 2-19. ΔV IMPULSE DELIVERY DIRECTION ACCURACY DATA
FOR PROBE MIDCOURSE ΔV

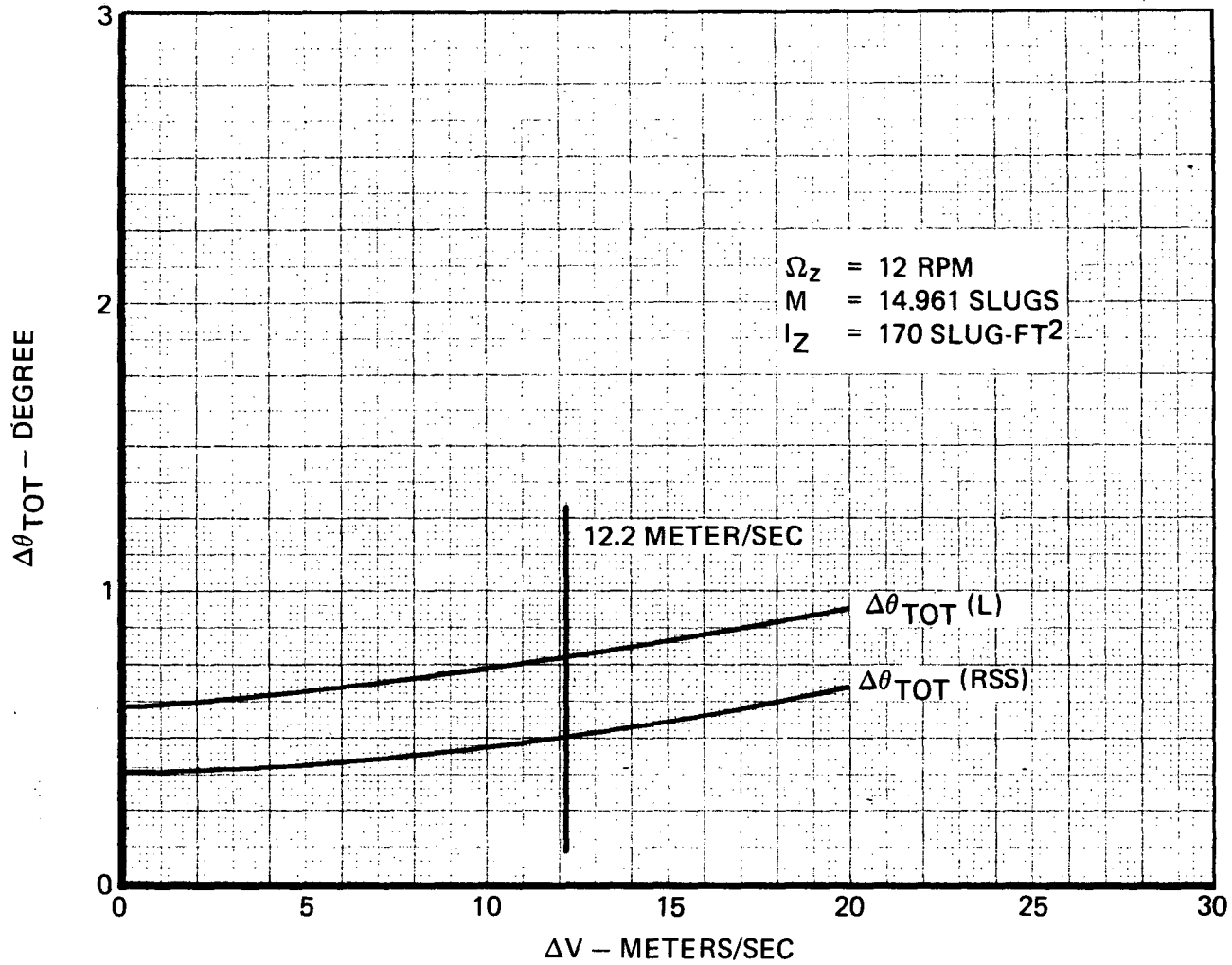


Figure 2-20. ΔV IMPULSE DELIVERY DIRECTION ACCURACY DATA FOR PROBE TARGETING BEFORE SPIN-UP

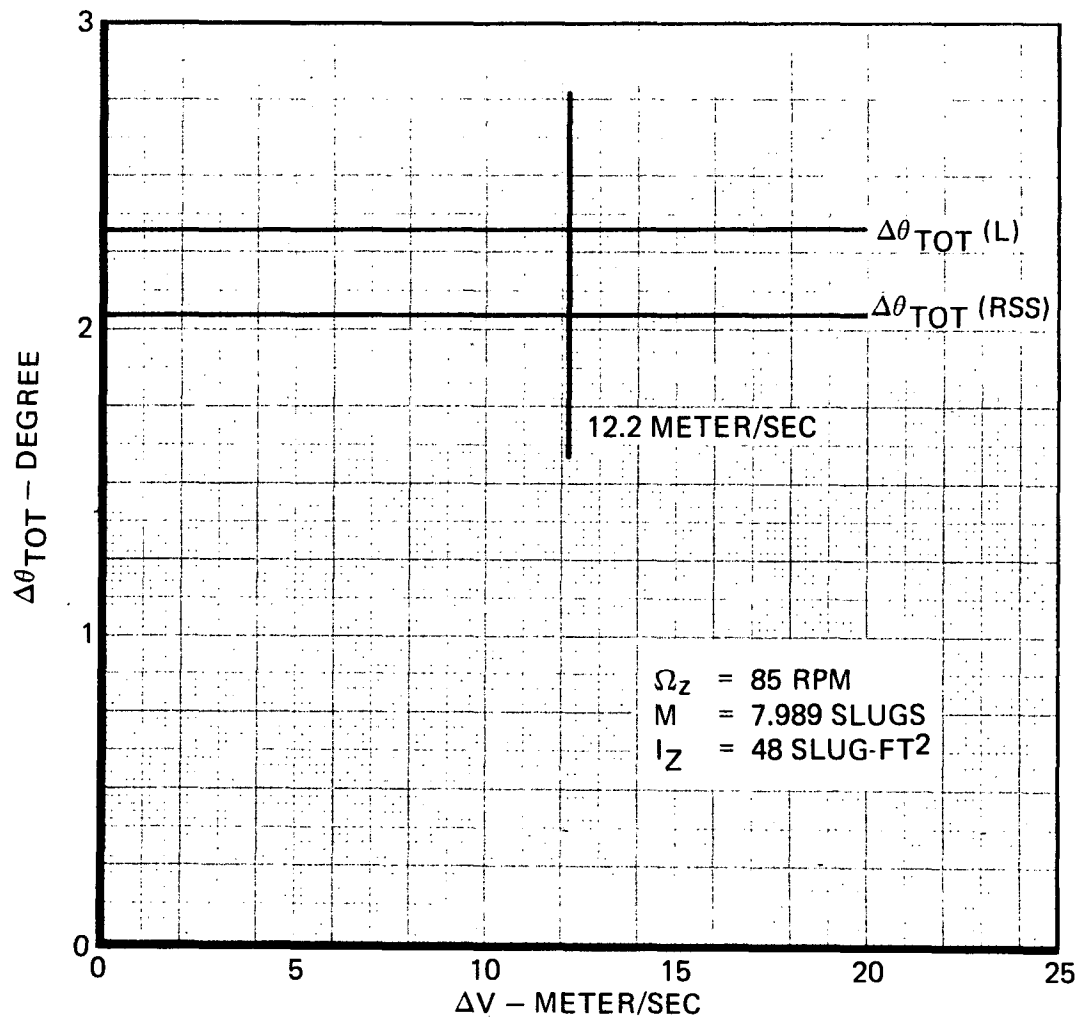


Figure 2-21. ΔV IMPULSE DELIVERY DIRECTION ACCURACY DATA FOR PROBE LATE MISSION ΔV RETARGETING AFTER MINI PROBE RELEASE

Table 2-16. ONE ENGINE OUT EFFECTS ON CONFIGURATIONS B AND F

Spacecraft	$I_o(\Delta V)$ (lbf-sec)	Ω_z (rpm)	I_z (slug-ft ²)	M_z (slug-ft ² /sec)	$\Delta\theta$ (about x degrees)	Allowed $\Delta\theta$ (deg)	Allowed ΔV (m/second)
Orbiter	8198	15	68	106.8144	117.287	7	6.44
Orbiter	8198	60	68	427.2576	29.322	7	25.76
Probe	9695	12	181	227.4518	28.938	7	26.10
Probe	9695	60	181	1137.2592	5.788	7	130.50

The orbiter, rotating at 15 rpm, would clearly be in trouble if an engine failed closed at the beginning of the maneuver. If the orbiter were spinning at 60 rpm, a preprogrammed velocity change of 30 m/sec could probably be executed satisfactorily.

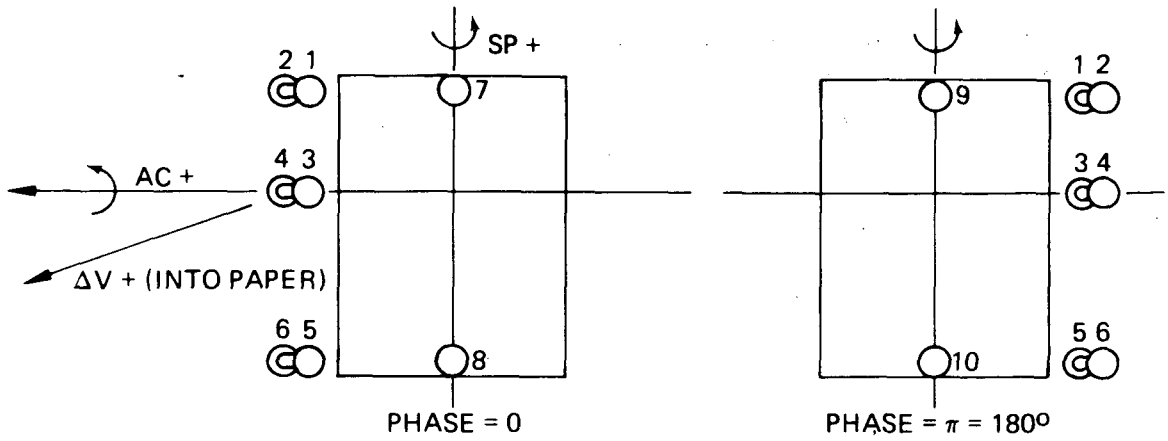
Engine out disturbance effects on spin rate for the C and D-2 configurations may be evaluated in terms of spin rate change. In particular, the delivery of one-half of the orbiter's 108 m/sec velocity change midcourse correction impulse through one engine nonopposed would produce a spin rate change of 1,264 rpm. For the probe, a similar circumstance would produce a spin rate change of 562 rpm.

2.2.7 Attitude and Spin Control Motor Mounting Configuration Flexibility

The criteria and analysis results discussed above clearly support the Configuration B and F ΔV motor mounting approach, which is to mount one radially firing thruster immediately below (about 0.0105 foot) the lowest predicted point of center of gravity excursion and the other motor 0.0105 foot above the highest predicted point of center of gravity excursion in order to minimize the radius arm through which the uncertainty torques can act to change the spin axis attitude or spin rate. The number 0.0105 foot is computed as the sum of the center of gravity uncertainty along Z, the motor mounting uncertainty along Z, and the effect of motor mounting angular uncertainty. Deviation from this criteria will produce an engine configuration that is more susceptible to "engine-out" type failure and is not capable of executing a single uninterrupted ΔV maneuver of at least 100 ft/second.

After the criteria for selecting mounting positions for the ΔV motors are firmly established, the mounting locations for the attitude control and spin motors must be chosen. In general, it can be stated that the torque arm lengths should be maximized to minimize the propulsive impulse (lbf-sec) required to deliver the needed torque impulse (lbf-ft/sec) and that the motors should be mounted to minimize the cross coupling effects discussed above. A third criterion to be considered is the flexibility of a particular mounting arrangement with regard to the number of motors required to produce attitude control, spin plus, and spin minus maneuvers.

In order to determine the flexibility of various designs, an exercise was made to determine all possible effects of a motor firing. Figure 2-22 shows the results of such an exercise.



MOTOR FIRING NO.		$\Delta V +$	$\Delta V -$	AC +	AC -	SP +	SP -
0	π			PRIME	BACKUP		
1		X ⁽¹⁾		X			X
	1		X		X		X
3		X					X
	3		X				X
5		X			X		X
	5		X	X			X
7		X		X			
	7		X		X		
8		X			X		
	8		X	X			
2			X		X	X	
	2	X		X		X	
4			X			X	
	4	X				X	
6			X	X		X	
	6	X			X	X	

(1) X INDICATES MOTOR FIRING

Figure 2-22. ATTITUDE AND SPIN CONTROL THRUSTER STUDY

A review of the data shows that motors 1 and 6 or 2 and 5 taken in pairs, each will provide four primary functions, as follows: attitude control plus, attitude control minus, spin plus, and spin minus. When all four engines are available for use, $\Delta V+$ and $\Delta V-$ can also be performed as a backup to the primary ΔV motors.

In contrast, motors 7 and 8 in Figure 2-22 can be used to perform attitude control plus or attitude control minus only, and motors 3 and 4 can be used for spin plus and spin minus only. As a consequence, the (1, 6) and (2,5) engine pairs provide complete redundancy in the execution of attitude and spin control using only four motors. Configuration F required twice as many motors to accomplish the same task.

2.2.8 Vehicle Dynamics Study Conclusions and Configuration Selection

Configuration selection and performance predictions for the preferred configuration are two prime goals of the vehicle dynamics study. As has been stated previously in this section, Configuration B was selected as superior to other configurations originally proposed and to the performance baseline configuration, F, evolved for this study. The reasons for this are as follows:

- a. The ΔV motor arrangement consists of two radially firing thrusters placed along the Z axis immediately above and below the highest and lowest points of the center of gravity's anticipated excursions during the mission. As a result, one of the two motors is always placed as closely as possible to the center of gravity during the ΔV maneuver phases of the mission, which occur during cruise and late in the mission for both the orbiter and probe.
- b. The attitude and spin control motor assemblies consist of two sets of two motors each. Each set includes a forward facing motor placed above (below) the center of gravity at the greatest possible distance from the center of gravity and a rearward facing motor placed below (above) the center of gravity at the greatest possible distance available for mounting. As a result, the attitude control moment arm is maximized. Because the two motors are mounted tangentially with Y coordinate values of 2.196 feet, either set of motors can execute attitude control positively or negatively about any axis and spin control positively or negatively.

The effects produced by these arrangement characteristics are as follows with respect to the selection criteria:

Criterion	Relative Position of Configuration B
ΔV max (early and late mission)	Superior to all ⁽¹⁾ , because of close coupled upper and lower motor mounting positions
Total usable weight	Superior to all ⁽²⁾ , because of minimal ΔV cross coupling into attitude and spin effect areas
Total usable fuel plus thruster weight	Superior to all, because of minimal cross coupling and minimum thruster quantity requirement

Criterion	Relative Position of Configuration B
Thrust vector directional delivery accuracy	Superior to all ⁽¹⁾ , because of minimal ΔV motor cross coupling
Single engine out Sensitivity during ΔV maneuver	Superior to all ⁽¹⁾ considering both cruise mode and late mission maneuver requirements, because of ΔV motor close coupled mounting approach
Number of engines required	Equivalent to all except A, E and F ⁽³⁾

- (1) Equal to performance of baseline system, F.
- (2) Slightly inferior to F
- (3) The gimbale engine configurations required fewer motors (only 6), but were eliminated from the competition for other reasons. The F configuration requires 12 motors.

In order to more fully appraise the findings of this study, the deficiencies of the nonoptimum systems are discussed below.

Configuration F – Configuration F was defined during the course of the study as the effects of engine mounting location on ΔV_{\max} and cross coupling torques became clear. From the point of view of maximizing ΔV_{\max} and minimizing cross coupling, F is optimum; however, it requires four more engines than any other configuration considered.

Configurations A and E – These two configuration concepts employ a single radially firing gimbale engine with thrust vector always pointed through the center of gravity for ΔV maneuvers. The gimbale engine configurations were rejected for several reasons, the prime one being that the large center of gravity excursion of about 1 foot on the probe would require the engine to rotate through a total angle of 26 degrees, i.e., ± 13 degrees, which grossly exceeds the specified spacecraft-sun line/spacecraft spin axis, included angle allowed variation range of ± 6 degrees (maximum). The gimbale motor concepts were also rejected because of limited qualification status for the gimbal mechanism in the preferred engine size; because of additional thrust vector pointing inaccuracies associated with this system; and because of the additional continuous attitude correction requirement associated with gradually rotating the spacecraft to maintain thrust vector direction, as the center of gravity moves.

Configuration C – This arrangement suffers for the following reasons:

1. The ΔV motors fire tangentially rather than radially, thereby potentially producing a large cross coupling into the spin mode.
2. The lower set of ΔV motors is located too far below the center of gravity for satisfactory late mission ΔV delivery on the probe.
3. The attitude control moment arm is not maximized. If it were, the upper set of ΔV motors would have to be placed too far above the center of gravity for late mission orbiter cruise mode ΔV maneuvers.

Configuration D-1 – In this arrangement, the lower ΔV motor is too far below the lowest point of center of gravity excursion for the early orbiter mission maneuvers and for the late probe mission

maneuvers. The upper ΔV motor is satisfactory for late mission orbiter maneuvers and early mission probe maneuvers. The D-1 configuration is also deficient because the attitude control torque arm is not maximum.

Configuration D-2 – The upper set of ΔV motors, which delivers most of the velocity correction impulse, fires tangentially, thereby producing a significant cross coupling into spin as in the case of Configuration C. Because the lower ΔV motor (also used for attitude control) is located at the lowest possible mounting point and the upper attitude control motor (which is also used for late mission orbiter ΔV) is located at the highest possible mounting point, the orbiter cruise ΔV suffers somewhat and the late mission orbiter ΔV suffers excessively. Similarly, the probe cruise suffers somewhat relative to B or D-2 and the late mission probe ΔV 's suffer excessively.

Because of the relatively large spin rate proportional error produced in the direction of delivery of velocity correction impulse bits, especially during the late probe mission when $\Omega_Z = 85$ rpm, it will be necessary to take one or more of the following actions:

- a. Relax the existing ± 0.5 -degree ΔV maneuver mean directional accuracy requirement
- b. Conduct the ΔV maneuver in a series of small ΔV steps
- c. Correct uncertainty effects by:
 1. Calibrating out fixed uncertainties
 2. Monitoring and compensating time varying uncertainties on board the spacecraft.

2.2.9 Sensitivity of Conclusions to Assumptions

The various assumptions made were reviewed to determine their impact on the conclusions. Critical assumptions were those relating to the magnitude and character of the thruster impulse bit repeatability and the worst-case method of combining errors. Other assumptions relating to errors in thruster and center of gravity location and pulse centroid repeatability are, within reasonable limits, of secondary importance. These factors tend to increase or decrease the values of ΔV_{\max} somewhat but have little impact on the relative ranking of the candidate configurations. As shown in Tables 2-5 and 2-6 for Configuration B, use of an RSS method on combining error effects tends further to suppress the effects of the small errors and results in general in an increase in ΔV_{\max} of in the order of 60%. The same general trend would be true for the other configurations. This leaves the assumptions relating to impulse bit repeatability as a major factor in differentiating between the various candidates.

Impulse bit nonrepeatability was assumed to have a constant value of $\pm 5\%$. While this is a very simple characterization, it is adequate to permit a valid comparison of the candidate configurations. Nonrepeatability of impulse bits typically increases with decreasing pulse width. While the 5% value is felt to be attainable, it is nevertheless an optimistic goal considering engine-to-engine variations and the gross difference in pulse widths and duty cycles required of upper and lower ΔV engines. This is particularly true for the C and D-1 configurations, where the duty cycle differences between upper and lower engines are greatest. As discussed paragraph 4.1.2.3, the lower thrusters in a C configuration installation may be required to deliver a single minimum impulse bit (24.4 milliseconds) for every 14 nominal (586 milliseconds) pulses of the upper engines.

The effect of reducing the assumed impulse nonreproducibility to 2.5% was also evaluated as shown in Tables 2-5 and 2-6. This might be achieved with careful engine matching but would be difficult to verify experimentally in engine acceptance tests. For the B configuration this is shown to have a beneficial effect of increasing ΔV_{\max} for torques about some axes, not necessarily, however, those that are limiting. For the other configurations with large moment arms about the center of gravity, the increase in begin with. In order to make the C configuration comparable to the B configuration with regard to precessional disturbances, a reduction in impulse nonreproducibility of approximately an order of magnitude would be required.

It might be postulated that with careful engine matching, in-space calibration, and assuming a normal statistical distribution of per pulse total impulse in a long train of engine pulses, that an effective improvement in reproducibility of the mean impulse bit of this order could be attained. This is based on the fact that the standard deviation of the mean of a sample from the mean of the total population decreases inversely as the square root of the sample size. Examination of actual engine pulse mode test data indicates that although there is a trend in this direction, the impulse bit sizes are not normally distributed. The thrusters can operate at a quasi-stable level for one sequence of highly reproducible pulses and then shift to another level for subsequent pulses. This mode of operation is attributed to bistability in injector and orifice flow and variations in decomposition fronts within the catalyst bed. Operation of this type could lead to worst-case error torques of the type assumed in the dynamics analysis.

Because of the uncertainties involved in impulse predictability, the approach of using a worst-case analysis and selecting the thruster arrangement least sensitive to induced errors is felt to provide minimum program risk.

2.3 CONTROL RATES

2.3.1 Attitude/Spin Control

In order to determine the most suitable thrust levels from the discrete choices available and to establish the validity of the specified requirements as they relate to the candidate configurations, attitude/spin control rates and resolution were investigated.

2.3.1.1 Attitude Control

Precession functions are performed by pulsing opposed pairs of thrusters to minimize ΔV dispersions. Precession rate is determined by firing time per revolution and number of revolutions per second. Resolution is fixed by the minimum orientation change for each pulse from the thruster pair. The relationship between these variables is presented in Figure 2-23. It is evident from the curve that the required resolution cannot be met at the precession rates specified for large attitude changes at the 12-rpm spin rate. A final vernier correction at a lower rate will be needed to provide the required resolution. At the spin rate of 15 rpm it is marginally possible to satisfy both the rate and resolution requirements with a single pair of thrusters as shown in the figure.

Precession rate is presented as a function of thrust level for the orbiter and probe spacecraft in Figures 2-24 and 2-25. Nominal cruise conditions used were moments of inertia of 68 slug-ft² and 181 slug-ft² and spin rates of 15 rpm and 12 rpm for the orbiter and probe configurations

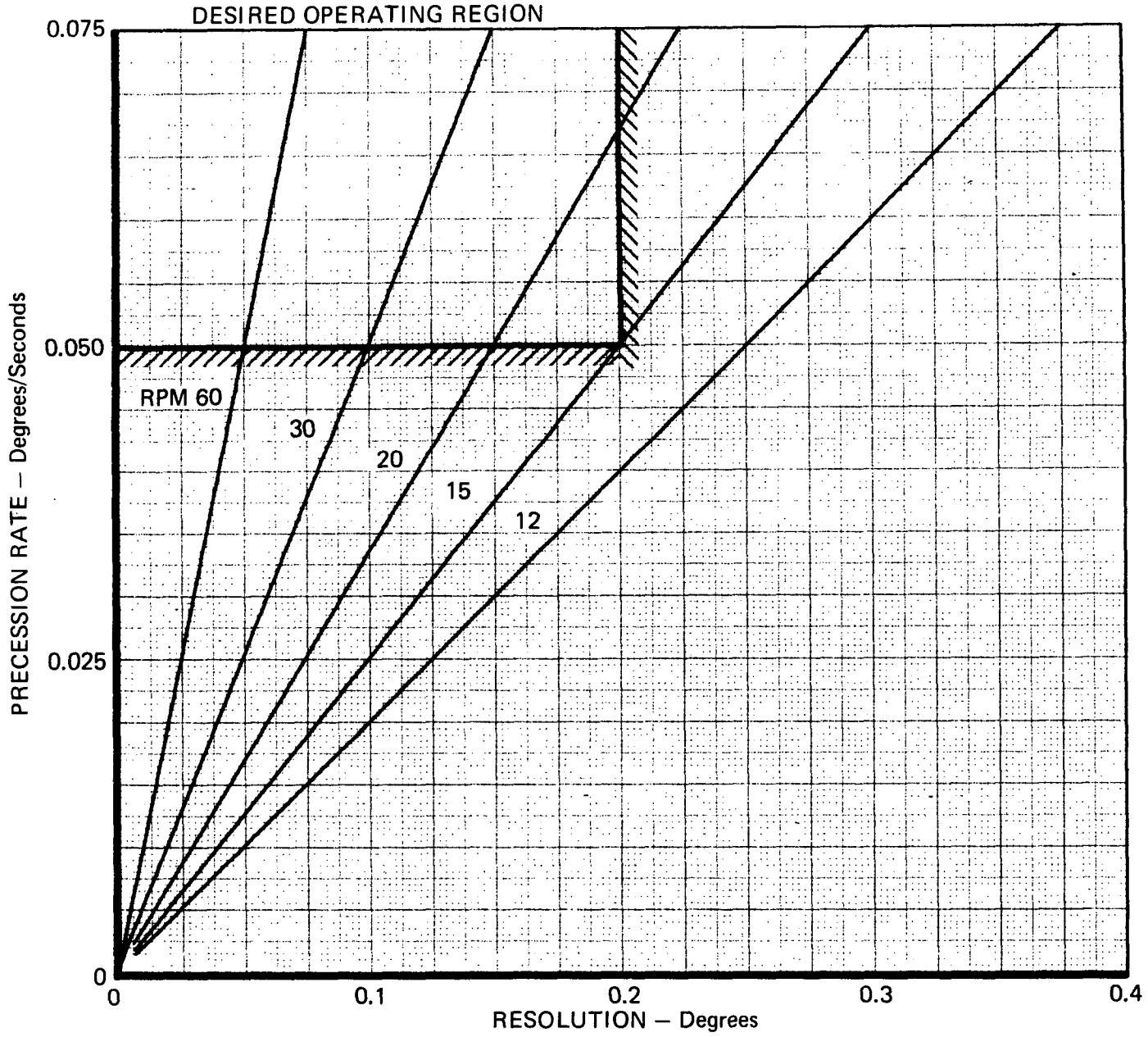


Figure 2-23. PRECESSION RATE VS RESOLUTION

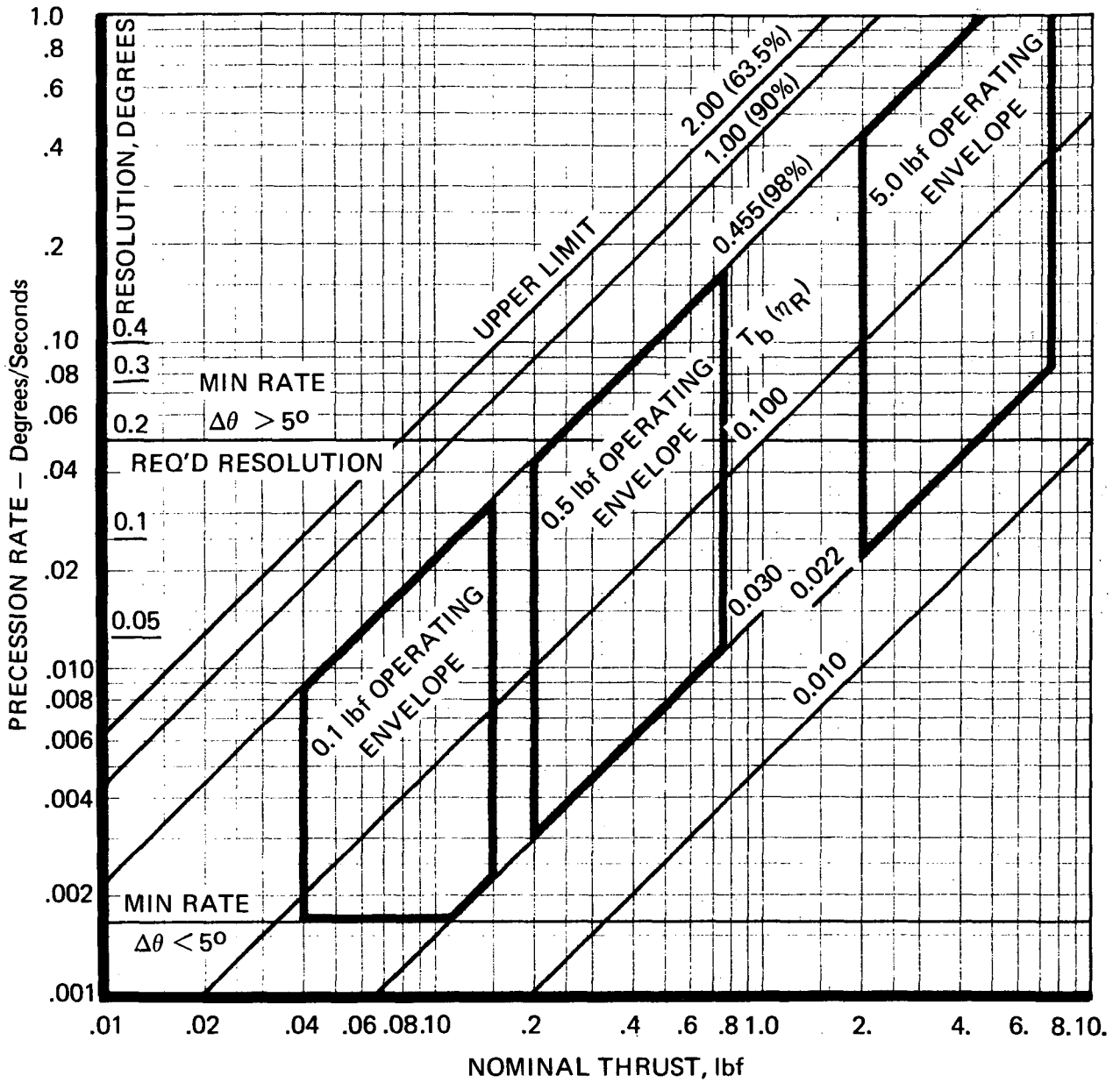


Figure 2-24. ATTITUDE CONTROL — ORBITER VEHICLE
 ($I = 68 \text{ SLUG-FT}^2$, $\omega = 15 \text{ rpm}$)
 (ONE THRUSTER PAIR, 44.88 in. SPACING)

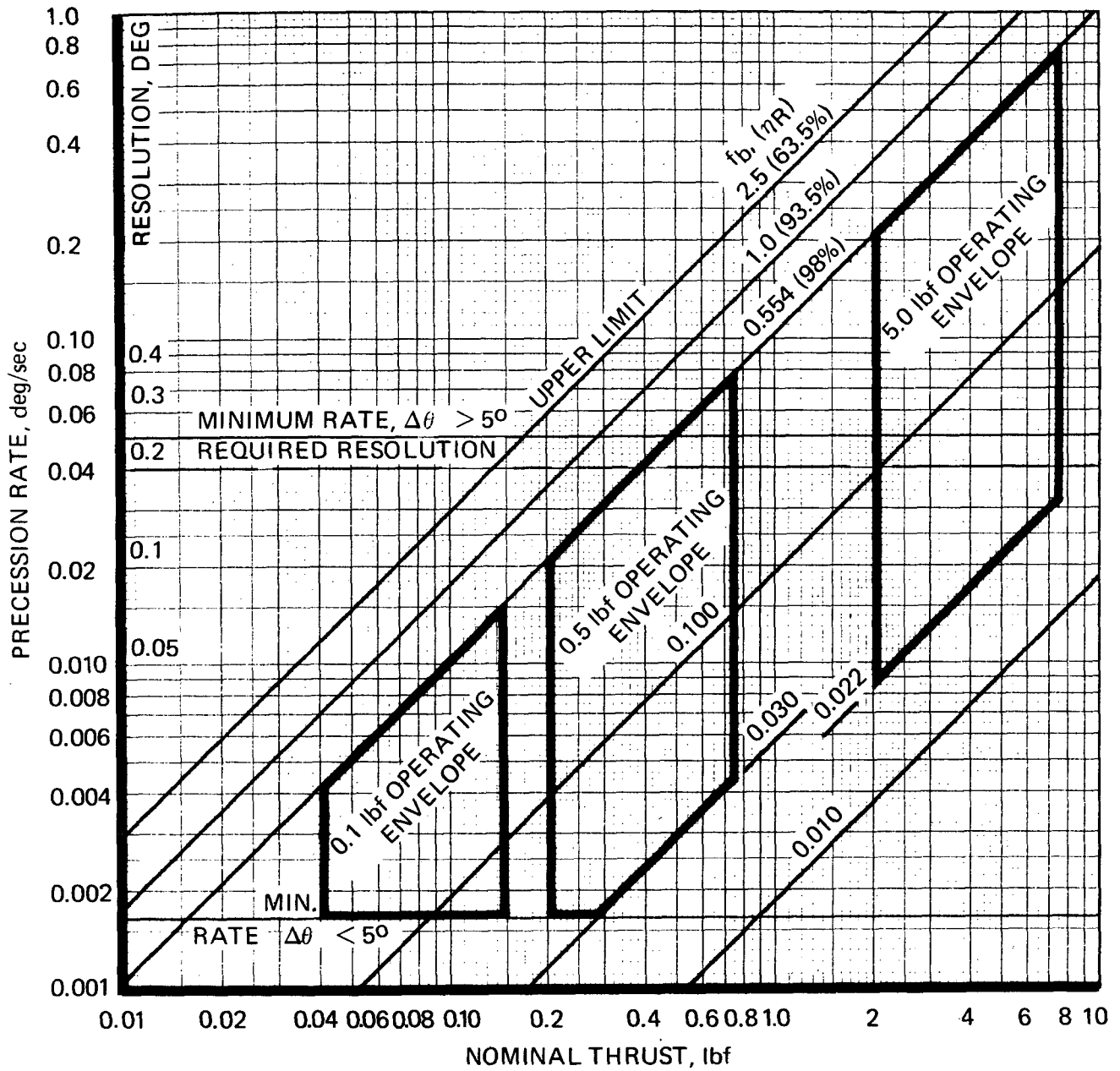


Figure 2-25. ATTITUDE CONTROL – PROBE VEHICLE
 ($I = 181 \text{ SLUG-FT}^2$, $\omega = 12 \text{ rpm}$)
 (ONE THRUSTER PAIR, 44.8 in. SPACING)

respectively. The curves are based on operation of a single pair of precession thrusters. Pulse width and related rotational efficiency along with the resolution are indicated parametrically. In actual use, the pulse width would be rounded off to correspond to the nearest whole number of sectors (a sector being 1/1,024 of a revolution) as discussed in paragraph 4.1. The nominal thrust ranges for thrusters of 5, 0.5, and 0.1-lbf nominal thrust operating over fairly large blowdown ranges are also indicated. These curves define an operating envelope for each of the candidate thrusters in terms of its operating parameters and the resultant maneuver rate and resolution.

An absolute upper limit to this envelope is defined by that pulse width which corresponds to a 180-degree firing sector angle (2 seconds for the orbiter and 2.5 seconds for the probe vehicle). Increasing pulse width beyond this value results in reducing precession rate. A more practical limit is, however, defined by that pulse width which corresponds to the design value of rotational efficiency of 98%. This is also indicated on the figures.

The lower limit of the envelope of thruster operation is defined by the smallest pulse width that gives acceptable reproducibility. This is assumed to be 30 milliseconds except for the MR-50 5-lbf thrust engine which has undergone extensive qualification testing at 22-millisecond pulse widths. Should this minimum pulse width result in precession rates below the minimum specified for small angle changes, the lower limit of the operating envelope is considered to be defined by that pulse width which ensures meeting the minimum rate over the thruster blowdown range.

As shown in Figure 2-24, the 0.5-lbf thrust level is near ideal for the orbiter mission in that it is able to maintain the minimum precession rate to the end of its blowdown range when operating at the 0.455-millisecond pulse width which corresponds to the design rotational efficiency. The resolution requirement can be accommodated over the entire blowdown range with pulse widths in excess of 100-millisecond duration. For the 5-lbf thruster, on the other hand, pulse widths of slightly over 10 milliseconds would be required to meet the resolution requirement at the upper limit (over 4.5-lbf thrust) of the blowdown range. In order to meet the requirements with a 5-lbf (nominal) thruster, the thrust/blowdown schedule must be such that the initial thrust level is less than approximately 4.5 lbf. A reduced moment arm could of course produce less torque for a given thrust level. The precession rate requirement, of course, presents no problem at these thrust levels. The 0.1-lbf thruster, while able to deliver impulse bits corresponding to resolution meeting the specified value, cannot meet the minimum precession rate requirement at any point in its blowdown range. Active use of both the primary and backup thruster pairs can be used to double the precession rate without reducing resolution. Longer pulse width with corresponding reduction in efficiency can also be considered. Use of these approaches will still not enable a system of 0.1-lbf thrusters to meet the specified precession rate over the entire blowdown cycle.

For the probe spacecraft, because of its higher moment of inertia, only the 5-lbf thruster can satisfy both requirements over its entire operating range. The 0.1-lbf thruster cannot meet the minimum rate requirement for large angle changes at any point in its operating envelope. For the 0.5-lbf thrust engine, increased pulse width or use of both thruster pairs would be necessary to provide the minimum rate over most of the thrust range or both could be used to cover the entire range. It should be noted that the lower part of the thrust blowdown cycle should correspond to the latter part of the mission when spacecraft moment of inertia is reduced by consumption of propellant and/or probe release.

2.3.1.2 Spin Control

Spin control was also investigated for the range of thrust levels considered for attitude control. Maximum spin rates of change (continuous firing) for the probe and orbiter are shown in Figure 2-26. Minimum rates (without ΔV disturbance) are obtained by firing minimum impulse bits 180 degrees apart. These rates, for 30-millisecond pulses, are also shown on the curve. These rates are averaged over the period of rotation; hence, the incremental change in spin is numerically equivalent to four times the minimum rate shown for the orbiter and five times that shown for the probe. A pair of 5-lbf thrusters can provide the desired spin change rate over its entire blowdown range. The minimum incremental change requirement (0.25 rpm) can also be met. The 0.5-lbf thruster as well as the 0.1-lbf thruster can provide the required resolution; however, the specified rate change is met only by the 0.5-lbf engine at the initial phase of the blowdown cycle for the orbiter spacecraft. Since it is also required that these rates and resolution requirements be met in the secondary (one-engine-out) mode, it is evident that only the 5-lbf (nominal) thrust engine can be considered for those configurations providing spin control initially with a two-engine couple. For a single engine, a minimum thrust of approximately 3 lbf is necessary to meet the spin rate change requirement for the probe vehicle in its cruise configuration. This means the spin thruster pairs must begin their blowdown at a thrust near the 7.5-lbf level or blowdown ratio be limited. At this level the minimum incremental rate change requirement is just met.

2.3.1.3 Summary and Conclusions

Control rate and resolution limits for the nominal operating ranges of the three candidate thrusters are summarized in Table 2-17. These data are based on the maximum moment arms that can reasonably be accommodated by the spacecraft bus, assuming a single pair of thrusters providing a control couple and a 2.5:1 thrust blowdown ratio. Specification values are also given in the table and noncompliance indicated by underlining the appropriate entry. The spin rate change, already one of the more difficult requirements to meet, would be halved for degraded mode (one-thruster-out) operation.

Table 2-17. ATTITUDE/SPIN CONTROL PERFORMANCE LIMITS

	Nominal Thrust Level					
	5 lbf		0.5 lbf		0.1 lbf	
	Orbiter	Probe	Orbiter	Probe	Orbiter	Probe
Precession resolution, deg. (Specification: 0.2 max.)	<u>0.33</u>	0.15	0.044	0.022	0.009	0.008
Precession rate, deg/sec. (Specification: 0.05 min.)	0.43	0.21	<u>0.043</u>	<u>0.021</u>	<u>0.009</u>	<u>0.004</u>
Spin rate resolution, rpm (Specification: 0.25 max.)	0.2	0.1	0.02	0.01	0.01	0.01
Spin rate change, rpm/sec (Specification: 0.33 min.)	1.2	0.4	<u>0.12</u>	<u>0.04</u>	<u>0.02</u>	<u>0.01</u>

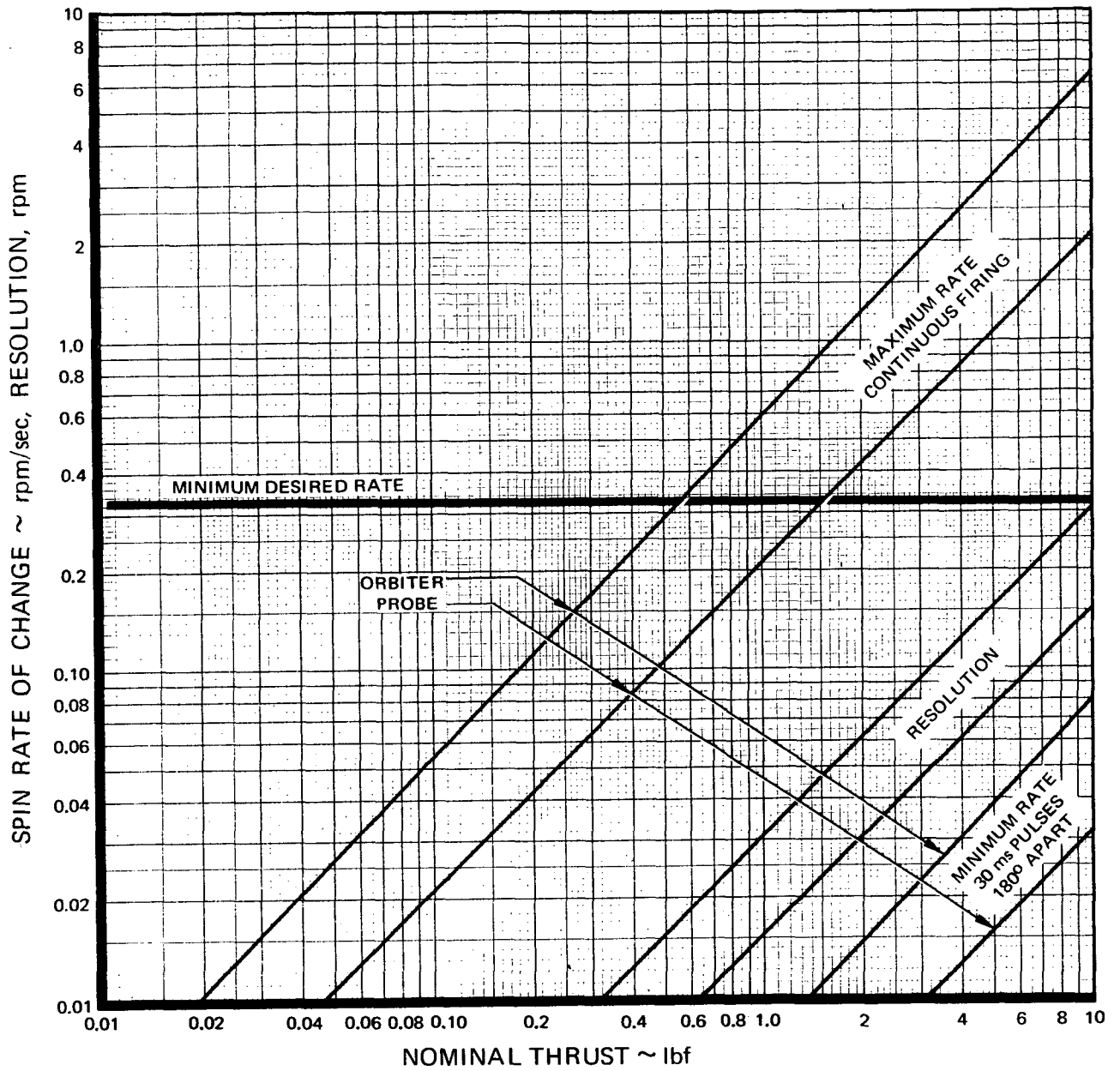


Figure 2-26. SPIN RATE OF CHANGE VS THRUST
(ONE THRUSTER PAIR)

For precessional control, the acceptable range of thrust levels is approximately 0.5 to 5 lbf. Thus, the 0.1-lbf thruster and the 0.5-lbf thruster (unless uprated to provide 0.4- to 0.5-lbf thrust at the end of its blowdown cycle) are inadequate if all current requirements are to be met. Satisfactory use of the 5-lbf thruster will depend on limiting the initial thrust for use on the orbiter vehicle to between 4 and 5 lbf. The use of thrusters at an initial thrust of 7.5 lbf and limited in blowdown to 2.5 can be used to meet the spin control requirements for both the orbiter and probe vehicles in both primary and degraded mode operation. Somewhat lower initial thrusts and larger blowdown ranges could, of course, be used for the orbiter vehicle only.

Control parameters for the candidate configurations and at various thrust level combinations are given in Table 2-18. Specification requirements are noted and noncompliance indicated by underlining the appropriate entry. Attitude resolution of 0.22 degree and a spin rate of change of 0.32 rpm/sec may be considered acceptable, although the specified values are 0.20 maximum and 0.33 minimum, respectively. These requirements could be met by slightly lowering the initial thrust or increasing moment arm for orbiter missions and slightly limiting blowdown ratio for probe missions. The latter may not be necessary, since vehicle moments of inertia are reduced by probe release as the engine nears the low thrust end of the blowdown cycle.

The data of Table 2-18 show that none of the thruster arrangements allow Configuration A to meet all the requirements. This is due primarily to the limitation on minimum pulse width (0.022 sec) and the fact that the attitude control couple is comprised of three engines. The shorter moment arm helps the attitude resolution situation somewhat; however, a propellant weight penalty is incurred.

For the remaining configurations, all the requirements can be met through the use of all 5-lbf nominal engines with feed pressure schedules adjusted to provide an initial thrust of 7.5 lbf for the probe mission and approximately 5 lbf for the orbiter mission. Thrust blowdown ratio must be limited to about 2.5. Lower blowdown ratios and lower initial thrusts are practical as discussed in paragraph 4.1.

In the case of Configuration C, tangential doublets, it is possible to use a system of all 5-lbf nominal initial thrust engines for both missions. This is based on the assumption that three thrusters would be available for spin control in the secondary (one-engine-out) mode. If the failure is such that half the system is permanently isolated and inoperative, the different thrust schedule approach for the orbiter/probe is the only technique that will enable meeting all requirements.

In the case of Configuration D, rectangle, two other possibilities exist. These are where the tangential thrusters have an initial thrust of 7.5 lbf (5 lbf could be used for orbiter missions only), and the radial thrusters are 5- or 1-lbf initial thrust units. Operation of the same basic thrusters from the same feed system at considerably different thrust levels, although feasible through the use of trim orifices, is somewhat undesirable due to the obvious feed pressure discrepancy. The other approach requires uprating the 0.5-lbf thruster to 1 lbf. Although this uprating is currently underway on an existing program, this approach also suffers from feed system pressure incompatibility.

**Table 2-18. ATTITUDE/SPIN CONTROL OPERATING PARAMETERS
ORBITER/PROBE DATA**

System	A Gimbal			B Radial Pairs			C Tangential Doublets			D Rectangle			E Alternate Gimbal		
	All 7.5	All 5.0	Orb 5.0/ Prb 7.5	All ACS 1.0	All ACS 5.0	Orb 5.0/ Prb 7.5	All 1.0	All 5.0	Orb 5.0/ Prb 7.5	Tang. 7.5 Radial 1.0	Tang. 7.5 Radial 5.0	Orb 5.0/ Prb 7.5	All ACS 1.0	All ACS 5.0	Orb 5.0/ Prb 7.5
Thrust levels*	All 7.5	All 5.0	Orb 5.0/ Prb 7.5	All ACS 1.0	All ACS 5.0	Orb 5.0/ Prb 7.5	All 1.0	All 5.0	Orb 5.0/ Prb 7.5	Tang. 7.5 Radial 1.0	Tang. 7.5 Radial 5.0	Orb 5.0/ Prb 7.5	All ACS 1.0	All ACS 5.0	Orb 5.0/ Prb 7.5
Attitude resolution, deg (Specification: 0.2 max)	<u>0.45/0.40</u>	<u>0.30/0.17</u>	<u>0.30/0.40</u>	<u>0.06/0.03</u>	<u>0.22/0.10</u>	<u>0.22/0.15</u>	<u>0.06/0.03</u>	<u>0.22/0.10</u>	<u>0.22/0.15</u>	<u>0.06/0.03</u>	<u>0.22/0.10</u>	<u>0.22/0.15</u>	<u>0.06/0.03</u>	<u>0.22/0.10</u>	<u>0.22/0.15</u>
Precession rate, deg/sec (Specification: 0.045 min)	0.44/0.27	0.30/0.17	0.30/0.27	0.09/0.045	0.44/0.20	0.44/0.30	0.09/0.045	0.44/0.20	0.44/0.30	0.09/0.045	0.44/0.20	0.44/0.30	0.09/0.045	0.44/0.20	0.44/0.30
Spin rate resolution, rpm (Specification: 0.25 max)	0.23/0.11	0.15/0.075	0.15/0.11	0.015/0.01	0.15/0.075	0.15/0.11	0.015/0.01	0.15/0.075	0.15/0.11	0.23/0.11	0.23/0.11	0.15/0.11	0.015/0.01	0.15/0.075	0.15/0.11
Spin rate change**, rpm/sec (Specification: 0.33 min)	<u>0.90/0.32</u>	<u>0.60/0.21</u>	<u>0.60/0.32</u>	<u>0.11/0.042</u>	<u>0.60/0.21</u>	<u>0.60/0.32</u>	<u>0.35/0.12</u>	1.8/0.60	1.8/0.90	<u>0.90/0.32</u>	<u>0.90/0.32</u>	<u>0.60/0.32</u>	<u>0.11/0.042</u>	<u>0.60/0.21</u>	<u>0.60/0.32</u>

*Initial thrust: 2/3 max thrust blowdown ratio assumed

**In secondary (single failure) mode if critical

Within the constraints of the specified requirements, the selected candidate configurations and the use of existing thrusters, the best approach appears to be use of 5-lbf (nominal) thrust engines for all attitude/spin control functions; these must, however, be uprated for the probe configuration spacecraft and somewhat derated for the orbiter. Blowdown ratio must be limited to less than 2.5:1.

2.3.2 Velocity Control

In the preceding section it was established that 5-lbf (nominal) thrusters provide the best approach to meeting the attitude/spin control requirements. Few requirements exist which would limit the choice of thrust level for velocity control. The major concern is avoiding excessively long maneuver durations. In view of the desirability of employing only one size thruster and recognizing that in some configurations the attitude/spin control engines would also be used for velocity corrections, the suitability of 5-lbf thrusters for velocity control was investigated. Figure 2-27 presents midcourse maneuver duration as a function of required ΔV and firing sector angle. Using a single 5-lbf (mean thrust over the blowdown assumed to be 4.25 lbf), the duration for a maximum midcourse correction would be approximately 4.4 hours at the 42-degree firing sector angle which corresponds to the design rotational efficiency of 98%. This is well under the 8-hour maximum called out in the specification. For required midcourse corrections less than the maximum, the time required will be correspondingly less. The duration can be further reduced by increasing the firing sector angle. This shows the small corrections in the order of 30 meters/sec can be accomplished in less than 30 minutes. If the excess midcourse propellant is to be retained for additional orbit maneuver capability (see paragraph 4.3), the correction time would be more than twice that.

Conditions are similar for the probe mission except in that case there is less concern for retaining the propellant for added post-midcourse maneuver capability.

The durations shown can be halved by firing both the primary and the backup system with 180-degree phasing. In some configurations, more than one thruster is used for midcourse correction. In those cases, the maneuver time would be further reduced. Typical reductions would be by 2 to 20% of the times shown in the curve.

A further constraint on velocity control thrust is the requirement for performing the periapsis change maneuver within the 170 to 190-degree true anomaly angle range. Tank pressure blowdown calculations indicate that a 5-lbf thruster may drop to as low as 2.7-lbf thrust at the time of propellant depletion for the orbiter configuration. At this thrust level and at the design firing sector angle, the total impulse required for a 100-kilometer periapsis change will be delivered in approximately 1,500 seconds by a single engine. Near apoapsis, this corresponds to approximately 6 degrees of arc. A maximum periapsis change maneuver can then be accomplished well within the specified range for any of the configurations using 5-lbf nominal thrusters.

It is concluded that 5-lbf (nominal) thrusters are adequate to perform the velocity control functions at reasonable rates for all configurations. Since the attitude/spin control requirements also dictate use of 5-lbf thrusters, the remainder of the study will be based on use of this thrust size for all locations on all configurations.

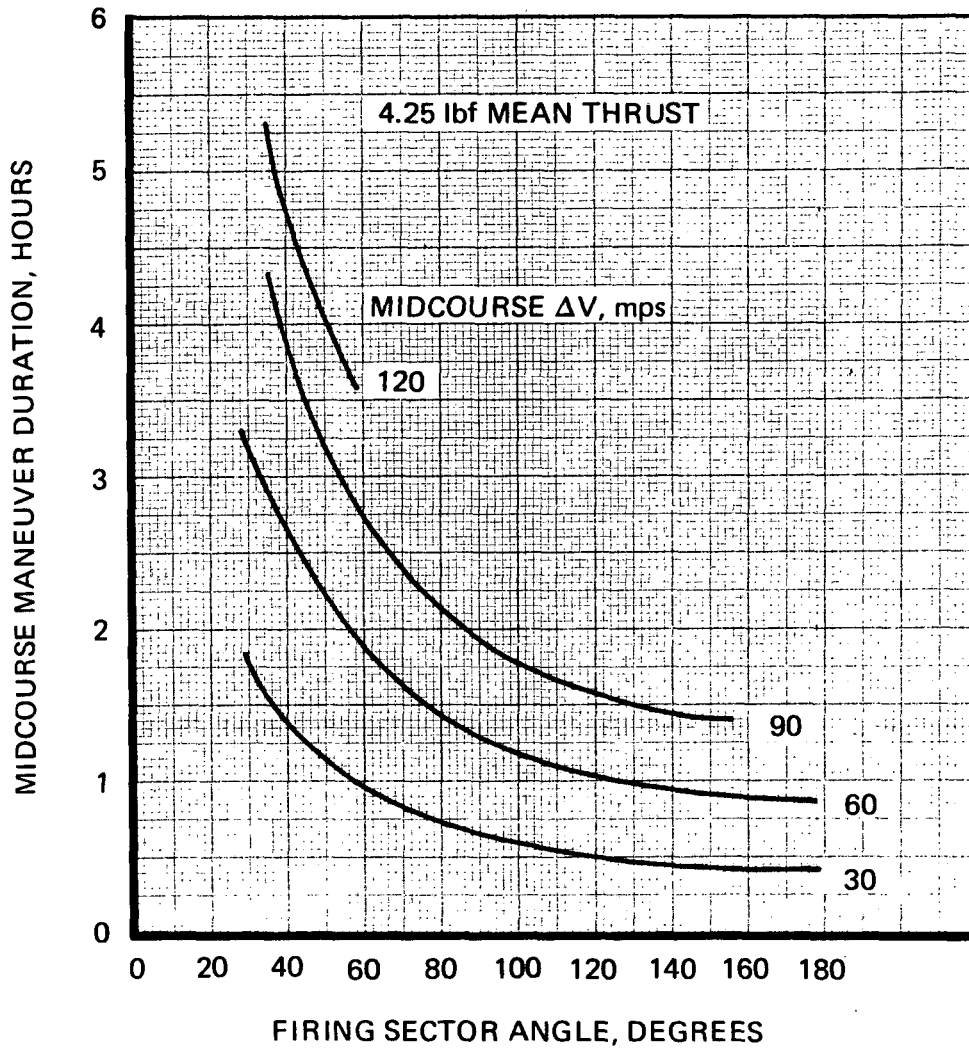


Figure 2-27. MIDCOURSE MANEUVER DURATION

3.0 RELIABILITY

3.1 FAILURE MODE/REDUNDANCY ANALYSIS

The candidate propulsion systems were subjected to an analysis of system failure modes and the effects of various forms of redundancy. The analysis proceeded from a general review of system level operation (as affected by thruster location) to a failure mode and effects analysis (FMEA) conducted at the component level.

The object of these analyses was to:

- a. Identify and, if possible, eliminate critical configuration-peculiar failure modes.
- b. Determine optimum means of incorporating redundancy into the propulsion system.
- c. Identify, as an aid to overall system ranking, those configurations with the least-critical failure modes.

3.1.1 Effect of Thruster Location and Valve Type on System Failure Modes

Each of the propulsion system configurations is required to perform the functions of velocity correction, attitude control, and spin control. The velocity and attitude control functions may be performed by proper combinations of thrusters mounted to fire either radially or tangentially while the spin control function must be performed by tangentially mounted thrusters.

The additional constraints imposed on the analysis are the general philosophy of "open-loop" operation and consideration of the communications time lag for interplanetary operation and/or failure correction.

One redundancy concept in general use is that "no single failure shall cause loss of mission." This is achieved for many applications by incorporating redundant thrusters and various combinations of latching or explosive valves to isolate failed thrusters. This concept is satisfactory for near-Earth operations where fault detection and isolation can be relatively rapid. For interplanetary distances, the delay time is such that vehicle gyrations and loss of propellant could cause loss of mission before the fault could be detected and corrective action taken.

From these considerations, it is apparent that any system redundancy concepts considered should be aimed first at eliminating single failures which may occur in the critical failure modes and that thruster locations should be selected to minimize the criticality of failures, consistent with other operational requirements.

The general effects of open and closed valve failures for the three propulsion functions, considering radial or tangential mounting of the thrusters, is shown in Table 3-1.

Table 3-1. EFFECT OF VALVE FAILURE ON SYSTEM FUNCTION

Function	Thruster Mounting	Type of Failure	Effect of Failure on System			
			Propellant Loss*	ΔV	Precession	Spin
Velocity Correction	Radial	Closed	—	<Desired	X	—
		Full open	Major	<Desired	X	—
	Tangential	Closed	—	<Desired	X	Excessive Change
		Full open	Major	<Desired	X	Excessive Change
Attitude Control	Radial	Closed	—	X	<Desired	—
		Full open	Major	X	<Desired	—
	Tangential	Closed	—	X	<Desired	Excessive Change
		Full open	Major	X	<Desired	Excessive Change
Spin Control	Tangential	Closed	—	Minor	Minor	<Desired
		Full open	Minor	Minor	Minor	>Desired

* Assumes latching valve opened prior to maneuver and closed following maneuver. Thus, open failure during maneuver (except spin) can cause large propellant loss.

X Indicates an undesirable component produced by the failure.

— Indicates no effect from the failure.

Spin Control – Single thruster failures are least critical in the spin mode and essentially identical for all configurations. The reason for this lies in the normal modes of operation for spin changes. These modes are either continuous-on (for maximum spin rate of change) or equal small pulses fired 180 degrees apart to achieve minimum corrections. Assuming for these maneuvers that the latching valve is commanded open just prior to the firing and commanded closed just after its completion, the worst-case single failure would be that caused by continuous-on firing of a single thruster for one-half revolution when only a pair of minimum impulse bits had been commanded. The latching valve is capable of preventing catastrophic changes in spin rate because of its timely sequencing for this mode. Assuming a 5-lbf thrust condition (failure occurring at maximum feed pressure) and the orbiter vehicle (minimum moment of inertia) at 15 rpm and being commanded to spin down, the spin rate is reduced by 3.2 rpm down to 11.8 rpm. Since burn time is longer if a single thruster is used (and couples are not required since the induced ΔV 's cancel if pulses are fired 180 degrees apart), it is apparent that single thrusters are best for the spin maneuvers from a potential failure standpoint. For the worst-case failure occurring during a small correction as discussed above, a single thruster will be on for a longer portion of the total on-plus-off time, hence making the impact of an open failure even less critical in relation to the commanded maneuver.

Attitude Control – For attitude control thrusters, whether radially or tangentially mounted, a valve open failure is the most critical since it can cause a gross loss of propellant. This loss is due to the fact that the nominal pulsing duty cycle is on the order of 10%; hence, the latching valves remain open for a relatively long period of time during a maneuver, providing an opportunity for excessive propellant loss if a thruster valve should fail open. For a radially mounted thruster, the propellant loss is the major effect of an open failure with the net precession being less than that commanded and with some net velocity produced. If the thrusters are mounted tangentially, an open failure will produce excessive spin change as well. In the case of a thruster failed closed, the general effects for each thruster location are the same (differing in spin change magnitude and direction) except no propellant is lost.

From these descriptions, it would initially seem that the ideal location for attitude control thrusters would be the radial pointing location; however, several factors make the tangential location more attractive.

The first of these is that it is not easy to sense a valve open failure during an attitude maneuver with thrusters pointing radially. The only readily monitored parameters that would provide an indication are actual precession rate (difficult to determine without additional on-board electronics) and propellant tank pressure (which would decay faster than nominal but would be difficult to interpret on-board due to the various possible duty cycles). By contrast, the tangential location provides simple sensing of failures since both open and closed thruster failures will induce a spin change. Spin rate is being continuously monitored for the sectoring system; thus it could be a relatively simple matter to incorporate limits on spin change which, if exceeded, result in the termination of all propulsion commands and generation of a command to close the latching valve. This approach of rapidly sensing the failure and terminating the commands minimizes the velocity increment delivered to the vehicle as a result of the failure. Other data, such as thruster temperatures, may

then be used to discriminate open or closed failures and isolate the faulty thruster. A second consideration is the fact that a tangential location for the attitude thrusters results in better impulse distribution between thrusters, since both attitude control and spin control would be performed on the tangential thrusters and only velocity corrections on the radial thrusters.

Velocity Correction – Problems associated with failures of the velocity correction thrusters are, in general, similar to those of the attitude correction system. Open or closed valve failures with tangential thrusters produce excessive spin changes. These may be detected and limited by a spin sensing control as discussed above. However, as discussed previously, the tangential location is not desirable for the velocity control thrusters because of thrust and alignment tolerances inherent in normal thruster operation. Therefore, it is necessary to analyze the radial thruster location to determine methods of minimizing the failures or effects thereof.

The probability of the open failure mode is a function of the type of valve configuration selected for the thruster and may be minimized as discussed in paragraph 3.1.2 below.

The fail closed case is the primary failure mode to be analyzed for effect on the system. Failure of a radial thruster will induce precession, the amount being a function of the thruster moment arm to the vehicle center of gravity. This distance is minimized by the arrangement employed in Configuration B, which was used for the analysis. For the orbiter configuration, and assuming a maximum first midcourse maneuver with the spacecraft spin rate increased to 50 rpm (to minimize attitude perturbations due to normal tolerances), the worst-case precession induced by immediate failure in the closed position of either thruster is on the order of 35 degrees. This precession, while undesirable, is not catastrophic, and since velocity correction is being commanded, the net effect is only to reduce the delivered velocity which can be imparted in an additional maneuver. This aspect was also discussed in paragraph 2.2.6 with data presented in Table 2-16. It should be noted that if the velocity correction is being performed using both primary and backup pairs of thrusters, the worst-case precession is half that computed above, since pairs of engines are each delivering one-half the total impulse. Other velocity corrections are of sufficiently smaller magnitude compared to the first midcourse that the precession effect caused by a failure is less than that computed above.

3.1.2 Thruster Valve Combinations

Various combinations of thruster valves and latching valves are considered, together with the effect of open or closed failures on the vehicle, in Table 3-2. Several of these concepts and the approach leading to the selection of a valve configuration are presented below.

Single Thruster Valves – Single thruster valves without a latching valve are unacceptable. Failure of a thruster valve in the leakage or open modes would cause loss of the redundant features, since no means of isolating the failure is provided.

Single Thruster Valves Plus Latching Valve – This concept represents an improvement, since a leaking or open thruster valve can be isolated by the latching valve and the redundant half of the propulsion system may be employed.

Table 3-2. VALVE CONCEPTS

Valve Concept	Effect on System of Valve Failure Mode				
	Failure to Open	Failure to Close		Comments	Criticality
		Leakage	Full Open		
1) Single thruster valves, (single seat), no latching valve	Thrust backup mode is available	Gradual loss of propellant, vehicle perturbation.	Complete loss of propellant or violent vehicle maneuver.	Negates effect of redundant thrusters in open or leakage failure modes.	Critical
2) Single thruster valves plus latching valve	Thrust backup mode is available	Loss of propellant and minor vehicle perturbation until latching valve closed.	Major loss of propellant and large vehicle perturbation (dependent on thruster location) until latching valve closed.	Some propellant loss may be acceptable if vehicle not grossly perturbed.	Major
3) Single thruster valves, dual seat (pushrod)	Thrust backup mode is available	Two seats reduce leakage potential unless particle on downstream seat is large enough to cause liftoff of upstream seat.	Complete loss of propellant if downstream seat fails open. Possible leakage loss of upstream seat.	Partially compromises redundant thruster concept. Less likely to fail open in leakage than (1).	Major
4) Dual (independent) thruster valves	Thrust backup mode is available	Two seats reduce leakage potential. Seats not connected.	Redundantly actuated valves reduce probability of full open failure. Open failure of downstream valve affects I-bit and centroid.	High probability of success. Some degradation of operation if downstream valve fails open.	Minor
5) Single thruster valves, dual seat (pushrod) and latching valve	Thrust backup mode is available	Two primary valve seats reduce leakage potential. Latching valve eliminates leakage after mission function if large particle holds downstream seat off.	Major loss of propellant and large vehicle maneuver (dependent) on thruster location) until latching valve closed.	Less reliable than (4) for open failure during maneuver.	Minor or major
6) Dual (independent) thruster valves and latching valve	Thrust backup mode is available. Some compromise in opening reliability.	Two primary seats plus latching valve minimize chance of leakage.	Redundantly actuated valves reduce probability of full open failure. Downstream failure affects I-bit and centroid.	Most reliable, some performance degradation if downstream seat fails open.	Minor

Dual-Seat or Dual-Independent Valves Plus Latching Valve – The most desirable feature for thruster valves employed for repetitive pulsing is that the valves have no sliding parts. This helps to ensure repeatable cycling and reliable operation. In particular, this concept, together with mechanical force-bias toward the closed position virtually eliminates the possibility of a full-open failure (excluding the case where a failure in the guidance and control or electrical system keeps power applied to the valve). The remaining primary failure modes are failure to open (principally coil short or open or wire break) or failure to close completely (leakage mode). Results of testing with typical propellant valves of this type show that an overwhelming majority of the failures occur in the leakage mode.

Thus, leakage is seen to be both the most likely failure mode as well as the most likely failure mode which will require closing of the latching valve, resulting in a loss to the system of three additional thrusters as well as of the failed unit.

Dual-seat or dual independent valves may be employed to counteract this problem, the dual seat in each case aiding to prevent leakage. The dual-independent valve is functionally identical to taking two completely separate valves and joining them together, each half containing its own coil, actuator, and seat.

This latter concept, in addition to providing leakage protection, provides protection against a failure in the open position since the actuation of each seat is completely independent. However, as noted earlier, this failure mode is unlikely because of the type of valves employed. The penalty paid by the dual-independent valve for improved protection against open failures (leakage or wide-open) is a higher probability that the valve will fail to open since there are twice as many coils, wires, etc., that must successfully operate to get the valve open.

As shown in Table 3-2, the most reliable valve concept is the dual independent thruster valves (concept number 6). There is not presently a developed and qualified dual independent propellant valve available as discussed in section 5.3.2. The use of the dual seat (pushrod) valve concept is currently possible through use of the existing Hydraulic Research dual seat valve.

A latching valve is provided upstream of the thruster valves to permit system isolation in the event of a failure to retain full use of the system's built-in functional redundancy.

3.1.3 Driver Circuit Redundancy

Possible redundancy of driver circuit configurations was considered for the Planetary Explorer vehicle. The three primary approaches compared (also summarized in Table 3-3) are as follows:

- a. Nonredundant configuration of one driver circuit per thruster
- b. Redundant configuration wherein two driver circuits may be individually switched between two opposed thrusters.
- c. Multiple driver circuits which may be switched to any desired thruster.

The primary advantage of the fixed, individual driver circuits is that they are permanently wired and that no additional commands or logic are required for their operation beyond the normal thruster commands. This approach is also consistent with a philosophy that no single failure can cause loss of function since the thrusters/driver circuit combinations are themselves redundant.

Table 3-3. DRIVER CIRCUIT REDUNDANCY COMPARISONS

Circuit Arrangement	Failures Necessary to Cause Loss of a Specific Primary Propulsion Function	Comments
A. One driver circuit/thruster (direct connected)	Two thrusters or two driver circuits or one thruster and driver circuit on opposite thruster.	<ul style="list-style-type: none"> ● No additional logic required ● No additional switch unreliability ● Least ground commands
B. Two driver circuits switchable between two thrusters of same function	Two thrusters or two driver circuits	<ul style="list-style-type: none"> ● Improves overall reliability ● Requires additional switching ● Requires additional logic in guidance system ● Requires additional ground commands
C. N driver circuits switchable between M thrusters, with maximum of F thrusters firing at one time $N \leq M$ $N > F$	Two thrusters or $(N - F + 1)$ driver circuits	<ul style="list-style-type: none"> ● Highest system reliability ● Most switching required ● Most logic required ● Most additional ground commands ● Should include self-test feature

The addition of switching capability between pairs of thrusters and driver circuits removes the single thruster, opposite driver circuit failure mode inherent in the fixed wired configuration. This configuration requires additional components (switches) and logic capability. The system could be set up with a basic switch position which was changed to the alternate position by ground command and then reverted to the original position upon termination of the commanded maneuver. Alternately, the switch setting could always remain in the last commanded position. The approach to be employed would ultimately have to be selected from consideration of the effects of possible failure modes, such as stray signals, on the reliability of commanding the desired path.

The third approach consists basically of a "switchboard" which connects driver circuits to selected thrusters. Dependent upon the number of driver circuits and maximum number of thrusters required to perform a given propulsion function, the reliability of having sufficient operative driver circuits can be made very high, possibly with a reduction in the total number of driver circuits. Thus, dependent on the reliability of the switching circuitry, another (possibly large) improvement in reliability may be possible. Ground commands may be necessary to assign driver circuits to the desired thrusters. As an alternate, on-board logic could be employed which would automatically connect a driver circuit to a commanded thruster. This circuit would step through the driver circuits, perform an automatic test for function, and connect only functioning circuits to the thrusters. This method prevents inadvertent ground command of a driver circuit, previously unused, which may have developed a malfunction.

The most significant criterion for deciding whether to incorporate redundant driver circuits lies in a comparison between the reliability of the driver circuit and other elements in a chain such as the vehicle receiver, decoder, and guidance computer. If the driver circuit is equivalent in reliability to these items, and they are not redundant, then no useful purpose is achieved by making the driver circuit redundant. If, however, the driver circuit is inherently less reliable because of its requirement to handle higher currents, then redundancy offers system advantages. It is assumed that switching driver circuits during a particular maneuver is undesirable.

Review of the candidate thruster configurations indicates that for Configurations B and D up to six thrusters may be fired during a velocity-control maneuver if maximum rates are to be achieved (both primary and secondary thrusters operating) and simultaneous correction of predictable error torques is employed. For Configuration C up to eight thrusters may be required while for Configurations A and E, the maximum is four.

Lacking information on driver circuit, switching, command, and other associated spacecraft systems, the most straightforward approach of using a single fixed wired driver circuit for each thruster valve would be most consistent with the basic concept of simplicity and low cost.

3.1.4 System Plumbing

In order to maintain the desired system redundancy, it is necessary to group thrusters together so that each redundant half of the system contains all functions, i.e., velocity, attitude control, and plus and minus spin capabilities.

This may be accomplished for all configurations studied. For Configurations C and D, a conflict exists between the need to fire thrusters on the same side of the spacecraft (for ΔV) and the requirement for couples for attitude control with upper and lower thrusters on opposite sides of the spacecraft. Since the duty cycles for the velocity control thrusters are not equal, in general, the second thruster of the ΔV pair is separately programmed to delay its firing in multiples of one-half revolution, thus delivering its impulse along the desired vector. For simultaneous firing both isolation valve branches must be opened. This could be considered the primary operational mode until a failure occurred which necessitated permanently isolating one-half of the system.

3.1.5 Feed System Isolation Valve Configurations

Three different combinations of feed systems incorporating latching and/or explosive isolation valves were analyzed. These configurations were presented in Figures 1-6, 1-7, and 1-8.

The selection of the correct placement of isolation valves in the system is strongly affected by the use of the isolation valves during system operation.

Analyses were performed using representative reliability numbers for the thruster groups and latching valves to aid in identifying the optimum method of using the latching valves. Actual reliability calculations are presented in paragraph 3.2.

The following assumptions were employed:

- a. Reliability of a thruster group (four thrusters) of successfully performing a complete mission, 0.995.
- b. Latching valve or explosive valve failure rate of 0.2×10^{-6} failures per actuation (open-to-closed or closed-to-open).
For a single cycle, $R = 0.9999998$.
For 200 actuations (100 discrete propulsion functions), $R = 0.99996$ and $R_{\text{opening}} = R_{\text{closing}} = 0.99998$.
- c. For simplicity, the calculations exclude failures due to feed system leakage in order to focus on the latching valve operational modes since leakage is common to all systems.

Now, for feed system Configuration 1, with only downstream latching valves, and assuming that the latching valves are both required to cycle open once and one latching valve is required to close (if a thruster in its branch fails) in order to obtain the redundant propulsion functions, the following results may be calculated.

Reliability of all thrusters operating successfully with propellant available:

$$R = (0.995) (0.9999998) (0.995) (0.9999998)$$

$$R = 0.99002$$

Reliability of at least one thruster group operable with opposite propulsion branch successfully closed:

$$R = (0.9999998) (1 - [1 - (0.995) (0.9999998)]^2) = 0.999975$$

For the same feed system configuration, but with the assumption that the latching valves are opened prior to and closed after each discrete propulsion function (as discussed in paragraph 3.1.1 to prevent certain types of potentially catastrophic failure modes or low level leakage), the calculations may be repeated. One hundred discrete functions (200 valve actuations) were considered. The corresponding results are:

Reliability of all thrusters successful:

$$R = (0.995) (0.99996) (0.995) (0.99996) = 0.98995$$

Reliability of at least one thruster group successful:

$$R = 1 - (1 - (0.995) (0.99996))^2 = 0.9999746$$

The operations using Configuration 3 result in essentially equivalent numbers since the parallel explosive valves only contribute to a very high opening reliability, after which, actuation of the latching valves must proceed based on either of the two situations described above.

With Configuration 2, different options are available. The parallel latching isolation valves are closed at launch with the downstream valves left open. This provides the highest possible reliability that propellant will be available to both groups of thrusters. Since the parallel valve configuration is highly reliable in opening, it should be employed for performing the system lockup function as well. In this regard, it should be noted that both valves must close for lockup; however, this is no worse than the case where the thruster group valves are used for lockup; since both of these valves must close after each propulsion function if protection against certain failure modes is to be ensured.

With this philosophy employed, the thruster group latching valves may be used as the final backup to lock up one-half of the system when needed in the event of a failure of one of the upstream latching valves in the open position.

The reliability of opening the parallel flow paths 100 times is then:

$$R_{\text{opening}} = 1 - (1.0 - 0.99998)^2 = 0.999999996$$

The reliability of closing both parallel flow paths 100 times is:

$$R_{\text{closing}} = (0.99998)^2 = 0.99996$$

The reliability of successful redundant operation, including one cycle of a branch valve to close off a thruster group on the assumption that both a thruster valve has failed open and one of the parallel latching valves has also failed open, is given by:

$$\begin{aligned}
 R &= (R_{\text{opening}}) (R_{\text{closing}}) (R_{\text{thruster redundant operation}}) \\
 R_{\text{opening}} &= \text{Parallel flow paths} = 0.9999999996 \\
 R_{\text{closing}} &= 1 - [(1 - 0.99996) (1 - 0.9999998)] = 0.9999999992 \\
 R_{\text{thruster}} &= 1 - (1 - 0.995)^2 = 0.999972 \\
 R &= 0.999975
 \end{aligned}$$

From these analyses, it is apparent that the thruster group reliability is the limiting factor in the chain, any of the assumed feed systems being sufficiently reliable so as not to degrade overall mission reliability. The calculations do show, however, that Configuration 2 is significantly higher in reliability in performing its functions. Therefore, if any doubt exists as to the failure rates of the latching valves, Configuration 2 should be selected.

The optimum strategy for employing this configuration, assuming that the system is to be locked up after each discrete firing sequence, is as follows:

- a. Launch with parallel latching valves closed and thruster group latching valves open.
- b. Employ the parallel latching valves for all normal opening/lock-up operations.
- c. If a failure to open is detected in one of the parallel latching valves, discontinue operation with these valves, thus ensuring at least one in the open position.
- d. Employ the thruster group valves for:

Lockup of a thruster group if a thruster valve fails (primary function), opening/lockup functions for the system if one of the parallel latching valves fails in the closed position (secondary function).

Used in this manner, this configuration of latching valves provides maximum reliability of functional operation while also providing protection against certain failure modes.

3.1.6 Failure Mode/Effects Analysis

A preliminary FMEA has been conducted at the component/piece part level. The results of this analysis are presented in Appendix B. As an aid to understanding the material in this appendix the following definitions are given.

Criticality has been estimated by the following criteria:

- I *Critical* – Catastrophic to mission equipment, mission abort, or severe degradation to mission performance, or death or severe injury to personnel
- II *Major* – Loss of 50% of mission function, performance, or availability or time-loss injury to personnel

III *Minor* – Essential mission functions performable but with decreased capability or availability; “no time-loss” injury to personnel

Although probabilities of failure modes have not been assigned, a review of the reliability analysis indicates that fair allocation of component failure rates to the modes would show that I or II ratings would have a very low probability of occurrence.

3.2 RELIABILITY ANALYSIS

3.2.1 Summary

Reliability analyses have been made of five candidate propulsion configurations for the Planetary Explorer for both the orbiter and probe missions. Three propulsion functions have been reviewed for each: delta velocity, attitude control (precession), and spin. For each function, three functional modes have been considered: primary–dual (duplicate assemblies 180 degrees from each other), primary–single (assembly on one side), and secondary (single assembly redundant with its identical assembly 180 degrees related). The reliability data for these analyses are summarized in Table 3-4 for both the orbiter and probe missions. The data are shown at the subsystem level, as a product of the three propulsion functions noted above.

Table 3-4. RELIABILITY TABULATION – THRUSTER GROUPS

Mission	Mode	Configuration				
		A	B	C	D	E
Orbiter	Primary (dual)	0.99178	0.99257	0.9926	0.99276	0.99191
	Primary (single)	0.99409	0.99425	0.99427	0.99443	0.99422
	Secondary (redundant)	0.999965	0.999967	0.999967	0.999969	0.999966
Probe	Primary (dual)	0.99397	0.99503	0.9951	0.99517	0.99398
	Primary (single)	0.99628	0.99671	0.99678	0.99685	0.99629
	Secondary (redundant)	0.999986	0.999989	0.99999	0.99999	0.999986

In addition, reliability analyses have been performed on three feed system configurations, each with respect to both the orbiter and probe missions. These data are presented in Table 3-5. A system reliability summary, combining both subsystems, is presented in Table 3-6.

Estimated parameters of cumulative engine burn time and pulses for each configuration and function were used as bases for the propulsion subsystem analyses. These are presented in Table 3-7, and their functional relationships are shown in Table 3-8. The several propulsion and feed subsystem configurations are shown schematically in Figures 1-1 to 1-8.

Table 3-5. PRESSURIZATION/PROPELLANT FEED SUBSYSTEM

Mission	Configuration Number		
	1	2	3
Orbiter	0.99086	0.99055	0.99055
Probe	0.99502	0.99579	0.99579

Table 3-6. SYSTEM RELIABILITY SUMMARY

The following data combine the reliability of Configuration 2 feed (pressurization/propellant) subsystem from Table 3-5, with the primary--single mode of the indicated thruster group configuration from Table 3-4.

Mission	Propulsion Subsystem Configuration				
	A	B	C	D	E
Orbiter	0.98470	0.98485	0.98487	0.98503	0.98482
Probe	0.99109	0.99152	0.99159	0.99166	0.99110
Ranking					
Orbiter	5	3	2	1	4
Probe	5	3	2	1	4

3.2.2 Conclusions

3.2.2.1 Propulsion Subsystem Configurations

Table 3-4 shows the reliability tabulation for the several configurations. It will be noted that the primary (dual) mode in all configurations is somewhat less reliable than the primary (single) mode. This results chiefly from the increased number of cold starts and the number of TCV's exposed to potential leakage as compared to when a single assembly is performing the function. Internally series-redundant (two seats "push rod" linked) TCV's have been assumed in the calculations.

On the basis of probability, assuming the exponential failure distribution and a constant failure rate, the reliability of any assembly depends on the total time (operating and nonoperating) and/or cycles involved in the function. The analysis, therefore, indicates a slight gain in operating in the primary--single (versus dual) mode. However, since full redundancy is available in all these

Table 3-7. ESTIMATED FIRING DATA

Configuration	Parameter	Orbiter Mission			Probe Mission			Totals	
	Function	ΔV	AC	Spin	ΔV	AC	Spin	Orbiter Mission	Probe Mission
A	Hours	1.294	0.154	0.0284	0.667	0.0753	0.0467	1.476	0.789
	Pulses	9,935	2,364	218	3,746	846	262	12,517	4,854
B	Hours	1.293	0.1184	0.0335	0.6666	0.0637	0.053	1.445	0.7833
	Pulses	12,405	1,818	257	4,680	716	299	14,480	5,695
C	Hours	1.281	0.1747	0.1	0.6604	0.0728	0.0821	1.556	0.8203
	Pulses	10,929	2,682	771	4,121	818	489	14,382	5,428
D	Hours	1.281	0.1733	0.0284	0.6604	0.0698	0.0504	1.483	0.6604
	Pulses	10,929	2,660	218	4,121	784	283	13,807	5,188
E	Hours	1.294	0.1223	0.0307	0.667	0.0674	0.0484	1.447	0.7828
	Pulses	9,935	1,877	236	3,746	757	272	12,048	4,775

Table 3-8. THRUSTER FUNCTIONAL MODES

Function	Mode	Configuration Number				
		A	B	C	D	E
ΔV	Primary (dual)	1 & 2	1 & 2, +3 & 4	1, 3, 5, 7 & 2, 4, 6, 8	1, 5, & 7 + 3, 6 & 8	1 + 2
	Primary (single)	1	1 & 2	1, 3, 5, 7	1, 5, & 7	1
	Secondary (redundant)	1 or 2	1 & 2 or 3 & 4	1, 3, 5, 7, or 2, 4, 6, 8	1, 5, & 7 or 3, 6 & 8	1 or 2
AC (Precession)	Primary (dual)	1, 4, 6 + 2, 3, 5	5 & 8 + 6 & 7	1, 5, 4, 8 & 2, 6, 3, 7	1 & 4 + 2 & 3	3 & 6, + 4 & 5
	Primary (single)	1, 4, 6	5 & 8	1, 5, 4, 8	1 & 4	3 & 6
	Secondary (redundant)	1, 4, 6, or 2, 3, 5	5 & 8 or 6 & 7	1, 5, 4, 8 or 2, 6, 3, 7	1 & 4 or 2 & 3	3 & 6 or 4 & 5
+ Spin	Primary (dual)	4 & 5	6 & 8	2, 4, 5, 7	6 & 7	4 & 6
	Primary (single)	4	6	2 & 5	6	4
	Secondary (redundant)	4 or 5	6 or 8	2 & 5 or 4 & 7	6 or 7	4 or 6
- Spin	Primary (dual)	3 & 6	5 & 7	1, 3, 6, 8	5 & 8	3 & 5
	Primary (single)	3	5	1 & 6	5	3
	Secondary	3 or 6	5 or 7	1 & 6 or 3 & 8	5 or 8	3 or 5

NOTE: + and - spin have been combined in the reliability calculations.

assemblies, it is obvious from the high values associated with the secondary (redundant) modes that the spacecraft system should be designed to use this redundancy. Redundancy is based on a primary–single group being redundant to its corresponding group 180 degrees related.

3.2.2.2 Pressurization/Propellant Subsystem Configurations

The analysis shows that Configuration 1 is the most reliable in both the orbiter and probe missions. This results chiefly from the fact that there are fewer parts and joints that result in leakage paths. Most of the failure rate in pressurized components consists of the leakage failure mode, and the cyclic operation of the latching (or explosive-operated) valves is a small part of the total unreliability. However, the foregoing failure mode analysis indicates that Configuration 2 is the most effective considering all failure criticalities.

In Configurations 2 and 3, whether latching or explosive-actuated valves are used in the redundant assembly has negligible effect on reliability since the redundant capability provides such a high reliability. Whether the addition of this redundant assembly is of value (compared to Configuration 1) depends on the criticality of this function to the mission. Whether the latching valves on the propulsion branches are open or closed at launch on these two configurations is negligible in terms of reliability. However, since the upstream valves are available, it is best to leave them open at launch to take advantage of every bit of reliability available. It is a fact of any reliability consideration that the prediction is a probability, but since failures are assumed randomly distributed (assuming no wearout), a failure of even remote probability could occur in the first instant of operation.

3.2.3 Discussion

3.2.3.1 Models

The exponential relationship and distribution has been assumed.

Therefore:

$$R = e^{-\lambda_t T n}$$

Where:

- R = Reliability (probability of no failure)
- λ_t = Failure rate (failures/hour)
- T = Time (hours)
- n = Number of identical elements

Expressed in cycles, this becomes

$$R = e^{-\lambda_c N n}$$

in which:

- λ_c = Failure rate (failures/cycle)
- N = Number of cycles

Some parts operate in both time and cyclic domains, with appropriate time-related or cyclic-related failure rates. The following is used to express these combined effects:

$$R = e^{-(\lambda_t T + \lambda_c N)n}$$

For this analysis, the final exponent is made a summation of the failure rates, times, and cycles as listed in the columns of the typical data and calculation sheets shown as Tables 3-9 and 3-10.

These are the basic building blocks used to derive the system reliability consistent with the following logic model:

$$R_S = R_V R_A R_S R_F$$

Where:

- R_S = System reliability
- R_V = Velocity function reliability
- R_A = Attitude control function reliability
- R_S = Spin (+ and -) function reliability
- R_F = Feed (pressurant/propellant) S/S reliability

3.2.3.2 Duty Cycles and Mission Profiles

Five cold starts for the reactor (thruster) have been estimated for each thruster. The total number of hot pulses to which the thrusters are subjected has also been accounted for by appropriate failure rates. Configurations A and E both use gimbaled thrusters, which involve additional reliability penalties to account for the actuators and position sensing. A valid failure rate for the actuators is not available since the proposed unit would have to be designed and built. It is planned to be an electrically driven ball-screw linear driver. Therefore, assuming a well-designed, -built, and -qualified unit, the time-and-cyclic-related failure rates (noted in Table 3-9) are based on engineering judgment. Table 3-6 lists the duty cycles for each configuration, showing the required total expenditure in burn time and pulses for all functions. This table also shows the proportional distribution of these totals that is expended in the ΔV , attitude control, and spin functions by the different thruster assemblies in each configuration.

The orbiter mission has 195 days in transit plus 60 days in orbit, a total of 6,120 hours. Longer times in orbit would tend to reduce the mission reliability slightly but would not alter the ranking. The probe mission has 195 days in transit plus a day for final maneuvers, a total of 4,704 hours. All pressurized components are assumed fully operating for the full mission duration, hence, subject to a leakage failure mode. Failure rates characteristic of the nonoperating periods of thrusters and valves are proportionately small, and have not been included in this study. The cumulative burn time and cycles for all mission phases have been used, rather than attempting to present the reliability by successive mission phases (midcourse corrections, orbit maneuvers, etc.).

Table 3-9 – PROPULSION SUBSYSTEM FAILURE RATE DATA (TYPICAL)

CONCEPT A-ORBITER, PROPULSION FUNCTION: $\Sigma \Delta V$, AC, SPIN
 (All exponents $\times 10^{-6}$)

Mode	Component	(n) Qty	(T) Time (hours)	(N) Cycles	λ_t	λ_c	$\lambda_t T_n$	$\lambda_c N_n$	$\Sigma \lambda T/N$	
Primary	Actuators	2	1.476 ^(a)	212	50	5	73.8	2120	2194	
	Thrusters	6		5 ^(b)		23.1		693	693	
	Valves	6	6120		0.05 ^(d)		1836		1836	
	Thrusters & Valves	all ^(c)	1.476	12,517	17.3 ^(e) 2.0 ^(f) (19.3)	0.23 ^(e) 0.05 ^(f) (0.28)	28.5	3504.8	3533	
					Dual: R = 0.99178 Single: R = 0.99409				8256	
Secondary – Redundant	Actuators	1	1.476 ^(a)	212	50	5	73.8	1060	1134	
	Thrusters	3		5		23.1		346.5	347	
	Valves	3	6120							
	Thrusters & Valves	all ^(c)	Same as for primary (dual)							3533
					R = 0.999965				*5932	

- Notes: (a) Cumulative time – applies to either 1 or 2 units
 (b) Cold-start cycles
 (c) Time- and cyclic-related failure rates apply as a block to all thrusters and TCV for the mission—see Table 3-7. In addition thrusters and TCV are charged with rates noted in (b) and (d).
 (d) Leakage failure rate (operating) applicable for mission duration. See paragraph 3.2.3.2. All pressurized components considered fully operating in the leakage mode.
 (e) For thrusters.
 (f) For TCV.

The latching valves in the propulsion branches are considered to be cycled after each discrete propulsion function. This activity has been estimated as 90 cycles for the orbiter mission and 30 cycles for the probe mission. These operations have been accounted for in the reliability predictions.

The pressure transducer for the propellant/pressurization subsystem is assumed to be functionally redundant with a system operating mode in which system parameters could provide backup information equivalent to that normally supplied by the transducer. If the transducer fails, it is possible to calculate the required firing duration based on an assumed pressure derived from the transducer readings prior to its failure (as well as accounting for known or assumed propellant leakage). After each firing, a new system pressure could be calculated from the firing data, total impulse, and resultant propellant consumed during the burn. Tracking data could provide a feedback of information to determine the actual total impulse delivered to aid in cross checking the calculations. Therefore, to estimate this functional redundancy, an "equivalent" transducer was assumed having a failure rate double that of the operational unit. This increased failure rate provides for lack of timeliness of the data and possible degraded mission operations or duration due to maneuver over-compensation and correction that could result from the functional backup mode. If pressure transducers were to be used in the propulsion branches, they would add slightly to the overall redundant reliability but would lose more in unreliability by increasing the potential leakage paths.

The propellant supply line to the TCV has been assumed attached to the TCV by a mechanical fitting, and likewise, the pressure line to the pressure transducer. Hence, a greater failure rate has been applied to these fittings to account principally for leakage, as compared to the brazed fittings and connections elsewhere. It must be noted that the fitting leakage failure rate for the TCV was included with the analyses of the respective propulsion subsystem configurations (rather than at the system level) to properly handle the primary (dual/single) and secondary (redundant) operating modes.

Temperature transducers have not been included in the analyses, since they were not considered essential to mission success.

It should be noted that for most propulsion maneuvers, e.g., delta velocity, an element of either precession or spin control, may be used for stability. These elements are included in the total burn time and pulses of all functions. Therefore, the reliability product of these functions for a given configuration yields its effective overall reliability.

3.2.3.3 Failure Rates

Sources of data on missiles and satellite electrical, electromechanical, and mechanical parts include RRC test data for thrusters and valves, Dynasciences (Reference 3) for pressure transducers, Rome Air Development Center (RADC) (Reference 4) for nonoperating rates, and Apollo Support (General Electric) (Reference 5) for general data. Some data have been modified by engineering judgment.

A failure rate modifier to adjust failure rates for the intensity of the boost phase environment has not been applied. A $K_m = 1$ modifier has been applied to the mission phases. No manufacturing and assembly (human) error factors were included to modify basic failure rates. Quality control screening and inspection procedures and in-process testing and acceptance testing, both by RRC and its suppliers, reduce fabrication and assembly errors to a random minimum.

Both operating and nonoperating failure rates have been applied to some components, the latter to account for "standby" time between functioning periods (see Table 3-10, Note 7).

A complete listing of components, operating times/cycles, failure rates, and modifiers and their exponent summations are presented in Tables 3-9 and 3-10, which are typical of all configuration analyses.

Table 3-10. FAILURE RATE DATA

SYSTEM/SUBSYSTEM Feed (Pressurant/Propellant)

Configuration B (Orbiter)

PART OR COMPONENT	Q QUANTITY (5)	OPERATING PHASES		NONOPERATING PHASES (HOURS)		FAILURE RATES x 10 ⁻⁶			λ _t T _n x 10 ⁻⁶			λ _c T _n x 10 ⁻⁶	Σλ _{T/N} x 10 ⁻⁶
		TIME, HRS (T) (1)	CYCLES No. (N)	MISSION K _M =	BOOST K _B =	OPERATING λ _t	NON-OPERATING λ _t	CYCLIC λ _c	OPERATING	NON OPERATING	BOOST	CYCLIC	
Fill/drain valve	2	6,120	(2)			.01			122.4				122.4
Tank	9	↑				.10			5,508				5,508
Latching valve	1	↓	1			.01		.5	61.2			.5	(3) Neglect
Latching valve (3)	1	6,120	1			.01		.5	61.2			.5	122.4
Filter	1	2.15				.10			.2				.2
Latching valve	2	6,120	90			.01	.001(7)	.5	122.4	12.2		90	224.6
Pressure transducer (with fitting leakage) (3)	1	↑				5.05			30,906			(3)	1,891.4
System mode(6)		↓				10			61,200				1,621.8
Lines/fittings (leakage) (4)	53	6,120				.005			1,621.8				9,490

R = e^{-.009490}
= .99055

- NOTES
- (1) 195 days (4,680 hours - transit) plus 60 days (1,440 hours - orbit).
 - (2) All pressurized components considered operating for full mission duration.
 - (3) Redundant effective exponent is shown.
 - (4) Leakage for thrust chamber valves (at a different failure rate) combined with propulsion system analysis (see paragraph 3.2.3.2).
 - (5) Leakage for redundant valves is additive.
 - (6) See paragraph 3.2.3.2.
 - (7) The thruster group I.V are in a standby mode, hence have a nonoperating failure rate also.

3-20

Table 3-10. FAILURE RATE DATA (Concluded)

SYSTEM/SUBSYSTEM Feed (Pressurant/Propellant) Configuration B (Probe)

PART OR COMPONENT	QUANTITY (5)	OPERATING PHASES		NONOPERATING PHASES (HOURS)		FAILURE RATES $\times 10^{-6}$			$\lambda_i T_n \times 10^{-6}$			$\lambda_c T_n \times 10^{-6}$	$\Sigma \lambda_{T/N} \times 10^{-6}$	
		TIME, HRS (T) (1)	CYCLES No. (N)	MISSION $K_M =$	BOOST $K_B =$	OPERATING λ_t	NON OPERATING λ_t	CYCLIC λ_c	OPERATING	NON OPERATING	BOOST			CYCLIC
Fill/drain valve	2	4,704				.01			94.1				94.1	
Tank (2)	6	↕				.10			2,822.4				2,822.4	
Latching valve	1	↕	1			.01		.5	47			.5	(3) Neglect	
Latching valve (3)	1	4,704	1			.01		.5	47			.5		
Filter	1	1.96				.10			.2				.2	
Latching valve	2	4,704	30			.01	.001(7)	.5	94.1	9.4		30	133.5	
Pressure transducer (with fitting leakage) (3)	1	↕				5.05			23.755			(3)	1,117.4	
System mode(6)		↕				10			47,040					
Lines/fittings (Leakage) (5)	41	4,704				.005			964.3				964.3	
												5,226		
												$R = e^{-.005226}$		
												$= .99479$		

NOTES

- (1) 195 days (4,680 hours transit) plus 1 day (24 hours orbit insertion).
- (2) All pressurized components considered operating for full mission duration.
- (3) Redundant effective exponent is shown.
- (4) Leakage for redundant valves is additive.

- (5) Leakage for thrust chamber valves (at a different failure rate) combined with propulsion system analysis (see paragraph 3.2.3.2)
- (6) See paragraph 3.2.3.2.
- (7) The thruster group IV are in a standby mode, hence have a nonoperating failure rate also

3-21

4.0 OPERATIONAL CONSIDERATIONS

4.1 MISSION PROFILES

4.1.1 Mission Sequence

The hydrazine propulsion system maneuver sequence for the probe and orbiter missions is described in Table 4-1 and 4-2 respectively. It should be noted that the initial cruise orientation maneuver is performed in conjunction with the midcourse correction rather than immediately after separation from the final launch vehicle stage. These sequences show the course correction occurring in four phases, an in-flight calibration and three velocity-control maneuvers of progressively smaller magnitude.

The magnitude of the in-flight calibration maneuver would be the maximum that could be imparted to the vehicle and still guarantee that the attitude would not drift outside the prescribed limits of 6-degree precession about the X axis (thrust axis) and 1-degree precession about the Y axis. Following this maneuver, an attitude determination would be made which, when compared to premaneuver data, would provide the information necessary to adjust the individual engine firing cycles so as to cancel out, insofar as possible, those disturbance torques induced by dimensional alignment errors and nonrandom engine variations. Depending on the magnitude of the additional velocity correction required, an increased spin rate providing increased vehicle stability will also be determined. For some of the configurations and for maximum velocity corrections, it may still be necessary to divide the remaining maneuver into two or more firing periods to ensure that the induced precessional drift does not exceed the prescribed values. Maximum values of initial calibration maneuvers, required spin rates, and nominal number of firing periods for a maximum course correction maneuver are given in Table 4-3.

Spin rate perturbations, which can be large for some of the configurations, may impose additional limitations on operational maneuvers as discussed in Section 2.0.

4.1.2 Duty Cycles

In reviewing duty cycle requirements, the main concerns are endurance (as characterized by total accumulated burn time and the number of cold starts required) and thermal soakback during low duty cycle operation. The range of duty cycles required for Planetary Explorer missions is within the operating envelope of the MR-50 thruster, and, while of interest in establishing general feasibility and identifying potential problem areas, does not in general provide a basis for differentiating among the candidate configurations. Typical duty cycle requirements as related to the system propulsive requirements are shown in Table 4-4 and discussed below.

4.1.2.1 Spin Control

Spin control typically calls for steady-state thruster operation. The longest burn time requirement is associated with the spinup maneuver prior to release of the small probes. A burn duration of 50 to

Table 4-1. MISSION SEQUENCE—PROBE VEHICLE

Event	Spin Control ΔS , rpm	Attitude Control ΔA , degrees	Velocity Control ΔV , meters/sec	Notes
1. Despin	40			
2. Orient for midcourse		45		
3. Calibration firing			See note	Configuration dependent
4. Spinup	See note			Configuration dependent
5. First course correction			See note	Events 3 and 5 total 108 meters/sec; may have to be divided into more than one firing period.
6. Spin down	See note			Equivalent to event 4 numerically
7. Acquire cruise attitude		45		
8. Orient for second midcourse		45		
9. Second course correction			10	
10. Acquire cruise attitude		45		
11. Orient for third midcourse		45		
12. Third course correction			2	
13. Orient for main probe release		45		
14. Retarget for miniprobe release			5	
15. Spinup	73			
16. Retarget bus			18	
17. Maintain sun angle		18		
18. Reorient for encounter		12		
19. Attitude maintenance		110		
Totals	113 (min)	410	143	

160 seconds would be required, depending on the quantity of propellant expended for midcourse correction and whether one or two engines were used to perform the maneuver. Steady-state burn durations of this order present no problem. Small spin rate changes for fine resolution or correcting induced perturbations would require low duty cycles. Continuous operation at these low on-times is not required. Only 2 to 5% of the system total impulse capability is required for the basic mission spin profile. Additional capability may, of course, be required where additional midcourse spin stabilization and large spin perturbation corrections are required.

Table 4-2. MISSION SEQUENCE—ORBITER VEHICLE

Event	Spin Control ΔS , rpm	Attitude Control ΔA , degrees	Velocity Control ΔV , meters/sec	Notes
1. Despin	49			
2. Orient for midcourse		10		
3. Calibration firing			See note	Configuration dependent
4. Spinup	See note			Configuration dependent
5. First course correction			See note	Events 3 and 5 total 108 meters/sec; may have to be divided into more than one firing period.
6. Spin down	See note			Equivalent to event 4 numerically
7. Acquire cruise attitude		90		
8. Orient for second midcourse		10		
9. Second course correction			10	
10. Acquire cruise attitude		10		
11. Orient for third midcourse		10		
12. Third course correction			2	
13. Acquire cruise attitude		10		
14. Orient for retro		90		
15. Orient for orbit maneuver		90		
16. Orbital maneuvers			195	Minimum of 15 steps
17. Orient for orbital maneuvers		1,000		30 to 50 individual maneuvers
18. Attitude maintenance		180		Typically 3 to 6 degrees
19. Spin maintenance	51			
Totals	100 (min)	1,500	315	

4.1.2.2 Attitude Control

Typical attitude control mode duty cycles consist of pulse widths of 80 to 600 milliseconds at 10 to 15% on-time, depending on the spin rate and the pitch rate required. Short pulse widths may be required for small angle changes and fine resolution. Long trains of short pulses, however, are not generally called for. Duty cycles of this type present no problems. Approximately 8 to 10% of the system impulse capacity is used for attitude control.

4.1.2.3 Velocity Control

In the order of 80% system total impulse capability is required for velocity control. This also demands the widest range of operational duty cycles. For a given spin rate, the bulk of the required impulse would be imparted by firing through a rotational sector corresponding to approximately 42

Table 4-3. FIRST MIDCOURSE CALIBRATION AND STABILIZATION

	Maximum Calibration Firing, ΔV , meters/sec		1st Midcourse Spin Rate, rpm		No. of 1st Midcourse Firing Periods	
	Probe	Orbiter	Probe	Orbiter	Probe	Orbiter
A, E (gimbal)						
B (radial pairs)	22.7	11.2	12	60	2	3
C (tangential doublets)	10.9	3.2	60	60	3	15
D-1 (rectangle-radial)	22.7	5.2	12	60	2	14
D-2 (rectangle-tangential)	10.0	5.4	12	60	5	5

NOTE: Values are based on limiting X-axis precession to 6° and Y-axis precession to 1° . Spin perturbations may impose other limitations (see paragraph 2.2).

degrees (120 sectors). This corresponds to 11.7% on-time and gives the design rotational efficiency of 98%. Pulse widths at cruise conditions are nominally 469 milliseconds for the orbiter (15 rpm) and 586 milliseconds for the probe (12 rpm). Somewhat longer pulse widths may be used to reduce maneuver duration at some loss in rotational efficiency. Higher spin rates, such as the 85 rpm used in the terminal phases of the probe mission, would in general require correspondingly shorter pulse widths. At this spin rate, the pulse width corresponding to 120 sectors on (11.7% duty cycle, 98% rotational efficiency) is 82.7 milliseconds. Intermediate spin rates, where required for additional midcourse maneuver stabilization, would require intermediate pulse widths.

Duty cycles of this type should be well within the capabilities of any of the developed engines, since average propellant flow rates are high enough to provide a large cooling margin. The most difficult duty cycles, from the thruster standpoint, are generally those in the 0.1 to 1% on-time range. At duty cycles typically in this range, thermal soak produces maximum injector temperature and, if the engine is not designed for operation in this regime, possibility of injector boiling with accompanying pulse performance deterioration. Peak thrust chamber valve temperatures typically occur at duty cycles of this order.

For those spacecraft/thruster configurations using axial engine displacement and pulse balancing (all except the gimbaled engine), the thruster furthest from the cg must be capable of sustained operation at these low duty cycles. (Where preprogrammed attitude/spin balancing based on a calibration of the final installation is used during velocity control, the thrusters providing the attitude/spin functions may also be required to operate at low duty cycles.)

For the probe mission first midcourse, for example, velocity control engines on the aft skirt (Configuration D-1) are required to provide less than 1% of the total impulse. With the forward engines operating in their normal mode (0.586 second on at 0.2 cps), the aft engines would only be required to deliver a 24.4-millisecond pulse (5 sectors) every 14 spacecraft revolutions. This corresponds to 0.014 cps and 0.03% on-time. For the tangential doublets configuration, this impulse would be divided between the two aft engines. Corresponding values for the radial pairs configuration would, typically, be one pulse every three revolutions or 0.01% on-time. The MR-50 thruster has demonstrated capability for operation over the complete spectrum of duty cycles required for Planetary Explorer.

4.1.2.4 Cold Starts

Past experience with monopropellant engines has indicated that repetitive cold starts represents a major source of engine degradation. The MR-50 REA used as a baseline for this study has been flight qualified for a cold-start capability of 50. Additional work is under way under an Air Force contract to study in more detail engine degradation under repeated cold starts.

Review of the Planetary Explorer mission profiles reveals that only a very limited number of cold starts is necessary. Equilibrium thruster temperatures in the vicinity of Venus are above the cold start level; hence, only the initial phases of the mission (up to acquisition of cruise attitude after second midcourse correction) are of concern. An exception to this might occur if the engines were required to fire after cooldown in the shadow portion of Venus orbit.

Examination of the three basic propulsive functions separately for the basic mission sequences indicates that the spin control can be accomplished with only three cold starts, attitude control with four, and velocity control with two. Review of the basic thruster/spacecraft configuration indicates that the cold starts for spin and attitude control are, because of the sharing of the functions by the various engines, not additive; hence, the maximum number of cold starts a particular engine may see in the basic mission profile is four. Two additional starts were added to account for spin/attitude maintenance contingencies to give the values in Table 4-4. Thus, a very high margin exists between demonstrated cold-start capability of the engine and that required for the Planetary Explorer mission. Cold starts do not, therefore, represent any problem or concern for the study herein.

4.1.3 Thrust/Pressure Profiles

The propulsion system thrust profiles are dependent on total tank volume and required propellant as well as on the characteristics of the thruster used. Figure 4-1 shows tank pressure blowdown ratio as a function of propellant required for six and nine tank groups of the two most likely tank candidates. Also indicated on the curves are the corresponding values for each of the candidate configurations. These blowdown ratios depend directly on the candidate propellant requirement. Higher blowdown ratios will occur on the probe vehicle and in the INTELSAT-III tank.

Pressure drop characteristics of the MR-50 engine are shown in Figure 4-2 where vacuum thrust is plotted as a function of propellant tank pressure. Curves are provided for use of the nominal trim

Table 4-4. NOMINAL DUTY CYCLE REQUIREMENTS

	Function		
	Spin Control	Attitude Control	Velocity Control
Typical duty cycle	Steady-state burn up to 240 sec	Pulse widths of 0.025 to 0.600 sec at 10% on-time	Pulse widths of 0.025 to 0.600 sec at 0.01% to 10% on-time
Total cycles *	10	10^3	10^4 ⁽¹⁾
Total impulse (lbf-sec)	0.08×10^3	1.2×10^3	1.2×10^4
Cold starts	5	6	2

(1) Midcourse spin stabilization to 60 rpm could increase cycles to 3.5×10^4

30

11040-30

4-7

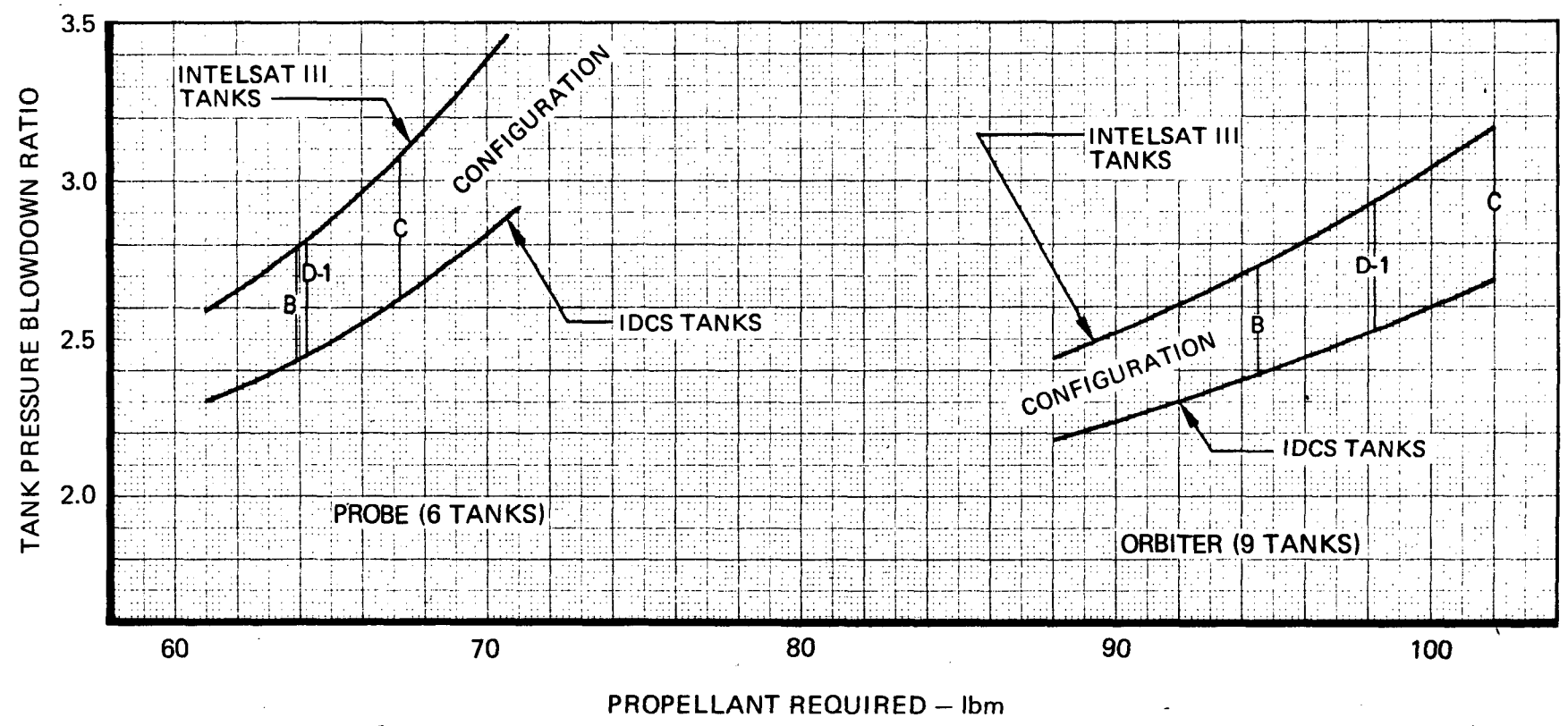


Figure 4-1. EFFECT OF TANK SELECTION AND PROPELLANT REQUIREMENT ON BLOWDOWN RATIO

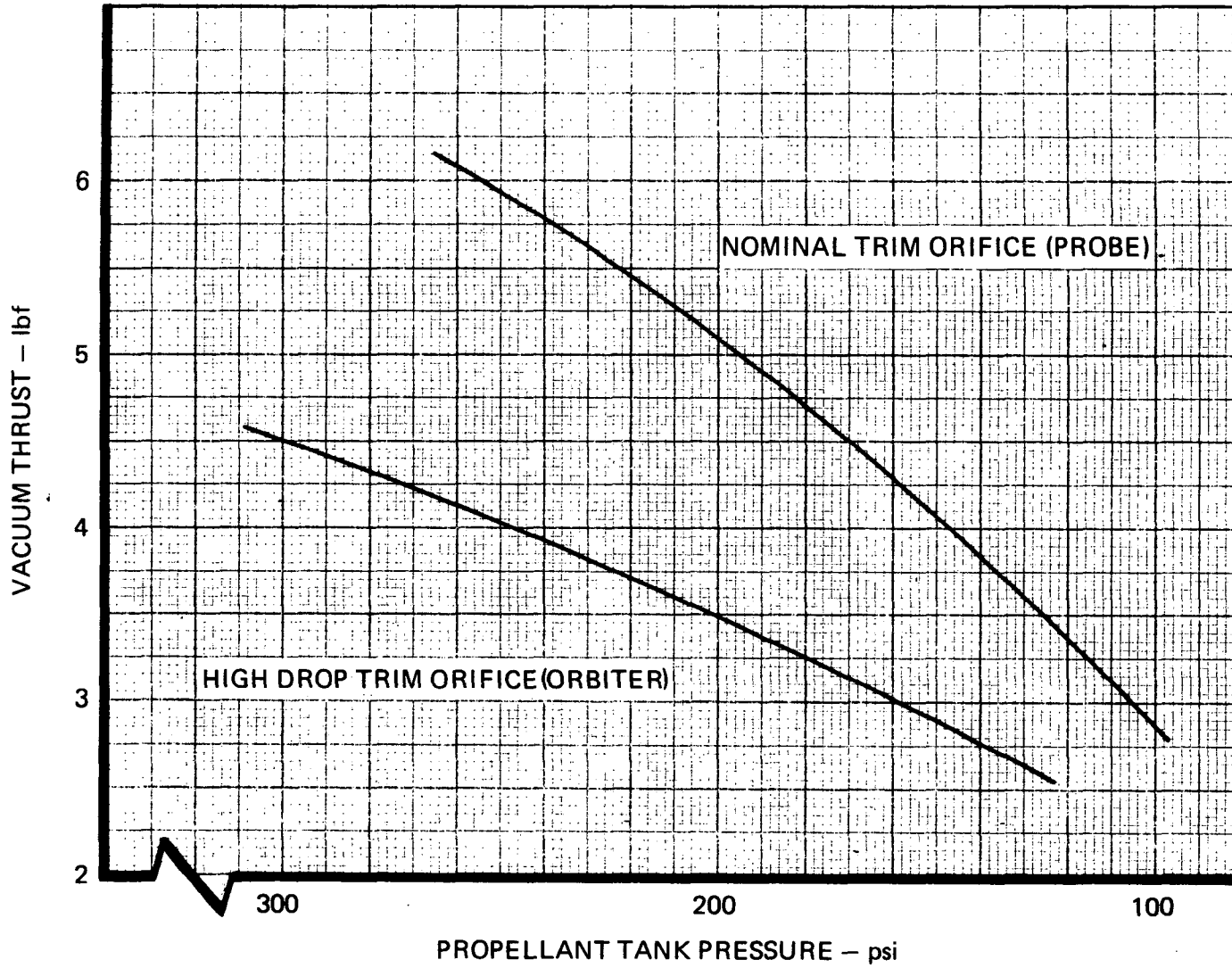


Figure 4-2. MR-50 THRUST/PRESSURE PROFILE

orifice or the high pressure drop trim orifice. As indicated in paragraph 2.2, a major concern in setting the thrust schedule for probe vehicles is maintaining a minimum thrust of approximately 3 lbf at the end of the blowdown cycle in order to maintain capability to meet the spin rate change requirement in the degraded (one-engine-out) mode. From Figures 4-1 and 4-2, it can be seen that it is possible to meet this condition for the lower propellant weight systems without incurring excessively high initial tank pressures or thrust levels with the nominal thruster trim orifice and the IDCS tank. For the orbiter vehicle, initial thrust should be limited to about 4.5 lbf in order to meet the attitude resolution requirement in the early phases of the mission. In order to do this and not have the end-of-mission thrust fall to an excessively low level (outside the qualification test range), it appears necessary to use the high pressure drop trim orifice and the ICDS tank. Because of the low initial thrust requirement, initial tank pressure will not be excessively high.

More detailed thrust schedules are presented in Figures 4-3 and 4-4 and Table 4-5. These are based on the propellant requirements of the radial pairs ("B") configuration. Figure 4-3 presents thrust level as a function of propellant consumed and indicates the thrust levels at which the various mission maneuvers will be conducted. Similar curves for other configurations can be readily prepared from Figures 4-1 and 4-2. Table 4-5 gives a detailed breakdown of the various operating parameters and pressure drops for the initial and final points on the blowdown cycle.

4.1.4 Power Profiles

The propulsion system power demands are summarized in Table 4-6. The requirements are given for the various propulsive maneuvers and for other power-consuming components which make up the propulsion system. These data enable constructing a power-time profile for any mission sequence. The only configuration dependent item is the thrust chamber valve power during velocity control maneuvers. The differences shown are brought about by the numbers of thrusters required for velocity correction for the various candidate configurations. The ranges shown correspond to the range of power demands corresponding to the percent use of the upper and lower thrusters which will be programmed to prevent excessive disturbance torques. The values are based on average thrust levels and spacecraft mass properties. To a first approximation, the reduction in thrust level due to feed pressure blowdown and the reductions in spacecraft weight tend to keep these rates somewhat constant.

The maneuver data are further based on the 42-degree (120 sector) firing angle which corresponds to the design rotational efficiency of 98%. Maneuver duration can be shortened by increasing the firing sector angle. This will result in a corresponding increase in average power consumption. Peak power will be unaffected.

Instrumentation excitation power is listed on a per-channel basis, since some flexibility exists in establishing the flight instrumentation. Recommendations are given in the next section. Pressure transducer power requirements could be considerably reduced through the use of a potentiometer-type unit.

A discussion of power reduction concepts is provided in Appendix C.

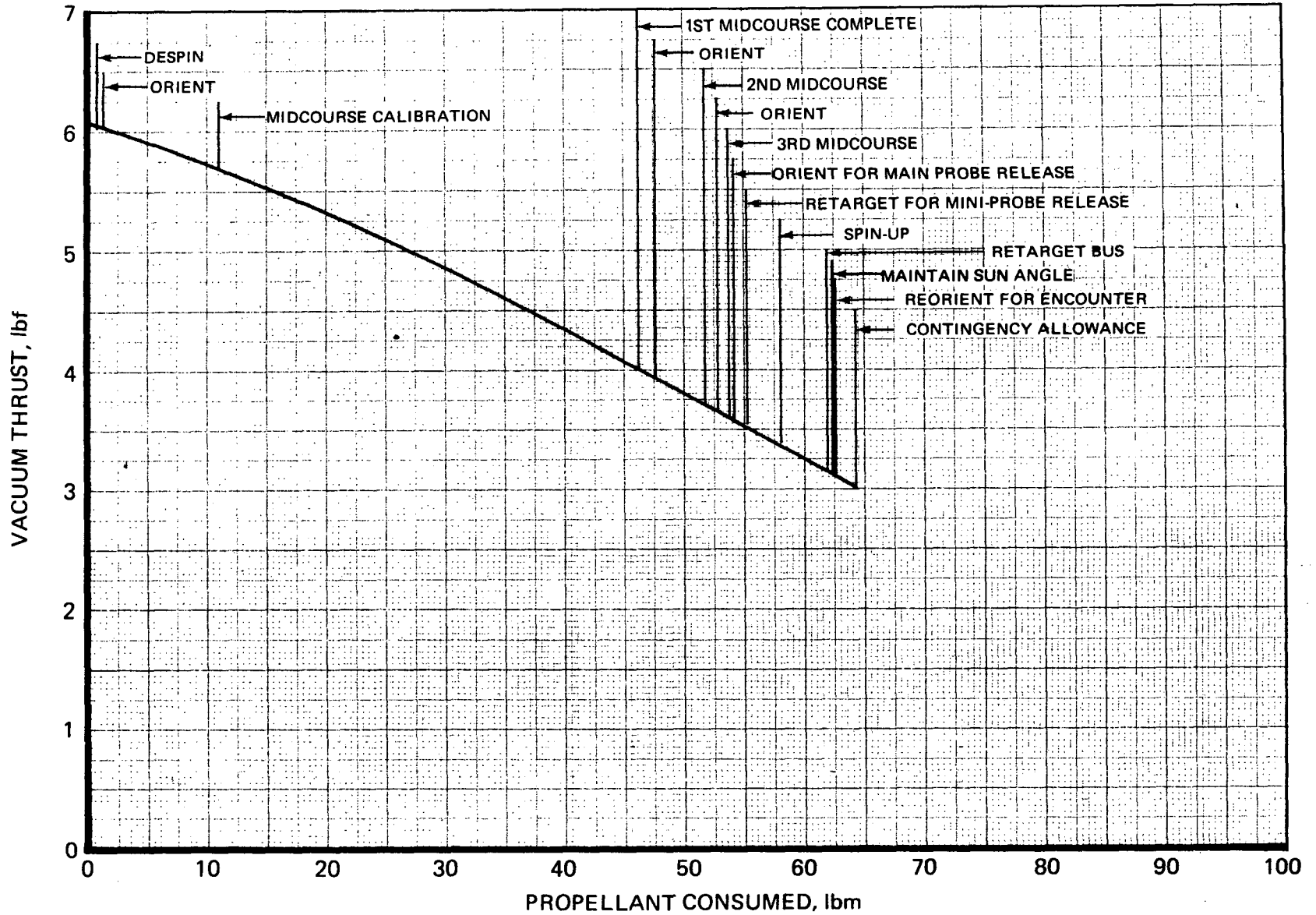


Figure 4-3. TYPICAL THRUST/MISSION PROFILE – PROBE (CONFIGURATION B)

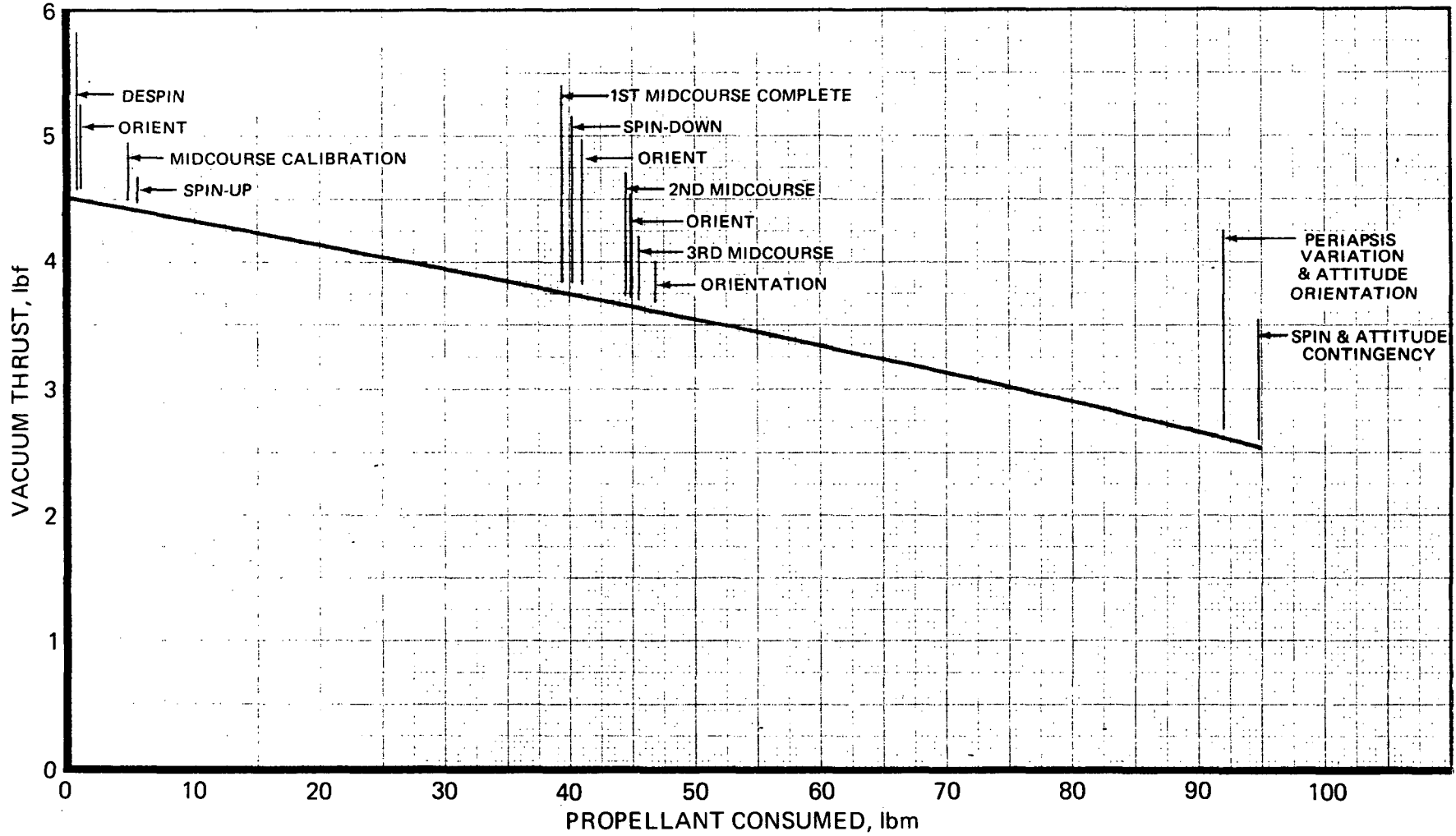


Figure 4-4. TYPICAL THRUST/MISSION PROFILE – ORBITER
(CONFIGURATION B)

Table 4-5. THRUST AND PRESSURE SCHEDULE

	Probe		Orbiter	
	Initial	Final	Initial	Final
Tank Pressure, psia	260.0	106.3	300.0	124.8
Performance parameters				
Thrust, lbf	6.11	3.03	4.53	2.53
Specific impulse, lbf-sec/lbm	227.9	226.5	227.3	226.1
Flow rate, lbm/sec	.0268	.0134	.01991	.01119
Characteristic velocity, ft/sec	4,245	4,230	4,239	4,226
Thrust coefficient	1.727	1.723	1.725	1.722
Chamber pressure, psia	114.7	57.1	85.1	47.7
Bed loading, lbm/sec-in ²	.0246	.0123	.0182	.0103
Ammonia dissociation, %	63.2	65.6	64.2	66.3
Pressure drops, psid				
Feed system	6.7	1.7	3.7	1.2
Orifice	26.3	6.6	139.0	43.9
TCV	38.1	10.9	22.3	7.9
Injector	52.4	17.7	32.9	13.4
Upper bed	10.9	6.1	8.5	5.3
Lower bed	10.9	6.2	8.6	5.4

4.1.5 Instrumentation Recommendations

The basic concept of ground commanded operation and availability of primary/secondary operational modes implies the need of fairly extensive instrumentation for command determination and diagnostic evaluation. Typical instrumentation recommendations are illustrated in Figure 4-5 and summarized in Table 4-7. The basic schematic diagrams provided at the outset of the study indicated a pressure transducer in the tank outlet line. This pressure transducer should be retained and supplemented with pressure instrumentation downstream of the isolation valves. This additional pressure measurement capability will provide a backup for the tank outlet pressure used for thrust/duty cycle determination and propellant reserve indication and, in addition, provide a positive indication of isolation valve functioning and filter condition.

Temperature measurement to verify operation of each thruster along with alternate propellant tank temperature indication to verify spacecraft thermal balance and provide fine correction for performance determination are also recommended.

Table 4-6. PROPULSION SYSTEM POWER CONSUMPTION

Event or Item	Power Reqmt, watt		Duration	
	Peak	Average	Orbiter	Probe
Spin change	22.2	22.2	0.45sec/rpm	1.05 sec/rpm
Attitude orientation	22.2	2.6	1.29 sec/degree	2.17 sec/degree
Velocity change: { A, E	11.1	1.3	136 sec/mps	160 sec/mps
Configuration { B, D	22.2	2.6-1.3	68-136 sec/mps	80-160 sec/mps
{ C	44.4	5.2-2.6	34-68 sec/mps	40-80 sec/mps
Isolation valve actuation	62.7	—	0.035 sec/actuation	0.035 sec/actuation
Heaters	0.1	0.1	Launch + 30 days	
Pressure transducers ⁽³⁾	0.28 watts/channel		(3 channels recommended)	
Temperature transducers ⁽³⁾	0.14 watts/channel		(11 channels recommended)	

NOTES: (1) See Appendix C for discussion of power reduction concepts.

(2) Maneuver data based on primary system only at average thrust level in cruise phase, double power, and halve valve duration for use of both primary and backup systems.

(3) Conditioning included, thermocouples assumed; thermistors can be used for tank temperature measurement (3 channels)

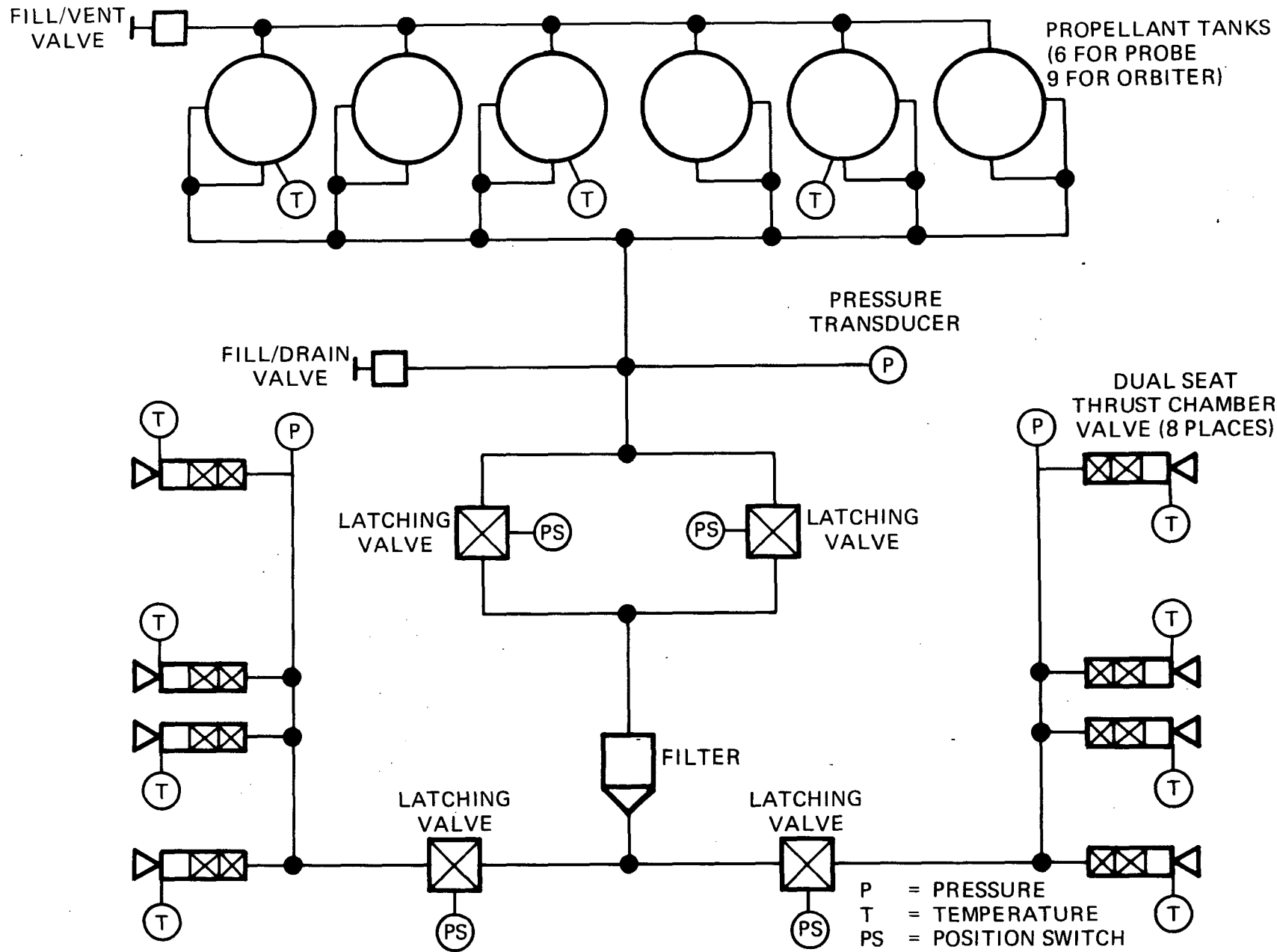


Figure 4-5. INSTRUMENTATION RECOMMENDATIONS

Table 4-7. PLANETARY EXPLORER PROPULSION INSTRUMENTATION

Measurement	Purpose
Tank outlet pressure	Performance/duty cycle prediction Propellant management
Thruster manifold pressure	Backup tank outlet pressure Verify isolation valve function Indicate filter condition
Propellant temperature	Propellant management Thermal balance
Thruster temperature	Thruster operation
Latch valve position	Isolation valve actuation

Latching valves should have position indication switches to indicate actuation. These switches will indicate only that the valve has stroked, however, and provide no indication of leakage.

If it becomes necessary to reduce the instrumentation, elimination of the thruster thermocouples on the backup thrusters and the pressure transducers in the thruster manifolds can be considered. This can be considered consistent with the single malfunction concept of redundancy. Should a malfunction occur in the primary branch, this could be isolated and operation switched to the second branch. A second malfunction would then be required to cause loss of propulsive capability. Consideration could also be given to reducing the number of temperature measurements. These reductions in instrumentation are undesirable, however, since they reduce the ability to determine and command the required propulsion maneuvers and the ability to isolate and correct or circumvent anomolous behavior should it occur.

4.2 COMMAND LOGIC

All maneuvers for the Planetary Explorer mission are to be ground commanded. The commands required depend on the on-board capability for a stored guidance logic program. That is, the number of command bits may be reduced by including more logic on-board. To demonstrate these alternate approaches, two command systems are considered, the first being primarily ground commanded and the second taking maximum advantage of on-board logic to reduce the number of commands. The same command systems are capable of controlling movement of the gimbal actuators, assuming that these actuators are controlled by stepper motors.

4.2.1 Ground Commanded Systems

The commands for each engine are derived from the following sequence which lists the commands, their purpose, and the number of bits required:

Command	Purpose	Number of Bits
1	Stop, thruster/actuator/latch valve	4
2	Start sector number (1-1,024)	10
3	Fire for (1-1,024) sectors	10
4	Fire every (1-16) spin periods	2-4
5	Fire (1-8,192) times	11-13

The 16 combinations obtained by decoding the first four bits are used to select/command the following functions. One combination (logically 0000) is employed as a stop command and, when decoded, immediately sends off commands to both latching valves, terminates all thrusters, and resets the command register. Four combinations are employed to command two gimbal actuators each in two directions. Eight combinations select up to eight thrusters, and two are used for latching valves. The remaining combination is employed as the "no-thruster" command used to fill out the command format when less than the full complement of thrusters is to be commanded on.

The second instruction provides for capability to start the commanded event at any rotational angle while the third instruction sets the duration of the pulse from one sector to steady state on time. Some configuration dependency may exist in Item 4. The gimbale velocity control engines would normally fire every spin period hence for configurations A and E. This instruction may be unnecessary. The velocity control engine furthest from the center of gravity in configuration B may fire once every three revolutions (2 bits) while on configurations C and D-1 this rate may be up to once every 14 revolutions (4 bits).

Item No. 5 generates the stop command by counting the number of firing pulses. There is no need to duplicate this for each engine, rather a master counter (with possible redundancy) would be used to terminate all engines. If an accelerometer or other device was used to generate the stop command the individual engines could be programmed with a 28 bit word. To these basic commands must be added a command for access to the guidance program and, finally, an execute command. The required combination of bits (exclusive of the access code) required for each configuration was determined on the basis of the thruster arrangement, maximum number of thrusters required for a given maneuver, simultaneous correcting disturbance torques, and use of a master termination counter. These results are as follows:

	Configuration	A	B	C	D	E
a.	For maximum rates (both redundant systems)	139	175	254	187	139
b.	Nominal rates	118	131	150	137	118

The basic logic for decoding and implementing one set of thruster commands is shown in block diagram form in Figure 4-6. The logic involves primarily setting up counters to control the timing and number of pulses. A post-maneuver "vernier" in which a high-rate maneuver is to be ended with a short pulse for fine resolution, would have to be commanded separately.

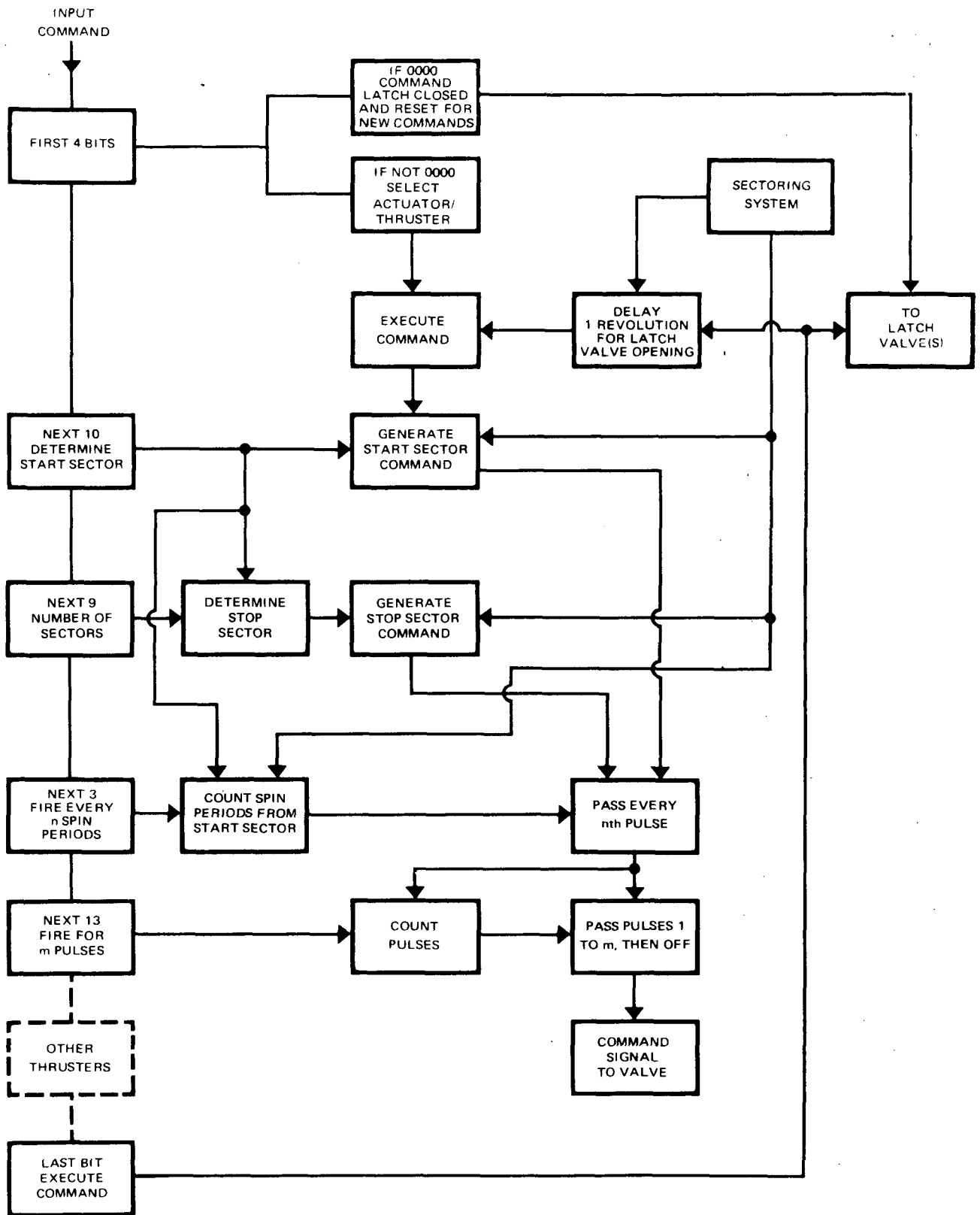


Figure 4-6. COMMAND LOGIC DIAGRAM

4.2.2 Command System Employing Maximum On-Board Logic

The second approach involves using one basic command and a set of differential commands to control a pair of engines. In order to minimize the extent of the differential commands, the engines must be opposed, that is, operate from opposite sides of the redundant pairs. This approach is most satisfactory for configurations such as B, C, D, and E, but with modification it could be adapted to A as well.

The format for these commands is as follows:

Command	Purpose	Number of Bits
1	Stop	1
2	Select mode (actuator, primary, backup, combined)	2
3	Select function (actuator up, actuator down, ΔV , precession, spin up, despin)	2
4	Start sector number (1–1,024)	10
5	Fire for (1–1,024) sectors	10
6	Fire every 1, 2, – 16, spin periods	2–4
7	Fire (1–8,192) times	11–13
8	Second engine start sector shift (0–15 sectors)	4
9	Start sector increase or decrease	1
10	Second engine pulse width increment (0–30) sectors	4–7
11	Pulse width increase or decrease	1
12	Execute	

With this command format, the first bit is the stop command, functioning as in the previous description. The next two bits select between four modes of operation which define whether both halves of the propulsion system are to be selected or which of the two redundant pairs is to be selected, or if the actuator is to be repositioned. The next two bits determine the function to be performed such as ΔV , precession, spin direction, or actuator direction. Since these combinations include six functions, two of the combinations carry double information such as spinup, actuator up as one combination, and spin down, actuator down as another. Which function is to be performed is determined by the previous mode selection; that is, previous selection of spin mode is used to select spin function from the spin/actuator combination. The next four commands are identical with the previously discussed command approach, defining pulse width and timing of the pulse. Decoding of the mode and function commands uniquely defines the engine to which the first set of commands is directed as well as the engine to-which the differential commands are applied (if maximum rates are being commanded).

The next four bits provide for a shift in start sector to account for known differences in centroid location between engines. The next bit in this command sequence defines the direction of the start shift as plus or minus.

Four bits define a pulse width increment of 0 to 15 sectors. This increment is added to or subtracted from the beginning and end of the pulse via the logic; that is, start time is one sector

greater or less and stop time is one sector less or greater, thus giving an effective change capability of 30 sectors. The next bit defines whether the pulse width increment is plus or minus. The second pair of engines would obtain a similar set of commands. With this command format configurations A and E require 112 bits and configurations B, C, and D require 103, 77, and 105 bits respectively. This includes capability for maximum rate maneuvers and simultaneous correction of attitude disturbance torques. A master counter or externally generated shutdown signal is assumed for ΔV maneuvers.

4.2.3 Effect of Gimballed Engine on Guidance Logic

The basic command logic is capable of actuating a stepper motor for a gimbal actuator as well as the propellant valves. The primary drawback of the gimbal actuator is that a delay timer may have to be introduced into the engine control circuit to allow time for the actuator to move the engine. Alternately, the actuator may be given a stepping sequence which permits it to roughly track the cg travel over the duration of the firing.

4.3 PROPELLANT DUMPING

4.3.1 Retaining Excess Midcourse Propellant

In view of the intuitively undesirable aspects of dumping propellant carried thus far in the mission, the implications of carrying the excess midcourse propellant into orbit were investigated.

The ratio of the injection velocity not attained during retromotor firing due to the added weight of the unused midcourse propellant to the velocity that can be derived from that excess midcourse propellant once injected into orbit is as follows:

$$f = \frac{g I_{ss} I_n \left(\frac{M_o - M_{pm}}{M_o - M_{pm} - M_{ps}} \right) - g I_{ss} I_n \left(\frac{M_o}{M_o - M_{ps}} \right)}{g I_{sm} I_n \left(\frac{M_o - M_{ps}}{M_o - M_{pm} - M_{ps}} \right)}$$

where:

- M_o = Initial mass
- M_{pm} = Monopropellant mass
- M_{ps} = Solid Propellant mass
- I_{ss} = Solid propellant specific impulse
- I_{sm} = Monopropellant specific impulse

This reduces to:

$$f = \frac{I_{ss}}{I_{sm}} \left[1 - \frac{I_n \left(\frac{M_o}{M_o - M_{pm}} \right)}{I_n \left(\frac{M_o - M_{ps}}{M_o - M_{pm} - M_{ps}} \right)} \right]$$

The monopropellant specific impulse should, of course, be adjusted for rotational efficiency. For all practical values of specific impulse and propellant load, the factor f is found to be less than unity, indicating a net gain in orbital maneuver capability by not dumping the excess midcourse propellant (see Figure 4-7).

For a typical Planetary Explorer mission, the increase in periapsis change capability as a function of unused midcourse propellant is shown in Figure 4-8. The total change capability and that required to make the necessary apoapsis altitude correction is indicated. A net increase in periapsis change capability of nearly 700 kilometers is indicated if no midcourse propellant is consumed prior to orbit injection. It should also be noted that the $\pm 1\%$ impulse predictability of the solid retromotor could result in an additional loss of slightly over 100-kilometer periapsis change capability.

Since the midcourse propellant load is based on 3-sigma injection errors and the total periapsis change capability actually required may be somewhat arbitrary, adjusting the total propellant load to deliver the specified 1,500-kilometer periapsis change capability at 50% confidence level suggests itself as a weight-saving measure. On the basis of nominal values, 8.5 pounds of propellant could be saved by this approach. If a 3-sigma midcourse correction must be made subsequent in orbit, periapsis change capability will only be reduced to approximately 1,200 kilometers.

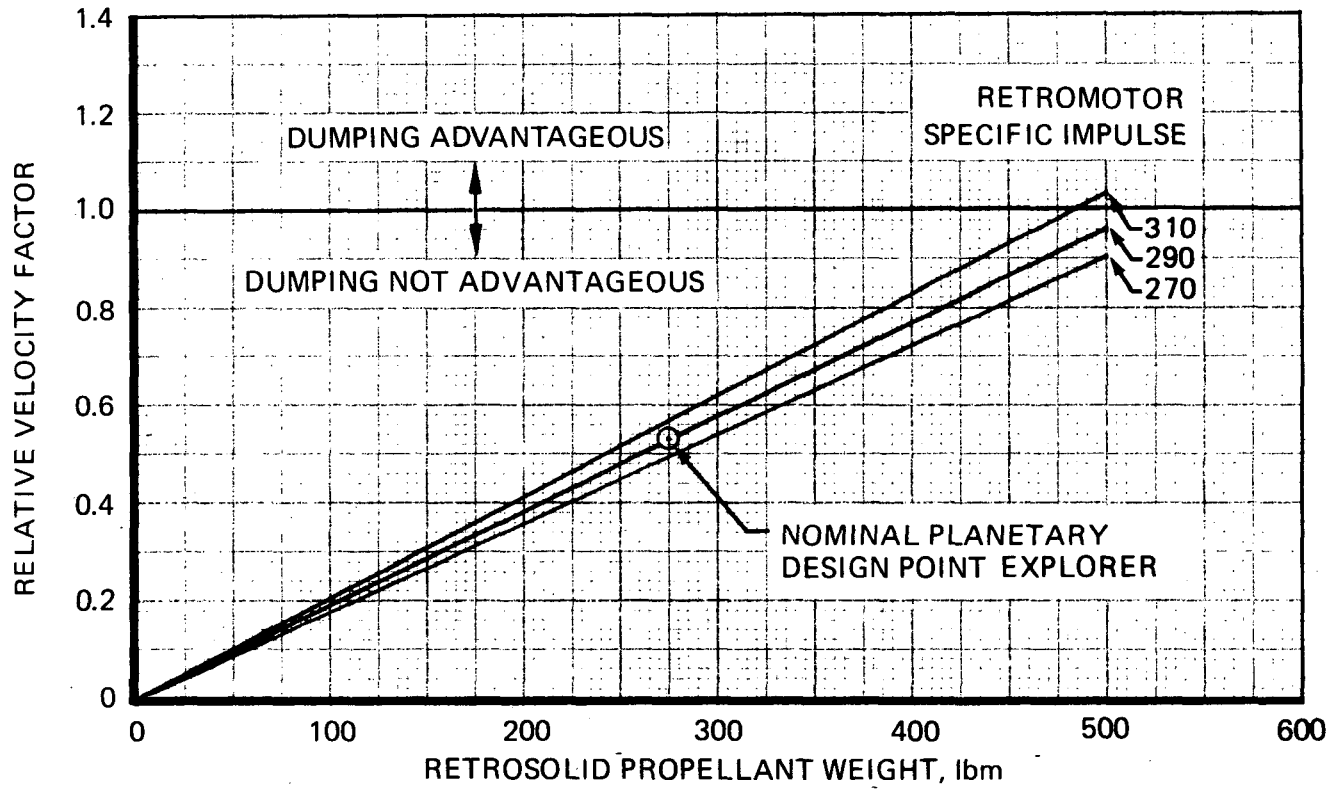
4.3.2 Varying Fixing Sector Angle

If dumping of unused midcourse correction propellant is to be required, this is best accomplished by increasing the thruster firing sector angle during midcourse correction firing so as to reduce directional efficiency and thus consume the excess propellant. This approach has the advantage of not requiring an additional maneuver or additional commands to the spacecraft and may reduce the total duration and number of pulses required for a given velocity correction. The functional dependence of various firing parameters on sector firing angle are shown in Figure 4-9.

Although total maneuver duration and number of firing pulses can easily be halved by increasing the firing sector angle from 40 to about 90 degrees, considerably larger angles are required to induce sufficient inefficiency to dissipate large amounts of excess propellant.

4.3.3 Varying Orbit Injection Retromotor Parameters

The desired initial orbit parameters could be attained with a range of excess midcourse propellant remaining by varying the injection point and firing angle of the retromotor. This approach, however, would result in a weight penalty in the form of additional solid propellant since the current approach of sizing the solid for periapsis injection with all midcourse propellant depleted represents the minimum energy case.



$M_0 = 747 \text{ lbm}$
 $M_{MP} = 42.55$
 $I_{SM} = 220$
 $R_R = 0.95$

Figure 4-7. REGIMES OF PROPELLANT DUMPING ADVANTAGE

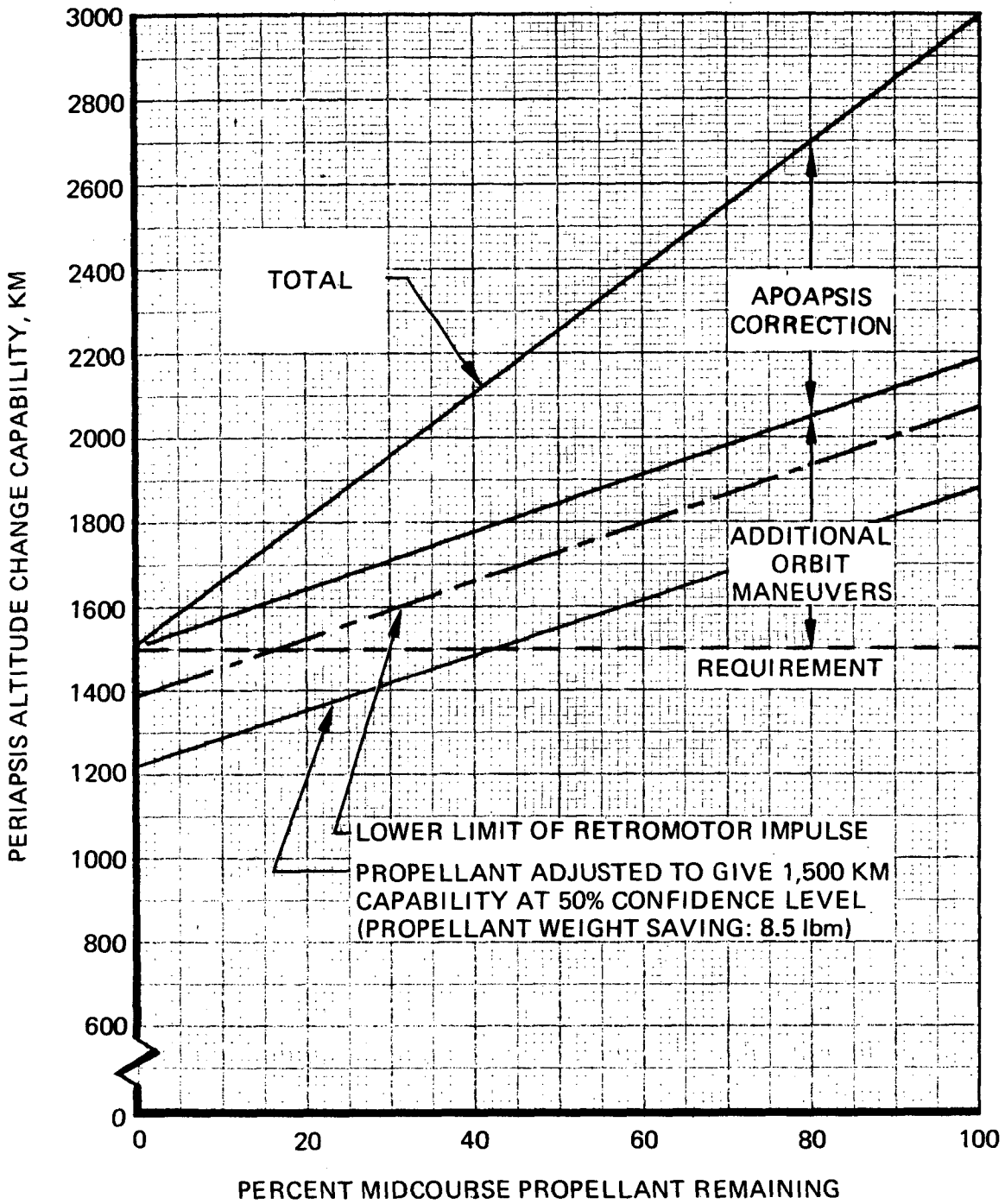


Figure 4-8. ORBIT MANEUVER CAPABILITY OF EXCESS MIDCOURSE PROPELLANT

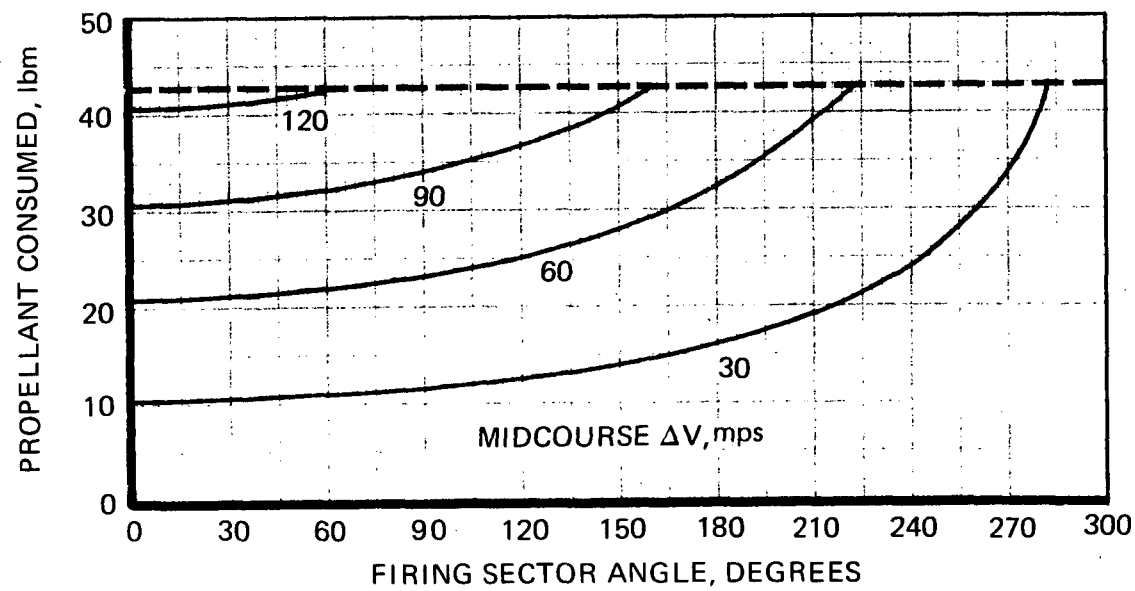
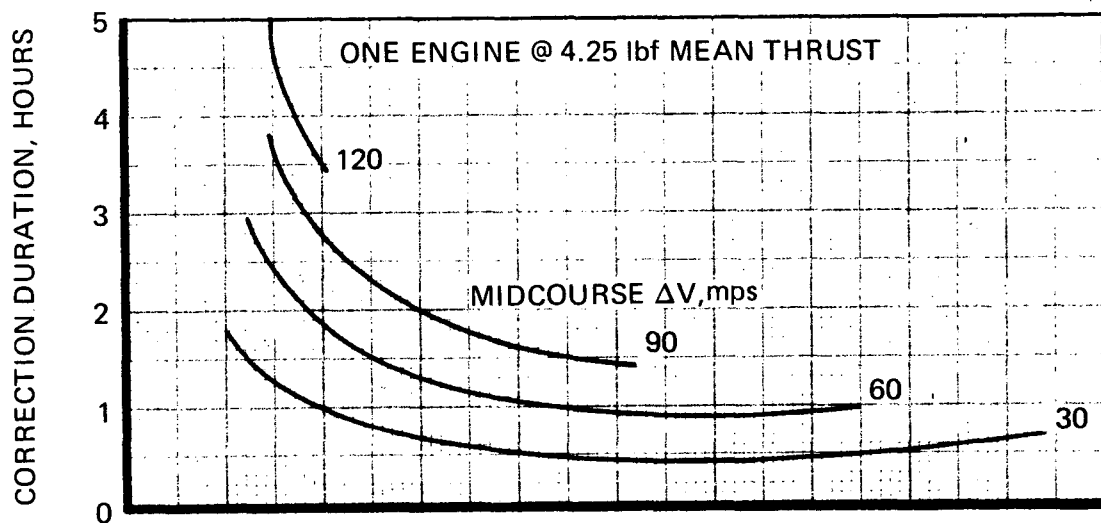
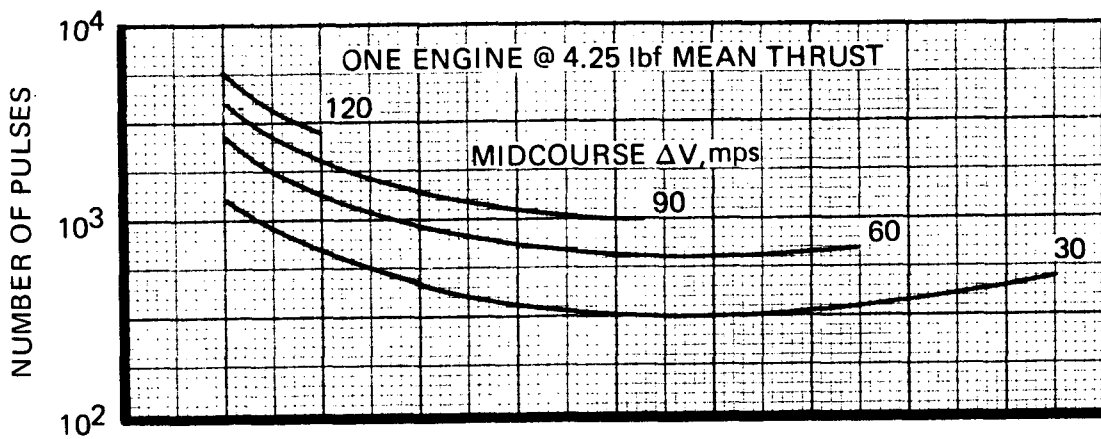


Figure 4-9. EFFECT OF FIRING SECTOR ANGLE ON MIDCOURSE AND DUMPING PARAMETERS

4.3.4 Recommendations

It is recommended that dumping of excess midcourse propellant not be included in the Planetary Explorer mission profile. This propellant should be carried into planetary orbit and used to increase the orbit maneuver capability of the spacecraft. Consideration should, if not excluded by other mission considerations, be given to reducing the total liquid propellant load to effect a subsystem weight saving at the risk of some reduction in orbit maneuver capability in the event of a very large initial trajectory injection error.

4.4 THERMAL DESIGN STUDY

The thermal design study reported in the following paragraphs was directed toward systematically developing passive design concepts compatible with the expected Planetary Explorer thermal environments using proven and durable hardware and fabrication techniques. Primary attention was focused on the thruster modules, because of their exposure to extreme solar radiation and deep space environments. These impose the most severe thermal problems. A highlight of the study was the development of an analytical procedure for computing directly, for any given module geometry, the surface radiation properties yielding minimum temperature perturbation in response to the interplanetary transit, vehicle maneuver, and Venus orbit heating/eclipse environments. The propellant tankage and line environments were also critically examined to optimize thermal control.

The design concepts presented are built around the MRM-50 rocket engine assembly which was thoroughly characterized thermally during the P-95 development program. This 5-pound thruster has been flight qualified for an extreme range of thermal environments and duty cycles. The thermal design is well suited, with minor modifications, for the Planetary Explorer vehicle. An especially useful feature is the integral radiation shield which, by channeling thruster radiation energy to space, protects the vehicle from direct exposure to hot surfaces.

The thruster modules are equipped with flat screw-on sheet metal valve cover plates to provide regular exterior surfaces which enable predictable radiation (solar absorptance/infrared emittance) properties and are easily removed for rework. Module thermal control coatings were chosen for durability and resistance to solar degradation.

Propellant tank temperature control is passive. Passive control for propellant lines is quite feasible; however, to guard against insulation damage and edge losses, those line sections which view the louvers and outer space are equipped with strip heaters. The total power requirement for the lines is 0.5 watt.

4.4.1 Hydrazine System Thermal Design Constraints

The determination of thermal design criteria for a liquid propulsion subsystem logically begins by identification of the constraints imposed by the range of mission environment and vehicle interface requirements specified by the customer and the hardware design limitations developed from RRC experience. These constraints are described below. The analyses of the following sections are aimed at systematically developing design concepts capable of satisfying these constraints.

4.4.2 Hydrazine Propulsion Systems Design Limitations

Design, fabrication, and test of hydrazine systems at RRC has identified thermal operating characteristics and hardware limitations that must be understood and considered to develop sound system thermal designs. These are enumerated below and, with the design margins computed during the analysis, are summarized in Table 4-8.

- a. All tankage, valves, and propellant lines must be maintained above the freezing point of hydrazine, 35.1°F, during operation.
- b. Maintenance of satisfactory catalyst bed operation throughout mission life requires control of bed temperature during "cold" starts.

During the Planetary Explorer Venus missions, cold-bed starts are anticipated only at initiation of the first, and possibly the second, midcourse correction.

- c. Maximum propellant inlet temperature and valve and injector design must be controlled to prevent propellant bulk boiling in the feed system. During REM-Mono overstress tests, RRC demonstrated successful pulse-mode operation feeding 160°F propellant through a valve artificially heated to above 250°F. Although design margin analyses indicated that higher operating temperatures were feasible, the demonstrated values represent realistic goals for system design.

4.4.3 Mission Thermal Constraints

The Planetary Explorer thermal environment and vehicle interface requirements for the Venus missions have been set forth in the GSFC Subsystem Specification, S-723-P-10, Reference 1. Further data on maneuver thermal constraints and on vehicle surface temperature and incident energy flux profiles were obtained from the "Planetary Explorer Phase A Report—Technical Plan," October 1969 (Reference 6). From these documents those conditions representing extreme thermal operating environments were abstracted and idealized into a worst-case mission profile. This profile, described in Table 4-9 and Figure 4-10, formed the basis for the design concept analyses following.

4.4.4 Thruster Module Thermal Design Analysis

To establish the feasibility of passive thruster module thermal control and to develop module thermal design criteria, a systematic analysis considering significant mission thermal environment constraints was conducted. The analysis focused initially on the extreme conditions of the interplanetary transit, then considered such transient episodes as vehicle maneuvers and Venus orbit shadow periods. The criteria thus evolved were used to develop a candidate thruster module design.

A detailed computer simulation of the candidate design yielded component temperature profiles and variances for the mission and thermal effects of the thruster module upon the spacecraft.

4.4.4.1 Passive Thermal Control Feasibility Analysis

4.4.4.1.1 General Mission Thermal Constraints

The most difficult thruster module thermal design problem considers the module mounted out from the spacecraft skin, relatively isolated conductively and radiatively from the vehicle. The significant

**Table 4-8. THERMAL DESIGN GOALS
(PASSIVE THERMAL CONTROL)**

Subsystem	Design Parameter	Potential Problems	Limiting Values	Design Goals	Predicted Values (Candidate Designs)
Propellant tanks and lines	Propellant temperature	1. Propellant freezing	1. 35.1°F	50°F	56-167°F ^③
		2. Propellant preheating causing injector boiling	2. 180°F	160°F	
Thruster modules	Heater power requirements	1. Propellant freezing in lines	35.1°F	Passive	0.02 watt maximum
	Minimum catalyst bed temperature	Excessive ignition delay causing bed damage	20°F	50°F	48°F (limiting)
	Valve operating temperature	1. Propellant freezing	35.1°F	50°F	57°F
		2. Propellant preheating	250°F ^①	225°F	186°F (extended operation) to 219°F (Venus orbital insertion) ^④
	Valve soakback temperature	1. Valve damage	300°F	250°F	≤235°F ^⑤
		2. Propellant boiling upon resumption of operation	280°F ^①		
	Module radiating area, solar absorption area	Acceptable temperature range	----	Optimize	----
Ratio of solar absorption areas = Z-axis normal/Z-axis pointing to sun line	Solar heating variations during maneuvers	----	Optimize	----	
Thermal control surfaces	Surface degradation caused by handling and solar exposure, elevated temperatures	----	No degradation	Gold, rhodium plating; silicone black paint	
Conduction, radiation heat transfer to vehicle	Perturbation of vehicle, solar cell heat balance	----	Minimize	Maximum instantaneous values: ^② Post mounted = 3.8 w/thruster to vehicle exterior (tangential) Skin mounted = 4.0 w/thruster to vehicle exterior, 4.1 w/thruster to interior (radial)	

① Strong function of feed pressure

② During thruster operation/soakback

③ Function of tank compartment insulation configuration (see paragraph 4.4.4.3)

④ To 241°F for configuration C

⑤ To 262°F for configuration C

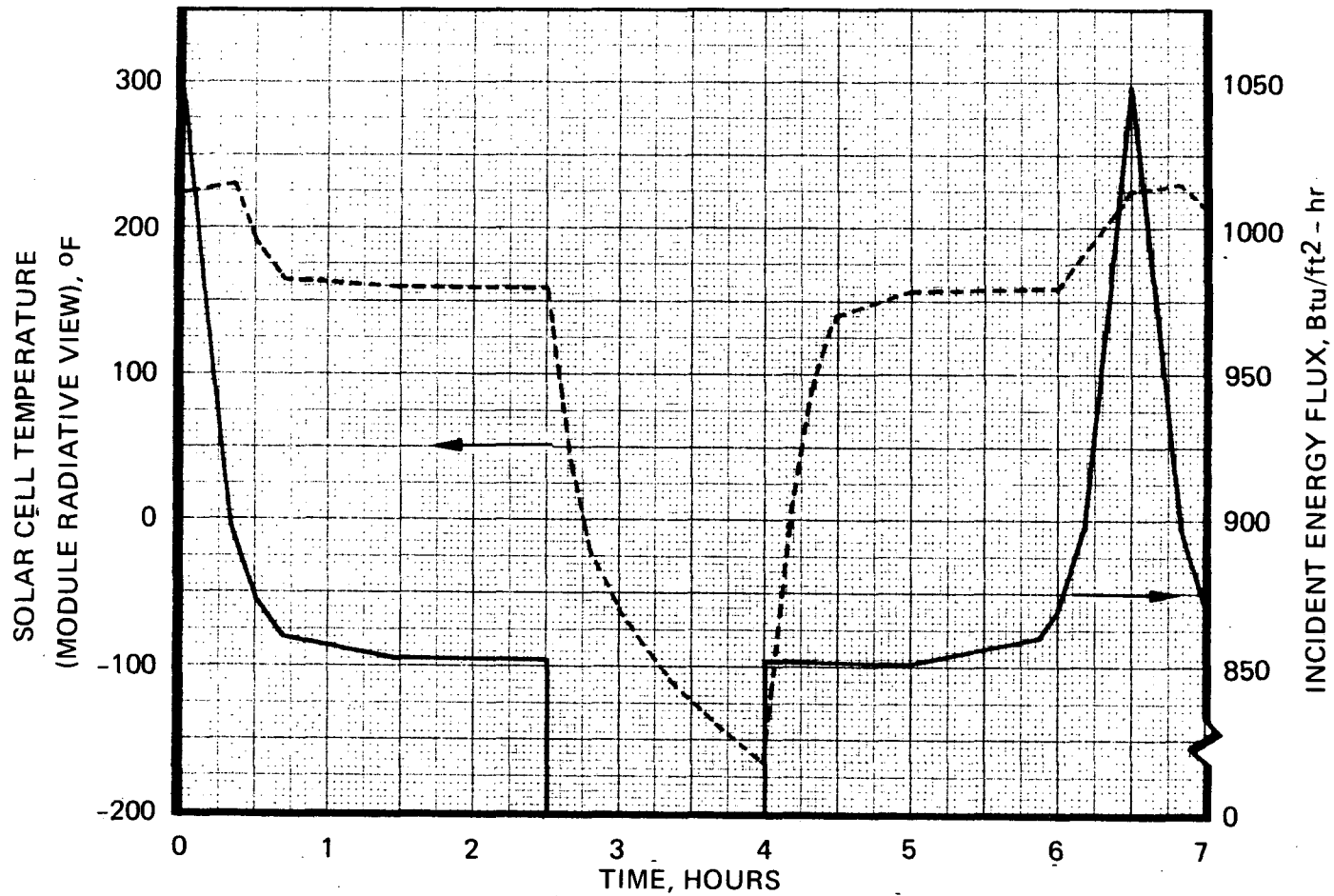
Table 4-9. IDEALIZED WORST-CASE THERMAL ENVIRONMENTS

Event	Duty Cycle (%)	Incident Energy (Btu/ft ² -hr)	Surrounding Temperatures (°F)	Comments
1. Earth vicinity (E)	---	442	Vehicle skin = 61°F Vehicle interior = 32°F conductive, -40°F radiative ¹	Minimum component temperatures
2. Venus vicinity (E)	0.1-10%	865	Vehicle = 156°F Propellant = 167°F	Maximum valve, injector operating temperatures
3. Shutdown from Event 2 (T)	---	865	Vehicle = 156°F	Valve soakback heating
4. 45°F spin axis shift on sun line for maneuvers (E)	---	858	Vehicle = 156°F (conservative)	Change in module solar exposure
5. Venus equatorial orbit, maximum shadow period (T)	---	0 to 1048	Vehicle skin = -166°F to +240°F Module mounts to 156°F	Maximum instantaneous heating Maximum (1.5-hour) shadow period

E = Equilibrium analysis

T = Transient analysis

¹Lower temperature as defined by Mr. Donald Miller at Concept Selection Meeting, RRC, 8-3-70.



ADAPTED FROM PLANETARY EXPLORER TECHNICAL PLAN
(PHASE A REPORT, PP 4-58, 4-59)
20,000 KM APOPSIS
1,000 KM PERIAPSIS

**Figure 4-10. THRUSTER MODULE
WORST-CASE VENUS ORBIT HEATING AND SHADOW ENVIRONMENT
(AS USED IN THE COMPUTER SIMULATION)**

thermal mission factors are solar heating and radiative cooling to space. Assuming as a first order approximation an isothermal module, the governing energy relation is:

$$c\rho V \frac{dT}{d\theta} = \alpha_s A_s K_s - \sigma \epsilon A_e T^4 \quad (4-1)$$

Where:

$c\rho V$ = Module thermal mass

T = Module temperature

θ = Time

α_s = Module average solar absorptance

ϵ = Module average infrared emittance

K_s = Solar heat flux

σ = Stefan-Boltzman constant

A_s, A_e = Effective areas for solar heating and radiation to space, considering reflections off the vehicle.

During the initial analysis phase, only the interplanetary transit is considered where K_s changes very slowly and $dT/d\theta \doteq 0$. Equation 4-1 may then be rearranged into two immediately useful forms. The first expresses the energy balance in terms of three dimensionless factors: a surface property term, a geometry term, and an energy term and for designated minimum module temperature goal of 50°F , sets a lower limit on the product of the surface and geometry terms.

$$\left(\frac{\alpha_s}{\epsilon}\right) \left(\frac{A_s}{A_e}\right) = \frac{\sigma T^4}{K_s} \geq 0.262 \quad (4-2)$$

The second form allows computation of the passive module temperature at any point in transit. In addition it affords an estimate of influence coefficients. Rearranging 4-1,

$$T^4 = \left(\frac{\alpha_s}{\epsilon}\right) \left(\frac{A_s}{A_e}\right) \frac{K_s}{\sigma} \quad (4-3)$$

Differentiating with respect to T

$$dT = \frac{K_s}{4\sigma T^3} \left[\frac{a_s}{\epsilon} d\left(\frac{A_s}{A_\epsilon}\right) + \frac{A_s}{A_\epsilon} d\left(\frac{a_s}{a}\right) \right]$$

Now substituting equation 4-3 back in and integrating yields for small parameter changes,

$$\Delta T = \frac{1}{4} T \left[\frac{\Delta(a_s/\epsilon)}{a_s/\epsilon} + \frac{\Delta(A_s/A_\epsilon)}{A_s/A_\epsilon} \right] \quad (4-4)$$

Equation 4-3 indicates that the module average temperature may be expected to rise to slightly below 150°F during transit to Venus, a temperature encouragingly well below the long-term component design goal of 200°F. Equation 4-4, however, indicates that the temperature effect of errors and unmodeled variations in module thermal properties, if undamped by conduction and radiation to the spacecraft, may be expected to range from 1.25°F/% variation at Earth orbit, to 1.5°F/% at Venus.

The errors and unmodeled variations most frequently encountered in radiation-dependent design are of the following types:

- a. Emittance and absorption measurement errors
- b. Errors in surface radiation modeling assumptions, such as specularly and spectral distributions
- c. Simplifications in view factor/radiation interchange factor computations
- d. Internal conductive path material and dimensional variations
- e. Surface degradation caused by handling, sterilization, salt spray, exposure and solar (e.g., UV) exposure.

Rocket Research Corporation's experience in the development and qualification of the HPM and REM-Mono hydrazine subsystem designs, which were, like the Planetary Explorer, propulsion subsystem thermal design, heavily radiation dependent, has demonstrated that the first four classes of variables above either tend to cancel out or can be detected and corrected during qualification and acceptance test. However, the surface degradation problem imposes two severe design restraints for Planetary Explorer propulsion subsystem passive thermal design. Propulsion subsystems are, during assembly, acceptance test, rework, shipping, mounting and ground checkout, subjected to considerable handling; this makes use of such finishes as anodizing, dielectric films, artificial oxidizing, etc., undesirable. During the expected Planetary Explorer mission, the exposed module surfaces may receive solar radiation exposures of as much as 4,000 sun-hours. Most paints used for spacecraft thermal control degrade substantially after a few hundred sun-hours. The above considerations effectively limit thruster module thermal control surfaces to black paint and noble metal plating (such as gold or rhodium), allowing surface a/ϵ values between approximately 1 and 7.

Substituting these values into equation 4-2 indicates a possible further constraint upon module design. For a minimum temperature design goal of 10°C (283°K) at Earth vicinity, equation 4-2 yields an allowable range for the geometry term of $3.8 \leq (A_e/A_s) \leq 26.7$.

The geometry constraint thus defined is illustrated in Figure 4-11 for some representative Planetary Explorer module surfaces. The figure indicates that the lower limit is somewhat beyond reach, eliminating the possibility of all black surfaces. However, the (A_e/A_s) range remains large, allowing a considerable variety of module design possibilities.

4.4.4.1.2 Transient Thermal Events

The results of paragraph 4.4.4.1.1 above indicate that during the Earth-Venus transit, passive thruster module thermal control can be attained with reasonable temperature margins and a substantial range of surface and configuration properties. It is worthwhile now to examine the mission transient events with an eye to optimizing the design parameters. The significant tradeoffs follow.

- a. To minimize thermal soakback loads following firing, it is desirable to maximize module surface emittance.
- b. However, radiative cooling of the module during Venus orbit shadow periods may constrain the maximum surface emittance values.
- c. Module temperature perturbations during spacecraft inclinations occurring during maneuvers may further constrain module geometry and surface properties.

Venus Orbital Shadow Periods – During long periods of inactivity in Venus orbit, a dynamic temperature equilibrium is achieved during which the thruster module energy loss during shadow periods balances the energy gain during periods of solar exposure. Expressed symbolically,

$$\int_{\theta_{\text{sun}}} c\rho V dT = \int_{\theta_{\text{shadow}}} c\rho V dT \quad (4-5)$$

To establish the conditions of dynamic equilibrium, reference is again made to the module energy balance:

$$c\rho V \frac{dT}{d\theta} = a_s A_s K_v - \sigma \epsilon A_e T^4$$

where in this case K_v includes the averaged solar, albedo, and infrared energy fluxes during the sunlit part of the orbit.

For shadow period $K_v \doteq 0$, and Equation 4-1 may be rearranged and integrated directly to yield a useful relationship between surface emittance, thermal mass, and temperature drop.

$$\frac{\epsilon A_e}{c\rho V} = \frac{1}{3\sigma \theta_{\text{shadow}}} \left[\frac{1}{T_{\text{min}}^3} - \frac{1}{T_{\text{max}}^3} \right] \quad (4-6)$$

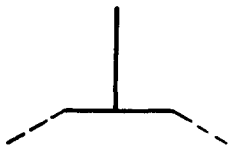
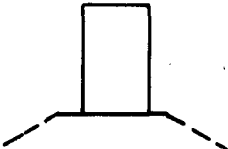
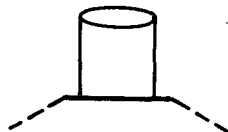
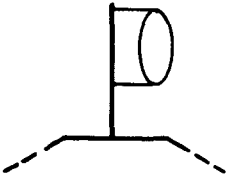
SHAPE	DESCRIPTION	GEOMETRY TERM
	PLATE PARALLEL TO FACET, NORMAL TO SUN LINE	$\frac{A_{\epsilon} \geq L \times D}{A_s \text{ per side} \leq \frac{1}{\pi} \times \frac{L}{D}} \doteq \pi$
	VERTICAL PLATE FACING TO SUN LINE	$\frac{A_{\epsilon} < 2 LD}{A_s > \frac{1}{\pi} LD} < 2\pi$
	VERTICAL PLATE PARALLEL TO SUN LINE	$\frac{A_{\epsilon} < 2 Ld}{A_s = 0} = \infty$
	LATERAL SURFACE OF CYLINDER NORMAL TO FACET	$\frac{A_{\epsilon} < 2\pi DR}{A_s > \frac{2}{\pi} DR} < \pi^2$
	CYLINDER CANTILEVERED OFF SUN-FACING BRACKET	$\frac{A_{\epsilon} < 2\pi DR}{A_s < \frac{2}{2\pi} DR} > 2\pi^2$

Figure 4-11. PLANETARY EXPLORER THERMAL ANALYSIS
THERMAL RADIATION A_{ϵ}/A_s VALUES FOR TYPICAL MODULE SURFACES
(FOR MODULE DIMENSIONS \ll VEHICLE DIMENSIONS)

where

$T_{\min, \max}$ = minimum and maximum orbital temperatures.

The temperature drop may be calculated using Equation 4-5. Rearranging 4-6 for solar exposure periods, and dividing both sides by A,

$$\frac{c\rho V}{\epsilon A_\epsilon} \frac{dT}{d\theta} = \sigma \left[\left(\frac{a_s}{\epsilon} \right) \left(\frac{A_s}{A_\epsilon} \right) \left(\frac{K_v}{\sigma} \right) - T^4 \right] \quad (4-7)$$

The first two quantities inside the brackets were defined and limited in Equation 4-2, paragraph 4.4.4.1.1 above, as

$$\frac{a_s}{\epsilon} \frac{A_s}{A_\epsilon} \geq \frac{\sigma T_{\min}^4}{K_e}$$

Substituting 4-2 into 4-7, multiplying through 4-6, and integrating

$$T_{\max} - T_{\min} = \frac{1}{3 \theta_{\text{shadow}}} \left[\frac{1}{T_{\min}^3} - \frac{1}{T_{\max}^3} \right] \int_{\theta_{\text{sun}}} \left[\left(\frac{K_v}{K_e} \right) T_{\min}^4 - T^4 \right] d\theta \quad (4-8)$$

Equation 4-8 is easily integrated numerically, and the result is shown in Figure 4-12. For the minimum design temperature goal of 50°F and the worst-case shadow orbit described in paragraph 4.4.2.1.1, it is readily calculated from Figure 4-12 and Equation 4-6 that

$$\frac{\epsilon A_\epsilon}{c\rho V} \leq 0.37 \quad (4-9)$$

For several candidate designs investigated, Equation 4-9 limited the average module emittance to space to about 0.25.

Maneuver Periods – Thus far the analysis has tacitly assumed that the module effective solar absorptance a_s and solar heating area A_s remain fixed; i.e., the orientation of the vehicle with respect to the sun line does not change. During maneuver periods, however, this orientation may vary as much as 45 degrees. Since the module solar heating parameter ($a_s A_s$) may be expected to vary with vehicle inclination, such periods may cause undesirable perturbations of the module heat balance. A first order estimate of the perturbation is obtained by subtracting Equation 4-2 from Equation 4-1 to yield

$$c\rho V \frac{dT}{d\theta} = \left[(a_s A_s)_i - (a_s A_s)_n \right] K_s - \sigma \epsilon A_\epsilon (T_i^4 - T_n^4) \quad (4-10)$$

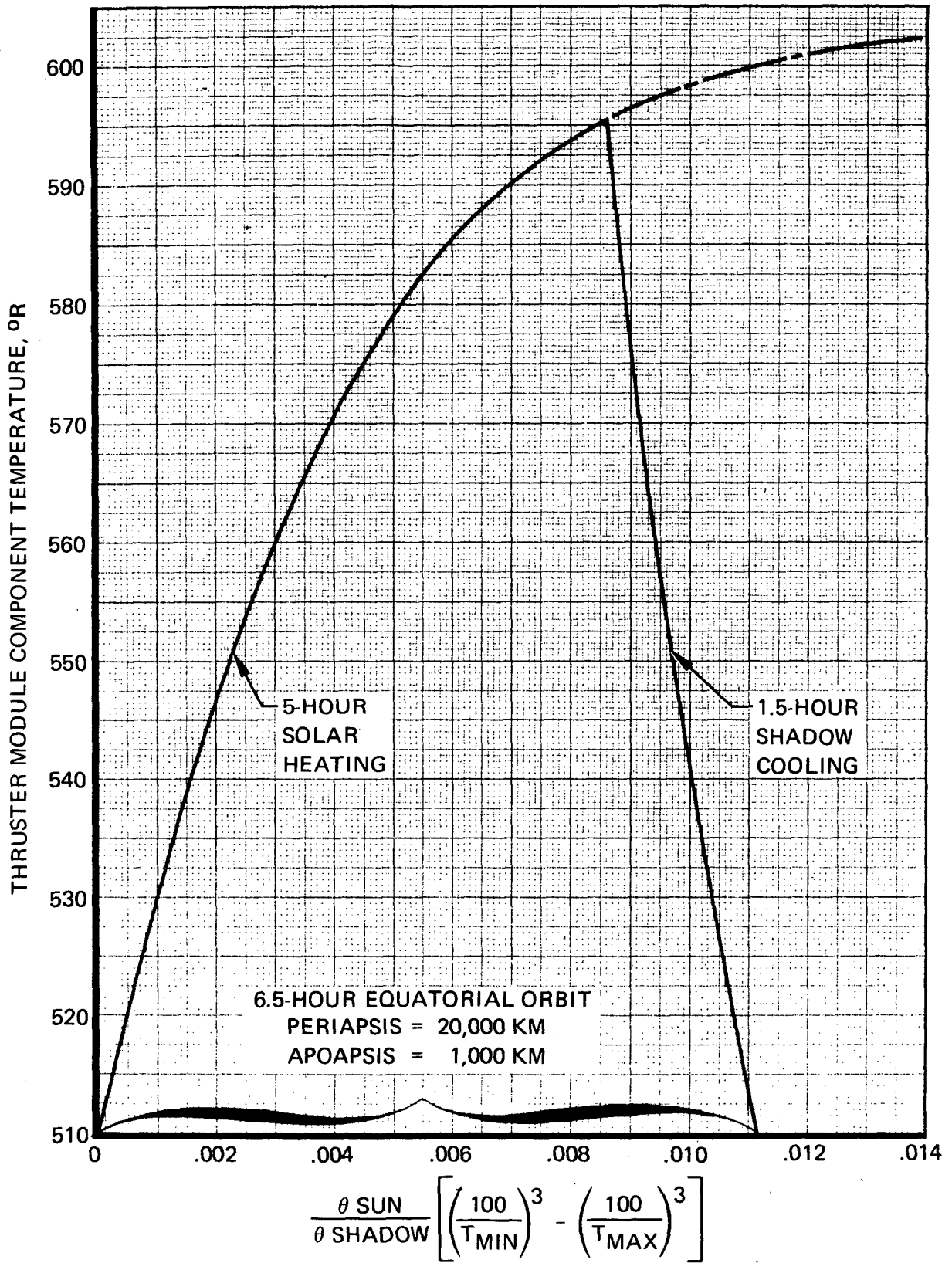


Figure 4-12. VENUS ORBIT SOLAR HEATING vs SHADOW COOLING

where the subscripts i and n denote conditions at the inclined and normal orientations respectively. Noting that maneuver periods may be long (as much as 5 hours), equilibrium ($dt/d\theta \rightarrow 0$) may be assumed and Equation 4-10 set in a more useful form

$$\frac{(a_s A_s)_i}{(a_s A_s)_n} = \left[\frac{(T_n + \Delta T_m)}{T_n} \right]^4 \quad (4-11)$$

where ΔT_m is the design margin allocated to perturbations in vehicle orientation.

Equation 4-11 allows ready evaluation of the allowable change in $(a_s A_s)$ for a given shift in vehicle inclination. Translation of this into a useful design concept, however, requires separation of the module surface areas and their solar absorptance values into orthogonal elements. Denoting parameter component normal and parallel to the vehicle XY plane by the subscripts n and z, restricting the sunline spin axis angle Φ to greater than 0 degrees, and assuming symmetry about the XY plane*,

$$(a_s A_s)_i \doteq a_n A_{sn} \sin \phi + 0.25 a_z A_{sz} \cos \phi \quad (4-12)$$

With an unlimited variety of thermal control surfaces to work with, it should in principle be possible to develop a module design to make $(a_s A_s)_i$ nearly invariant with vehicle orientation. However, the analysis of paragraph 4.4.4.1.1 above limited the usable thermal control surfaces for module design to essentially black paint coating on noncorrosive metal substrate, thus establishing a linear relationship between surface solar absorptance and emittance. In addition, the average infrared emittance has been limited by Equation 4-9. The following constraining relations may be written for $(a_s A_s)_i$. From Equation 4-9,

$$(\epsilon A_\epsilon)_i = A_{\epsilon n} \left[X_n \epsilon_c + (1 - X_n) \epsilon_m \right] + A_{\epsilon z} \left[X_z \epsilon_c + (1 - X_z) \epsilon_m \right] \leq 0.37 \text{ } \rho V \quad (4-13)$$

and from Equation 4-10

$$(a_s A_s)_i = A_{sn} \left[X_n a_c + (1 - X_n) a_m \right] \sin \phi + 0.25 A_{sz} \left[X_z a_c + (1 - X_z) a_m \right] \cos \phi \quad (4-14)$$

where X = fractional coverage of surface by paint and subscripts m and c denote metal, paint coating properties.

*A Z-axis shift results in solar heating on one end of the module while the other end remains shaded. The possibility of resultant local heating or cooling must, of course, be considered in the module internal thermal design.

Equations 4-9, 4-13, and 4-14 completely define the range of geometrics and paint patterns allowing passive thruster module thermal control. Figure 4-13 shows the simultaneous solution of the equations for representative values of module thermal properties and a maximum shift in Φ of 45 degrees. Although Figure 4-13 does not account for certain second-order factors such as variation in solar inter-reflections with Φ it provides a useful starting point for module design.

4.4.4.2 Detailed Computer Simulation of Candidate Thruster Module Designs

To test the validity of the Venus mission thermal design criteria developed in the previous subsection, detailed computer simulations of the candidate thruster module designs presented in Figures 5-3 and 5-5 were performed. The simulation ascertained mission temperature profiles and heat rejection rates to the spacecraft. In addition, thermal influence coefficients useful for estimating design margins were computed.

The analytical model used in the simulation was adapted from the REM-Mono thermal model which was instrumental in the design and qualification of the MRM-50 reaction engine assembly for the most extreme temperature and duty-cycle range yet attempted for hydrazine (Reference 7). This model incorporated several novel programming algorithms facilitating computation of radiative energy balances (Reference 8) and variation in hydrazine decomposition kinetics, and altitude chamber gas conduction with duty cycle (Reference 9).

4.4.4.2.1 Thruster Module Thermal Design

Thermal design of the candidate thruster modules was based on equations 4-9, 4-13, and 4-14 of the previous subsection. Surface radiation interchange factors to deep space and rotational average solar exposure areas for surface components normal and parallel to the vehicle XY plane were computed and inserted into the equations for solution. This procedure yielded optimum paint patterns with no need for iteration; however, control of valve soakback heating necessitated iteration to determine internal module conductive paths.

For the doublet module, separate paint pattern computations were required for the reactor shield and the valve mount bracket geometries because control of soakback loads required thermal isolation of these components. The shield and nozzle cavities presented special difficulties because of the uncertainties in analysis of specular reflectance of incident solar radiation within the cavities over the range of solar exposure angles encountered during a vehicle revolution. For the simulation, limiting values were found as follows. The rotational average absorption area-energy density product was computed for each component by numerical integration. Then for Earth vicinity, nominal material solar absorptivity values were applied (reflection ignored), and for Venus vicinity an apparent cavity absorptance accounting for reflection within the cavity was estimated using analytical data for regular cavity configurations (Reference 10). The shield paint pattern equations were adjusted for the cavity absorptances calculated for Earth vicinity, ensuring a conservative design.

MAXIMUM Z-AXIS SHIFT = 45°
 MODULE THERMAL MASS = $0.2 \text{ Btu}/^\circ\text{F}$
 EFFECTIVE EXPOSED AREA = 0.33 ft^2
 $A_\epsilon \equiv 7.5 (A_{sp} + A_{sn}); \epsilon = 0.22$
 THERMAL CONTROL SURFACES:
 BLACK COATING, $a/\epsilon = 0.90/0.90$
 GOLD SUBSTRATE, $a/\epsilon = 0.28/0.04$

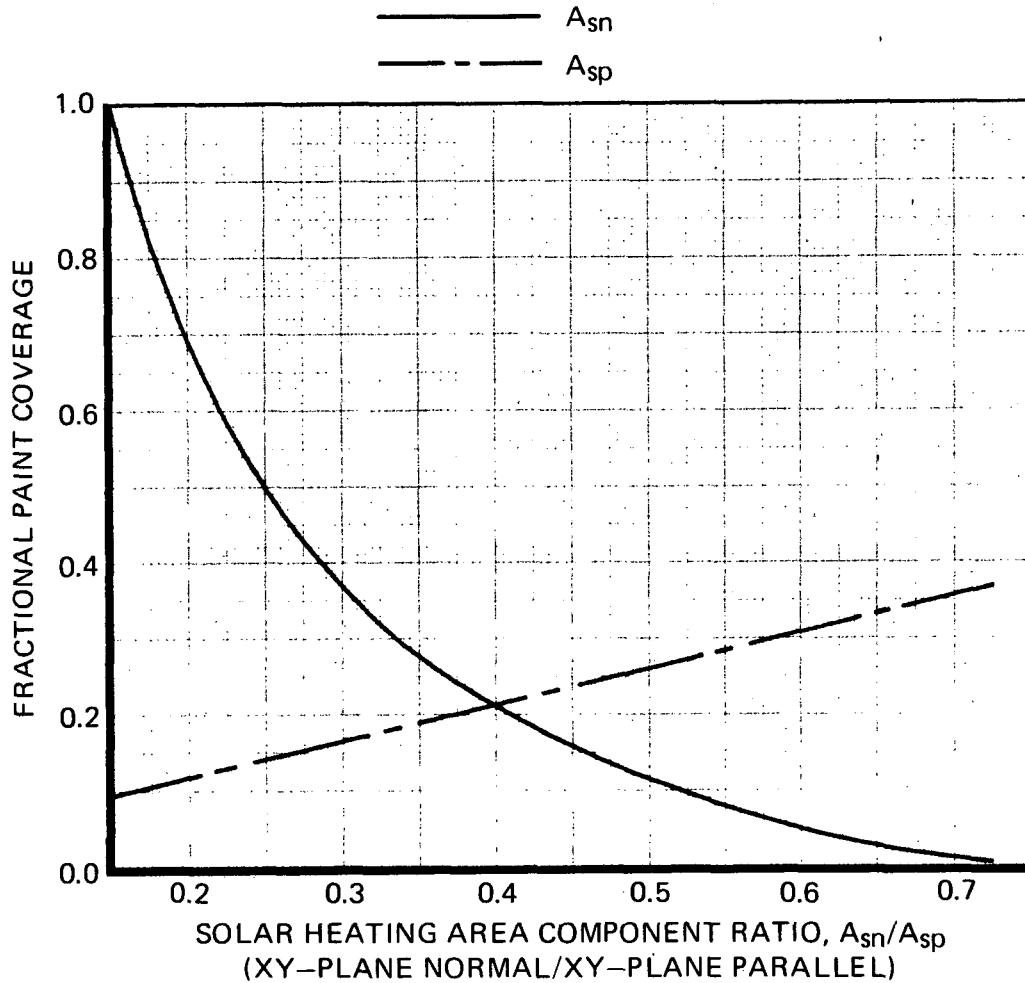


Figure 4-13. EXTERNAL THRUSTER MODULE DESIGN
 ALLOWABLE GEOMETRY FACTORS AND PAINT PATTERNS

The typical thruster mounting arrangement with resultant conductive heat transfer paths is shown in Figure 4-14. The MRM-50A thruster is thermally isolated from the module by its being supported with the feed tube and with thin tabs attached to the radiation shield. The radiation shield is designed to channel radiation from the thruster to space, thus protecting the vehicle surfaces from exposure to hot (1,500°F) reactor surfaces. Consequently, the temperature of the shield itself may exceed 400°F during operation and soakback. To protect the module from such loads, a flat 0.15-inch asbestos-reinforced phenolic insulating spacer is placed between the shield mounting bracket and the module frame. Protection from radiative soakback loads is provided by gold-plating those valve surfaces which directly view the thruster.

The module interior is designed for maximum heat transfer to evenly distribute soakback and solar loads. The valve is screwed directly to the module frame and torqued down; smooth, rigid mating surfaces ensure maximum contact conductance as was verified during the MRM-50A qualification program. The interior module surfaces and the valve surfaces they view are painted black to promote radiation heat transfer, thus further reducing module internal temperature gradients.

4.4.4.2.2 The Analytical Model

The computer simulation was performed by use of finite-difference techniques to solve an analog thermal network model of the thruster modules. The network schematic is shown in Figure 4-15. The model accounts for hydrazine propellant heat transfer in the feed system, decomposition and ammonia dissociation in the reactor, and attendant reaction and exit enthalpies. The associated computer program allows expression of such thermal parameters as material thermal conductivity and nodal heat generation as functions of time or temperature. An input option causes generation of thermal influence coefficients and variances (Reference 11).

Modeling of radiative heat transfer assumes diffuse, semi-gray surfaces. Computations were based on best available spectral emittance/absorptance data for temperature/wave length regimes of interest. Cavity radiation interchange factors were abstracted from detailed analyses by matrix methods of the nozzle and shield interiors. Though this approach glosses over significant specular components, the overall results agree reasonably with published data (Reference 11), and the agreement with test data has been excellent.

4.4.4.2.3 The Simulation

The computer simulation was performed for the mission conditions described in Table 4-9. For doublet module operation, firing of one thruster singly, or two simultaneously, over the full anticipated duty cycle range was considered. Effects of variations in material thermal properties were ascertained and design margins assigned.

The predicted temperature profiles for periods of inactivity during interplanetary transit and Venus equatorial orbit are shown in Figure 4-16 for the tangential doublet module.

Figure 4-17 illustrates operational temperatures and expected valve soakback loads for worst-case operation during orbital insertion (maximum solar energy absorbed). Sensitivity of the doublet module thermal design is indicated in Table 4-10.

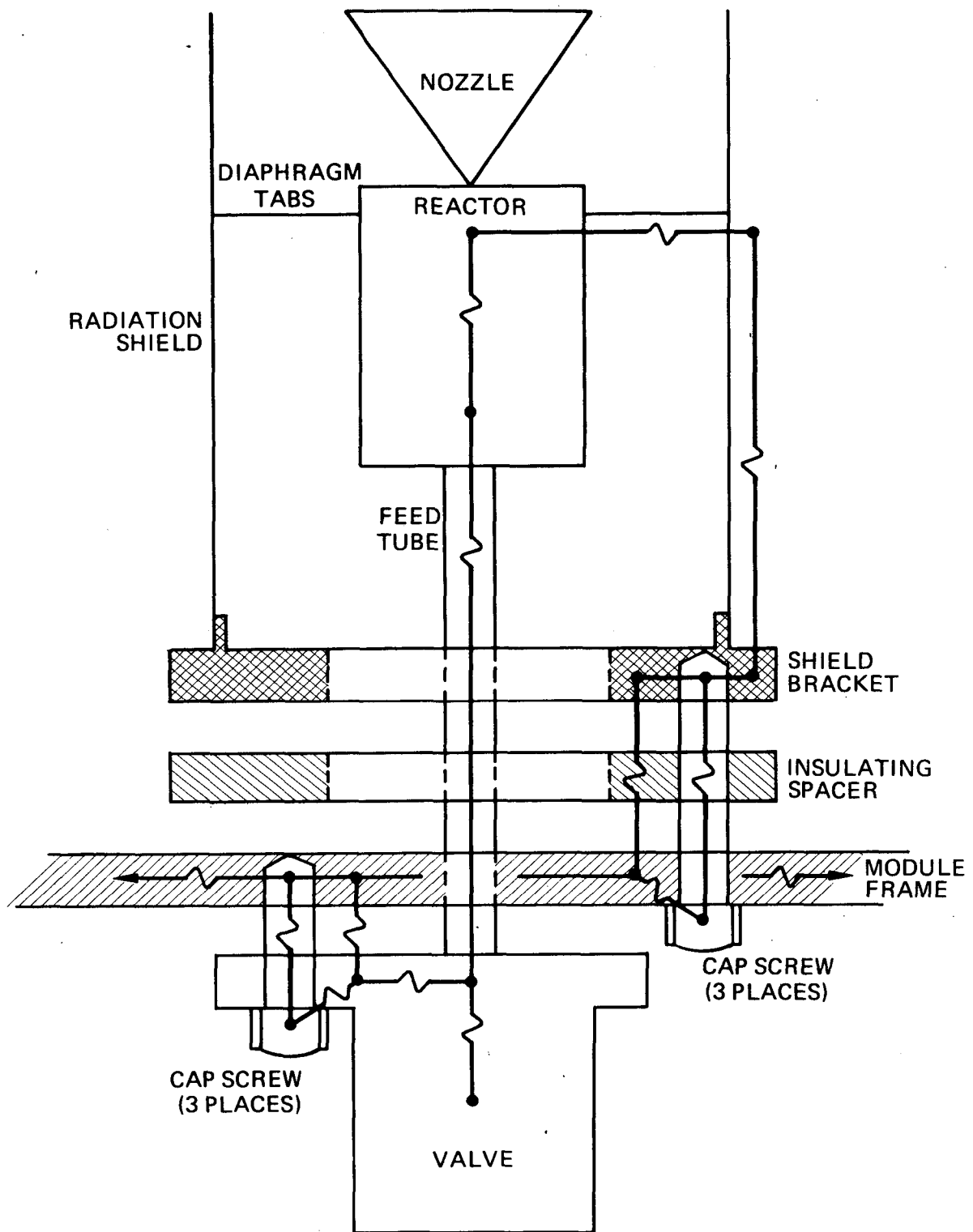


Figure 4-14. THRUSTER ASSEMBLY MOUNTING DETAIL (TYPICAL) SHOWING HEAT CONDUCTION PATHS

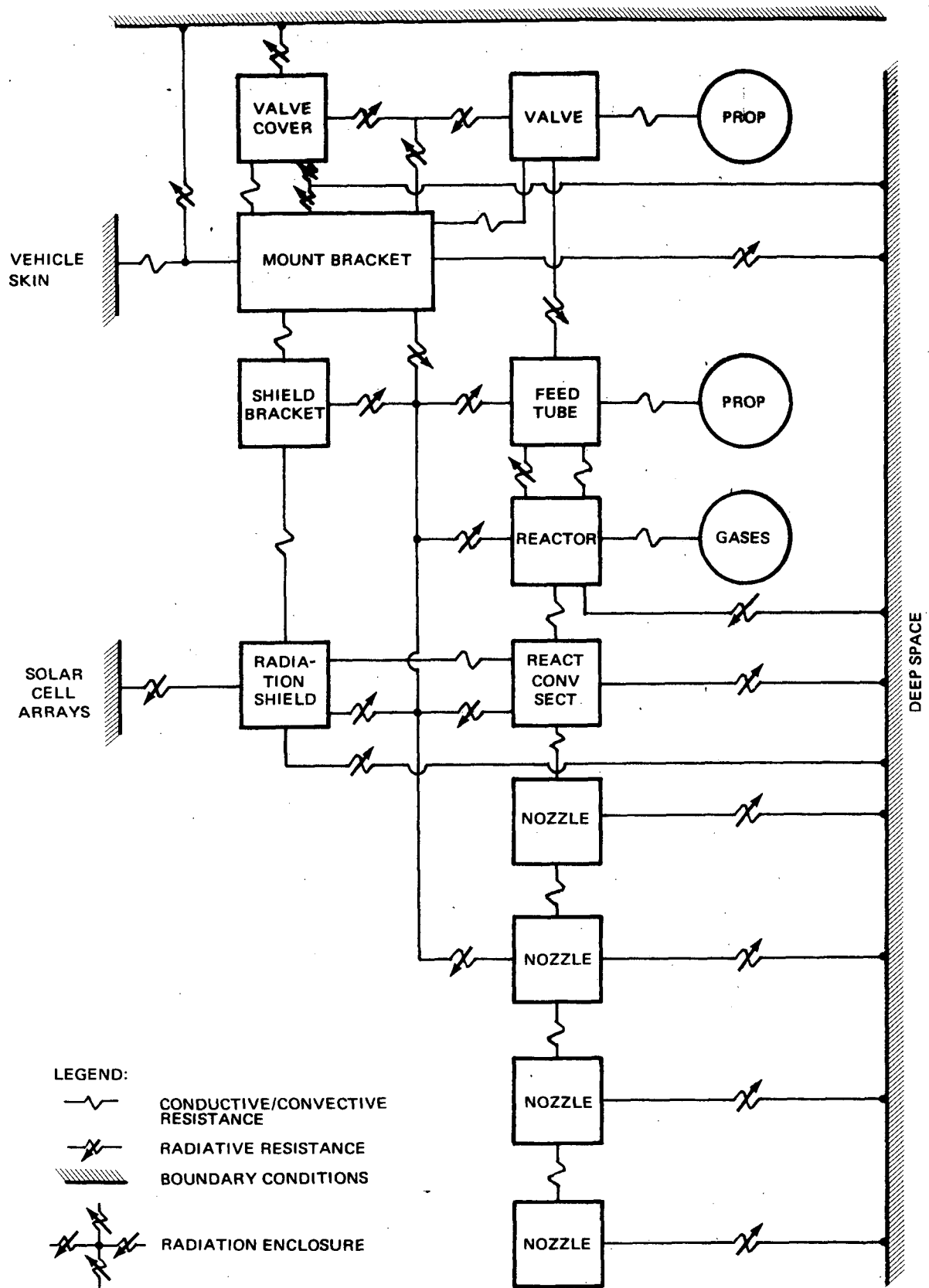


Figure 4-15. CANDIDATE TANGENTIAL THRUSTER MODULE THERMAL NETWORK SCHEMATIC (ONE HALF SHOWN)

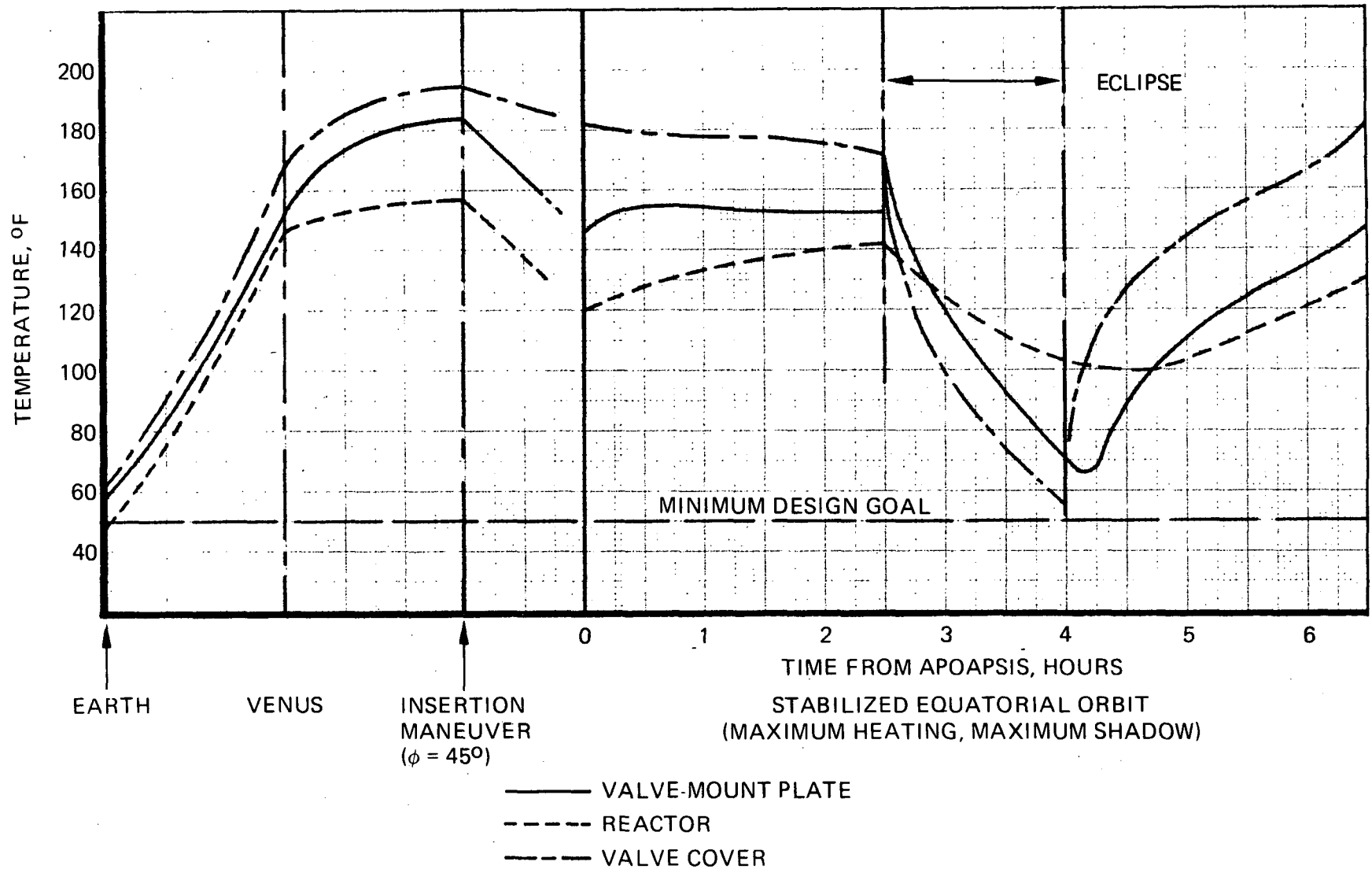
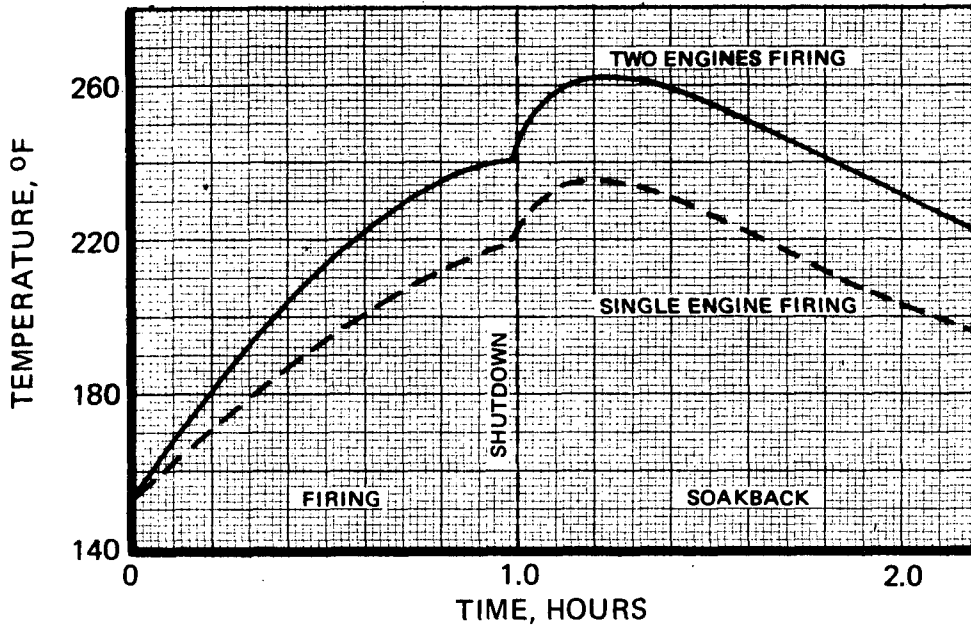


Figure 4-16. DOUBLET MODULE COMPONENT TEMPERATURES – VENUS MISSION (NO FIRING)

A. WORST-CASE VALVE SOAKBACK HEATING (1% DUTY CYCLE)



B. SOAKBACK FROM 10% DUTY CYCLE

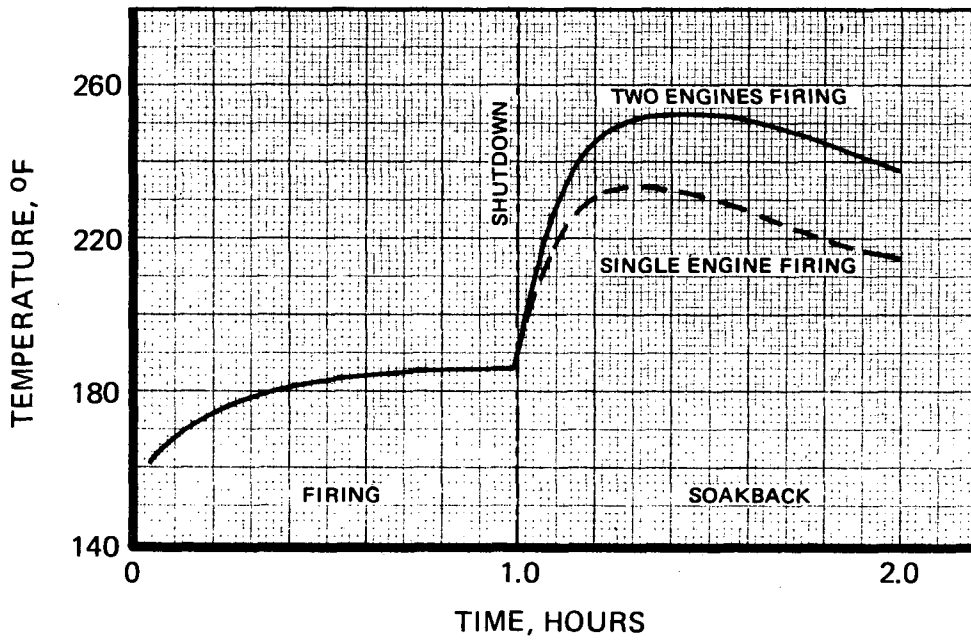


Figure 4-17. POST-MOUNTED DOUBLET MODULE – VALVE SOAKBACK HEATING (VENUS INSERTION MANEUVER – SPIN AXIS SUN-LINE ANGLE = 45°)

Table 4-10. CANDIDATE THRUSTER MODULE: MAXIMUM EXPECTED TEMPERATURE UNCERTAINTIES

Estimated Uncertainties

Radiation Properties:

Black paint = $\Delta a_s = 0.04$, $\Delta \epsilon = 0.03$

Gold/rhodium = $\Delta a_s = 0.03$, $\Delta \epsilon = 0.02$

Incident energy flux (solar, et al) = $\Delta a = 5\%$

Radiation interchange constant = $\Delta(AF) = 10\%$

Effective solar exposure area = $\Delta A_s = 10\%$

Conduction Properties:

Material conductivity = $\Delta K = 10\%$

Material dimensions = $\Delta(1/A) = 3\%$

Component	Environment	Uncertainties, °F			ΔT (RMS)	Design ^① Margin
		Radiation	Incident Energy	Conduction		
TC valve (Cold)	Earth vicinity	4.2	5.8	—	7.2	15.3°F
TC valve (Long-term operation)	Venus vicinity	8.0	7.1	3.6	11.3	25°F
TC valve (Soakback)	Insertion maneuver	8.4	6.2	3.6	11.0	7°F
Thruster (Cold)	Earth vicinity	2.9	2.9 ^②	—	4.1	-6.1°F

① Applying RMS uncertainties to simulation predictions.

② Mount plate/cover surfaces only. Limiting values were used for the thruster/shield simulation (see text).

Radial thruster thermal profiles are not shown. Simulation of a platform (angle bracket) mounted thruster yielded results nearly identical to the doublet module with both engines firing. Because of lessened solar absorption, the skin-mounted design produced lower valve soakback temperatures; however, the vehicle soakback energy rejection was higher, and much of this was to the vehicle interior. This is indicated in Table 4-8.

4.4.4.3 Thermal Management of Propellant Tankage and Lines

In the GSFC Subsystem Specification 5-723-P-10 upper (tank) compartment mission temperature ranges were given for adjacent solar cell arrays fully and partially backed by superinsulation. The analysis has thus far used the data for the partially insulated condition, yielding a propellant

temperature range of 56 to 167°F. Although the high end of this range is acceptable, a somewhat lower range would increase feed system temperature margins. It would therefore be desirable to design for a tank compartment minimum temperature between 40 and 50°F, resulting in a lower fuel temperature in Venus vicinity.

The problems of propellant feed lines exposed to adverse temperature environments were solved by RRC during development and qualification of the HPM hydrazine propulsion module. The approach used was to apply strip heaters to the propellant lines, followed by a wrapping of 10 to 20 layers of aluminized mylar multilayer insulation. The lines were attached to the vehicle by high resistance plastic clips.

For the MICOMACS, heaters are needed only for those sections of line beneath the louvers which have a partial view of deep space. In the equipment compartment (which has a minimum temperature of 32°F at Earth vicinity), the very large time constant of the superinsulation line, coupled with anisotropic conduction effects in the superinsulation blanket, would prevent line temperatures from dropping below 40°F. Those line sections viewing deep space would have heater power requirements of about 0.01 watt/foot; these heaters could be turned off just prior to the first midcourse correction to conserve power if necessary.

4.5 PLUME EFFECTS

4.5.1 Exhaust Contamination

Review of available data on optical surface contamination by thruster exhaust indicates that no problem should be encountered in the design and operation of the Planetary Explorer system. This is due primarily to the use of hydrazine propellant and to the thruster/spacecraft geometry.

The primary source of surface contamination has been identified as monomethyl-hydrazine nitrate formed during transient and off-mixture ratio pulse-mode operation of bipropellant thrusters (References 12 and 13). Direct jet impingement has also resulted in a "sandblasting" effect on the impacted surface, which is attributed to the presence of tramp metals in the propellant (Reference 12).

Use of anhydrous hydrazine monopropellant precludes the formation of MMH nitrate; and as shown by experimental studies reported (Reference 14), no measurable amounts of other contaminants are generated. Surface properties were, in some cases, affected but not seriously degraded. In these tests thermal control surfaces were located parallel to and in the order of one diameter away from the nozzle. Tangential thruster installations on the Planetary Explorer provide up to 2-1/2 nozzle diameters clearance for the 5.0-lbf thrusters. In addition, the back-to-back thruster modules are approximately equal in length to a spacecraft facet width; hence adjacent surface is not parallel to the jet immediately downstream of the exit, but rather drops away reducing further the likelihood of impingement problems. The testing reported in Reference 14 also included direct impingement on optical surfaces with no evidence of the "sandblasting" effect observed with bipropellant

thrusters. Trace metal content in typical hydrazine propellant, as reported by the supplier, is in the order of 4 ppm as compared to the 120 ppm reported for bipropellant N_2H_4/MMH in Reference 12.

No problems are anticipated with the radial thruster installations since the jet is directed away from the adjacent surfaces and, although Reference 13 shows that the chemical contaminants can migrate backwards from the nozzle exit plane, Reference 14 indicates no degrading compounds are generated by the hydrazine thruster.

The available data indicates that exhaust contamination does not constitute a serious risk for the Planetary Explorer mission.

4.5.2 Solar Array Nozzle Exhaust Plume Impingement Heating

A subject of considerable concern in spacecraft design is excessive heating of spacecraft components, such as solar cells, by energetic rocket motor exhaust gases. To determine whether such heating imposes constraints on the placement and orientation of the Planetary Explorer hydrazine thrusters, a detailed analysis of the MR-50 nozzle exhaust plume and its interaction with spacecraft surfaces was conducted.

The analysis indicated that for radially-mounted thrusters no energetic gases impact the spacecraft. For the tangential thrusters mounted with the nozzle exit plane parallel to the spacecraft facet edge, instantaneous local heating rates as high as 220 Btu/ft²-hr can be expected on the adjacent spacecraft facet. For steady-state operation (fuel dump, valve failure, or spin control) such heating could cause temperature rises to as much as 325°F (Venus orbit) for thermally isolated cells. However, because the radiative heat rejection capability of the solar arrays is quite large, cell time constants are order-of-magnitude higher than typical thruster pulse widths. Thus, for the maximum anticipated duty cycle (11%) expected, local temperature rises for a single thruster do not exceed 20°F.

4.5.2.1 Free Plume Computation

The free (unobstructed) nozzle exhaust plume properties for the MR-50 hydrazine monopropellant thruster were computed using the LMSC/HREC Method of Characteristics Plume Computer Program developed for NASA. The program, run on a CDC 6600, generated desired thermodynamic properties as a function of position within the plume. Temperature dependence of gas species properties was considered. Properties at several pertinent points in the impingement area were checked for reasonableness using approximate methods (Reference 15).

4.5.2.2 Plume Impingement with Heat Transfer to the Spacecraft

Piesik, et. al. (Reference 16), conducted extensive tests of plume heat transfer to flat plates, both parallel and canted to the nozzle axis, measuring pressure profiles and heating rates at the plate. Their data correlated well with a Newtonian impact analysis which assumed that the shock layer lies essentially on the plate and does not affect the plume free-stream. Additionally they found that impact pressure and density reach a maximum near the point of tangency of the lowest plume iso-Mach line with the plate; maximum heating rates also occur near this point.

Maddox (Reference 17), generalizing the work of Piesik and other investigators, developed a Stanton number correlation for heat transfer to blunt bodies from greatly underexpanded plumes. His correlating equation was modified slightly to accommodate thermochemical property data correlations developed from analysis of RRC hydrazine engine test data to yield

$$h_c = 0.6 c_{ps}^{0.4} k_s^{0.6} \mu_s^{-0.1} \left(\frac{\rho_s V_s}{\ell} \right)^{0.5} \left(\frac{T^*}{T_s} \right)^{\frac{n+1}{2}} \quad (4-15)$$

where:

- h_c = Heat transfer coefficient
- c_p = Specific heat-hydrazine decomposition product mix
- k = Thermal conductivity-hydrazine decomposition product mix
- μ = Viscosity-hydrazine decomposition product mix
- ρ = Density-hydrazine decomposition product mix
- V = Surface flow velocity
- T = Temperature
- ℓ = Distance from flow stagnation point

The subscript s indicates that properties are those of the surface boundary layer. T^* is evaluated for the boundary layer flow, rather than the free plume itself. The exponent term n comes from the exponential relationship between temperature and viscosity or thermal conductivity.

For the Planetary Explorer study, the spacecraft surface flow field was computed applying an ideal gas shock analysis to the impingement free plume; local heat fluxes were then obtained from equation 4-15 using the thrust chamber stagnation temperature as the driving potential. The impingement heat fluxes thus obtained are shown in Figure 4-18 superimposed on a sketch of the impinging free plume field. As was expected from Piesik's results the maximum surface pressure and density (not shown) appeared near station 6, where the Mach 15 line is nearly tangent to the canted surface. However, the maximum local heat flux appears near station 4.5; because of the cant the enthalpy of the incident plume is at a maximum here. The heat flux profile at station 4.5 in the plane normal to the paper is shown in the figure inset.

As a rough check of the analysis, the experimental data presented by Piesik was adapted to the present problem, scaling for cant angle and propellant enthalpy. The resultant heat maximum flux of 200 Btu/ft²-hr is in good general agreement with the results presented above.

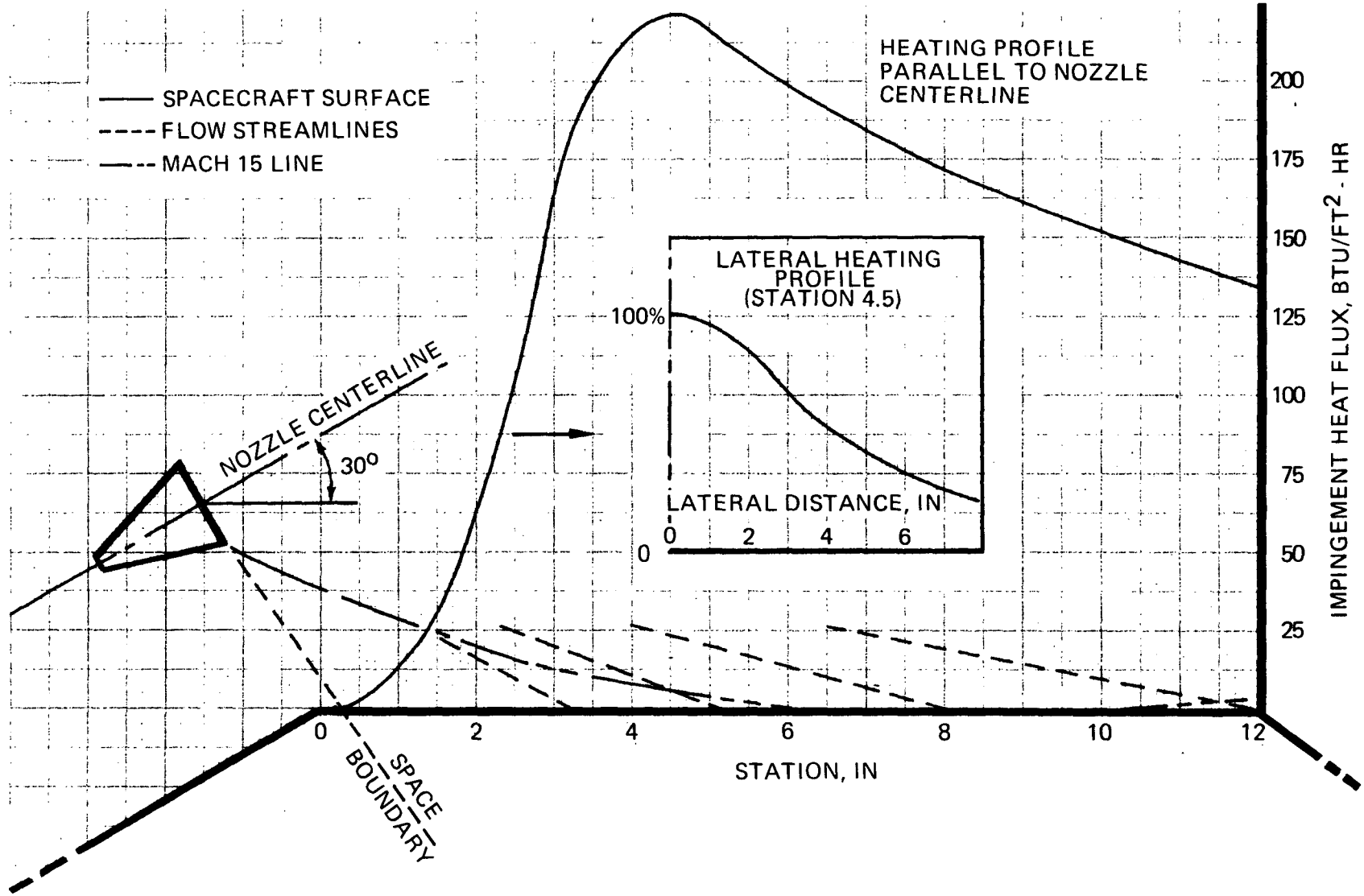


Figure 4-18. PLANETARY EXPLORER TANGENTIAL THRUSTER PLUME HEATING OF ADJACENT CANTED SOLAR ARRAYS ILLUSTRATING IMPINGEMENT FLOW FIELD

4.6 COMPUTER MODEL

Operational use of the system would be facilitated by implementation of a computer model to provide the information necessary to command a required maneuver. By use of measured or calculated values of hydrazine feed pressure, fuel temperature, and thruster temperature, and on the basis of input calibration factors and spacecraft mass properties, the program would compute the required duty cycle for each thruster required to perform the desired maneuver. The program would also compute the error margin and the total propellant consumption for mass property updating. A simplified block diagram of the program is provided in Figure 4-19.

INPUT PROPULSION SYSTEM DATA

FEED PRESSURE
FUEL TEMPERATURE
THRUSTER TEMP

SPECIFIC AND TOTAL
IMPULSE CENTROID
VS PULSE WIDTH
& NUMBER

THRUSTER
CALIBRATION
CONSTANTS
(ACCEPT TEST)

ERROR
MARGINS

INPUT SPACECRAFT DATA

THRUSTER
LOCATIONS

CALIBRATION
BIAS

DUTY CYCLE
PER ENGINE

M_0, I_z, Ω_z
MANEUVER REQ'D
MAX PULSE SECTOR

REQ'D TOTAL IMPULSE
& DISTRIBUTION

PROPELLANT
CONSUMED

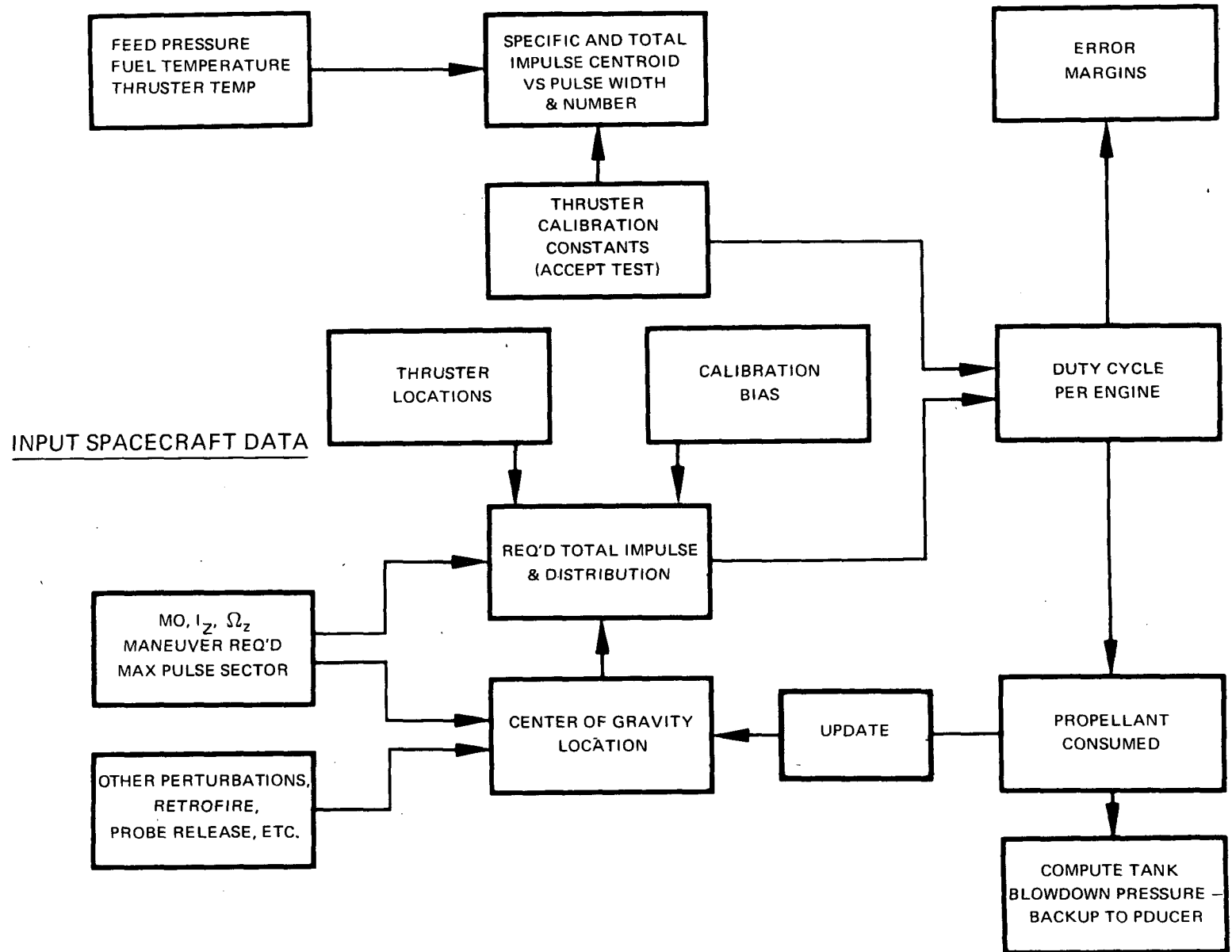
OTHER PERTURBATIONS,
RETROFIRE,
PROBE RELEASE, ETC.

CENTER OF GRAVITY
LOCATION

UPDATE

COMPUTE TANK
BLOWDOWN PRESSURE -
BACKUP TO PDU CER

Figure 4-19. PROPULSION COMPUTER MODEL



5.0 SYSTEM DESCRIPTION

5.1 SYSTEM DESIGN AND INTEGRATION

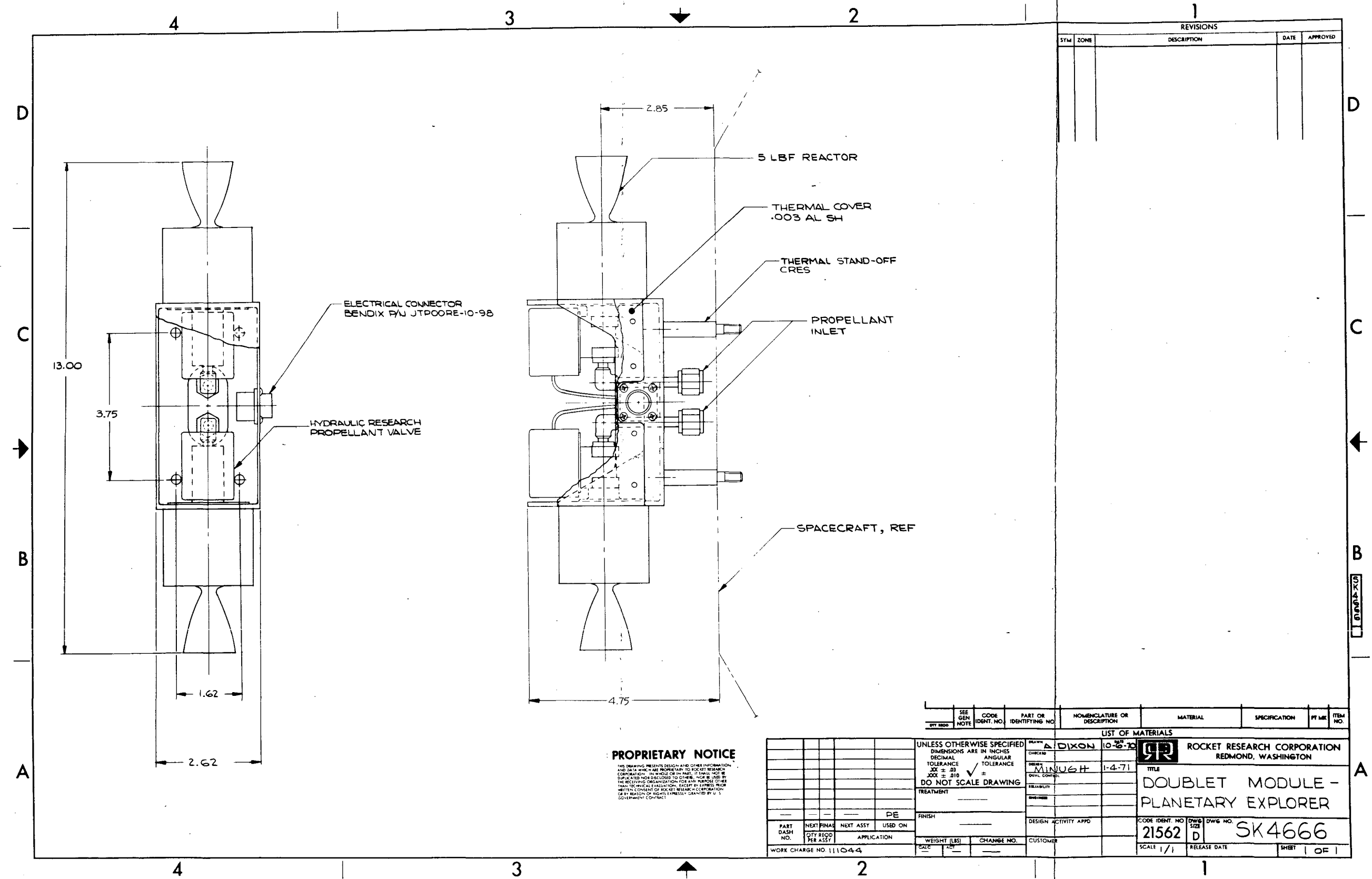
Preliminary design studies of the candidate configurations and the components and subassemblies that comprise them were conducted. The purpose of these studies was to identify areas of particular advantage or disadvantage for the various configurations and to establish the general mechanical compatibility of the system with the envelope and basic structural concept defined by AVCO drawing LA13230. Overall weights and power requirements, based on these selected or typical existing components, were also established.

It was concluded that complete modularization of the propulsion system into a single assembly prior to installation into the spacecraft is not practical. This is due to the necessity for locating thrusters centrally and/or at the extremities of the spacecraft and the size and location of the propellant tankage envelope.

The subsystem will be built up in a number of modules and these designed for simplicity of integration and assembly into the basic spacecraft structure. The propulsion system is logically divided into three types of module: a propellant tank module, a valve module, and the necessary thruster modules. All of the candidate configurations require a tangential thruster module consisting of back-to-back mounted engines. Differences are in the number and location of these thruster modules and the use of other radial or radial/gimbaled thruster modules. Figures 5-1 through 5-6 present preliminary design layouts of these basic building blocks. The individual modules are designed for functionality, compactness, and ease of installation and checkout. Intermodule interfaces should be selected so as to minimize final assembly splices and those located for accessibility of assembly and inspection.

The preliminary design study showed that the required propulsion system components and assembly were compatible with the spacecraft configuration and envelope (minor propellant line interferences were detected), and provided the mass properties and power data. It did not reveal, however, significant advantages or disadvantages to provide a positive basis for selection among the various candidates. All of the candidate configurations would use the same propellant tank and valve modules, the only differences being in the type and location of the thruster modules. From the mechanical design standpoint Configuration C, tangential doublets, is perhaps the most straightforward. This is because it uses four identical thruster modules. The tangential modules also minimize intrusion into the spacecraft (mechanical and thermal), particularly into the central equipment section. The gimbaled engine configurations, on the other hand, require design and development of an electromechanical device that exceeds in complexity any other component of the system. None of the configurations studied, however, presented design problems so difficult as to render them unfeasible.

Each of the major subassemblies is described below, followed by some comments on integration and assembly. Mass properties data are given in paragraph 5.2.



REVISIONS				
SYM	ZONE	DESCRIPTION	DATE	APPROVED

PROPRIETARY NOTICE
 THIS DRAWING PRESENTS DESIGN AND OTHER INFORMATION AND DATA WHICH ARE PROPRIETARY TO ROCKET RESEARCH CORPORATION. IN WHOLE OR IN PART, IT SHALL NOT BE REPRODUCED, COPIED, EITHER WHOLLY OR IN PART, OR IN ANY MANNER, WITHOUT THE WRITTEN PERMISSION OF ROCKET RESEARCH CORPORATION. EXCEPT BY EXPRESS WRITING FROM ROCKET RESEARCH CORPORATION OR BY REASON OF RIGHTS EXPRESSLY GRANTED BY U.S. GOVERNMENT CONTRACT.

QTY	SEE GEN NOTE	CODE IDENT. NO.	PART OR IDENTIFYING NO.	NOMENCLATURE OR DESCRIPTION	MATERIAL	SPECIFICATION	PT MK	ITEM NO.

DRAWN		CHECKED		DESIGNED		APP'D	
MINUGH	1-4-71	DIXON	10-26-70				

LIST OF MATERIALS			

UNLESS OTHERWISE SPECIFIED DIMENSIONS ARE IN INCHES		DRAWN BY		ROCKET RESEARCH CORPORATION	
DECIMAL TOLERANCE	ANGULAR TOLERANCE	MINUGH	1-4-71	REDMOND, WASHINGTON	
± .03	± .010			TITLE	
DO NOT SCALE DRAWING				DOUBLET MODULE - PLANETARY EXPLORER	
				CODE IDENT. NO.	
				21562	
				DWG NO.	
				D SK4666	
				SCALE	
				1/1	
				RELEASE DATE	
				SHEET 1 OF 1	

Figure 5-6. DOUBLET MODULE - PLANETARY EXPLORER

5.1.1 Propellant Tank Module

The propellant tank module, Figure 5-1, consists of an aluminum mounting ring, aluminum support struts, and, for the orbiter mission 9, propellant tank and associated plumbing. For the probe mission, three of the tanks will be replaced by aluminum spacers. Removal of these tanks will provide space to accommodate the three areas excluded from the allowable envelope as shown on AVCO Drawing LA13230.

Two tank candidates were considered in the design study – the 10-inch-diameter three-port tank supplied by Fansteel Advanced Structures Division for the IDCS program, and the 9.6-inch-diameter two-port tank supplied by Pressure Systems Incorporated for the INTELSAT III. The IDCS tank is preferable in that it, in its qualified configuration, has the more suitable three-port arrangement and a mounting arrangement more compatible with the available envelope. As discussed elsewhere, its larger size (497 in.³ as compared to 457 in.³) provides a lower blowdown ratio which helps maintain high vehicle control rates through the end of the mission. Although both tanks are specified at 1.6 lbm maximum by their suppliers, a weight of 1.38-lbf could be expected for the INTELSAT tank on the basis of actual weights of delivered tanks. This weight advantage could be largely offset by increased structural weight because of the more difficult mounting. In addition, altering the mounting or adding a third tank drain port could result in increased tank weight.

The tanks are mounted to tank support struts which, in turn, are attached to a mounting ring. The mounting ring is used to simplify the tank module/spacecraft center support interface.

A honeycomb mounting structure was investigated and discarded. The shape of the available tank envelope, notably the axial displacement of the tank location from the center support tube, requires additional structure to tie the tanks to the honeycomb platform and the platform to the center support. In addition, the cutouts required to accommodate the tanks would approach the platform width resulting in a loss of structural integrity of the platform. This could be particularly troublesome with the tank port trunion mounting currently used on the INTELSAT III tanks.

Slight envelope interference does exist with the recommended tank. As shown, this is in the area of the gas port. The tank could be moved slightly aft if interference at the propellant drain port could be more readily accommodated.

5.1.2 Valve Module

Preliminary design studies indicate that all of the control, servicing, and checkout components can be packaged into a compact modular assembly which will fit in one facet of the spacecraft between the upper and lower solar panel areas. Figures 5-2 and 5-3 show two valve module designs based on the candidate feed systems, namely the service and test valves and connector, pressure transducer, propellant line filter, and isolation valves. Figure 5-2 depicts a subassembly with one latching valve in each of the two thruster branches (feed system 1); that shown in Figure 5-3 is similar but incorporates the upstream parallel redundant isolation valve set. The drawing illustrates electroexplosive upstream isolation valves (feed system 3), but the installation with latching valves (feed system 2) would be essentially the same. The various service/test valve line connections would

be distinctly marked and of different size to preclude improper connection. As required, a mechanical joint is shown on the pressure transducer. Since this connection is located upstream of all isolation valves, considerable care must be exercised to ensure a leak-free joint. An MS27851 K-seal-type connector is recommended. The pressure transducer is located in the fuel lines rather than in the pressurant lines, since zero leakage is easier to guarantee with liquid as opposed to gas; and qualified, hydrazine-compatible units are available. This location also simplifies the plumbing.

5.1.3 Radial Thruster

The MR-50 5-lbf (nominal) thruster is used for all propulsive functions. On several of the candidate configurations it is used as a single radially mounted thruster. This basic engine is shown in Figure 5-4. In order to meet the requirement for series-redundant propellant valve seats this configuration is based on use of the Hydraulic Research and Manufacturing Company torque motor valve. This engine and valve are described in more detail in paragraphs 5.3.1 and 5.3.2.

The basic engine, in addition to its use where single radial thrusters are called for, is also used in the gimbaled engine module and the doublet module.

5.1.4 Gimbaled Engine

A gimbaled engine assembly consisting of a thruster, ball jackscrew/stepper motor actuator, mounting structure including flexural pivots, and the flexible propellant line would be integrated into a modular assembly such as that shown in Figure 5-5. This simplifies a vehicle mounting interface and permits bench functional testing and calibration of the actuator. A conceptual design of the actuator assembly is shown in Figure 5-7. In addition to the basic installation alignment tolerance, some additional thrust vector positioning uncertainties are inherent in this concept, due primarily to ballscrew backlash and stepper motor positioning. On the basis of typical values of ballscrew lead of 0.0625 inch, backlash of 0.004 inch, and stepper motor resolution of 15 degrees provided by component suppliers, a thrust vector positioning accuracy of ± 0.025 degree was established. A design investigation of a configuration with the gimbal pivot on the thrust centerline indicated increased envelope projecting into the interior of the spacecraft and somewhat higher bracket weight.

5.1.5 Doublet Module

A typical doublet thruster module is shown in Figure 5-6. This assembly uses two of the basic MR-50 engines (Figure 5-4), installed on an aluminum mounting bracket which in turn is installed on the spacecraft with thermal standoffs. The thrust chamber valves are wired to a common electrical connector. The propellant lines are plumbed independently to accommodate thruster coupling and facilitate thruster replacement if required, although downstream of the isolation valves MS27851 connectors should also be used here. A thin aluminum shield is shown over the thrust chamber valves. (See paragraph 4.4.) Subsequent thermal analysis indicates this shield may be eliminated.

5.1.6 Electrical Harness

A representative electrical harness was designed to permit further definition of the connector and cable requirements and weights. The design of the electrical harness represents a straightforward

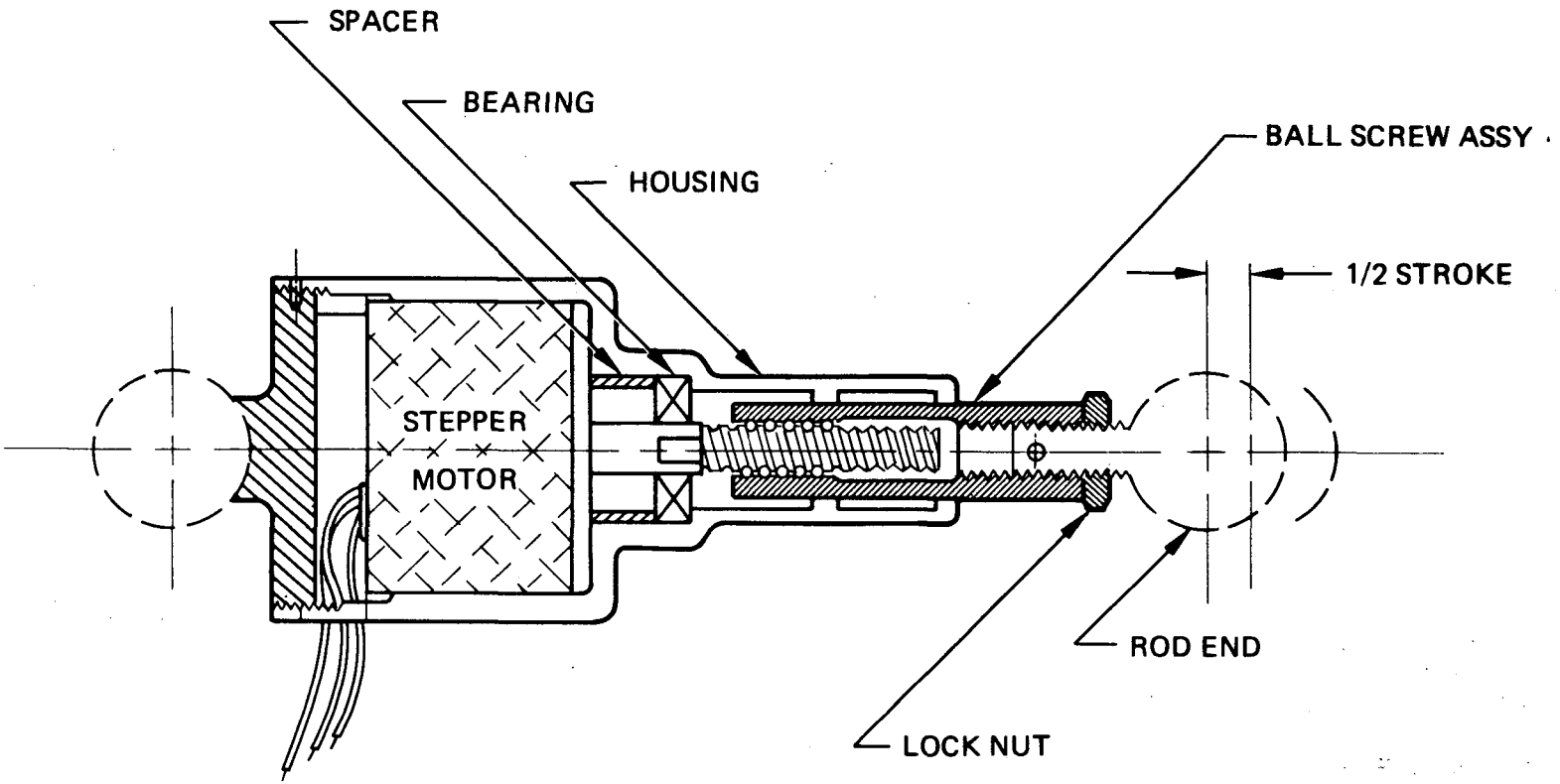


Figure 5-7. GIMBAL ACTUATOR CONCEPTUAL DESIGN

design task with no significant differences between the requirements of the candidate configurations. As such, it does not provide a basis for selecting among the candidate configurations.

A schematic for the design is shown in Figure 5-8. The harness includes a single interface connector and the required test connector. The baseline connector is a Bendix JTP-00RE 53 pin configuration which will accept the US Gauge No. 24 twisted and shielded wire which is sufficiently rated for the power handling requirements. To maintain serviceability throughout the subsystem, all cables to the valves and pressure transducer will terminate in hardware-compatible connectors. Although a single spacecraft interface connector is shown, the use of separate connectors for power, instrumentation and (if present) squib valves should be reviewed for compatibility with other spacecraft subsystems and design approaches.

It is further assumed that back voltage suppression circuitry will be integrated with the valve drivers on the spacecraft side of the interface.

The electrical design presented is based on candidate feed System No. 3, supplied by GSFC. Schematics for the other feed system candidates can be developed simply by eliminating (System No. 1) or substituting latch valves (System No. 2) for the squib isolation valves shown. Consistent with these feed system schematics only one pressure transducer is shown. If the instrumentation recommendations of paragraph 4.1.5 are adapted in whole or in part, the additional instrumentation must be integrated into the electrical design.

5.1.7 Assembly and Integration

The general arrangement of the various modules is shown in the system layout drawings, Figure 5-8 through 5-13. The specific locations selected for the thruster modules corresponding to each of the candidate configurations along with propellant line and electrical cable routing are also shown. The installation of the propellant tank and valve modules, typical of all configurations, shown in more detail in Figure 5-9. Propulsion module/spacecraft mechanical interfaces shown are suggested approaches; because of the lack of definition of the spacecraft structure, the mechanical attachment problem could not be worked in greater detail. The approaches shown should be helpful in design studies of the spacecraft structure and provide a starting point for further design iteration.

Intermodule plumbing interfaces can be quite simple. Depending on the extent of buildup of the basic structure at the time of propulsion system installation and the final propellant line routing, as few as one but in any case no more than four line splices will be needed to couple the system plumbing. This is exclusive of the thruster line attachment; these, however, are supplied with mechanical rather than weld or braze joints.

The main propellant feed line will have to be joined to the inlet at the valve module. It may be possible to include the pressurization line and the fill/vent valve as a part of the propellant tank module buildup. At the time of assembly then, this bulkhead-type fitting need only be secured to the valve module panel. If this is not possible, an additional assembly splice will be required. A similar situation exists for the thruster feed lines. These could conceivably be completed as part of

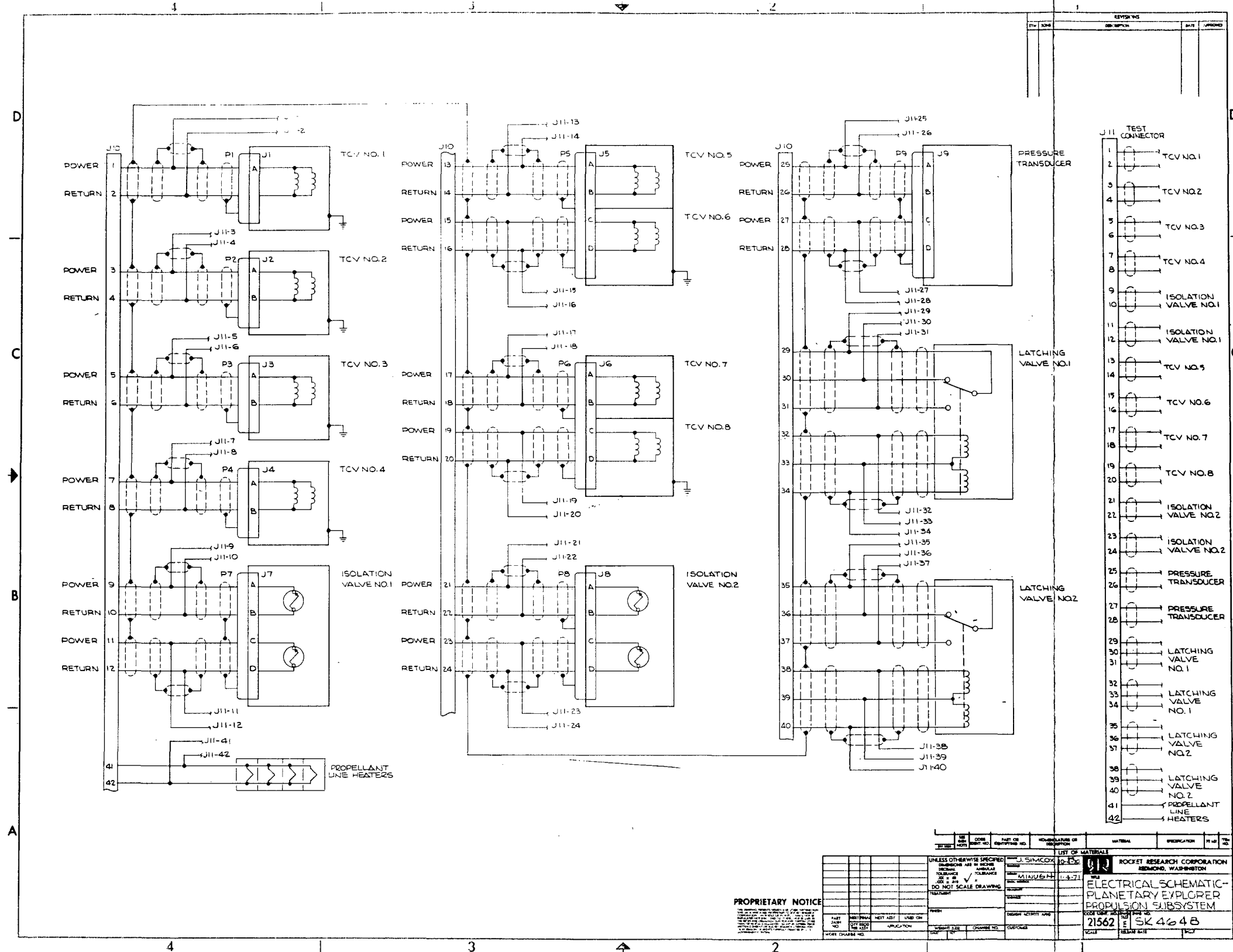
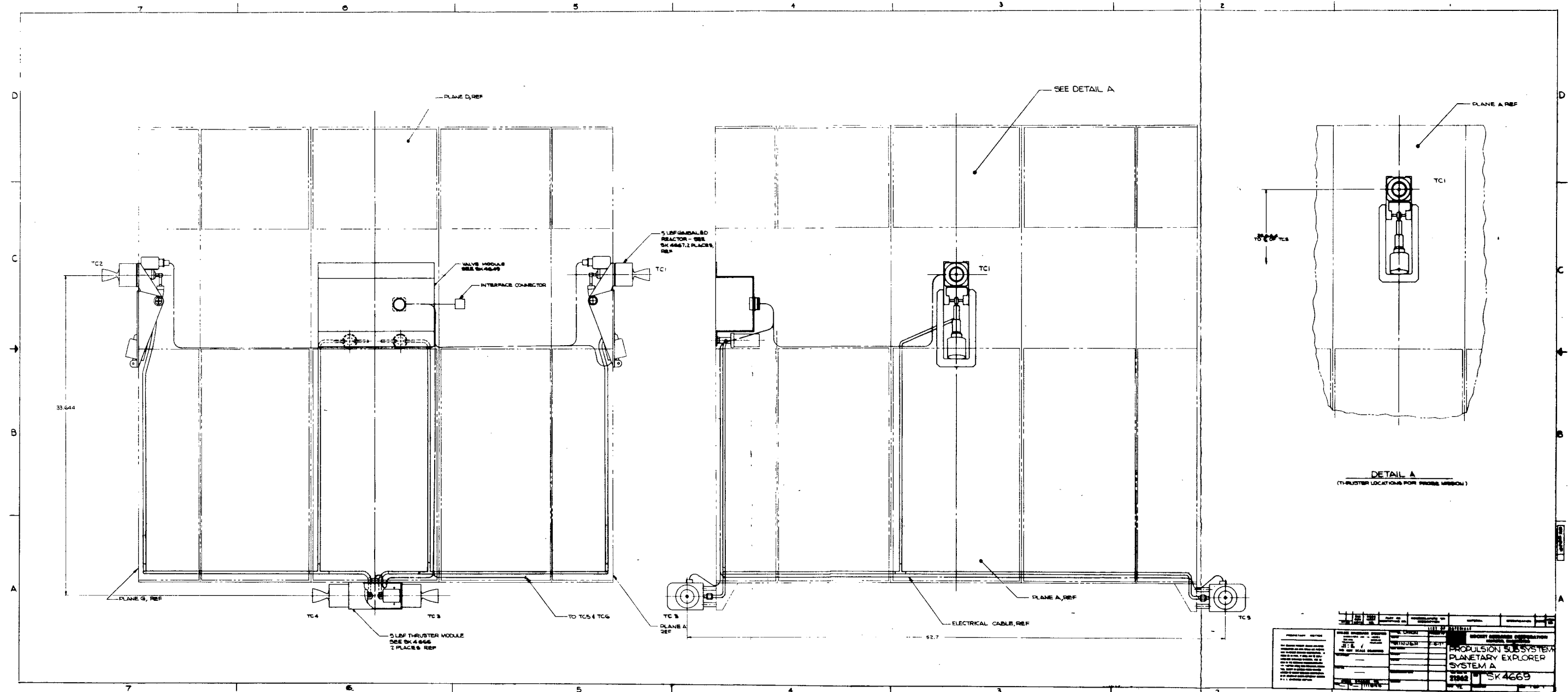


Figure 5-8. ELECTRICAL SCHEMATIC - PLANETARY EXPLORER PROPULSION SUBSYSTEM



TITLE PROPULSION SUBSYSTEM PLANETARY EXPLORER SYSTEM A		SK 4665	
DRAWN BY DATE	CHECKED BY DATE	DESIGNED BY DATE	APPROVED BY DATE
PROJECT NUMBER 211		DRAWING NUMBER SK 4665	

Figure 5-9. PROPULSION SUBSYSTEM PLANETARY EXPLORER SYSTEM A

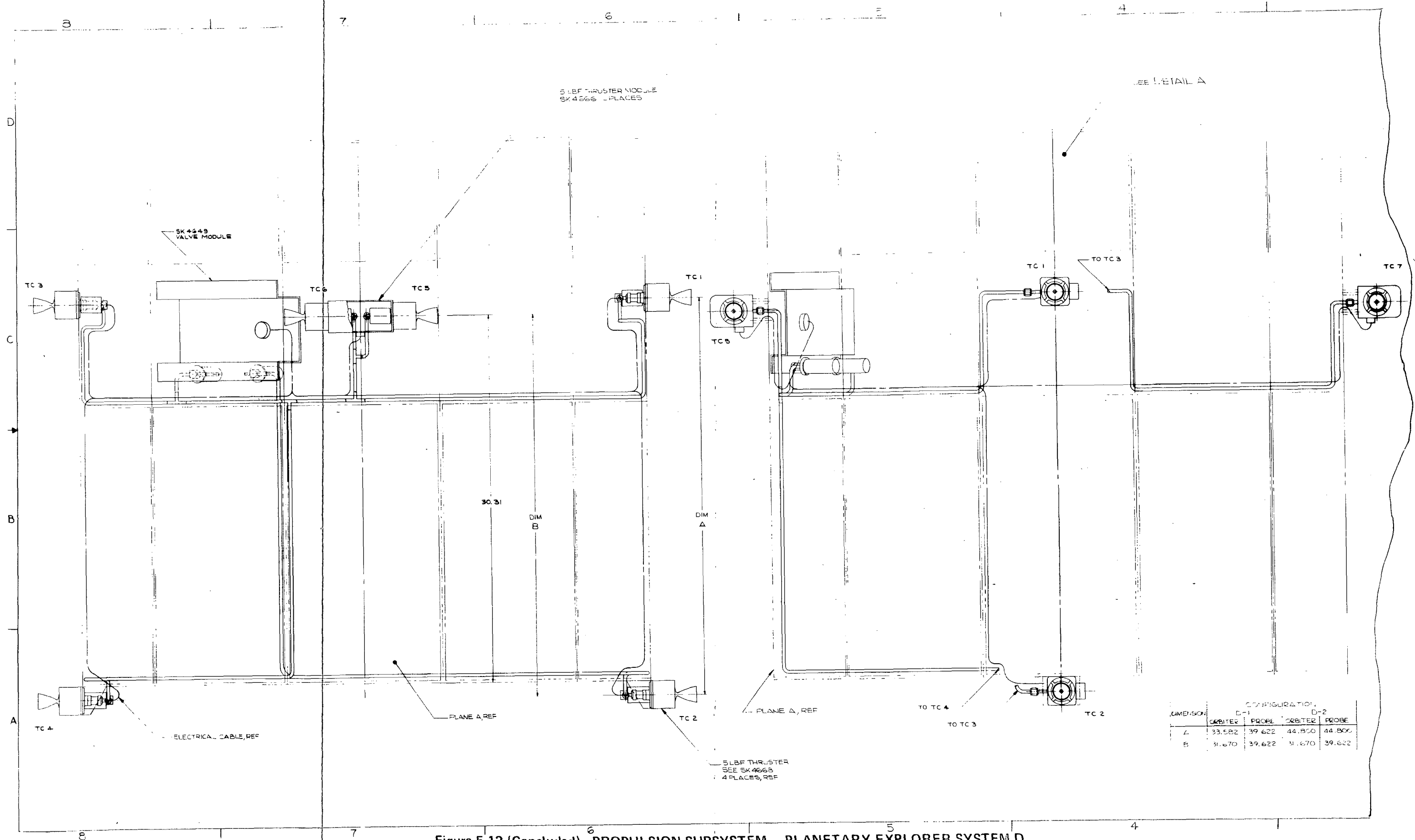


Figure 5-12 (Concluded). PROPULSION SUBSYSTEM - PLANETARY EXPLORER SYSTEM D

pgs. 5-26 + 5-27
blank

the valve module, leaving only securing of the mechanical joints to complete the system plumbing. If this is not practical, two additional assembly splices, one at the outlet to each isolation valve, will be required at system integration. Accessibility for inspection as well as installation is, of course, a design requirement. All propellant lines are 0.25-inch CRES tubing. Bimetallic transition tubes are required to connect the propellant tanks to the feed system plumbing. The design layouts (fittings, clearances, weight, etc.) are based on a brazed system. Use of a tube welding would not significantly alter the design.

Although course alignment can be accomplished at the time of thruster module installation, it is expected that a final check and adjustment, if necessary, will be made at the time of spacecraft balance and center of gravity determination. The propulsion supplier must build in the required adjustment capability; final alignment, however, should be the responsibility of the spacecraft integrator. It has been assumed that through the use of optical techniques, an alignment accuracy of 0.1 degree can be achieved. The accuracy in locating the thruster relative to the nominal vehicle reference is estimated as 0.020 inch.

5.2 WEIGHT AND BALANCE

5.2.1 Propellant Weight

Usable propellant requirements for the probe and orbiter missions are presented in Tables 5-1 and 5-2. Quantities are indicated for the various types of control required and for correcting the induced disturbances as derived in paragraph 2.2.4. A rotational efficiency of 98% was assumed. Propellant required for first midcourse spin stabilization is listed separately from that required for the specified mission spin profile.

Table 5-1. PROPELLANT REQUIREMENTS—ORBITER VEHICLE

	Configuration			
	B	C	D-1	D-2
Velocity control	78.003	78.001	78.001	78.003
Attitude control	8.392	10.729	10.729	8.392
Spin control	1.311	1.311	1.311	1.311
Spin stabilization	1.386	1.386	1.386	1.386
Disturbance correct:				
Attitude	0.755	2.201	2.098	0.808
Spin	0.698	4.713	0.392	4.289
Translation	4.217	4.322	4.322	4.215
	94.762	102.663	98.239	98.406

Table 5-2. PROPELLANT REQUIREMENTS—PROBE VEHICLE

	Configuration			
	B	C	D-1	D-2
Velocity control	51.272	51.272	51.272	51.272
Attitude control	5.343	5.966	5.966	5.343
Spin control	3.381	3.381	3.381	3.381
Disturbance correct:				
Attitude	0.577	0.709	0.427	0.508
Spin	0.581	3.113	0.376	2.851
Translation	<u>2.782</u>	<u>2.809</u>	<u>2.809</u>	<u>2.782</u>
	63.936	67.250	64.231	66.137

For all control maneuvers, average effective specific impulse included heatup losses for the number of thrusters required for the maneuver. Figure 5-14, based on actual MR-50 firing data, presents average specific impulse as a function of delivered total impulse. A midvalue of feed pressure is assumed. Attitude control contingencies were assumed to occur in 6-degree steps, and 25 orbital periapsis maneuvers were assumed to take place. Attitude perturbations induced during the first midcourse maneuver were assumed to occur and be corrected at the higher spin rates required for stabilization. For the orbiter vehicle average values of moment of inertia were used for the orbital maneuvers and contingencies while for the probe vehicle cruise conditions were assumed.

The propellant weight data clearly show the weak points of the various configurations. The susceptibility of configurations using tangential thrusters for velocity control to unbalanced spin torques is apparent in the large propellant weight penalty associated with spin disturbance correction. A moderate penalty is seen for those configurations using tangential thrusters for attitude orientation while minimum weight for this factor is incurred with the one configuration (D-1) which uses radial thrusters for both velocity and attitude control.

5.2.2 Module Weights

The weights of the various modules that make up the candidate configurations are presented in Table 5-3. A weight breakdown is provided giving weights for each of the components contained in the modules. Two valve module weights are given, one for feed system 1 (single latch valve pair) and one for feed system 3 (combined latch and explosive isolation valves). From the weight breakdown provided for feed system 3, it can be seen that the valve module for feed system 2 (redundant latch valve pairs) would be 0.52 lbm heavier for a total weight of 5.13 lbm.

5.2.3 System Weight and Balance

The dry weights for the candidate configurations are presented in Table 5-4. The weights of the required modules plus necessary electrical connectors, cable, and plumbing are indicated. These weights are combined with the propellant weights presented previously and with the required nitrogen pressurant to give the system weights presented in Table 5-5.

Figure 5-14. AVERAGE SPECIFIC IMPULSE MR 50 THRUSTER

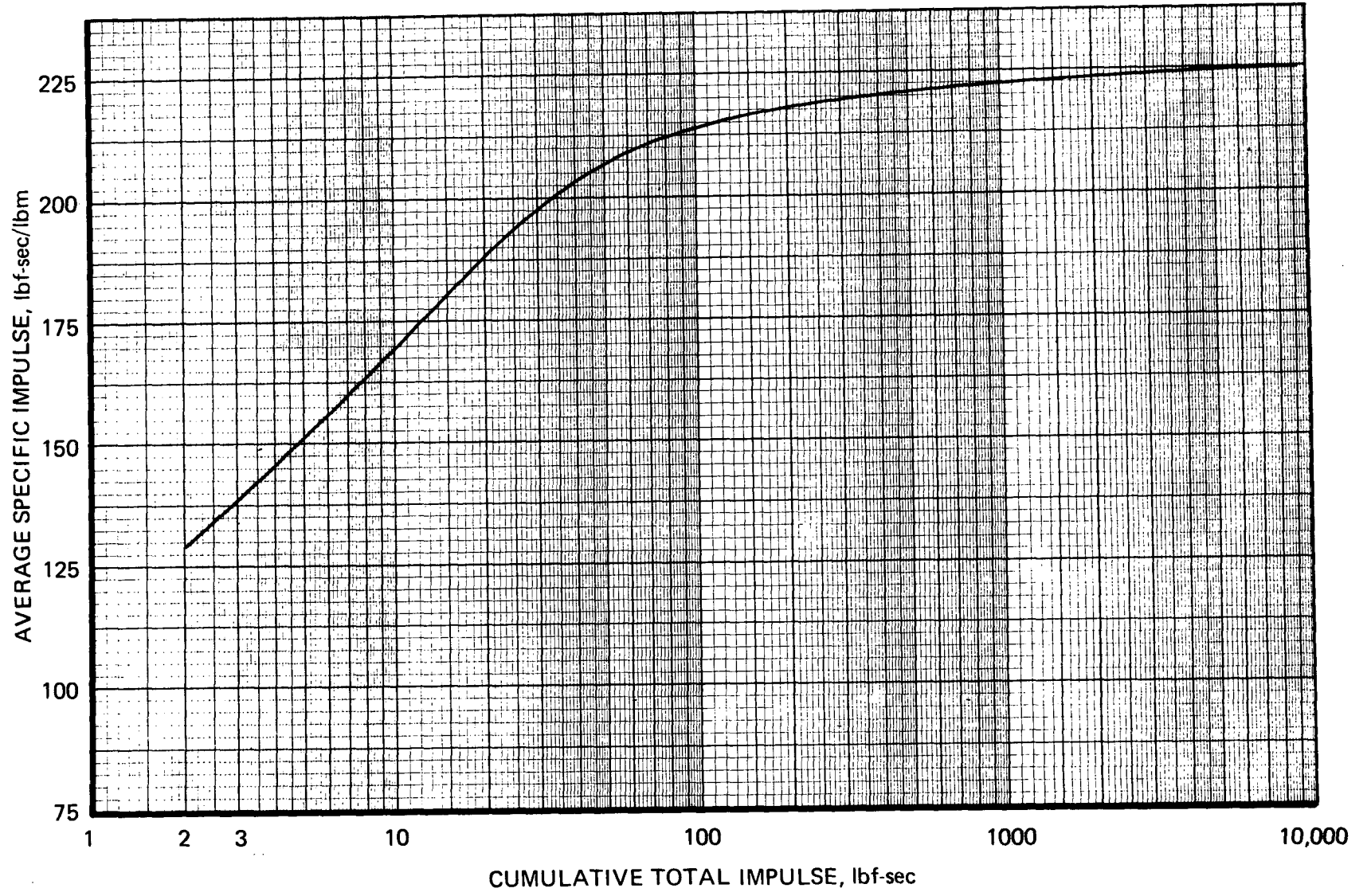


Table 5-3. MODULE WEIGHT SUMMARIES

Propellant Tank Module – Orbiter	
9 tanks @ 1.6 lb ea.	14.40 lb
Fittings	0.36 lb
Tubing	0.89 lb
Mounting ring	2.48 lb
Support brackets	2.75 lb
Fasteners	<u>0.38 lb</u>
Total	21.26 lb
Propellant Tank Module – Probe	
6 tanks @ 1.6 lb ea.	9.60 lb
Fittings	0.26 lb
Tubing	0.78 lb
Mounting ring	2.47 lb
Support brackets	2.40 lb
Tank spacers	0.50 lb
Fasteners	<u>0.38</u>
Total	16.39 lb
Valve Module, Feed System 3	
2 latching valves @ .61 ea.	1.22
2 explosive valves @ .35 ea.	0.70
3 fill/drain valves @ .22 ea.	0.66
1 filter	0.11
1 pressure transducer	0.41
Fittings & tubing	0.14
Mounting bracket	1.27
Fasteners & clamps	<u>0.10</u>
Total	4.61 lb
Valve Module, Feed System 1	
2 latching valves @ .61 ea.	1.22
2 fill/drain valves @ .22 ea.	0.44
1 filter	0.11
1 pressure transducer	0.41
Fittings & tubing	0.04
Mounting bracket	0.95
Fasteners, etc.	<u>0.05</u>
Total	3.22 lb

Table 5-3. MODULE WEIGHT SUMMARIES (Concluded)

Gimbaled Thruster Mode	
Stepped motor	0.89 lb
Ball screw assy & housing	0.251 lb
Motor bracket	0.322
Reactor bracket	0.194
Reactor	1.15
Rod ends	0.06
Propellant line fitting, etc.	<u>0.017</u>
Total	2.884 lb

Doublet Module	
2-5 lbf reactors & valves @ 1.15 ea.	2.30 lb
Electrical connector	0.06
Mounting bracket	0.363
Fittings, etc.	<u>0.06</u>
Total	2.783 lb

Table 5-4. DRY WEIGHT SUMMARIES

SYSTEM A		Wt (lb)
Thruster modules		
2 - 5 lbf gimbaled thrusters @ 2.884 lb		5.768
2 - 5 lbf doublet modules @ 2.738 lb		5.566
Valve module		4.61
Electrical		
4 - #10 electrical connectors @ 0.045 lb	0.18	
2 - #18 electrical connectors @ 0.11 lb	0.22	
64.6 feet wire	<u>1.00</u>	
	1.40	1.40
Plumbing		
4 @ 0.021 lb	0.064	
21.6 feet tube	<u>1.17</u>	
	1.234	1.234
Clamps and fasteners		<u>0.433</u>
	Subtotal	19.01
	9 tank module	<u>21.26</u>
	Dry weight orbiter	40.27
	6 tank module	<u>16.39</u>
	Dry weight probe	35.40

Table 5-4. DRY WEIGHT SUMMARIES (Continued)

SYSTEM B		Wt (lb)
Thrusters		
2 - 5 lbf doublet modules	2 @ 2.738 lb	5.566
4 - 5 lbf thrusters	4 @ 1.15 lb	4.60
Valve module		4.61
Electrical		
2 - #18 electrical connectors	@ 0.11 lb	0.22
6 - #10 electrical connectors	@ 0.045 lb	0.27
38.33 feet wire		<u>0.60</u>
		1.09
Plumbing		
fittings		0.074
18.8 feet tube		<u>1.02</u>
		1.094
Clamps and fasteners		<u>0.433</u>
	Subtotal	17.39
	9 tank module	<u>21.26</u>
	Dry weight orbiter	38.65
	6 tank module	<u>16.39</u>
	Dry weight probe	33.78
SYSTEM C		Wt (lb)
Thruster modules		
4 - 5 lbf doublet modules	@ 2.783 lb ea.	11.132
Valve module		
Electrical cable		
4 - #10 electrical connectors	@ 0.045 lb	0.18
2 - #18 electrical connectors	@ 0.11	0.22
56.3 feet wire		<u>0.88</u>
		1.28
Plumbing		
Fittings		0.08
26.83 feet tube		<u>1.45</u>
		1.53
Clamps and fasteners		<u>0.433</u>
	Subtotal	18.99
	9 tank module	<u>21.26</u>
	Dry weight orbiter	40.25
	6 tank module	<u>16.39</u>
	Dry weight probe	35.38

Table 5-4. DRY WEIGHT SUMMARIES (Concluded)

SYSTEM D		Wt (lb)
Thrusters		
5 - 5 lbf thrusters @ 1.15 lb		4.60
2 - doublet modules @ 2.783 lb		5.566
Valve module		4.61
Electrical cable		
6 - #10 electrical connectors @ 0.045 lb	0.27	
2 - #18 electrical connectors @ 0.11 lb	0.22	
50.42 feet wire	0.79	
	<u>1.28</u>	1.28
Plumbing		
Fittings	0.08	
22.58 feet tube	1.22	
	<u>1.30</u>	1.30
Clamps and fasteners		<u>0.433</u>
	Subtotal	17.79
	9 tank module	<u>21.26</u>
	Dry weight orbiter	39.05
	6 tank module	<u>16.39</u>
	Dry weight probe	34.18
SYSTEM E		Wt (lb)
Thruster modules		
2 - 5 lbf gimbaled thrusters @ 2.884 lb		5.768
2 - 5 lbf doublet modules @ 2.738 lb		5.566
Valve module		4.61
Electrical cable		
4 - #10 electrical connector @ 0.045 lb	0.18	
2 - #18 electrical connector @ 0.11 lb	0.22	
29.58 feet wire	0.46	
	<u>0.86</u>	0.86
Plumbing		
Fittings	0.042	
16.8 feet tube	0.91	
	<u>0.952</u>	0.952
Clamps and fasteners		<u>0.433</u>
	Subtotal	18.19
	9 tank module	<u>21.26</u>
	Dry weight orbiter	39.45
	6 tank module	<u>16.39</u>
	Dry weight probe	34.58

Table 5-5. SYSTEM WEIGHT SUMMARY

	B Radial Pairs	C Tangential Doublets	D-1 Rectangle Radial	D-2 Rectangle Tangential
Probe Mission				
System dry weight	33.78	35.38	34.18	34.18
Usable propellant	63.94	67.25	64.23	66.14
Residual propellant	.50	.50	.50	.50
Pressurant	.89	.83	.89	.85
Total wet weight	99.11	103.96	99.80	101.67
Orbiter Mission				
System dry weight	38.65	40.25	39.05	39.05
Usable propellant	94.76	102.66	98.24	98.41
Residual propellant	.70	.70	.70	.70
Pressurant	1.57	1.39	1.49	1.49
Total wet weight	135.68	145.00	139.48	139.65

Mass properties of the various modules as installed on the spacecraft are presented in Table 5-6. These are combined to provide the center-of-gravity location spin inertia, and spin unbalance for the candidate configurations in Table 5-7. These data are based on propellant loads of 61.50 lbm for the probe mission and 88.49 lbm for the orbiter configuration. The spin unbalance provides an indication of the balance that must be provided for by location of other spacecraft equipment. The axial and radial locations of these unbalanced masses are given in Table 5-6; the circumferential locations are apparent from the system layout drawings. Use of the propellant tanks for balance is not practical, since, because of the large weight of consumable fuel, spatial location of the individual tanks with respect to the spin axis must be paramount to minimize radial center-of-gravity translation as the propellant is consumed.

5.3 COMPONENT DESCRIPTION

Recommended typical components tentatively identified for the system are as follows:

Thrust chamber	Rocket Research Corporation	MR-50
TCV	Hydraulic Research	4800680
Isolation valve	Carleton Controls	2217001-2
Filter	Vacco	51-81847-1
Propellant tank	Fansteel	4425039
Fill/drain valve	Rocket Research Corporation	25030
Pressure transducer	Dynasciences	RRC-SCD-24948

These components are described in detail in the following paragraphs. All these components have a shelf life in excess of 4 years.

Table 5-6. PROPULSION MODULES MASS PROPERTIES

Component	Weight	Mass	Axial CG	Radial CG	Spin Inertia
	Pounds	Slugs	Feet	Feet	Slug Feet ²
9 tank module (loaded)	109.75	3.4084	2.365	—	8.5514
9 tank module (expended)	21.26	0.6602	2.283	—	1.1713
6 tank module (loaded)	77.83	2.4171	2.361	—	5.9710
Valve module System Δ	4.61	0.1432	1.229	1.754	0.4418
Valve module system C	3.22	0.100	1.287	1.686	0.2843
Radial thruster	1.15	0.0357	—	1.944	0.1349
Doublet module	2.783	0.0864	2.183	2.183	0.4120
Gimbaled thruster	2.884	0.0896	—	1.944	0.3385

Table 5-7. CANDIDATE SYSTEM MASS PROPERTIES

SYSTEM A

Spin Inertia (Slug Feet ²)					Axial CG Location*	Space Craft
Valve Module	Gimbaled Thrusters	Doublet Modules	Tank Module	Total		
0.2843	0.6770	0.8240	8.5514	10.3367	25.74	Orbiter (Loaded)
			1.1713	2.9566	18.648	Orbiter (Expended)
			5.9710	7.7563	25.164	Probe (loaded)
			0.8418	2.6271	18.216	Probe (Expended)
0.1686	—	—	—	0.1686		
Spin Unbalance (Slug Feet)						

*Inches from booster interface

Table 5-7. CANDIDATE SYSTEM MASS PROPERTIES (Continued)

SYSTEM B

Spin Inertia (Slug Feet ²)						
Valve Module	Radial Thrusters	Doublet Modules	Tank Module	Total	Axial CG Location*	Space Craft
0.2843	0.5396	0.8240	8.5514	10.1993	26.892	Orbiter (Loaded)
			1.1713	2.8192	22.480	Orbiter (Expended)
			5.9710	7.6189	26.410	Probe (Loaded)
			0.8418	2.4897	21.740	Probe (Expended)
0.1686	—	0.1886	—	0.3572		
Spin Unbalance (Slug Feet)						

*Inches from booster interface

SYSTEM C

Spin Inertia (Slug Feet ²)					
Valve Module	Doublet Modules	Tank Module	Total	Axial CG Location*	Space Craft
0.2843	1.6480	8.5514	10.5197	27.005	Orbiter (Loaded)
		1.1713	3.1035	19.104	Orbiter (Expended)
		5.9710	7.9393	25.350	Probe (Loaded)
		0.8418	2.7740	18.711	Probe (Expended)
0.1686	—	—	0.1686		
Spin Unbalance (Slug Feet)					

*Inches from booster interface

Table 5-7. CANDIDATE SYSTEM MASS PROPERTIES (Concluded)

SYSTEM D

Spin Inertia (Slug Feet ²)						
Valve Module	Radial Thrusters	Doublet Modules	Tank Module	Total	Axial CG Location*	Space Craft
0.2843	0.5396	0.824	8.5514	10.1993	26.724	Orbiter (Loaded)
			1.1713	2.8192	21.902	Orbiter (Expended)
			5.9710	7.6189	26.749	Probe (Loaded)
			0.8418	2.4897	22.780	Probe (Expended)
0.1686	—	—	—	0.1686		
Spin Unbalance (Slug Feet)						

*Inches from booster interface

SYSTEM E

Spin Inertia (Slug Feet ²)						
Valve Module	Gimbaled Thrusters	Doublet Modules	Tank Module	Total	Axial CG Location*	Space Craft
0.2843	0.6770	0.8240	8.5514	10.3367	25.944	Orbiter (Loaded)
			1.1713	2.9566	20.226	Orbiter (Expended)
			5.9710	7.7563	25.517	Probe (Loaded)
			0.8418	2.6271	20.209	Probe (Expended)
0.1686	—	0.1886	—	0.3572		
Spin Unbalance (Slug Feet)						

*Inches from booster interface

5.3.1 5-lbf Rocket Engine Assembly

The baseline 5-lbf Rocket Engine Assembly (REA) is the RRC MR-50 engine which has been designed, developed, and flight qualified for the LMSC P-95 Program. The MR-50 engine has been qualified as part of a four-engine module termed Rocket Engine Module-Monopropellant (REM-Mono). The REM-Mono four-engine module is shown in Figure 5-15, including four delivered modules. Production and delivery of 28 flight REM's (112 REA's) has been completed and the first follow-on buy of 26 REM's (104 REA's) is currently in process. Qualification testing of the MR-50 engine has been successfully completed and the tests are summarized in the following paragraphs.

5.3.1.1 MR-50A Qualification Test Summary

Qualification of the 5-lbf REA was conducted at the REM level. Each REM contains four REA's. Qualification testing was conducted on two REM's or eight REA's. Testing has been completed on both REM's and approved by Lockheed Missiles and Space Company.

Table 5-8 summarizes the types of requirements which had to be verified and indicates whether verification was by analysis, demonstration, or test. A summary of the qualification testing conducted on each of the REM's is contained in the following paragraphs.

5.3.1.1.1 Reaction Engine Module Serial Number 1001

Figure 5-16 depicts the qualification test sequence to which REM S/N 1001 was subjected. As indicated in the figure, functional tests were performed after each of the environmental tests. The following paragraphs summarize the tests conducted and the results obtained.

5.3.1.1.1.1 REM S/N 1001 Acceptance Test

The REM was subjected to two acceptance test sequences which consisted of random vibration and acceptance test firing of each REA in vacuum. Two acceptance test sequences were used to simulate a possible rework cycle and subsequent reacceptance testing of the REM. The random vibration level was 26.8 g rms applied in each of three axes for a duration of 60 seconds in each axis. The acceptance test conducted on the REM consisted of both pulse-mode and steady-state operations. A total of 210 pulses and two steady-state tests each of 100 seconds duration was conducted on each REA.

5.3.1.1.1.2 REM S/N 1001 Environmental Tests

5.3.1.1.1.2.1 Humidity Test

The humidity test was of 30 hours duration and consisted of subjecting the REM to a program sequence of relative humidity varying from room ambient to 95% at temperatures of +35 to +100°F.

5.3.1.1.1.2.2 Acoustic Test

The REM was subjected to an acoustic test of 3 minutes duration at an overall level of 152 decibels.

11027-53

5-45

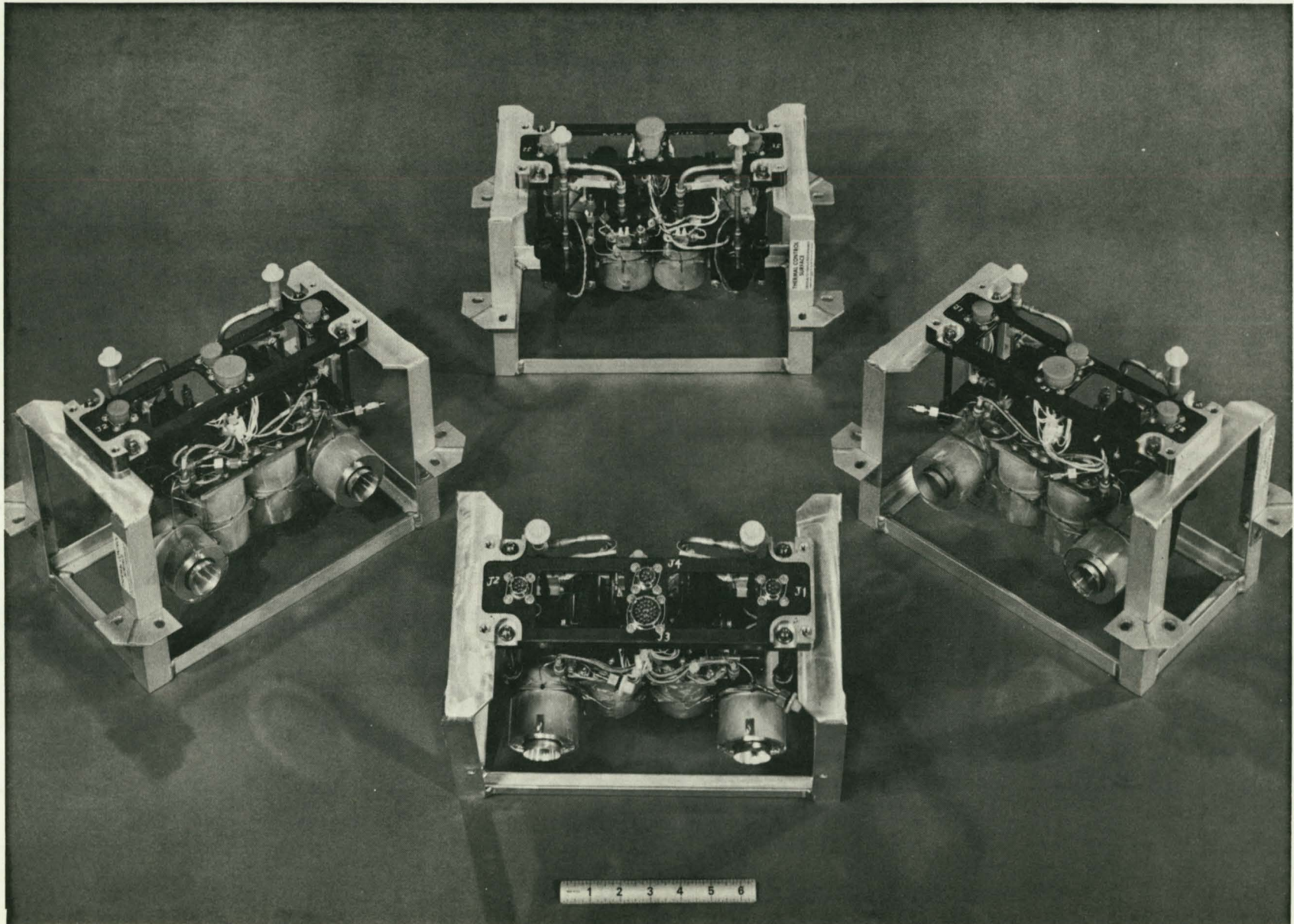


Figure 5-15. MRM-50A 5-lbf REACTION ENGINE MODULES

Table 5-8. MR-50A ROCKET ENGINE ASSEMBLY QUALIFICATION REQUIREMENT SUMMARY

Item	Method of Verification	Requirement
Thrust alignment	Analysis	Thrust vector within ± 0.5 degree of geometric centerline
Malfunction	Analysis	Failure of any one of two active REA's shall not effect operation of standby REA's
Reliability	Analysis	REM probability of success ≥ 0.999
Installation	Analysis	REM shall be installed as a single unit
Operating life	Analysis	Operating life shall not be less than 18 months
Prelaunch hold life	Analysis	Prelaunch hold capability a minimum of 33 days
Fungus	Analysis	REM shall meet performance after exposure to fungus environment per MIL-STD-810
Temperature	Analysis	REM shall meet performance after storage temperatures of -40°F to $+140^{\circ}\text{F}$
Transportation and handling	Analysis	REM shall meet performance after shock and vibration exposure requirements for air transportation
Storage	Analysis	REM shall meet performance after storage period of two years minimum
Propellant compatibility	Analysis	REM shall function normally after exposure to N_2H_4 fumes and splashes
Particle radiation	Analysis	REM must function normally after exposure to particle radiation for 6-month period per LMSC specification
Micrometeoroid	Analysis	REM must function normally after exposure to micrometeoroid environment for 6 months per LMSC specification
Solar radiation	Analysis	REM must function normally after exposure to solar radiation environment for 6 months per LMSC specification
Temperature	Analysis	The REM shall not be degraded by the transportation and handling environments
Loads	Analysis	Safety factor 1.25 applied to flight loads to obtain design flight ultimate loads and safety factor 1.5 for ground loads
Allowable stresses	Analysis	Allowable stresses shall be combined to provide required margin of safety under maximum combination of conditions
Ground safety	Analysis	REM shall be safe in electrical power failure mode
Moisture and fungus resistance	Analysis	All materials used in REM shall resist damage from fungus and moisture

Table 5-8. MR-50A ROCKET ENGINE ASSEMBLY QUALIFICATION REQUIREMENT SUMMARY (Continued)

Item	Method of Verification	Requirement
Electrolytic corrosion of metal parts	Analysis	The REM shall not use dissimilar metals in direct contact which accelerate electrolytic corrosion
Stress corrosion	Analysis	Materials, processes, and assembly techniques shall minimize stress corrosion
Liquid leakage rate	Demonstration	Internal liquid leakage of any REA shall not exceed 0.01 cc/hr and there shall be no external liquid leakage
Propellant	Demonstration	Propellant shall be per MIL-P-26536
Gases	Demonstration	Gases used in servicing checkout and cleaning shall be nitrogen per MIL-P-27401
Contamination levels	Demonstration	All fluids entering REM shall not contain particulate contamination in excess of limits of MIL-STD-1246 level 150 except quantity may include one fiber
Propellant saturation	Demonstration	REM shall meet performance when supplied with propellant completely saturated with nitrogen
Electrical characteristics	Demonstration	REA operating voltage 24 to 33 vdc. Maximum REA power 30 watts. Insulation resistance and dielectric strength per LMSC specification.
Instrumentation	Demonstration	Instrumentation to be provided to measure chamber pressure and temperature of active REA's, active REA's valve temperature, and REM mount plate temperature
Bleeding	Demonstration	Under normal conditions REM shall be as self-draining as possible
Draining	Demonstration	REM shall have capability of ready drainage and/or flushing in 1-g field under normal installation
Cleaning	Demonstration	REM manifold and passage upstream of valve seat shall have capability of cleaning after propellant loading by using rinse fluids and vacuum drying
Prelaunch life	Demonstration	REM shall meet all requirements after being loaded with propellant and pressurized for period of 13 days
Atmospheric pressure	Demonstration	REM shall have capability of operating safely without degradation at sea-level conditions
Pressure	Demonstration	Proof pressure shall be 1.5 times maximum operating pressure with 300 psia feed pressure and burst pressure shall be minimum of 2.0 under same conditions
Explosive and ordance safety	Demonstration	REM shall suffer no effect from exposure to explosive atmosphere and REM electrical equipment shall operate in such atmosphere without ignition occurring

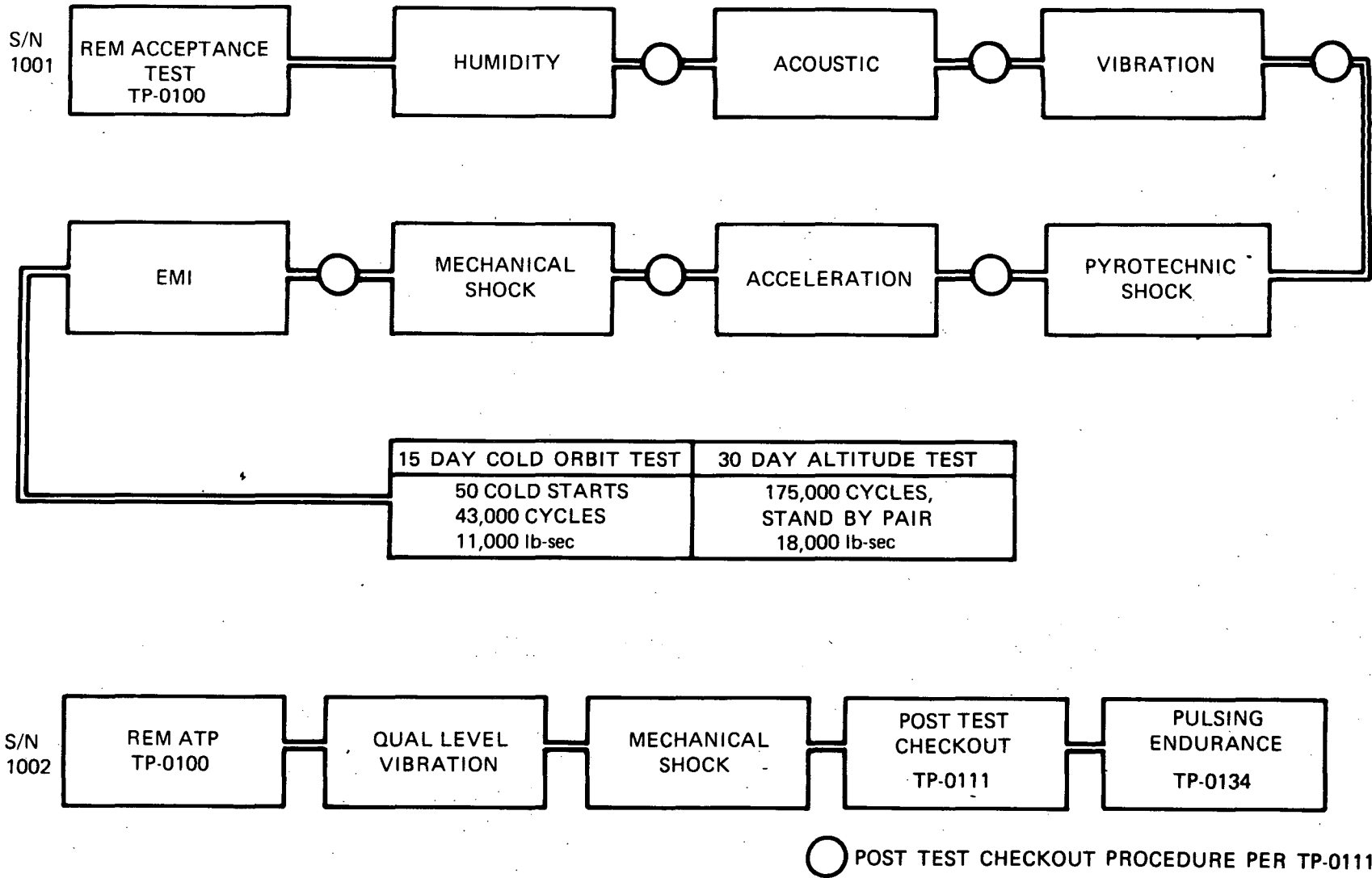
Table 5-8. MR-50A ROCKET ENGINE ASSEMBLY QUALIFICATION REQUIREMENT SUMMARY (Continued)

Item	Method of Verification	Requirement
Component filtration	Demonstration	REM shall contain filters for protection from contaminants during checkout servicing, testing, cleaning, purging, and operation
Propellant valves	Demonstration	Each REA shall have a single valve to control propellant flow and shall return to closed position if power failure occurs
Steady-state thrust	Test	Minimum steady-state thrust shall not be less than 2.5 lbf
Start and shutdown transients	Test	Thrust shall not exceed 10 lbf during start overshoot or shutdown transient
Ripple	Test	Thrust oscillation shall not exceed $\pm 25\%$ over REA life
Thrust repeatability run-to-run	Test	Variation in REA steady-state from run-to-run shall not exceed 8%.
Thrust repeatability REA-to-REA	Test	Two sigma variation in steady-state thrust between REA's of same or different REM's shall not exceed 10%
Total impulse	Test	Each REA shall have capability of producing 18,000 lbf-sec total impulse
Minimum impulse bit	Test	3-sigma minimum impulse bit shall not be greater than .15 lbf-sec or less than .03 lbf-sec at 22 ms pulse width over complete range of pressure and temperatures and duty cycles to 1 cps
Minimum impulse bit repeatability—run-to-run	Test	Variation in impulse bit of single REA shall not exceed $\pm 10\%$ run-to-run at 22 ms pulse width including instrumentation errors
Minimum impulse bit repeatability—REA-to-REA	Test	Variation in minimum impulse bit REA-to-REA of same or different REM's shall not exceed 22% two sigma including instrumentation errors
Steady-state specific impulse	Test	Minimum steady-state specific impulse shall exceed 205 lbf-sec/lbm
Pulsing specific impulse	Test	The minimum pulsing specific impulse operating at one 22 ms pulse every 100 seconds shall exceed 125 lbf-sec/lbm
Total firings	Test	Each pitch/roll REA shall be capable of 175,000 pulses including 10 cold starts. Each yaw REA shall be capable of 43,000 pulses including 50 cold starts.
Nominal duty cycle	Test	Maximum activity shall consist of steady state for 2 minutes and pulsing up to 5 cps. Minimum activity consists of one 22 ms pulse every 100 seconds.
Extreme duty cycle	Test	Maximum activity shall consist of steady state for 5 minutes and pulsing to 10 cps. Minimum activity shall consist of delivering 1.79 lbf-sec over 90-minute period.

Table 5-8. MR-50A ROCKET ENGINE ASSEMBLY QUALIFICATION REQUIREMENT SUMMARY (Concluded)

Item	Method of Verification	Requirement
Gas leakage rate	Test	Internal gas leakage rate shall not exceed 15 scc/hr GN ₂ and external leakage shall not exceed 1×10^{-4} scc/sec GN ₂
Steady-state start and shutdown response	Test	Rise time to 85% steady-state thrust shall not exceed 2.5 seconds and decay time to 10% steady-state thrust shall not exceed 150 ms
Pulsing response	Test	For minimum impulse bit operation (22 ms pulse width) 33% of impulse bit shall be delivered in 50 ms, 60% in 100 ms, and 75% in 150 ms
Propellant feed characteristics	Test	The REM shall operate at feed pressures as high as 315 psia and as low as 85 psia
Thermal characteristics	Test	Passive thermal control shall be utilized for normal operations. An active thermal control shall be used for nonstandard missions. Peak heat transfer to the vehicle shall not exceed 225 BTU/hr for two REA's firing steady state.
Blow-off covers	Test	A protective nozzle cover shall be provided that blows off at 9 ± 5 psi differential pressure
Orbital life	Test	Orbital life shall be a minimum of 45 days
Component life	Test	Propellant valves and pressure transducers shall have a minimum cycle life capability of 225,000
Relative humidity	Test	Up to 100% including condensation
Acoustics	Test	Overall sound pressure level 152 ± 3 db, 3 minutes
Vibration	Test	37.9 g rms, 180 seconds each axis. Sine vibration to be: 5 to 50 cps, 2.0 g's; 50 to 2,000 cps, 4.0 g's.
Mechanical shock	Test	30 g, half-sine wave, 8 milliseconds
Pyrotechnic shock	Test	8,000 g peak response acceleration at 4,000 cps
Acceleration	Test	Flight path: 8 g.s for 5 minutes; lateral: 3 g's for 5 minutes
Atmospheric pressure	Test	REM shall operate normally at altitudes of 260,000 feet or greater
Temperature	Test	REM shall operate normally when mounted to conductive surface and surrounded by totally absorbing thermal radiation environment. Temperature will vary from 0°F to +140°F.
Weight	Test	Dry weight of the REM shall not exceed 9.0 lbm
Electromagnetic	Test	REM shall comply with MIL-STD-826A, class AU type C plus special LMSC requirements

11027-59



S-50

Figure 5-16. QUALIFICATION TEST PLAN REM-MONO MRM-50A

5.3.1.1.1.2.3 Vibration

The REM was subjected to a random vibration testing at a level of 37.9 g rms for 180 seconds duration in each of three axes. After completion of the random vibration test the REM was subjected to a sinusoidal vibration test at a level of 2 g from 5 to 50 cps and 4.0 g from 50 to 2,000 cps in each of three axes. The sweep rate was 2 minutes/octave.

5.3.1.1.1.2.4 Pyrotechnic Shock

The pyrotechnic shock test was conducted with the REM mounted in a "barrel" which simulates the outer skin of the vehicle and has a detachable section to be blasted away by an explosive charge. Two pyrotechnic shocks were conducted. The applied pyrotechnic shock level was 25,000 g at 3,000 cps.

5.3.1.1.1.2.5 Acceleration

The REM was subjected to an acceleration of 8 g's for 5 minutes in the flight axis and 3 g's for 5 minutes each in two orthogonal axes.

5.3.1.1.1.2.6 Mechanical Shock

The REM was subjected to three 30-g shocks of 8 milliseconds duration in each of three axes in each of two directions (18 shocks total).

5.3.1.1.1.2.7 Electromagnetic Interference

The REM was tested for electromagnetic interference in accordance with methods 3001, 3002, 4001, 4002, 5001, 5006, and 6002 of MIL-STD-826A. In addition, the REM was checked for single event transient, ripple voltage and susceptibility to low-frequency ripple in accordance with LMSC specification requirements.

5.3.1.1.1.3 Orbital Life Test

A 45-day orbital life test in vacuum was conducted on the REM so that the active pair of REA's was subjected to 15 days of testing and the standby pair of 30 days of testing. The 15-day test on the active pair was designed to verify compliance with the specification requirements of 50 cold starts and to demonstrate the yaw REA duty cycle totaling 43,000 pulses and 11,000 lbf-sec total impulse. The 30-day test on the standby pair was designed to verify compliance with the 175,000 pulse and 18,000 total impulse requirement and to obtain a performance map of duty cycle, pressure, temperature, and pulse width which would verify compliance with specification performance requirements. All testing was conducted on a 24-hour-day basis.

Actual total impulse, number of pulses, and burn time accumulated on each of the active REA's during a 15-day orbital life test are as follows:

	Total Impulse lbf-sec	Number of Pulses	Burn Time seconds
Active yaw REA	11,760	60,942	2,801
Active pitch REA	14,955	92,897	3,835

Actual total impulse, number of pulses and burn time accumulated on each of the standby REA's during the 30-day orbital life test are as follows:

	Total Impulse lbf-sec	Number of Pulses	Burn Time seconds
Standby yaw REA	20,242	198,537	5,983
Standby pitch REA	20,554	182,502	4,831

5.3.1.1.2 Reaction Engine Module Serial Number 1002

Figure 5-16 depicts the qualification test sequence to which REM S/N 1002 was subjected. As indicated in the figure, the REM was subjected to an acceptance test sequence followed by qualification level vibration and mechanical shock. Following post-environmental test checkout, the engine was installed in the vacuum chamber and subjected to pulsing endurance testing.

5.3.1.1.2.1 REM S/N 1002 Acceptance Test

The acceptance test sequence for REM S/N 1002 was the same as that described in paragraph 5.3.1.2.1, except that only one acceptance test sequence was used.

5.3.1.1.2.2 REM S/N 1002 Environmental Tests

Upon completion of acceptance test, REM S/N 1002 was subjected to qualification-level vibration and mechanical shock testing as described in paragraphs 5.3.1.1.1.2.3 and 5.3.1.1.1.2.6 respectively.

5.3.1.1.2.3 Pulsing Endurance Test

REM S/N 1002 was subjected to the 15-day altitude pulsing endurance test. The following were the objectives of the test program:

- a. Demonstration of operating characteristics over the reactor life
- b. Demonstration of mission life capability
- c. Investigation of liquid leakage throughout reactor life
- d. Provision of backup data on repeatability and specific impulse.

Liquid leakage was investigated daily by maintenance of the REM at an inlet pressure of 233 psia and by the monitoring of flight temperatures for a minimum period of 4 hours to determine whether or not there was any temperature rise of the REA which would indicate liquid leakage.

The pulsing endurance test sequence was structured to accumulate a minimum of 175,000 pulses and 18,000 lbf-sec total impulse on each of the active REA's. This was followed by a switch-over and accumulation of the same life on the standby pair of REA's. Testing on each pair of REA's was accomplished in 7-1/2 days with testing conducted on a 24-hour-day basis.

The actual total impulse, number of pulses, and total burn time accumulated on each REA are summarized below:

	Total Impulse lbf-sec	Number of Pulses	Burn Time seconds
Active yaw REA	21,088	180,169	4,595
Active pitch REA	21,090	180,190	4,594
Standby yaw REA	26,346	187,388	5,807
Standby pitch REA	27,558	185,161	6,106

5.3.1.1.3 Summary of Test Results

Table 5-9 summarizes the major qualification test results and compares them to the specification requirements. All demonstrated performance values shown in Table 5-9 have added or subtracted, as appropriate, 2-sigma instrumentation errors so that demonstrated performance is within specification requirements considering measurement accuracies.

5.3.1.2 5-lbf REA Design

The REM-Mono engine design has evolved through a series of contracted and in-house research and development programs. In particular, the 5-lbf engine is based on previous experience on the Transtage 27-lbf engine that developed the basic engine design. The Transtage engine has been qualified and successfully flown on the Titan III-C vehicle. Many of the problems associated with obtaining engine life are not encountered until a formal engine qualification program is undertaken and the wide range of environments and operational modes fully explored. The extensive RRC contracted and in-house programs have clearly identified problems and design solutions associated with development of long-life hydrazine engines.

An AFRPL research contract is particularly significant in that RRC has been selected by AFRPL to conduct a long-life monopropellant hydrazine engine development and test program. This program will result in a 5-lbf engine capable of 1,000,000 pulses. This program uses the existing REM-Mono 5-lbf engine design as a baseline, and design modifications are being evaluated to further enhance engine life. This program will provide extended engine life capability for 5-lbf engines for future applications. The required duty cycle for the 1,000,000 cycle testing includes (45) cold-bed starts and will require approximately 2 months for the 1,000,000 cycles. The results of this long-life engine program will be available prior to the planned go-ahead for the Planetary Explorer Program. Engine design modifications will be evaluated during the long-life program which may be useful for the proposed Planetary Explorer Program.

The MR-50 monopropellant hydrazine 5-lbf REA is shown in Figure 5-17 using the Hydraulic Research series-redundant valve, and Figure 5-18 shows the REA using the Parker single-seat valve.

The Hydraulic Research valve is a minor modification of the flight-qualified Hydraulic Research INTELSAT IV valve. Modification of the valve is necessary to attach the valve to the RRC 5-lbf engine and will use a three-bolt hole pattern at the valve outlet. This minor modification will not affect the internal characteristics of the valve. This modification has also been currently proposed by RRC for the NASA/Goddard SMS program.

Table 5-9. COMPARISON OF QUALIFICATION TEST REQUIREMENTS TO DEMONSTRATED VALUES

Qualification Test Requirement		Demonstrated Values
LIFE		
175,000 cycles		181,515 cycles
18,000 lbf-sec		27,558 lbf-sec
45 days orbital		52 days
PERFORMANCE		
Thrust:	2.5 lbf average minimum 3-sigma steady-state	2.71 lbf min.
Start overshoot:	< 10 lbf	8.3 lbf
Ripple:	± 25% of maximum steady-state thrust	± 14%
Specific impulses:		
Steady state:	205 lbf-sec/lbm minimum 2 sigma	217 lbf-sec/lbm
Pulse mode +	125 lbf-sec/lbm at nominal minimum duty cycle, one REA firing	128.2 lbf-sec/lbm
Minimum impulse bit:	≤ 0.15 lbf-sec at maximum temperature and pressure conditions through 1 cps	0.125 lbf-sec
	≤ 0.18 lbf-sec at maximum temperature and pressure conditions above 1 cps	0.133 lbf-sec
	≥ 0.03 lbf-sec 3 sigma for all duty cycles up through 1 cps	0.0356 lbf-sec
Impulse proportionality (impulse bit versus pulse width):		Met specification requirement
Cold starts:	50	50
RESPONSE		
Steady state:	1 lbf in 60 msec (single REA start)	49 msec
	1 lbf in 90 msec (dual REA start)	66 msec
	85% steady state in 2.5 sec	2.44 sec
Pulse mode (during MIB operation):	33% impulse bit in 50 msec	49%
	60% impulse bit in 100 msec	65%
	75% impulse bit in 150 msec	75%

Table 5-9. COMPARISON OF QUALIFICATION TEST REQUIREMENTS TO DEMONSTRATED VALUES (Continued)

Qualification Test Requirement		Demonstrated Values
RESPONSE (Continued)		
Pulse mode (0.5 cps after REM inactivity):		
5th bit:	40% of equilibrium value	55%
10th bit:	50% of equilibrium value	57%
100th bit:	85% of equilibrium value	88%
Tailoff (steady state):	55 msec to 35% of steady-state value	51 msec
	150 msec to 10% of steady-state value	148 msec
REPEATABILITY		
Thrust:		
Run-to-run	±8%	±6.8%
REA-to-REA	±15%	±11.2%
MIB		
Run-to-run	±10%	< 10%
REA-to-REA	±22%	±21.4
DUTY CYCLE		
Nominal		
Maximum activity:	Steady-state operation for 2 minutes or 5 cps pulse mode	Conducted tests at required duty cycles
Minimum activity:	One MIB every 100 secs, single, alternate or any combination of firing REA's	Conducted tests at required duty cycles
Extreme		
Maximum activity:	Steady-state operation for 5 minutes or 10 cps	Conducted tests at required duty cycles
Minimum activity:	Impulse delivery not exceeding 1.79 lbf-sec over 90-minute period with off times up to 2,100 sec, single, alternate, or any combination of firing REA's	1.64 lbf-sec/90 min demonstrated

Table 5-9. COMPARISON OF QUALIFICATION TEST REQUIREMENTS TO DEMONSTRATED VALUES (Concluded)

Qualification Test Requirement		Demonstrated Values
THERMAL MANAGEMENT		
Active:	Redundant heaters employed when environmental surrounding temperature drops below 20°F	Heaters used at less than +20°F environment
Passive:	Passive thermal management at temperatures above 20°F and with extreme duty cycle	Passive control employed above +20°F
ENVIRONMENTAL		
Vibration		
Random:	37.9 g rms, 180 sec each axis	Unit successfully passed test
Sine:	5 to 50 cps, 2 g; 50 to 2,000 cps, 4 g	
Shock		
Mechanical:	30 g, half-sine wave, 8 milliseconds	Unit successfully passed test
Pyrotechnic:	8,000 g peak response acceleration at 4,000 cps	25,000 g at 3,000 cps
Acceleration		
Flight path:	8 g for 5 minutes	Unit successfully passed test
Perpendicular to flight path:	3 g for 5 minutes	
Acoustic (external, aft section):	Overall sound pressure level 152 ± 3 db, 3 minutes	152 db
EMI comply with MIL-STD-826A, Class AU, type C plus special LMSC requirements		Unit successfully passed test
Weight:	9 lbm maximum	8.62 lbm

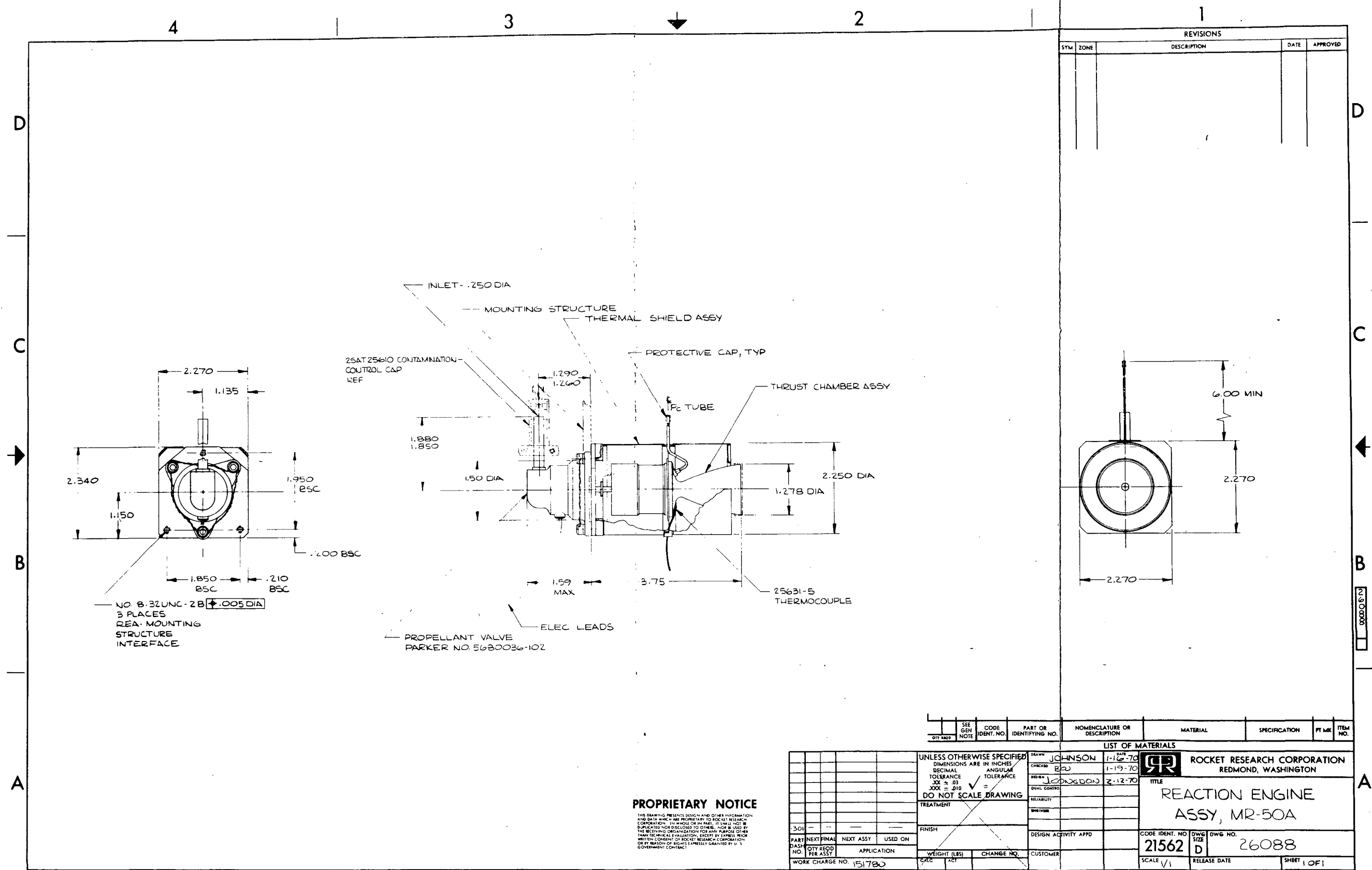


Figure 5-18. REACTION ENGINE ASSEMBLY, MR-50A

The Parker single-seat valve has been qualified as part of the MR-50A engine for the LMSC REM-Mono Program. The Parker valve would require no modification for the proposed Planetary Explorer application.

As discussed in the reliability section 3.1.2 and the valve section 5.3.2, a dual independent valve configuration should also be considered, since it has inherently higher reliability than either the single- or the dual-seat (pushrod) Hydraulic Research valve. This could be accomplished on the 5-lbf engine through use of two Parker single-seat valves in series. This design approach is currently being considered for the Viking lander and other applications and is similar to the Parker series valve design used by RRC on the Hydrazine Propulsion Module 0.5-lbf thrusters.

If the dual independent valve is developed and qualified at the 5-lbf thrust level, this configuration may be preferred. However, on the basis of using currently available qualified dual-seat valves, the Hydraulic Research valve has been shown throughout this study as a typical valve configuration, and the envelope for this configuration is typical of that required for the dual independent valve configuration.

Thruster performance used in calculating system propellant weights was presented in Figure 5-14. This curve is based on actual MR-50 thruster performance at a midrange feed pressure. Average specific impulse as a function of cumulative total impulse is shown. For a given maneuver, once the total impulse requirement is determined by vehicle requirements, an effective average specific impulse over that firing is provided by the curve. In this way, heatup losses are accounted for. Typical Planetary Explorer duty cycles are such that the collective total impulse from a pulse train may be used without significant error due to additional heat loss during engine-off periods.

5.3.2 Thrust Chamber Valves

Table 5-10 lists those propellant valves which in RRC's opinion are potential candidates for the Planetary Explorer thrust chamber valve, based on a review of the current status of existing valves and the following criteria:

- a. There must be less than 100-psid pressure drop at 0.022 lbf/sec N_2H_4 flow rate (5-lbf thrust).
- b. There must be no sliding fits.
- c. There must be test experience in an N_2H_4 system.
- d. There must be design precedent indicating ability to be produced in series-redundant seat configuration.

Rocket Research Corporation's valve data file was updated for the study by issuance of a request for current status data to valve supplies. Those valve manufacturers not listed in Table 5-10, and from whom information was solicited were Allen Design, Carleton Controls, Fairchild Hiller, Sterer Engineering, and Wright Components.

As seen in Table 5-10, all candidate valves except the Hydraulic Research P/N 4800680 (or 4801000) are either not qualified or do not provide seat redundancy. Therefore, on the basis of current status,

Table 5-10. CANDIDATE THRUST CHAMBER VALVES (5 LBF THRUST), PLANETARY EXPLORER N₂H₄ SYSTEM

Manufacturer	Hydraulic Research	Hydraulic Research	Moog Inc.	Moog Inc.	Moog Inc.	Parker	Parker
Part Number	4800680	4801000	010-57809	010-58321	010-50638	5680036	5690023
Weight, lbm	0.47	0.61	0.4 (incl. cable)	0.4 (incl. cable)	0.7	0.4	0.4
Approx. size, inches	1.33 x 2.4 x 2.17	1.33 x 2.4 x 2.17	1.3 dia x 1.55	1.01 dia x 1.9	1.5 x 3.0 x 1.9	1.4 dia x 1.53	1.4 dia x 1.53
Operating voltage range, vdc	24-36	18.6-32	20-33	20-32	24-32	19-33	24-33
Power, Watts at 70°F, 28 vdc	11.1	18.3	19.4	21.8	16.2	18.7	18.7
Opening response time 28 vdc, 70°F, ms	8 nom	7 nom	4.5 nom	10 nom	8 nom	5 nom	5 nom
Closing response time, 28 vdc, 70°F, ms	3 nom	3 nom	4 nom	2 nom	2 nom	5 nom	5 nom
Operating pressure, psia	0-300	0-300	0-300	0-300	0-300	0-750	0-300
Demonstrated burst pressure, psig	1270, predicted	615	>1200	>1000	>1000	>1200	>1200
Integral filter absolute micron rating	25	None	25	35	35	25	25
Rated flow, lbm/sec N ₂ H ₄	0.0224	0.025	0.022	0.025	0.025	0.022	0.022
Pressure drop, psid, at 0.022 lbm/sec	19.7	21.7	34.0	19.4	12.3	34.0	34.0
Operating temperature range, °F	40-250	40-280	40-250	40-250	40-250	40-250	40-250
Cycle life, qualified to	55,000	355,000	1,000,000	-	-	500,000	1,000,000
Cycle life, estimated capability	1,000,000	1,000,000	-	1,000,000	1,000,000	1,000,000	1,000,000
Seat type	Flat poppet, hard	Flat poppet, hard	Teflon poppet	Teflon poppet	Teflon poppet	Flat poppet, hard	Teflon poppet
Seat redundancy	Series	Series	None	Series	Series	None	None
Coil redundancy	*Partial	*Partial	None	None	*Partial	None	None
Valve type	Single torque motor, mech'ly linked seats	Single torque motor, mech'ly linked seats	Solenoid, flexure guided, non-sliding	Solenoid, flexure guided, non-sliding mechanically linked seats	Single torque motor, mech'ly linked seats	Solenoid, flexure guiding, non-sliding	Solenoid, flexure guided, non-sliding
Leakage, internal, sec/hr GN ₂	1.0	1.0	1.0	1.0	1.0	10.0	1.0
Leakage, external, sec/sec helium	6 x 10 ⁻⁶	6 x 10 ⁻⁶	6 x 10 ⁻⁶	10 ⁻⁵	10 ⁻⁴	6 x 10 ⁻⁶	6 x 10 ⁻⁶
Program application history	Qualified, 26 valves delivered for Skynet I and Natosat. Under contract for Skynet II	Qualified, 161 delivered for Intelsat IV and classified application	Qualified, Alternate for P-95 block III. None delivered	In house development	In house development. RRC has engine tested	Qualified, 250 delivered for P-95	Qualified. Under contract for 122, for P-95 block II
Remarks	*Operation in degraded mode if one coil fails. May need mu-metal shielding	*Operation in degraded mode if one coil fails. may need mu-metal shielding.	Not series redundant	Not qualified	Not qualified May need mu-metal shielding	Not series redundant	Not series redundant.

the Hydraulic Research valve is considered the prime candidate. Several other similar applications for 5-lbf size series-redundant valves such as the Viking (Mars Lander) attitude control and deorbit systems will precede Planetary Explorer in hardware development and are expected to stimulate more competition in this area. Rocket Research Corporation believes that several qualified series-redundant valves may be available in the 5-lbf thrust range when a final selection is made for Planetary Explorer. In particular, the Parker P/N 5690023 valve is ideally suited to assembly as a series-redundant pair, providing the type of redundancy shown as most desirable in Table 3-2. The series-redundant valve used on RRC's flight-qualified HPM and ERTS systems is a smaller version of the P/N 5690023 valve welded into a series-redundant pair. Power reduction can be accomplished, since the present Parker valve is designed for very fast response over a wide range of temperature, voltage, and pressures (750 psia).

The Hydraulic Research P/N 4800680 is preferred to the P/N 4801000 for use on the RRC MR-50 thruster because it requires less power and is lighter in weight as well as being significantly less expensive. The P/N 4801000 valve developed from the P/N 4800680 valve by increasing the power to reduce response time and beefing up the mounting. Because of the generally long pulse width duty cycles required, the shorter response time is not a requirement for the Planetary Explorer; and a revision to the mounting attachment is required in either case to adapt the valve to the MR-50 thrust chamber.

The Hydraulic Research P/N 4800680 valve is described in the next section.

5.3.2.1 Description of Hydraulic Research Valve

The Hydraulic Research valve P/N 4800680 currently recommended for the Planetary Explorer thrust chamber valve is shown in cross-section in Figure 5-19.

The Hydraulic Research valve is a normally closed torque-motor-operated, single-flapper shutoff valve. The valve incorporates two metal-to-metal flat-lapped poppets and seats in series to provide redundancy in the critical fail open mode. The poppet and seat material is extremely hard (1,800 to 2,000 Knoop) and, therefore, effectively resists damage by particles in the fluid.

All materials in the valve contacting the flowing propellant and N_2H_4 external spray or fumes are compatible with hydrazine. All joints in the hydrazine flow path are electron beam welded to provide maximum joint integrity, long-term storage capability and high thermal compatibility.

When no power is applied, the torque motor permanent magnet field is sufficient to overcome the torque tube spring force, which holds the armature against its closed stop. The flapper, which is rigidly connected to the armature, holds the downstream poppet against its seat and allows the upstream poppet coil spring to hold the upstream poppet against its seat. When power is applied to either or both coils (a minor wiring modification is required to change from parallel to independent coils), a magnetic flux is induced which bucks the permanent magnet field, allowing the torque tube to move the armature and flapper to the open position, opening both seats and allowing flow. When power is removed the permanent magnet field again closes the valve.

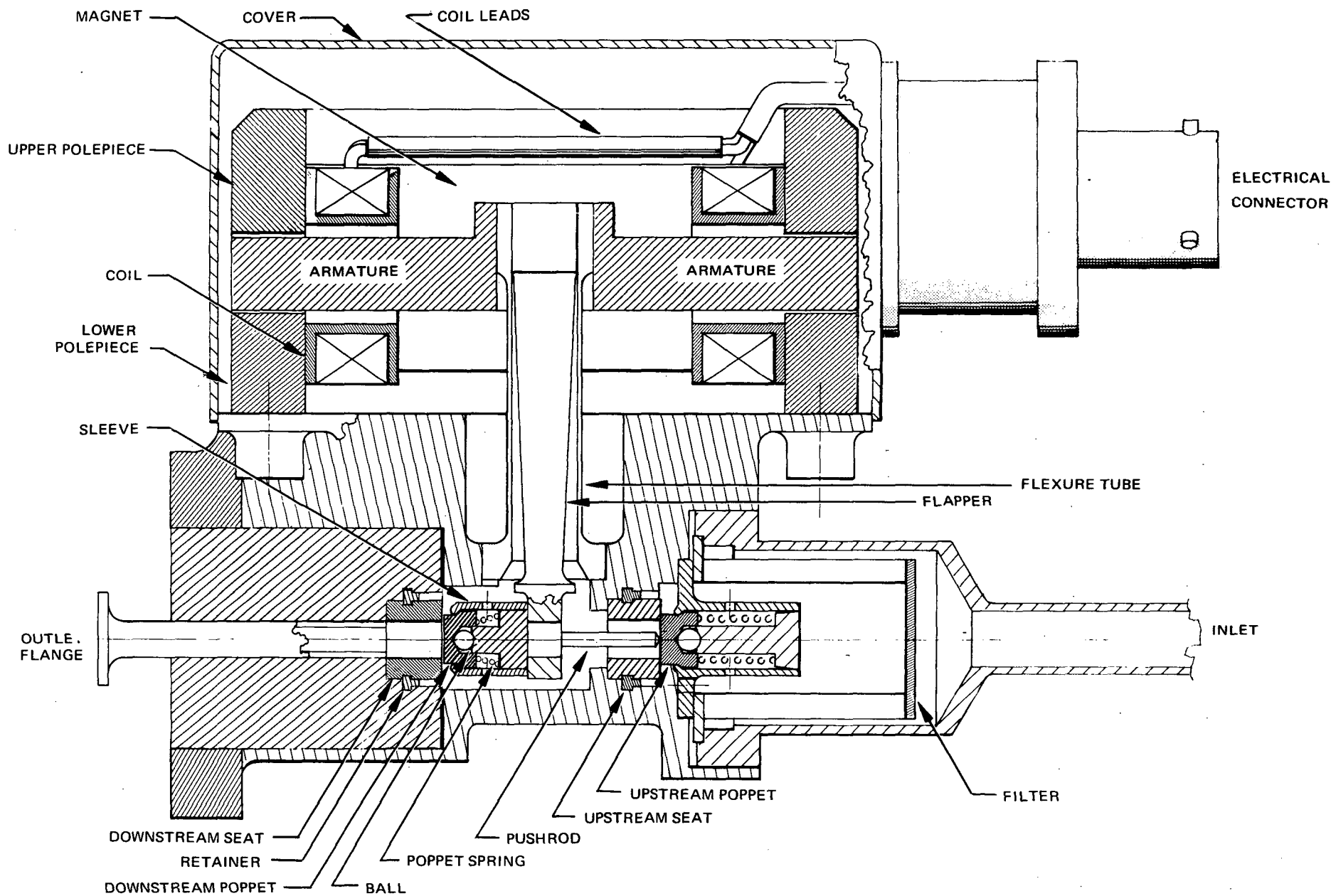


Figure 5-19. HYDRAULIC RESEARCH VALVE SCHEMATIC - PART NUMBER 48000680

Performance and electrical characteristics of the Hydraulic Research valve are summarized in Table 5-10. The environmental capability of the valve is given in Table 5-11.

Table 5-11. ENVIRONMENTAL CAPABILITY, RECOMMENDED THRUST CHAMBER VALVE

Environment	Planetary Explorer Requirement	Hydraulic Research P/N 4800680
Launch (non operating) Random vibration	12.8 g rms, 4 min/axis 20 to 300 Hz +4 db/oct 300 to 2000 Hz 0.09 g ² /Hz	20.3 g rms, 1.5 min/axis 20-1200 Hz 0.256 ² /Hz 1200-2000 Hz -6 db/oct
Shock	Flat at 600 g, 800 to 4000 Hz Rolloff to 75 g at 100 Hz	Not tested at valve level
Post launch (operating)		
Temperature, valve	40-200°F (probable max)	40-250°F
Temperature, fluid	40-140°F (probable max)	40-140°F
Ambient pressure	Hard vacuum	Over one year successful operation in earth orbit
Acceleration	5 g	Up to 25 g depending on temperature & voltage
Magnetic field generation	0.25 gamma after 50 gauss deperm	Not tested at valve level

5.3.2.2 Further Study Recommendations

As can be seen in Tables 5-10 and 5-11 most Planetary Explorer requirements are met by the Hydraulic Research valve. The following areas will require further study before a final valve selection is made:

- a. As shown in Table 3-2, the Hydraulic Research valve (dual-seat (pushrod)) configuration may not be as reliable as a dual (independent actuator) valve design. A weight/power/reliability tradeoff study must be done to evaluate the use of two independent single-seat valves in series.
- b. On the basis of mission duration, operating cycles, expected temperature, and leakage allowed, RRC believes that either soft (Teflon) or hard seats are capable of performing the mission. A liquid-gas leakage correlation study conducted for SAMSO (Report TOR-0059(6471)-17), using an RRC-supplied Parker P/N 5680036 (see Table 5-10) valve indicates that the 0.08-lbm/year N₂H₄ leakage specified for Planetary Explorer corresponds (conservatively) to 14.9 scc/hr of allowable GN₂ leakage. Further study of possible environmental effects should be accomplished.

- c. The Hydraulic Research valve must be tested to the Planetary Explorer shock level. Also, this valve possesses resonances in the 1,500 to 2,000 Hz range, and the random vibration spectrum to which it was tested rolls off from 1,200 Hz so the energy inputs at higher frequencies are not equivalent to the flat-to-2,000 Hz Planetary Explorer requirement.
- d. The permanent magnet torque motor will almost certainly require a modification providing magnetic shielding, if the spacecraft payload includes a magnetometer experiment.

5.3.3 Isolation Valves

Table 5-12 lists those isolation (latching) valves which in RRC's opinion are potential candidates for the Planetary Explorer mission, based on a review of the current status of existing valves and the following criteria.

- a. There must be a pressure drop of less than 10 psid at 0.022 lbf/sec N_2H_4 flow rate (5 lbf thrust).
- b. There must be no sliding fits.
- c. There must be test experience in an N_2H_4 system.
- d. Positive indication of valve positions must be provided.
- e. Weight must be less than 1 lbf.

The valve manufacturers solicited for thrust chamber valve data (see paragraph 5.3.2) were also asked to provide information on existing latching valves. As seen in Table 5-12, only two valves meet the above criteria, and only one of these, the Carleton Controls P/N 2217001-2, is currently in a qualified status. Parker-Hannifin Corporation and Consolidated Controls (was National Waterlift) manufacture flight-qualified N_2H_4 latching valves meeting all the above criteria except item e, being used in higher thrust level systems. Rocket Research Corporation expects that future latching valve applications at the 5-lbf thrust level will stimulate these companies and others to further development of valves suitable for Planetary Explorer.

The Carleton Controls valve described below meets Planetary Explorer requirements. The power consumption, now 63 watts for 30 millisecond at 28 vdc, can be reduced as required by a minor coil change at some sacrifice in response.

5.3.3.1 Description of Carleton Controls Valve

The Carleton Controls P/N 2217001-2 valve, shown in Figure 5-20, is a mechanically bistable latching valve, using a Belleville spring to produce the bistable latching force. The valve seat is an integral part of the CRES valve body. The valve stem contains a Teflon seal insert, well confined to control cold flow. Upstream and downstream of the seat welded CRES bellows are welded to the stem and body to seal the fluid passage and provide balancing to inlet and outlet pressures. The bellows/seat differential area and the Belleville spring latching force are set to relieve downstream pressure buildup due to thermal expansion of propellant locked up between the latching and thruster valves. Sliding seals of the garter-spring loaded Teflon slipper type are provided redundant to the bellows to prevent overboard leakage in case of an inlet-bellows leak or leakage into the actuator section in case of an outlet-bellows leak.

**Table 5-12. CANDIDATE ISOLATION VALVES (5 LBF THRUST SYSTEM)
PLANETARY EXPLORER N₂H₄ SYSTEM**

Manufacturer	Carleton Controls	Hydraulic Research
Part number	2217001-2	—
Weight, lbm	.54 (excl. cable)	.6 max
Approx. size, inches	1.25 dia x 4.5	1.33 x 2.4 x 2.17
Operating voltage range, vdc	18 - 50 vdc	24 to 36
Power, watts at 70°F, 28 vdc	62.7 (for 30 ms)	
Opening response time, 28 vdc, 70°F, ms	< 30	< 20
Closing response time, 28 vdc, 70°F, ms	< 30	< 20
Operating pressure, psia	0 - 300	0 - 300
Demonstrated burst pressure	No burst at 1200 psig	Predicted >1200 psig
Integral filter absolute micron rating	25*	25*
Rated flow, lbm/sec N ₂ H ₄	0.022	0.025
Pressure drop, psid, at 0.022 lbm/sec	1.0 max	7.7 max
Operating temperature range, °F	-30 to +140	40 - 250
Cycle life, qualified to	10,000	—
Cycle life, estimated capability	100,000*	100,000
Seat type	Teflon poppet insert	Hard **
Seat redundancy	None	None
Coil redundancy	None	Partial ***
Valve type	Solenoid operated, belleville spring latching, bellows isolation, no sliding in wetted section	Torque motor operated, permanent magnet latching
Leakage, internal, scc/hr GN ₂	1.0	1.0
Leakage, external, scc/sec helium	10 ⁻⁶	10 ⁻⁶
Program application history	Qualified for Intelsat IV and classified program	In house development. Probable usage for SMS program
Remarks	*RRC-proposed modification **50,000 in Hughes test Power can be reduced	*RRC-proposed modification **Soft seat in development ***Operation in degraded mode if one coil fails

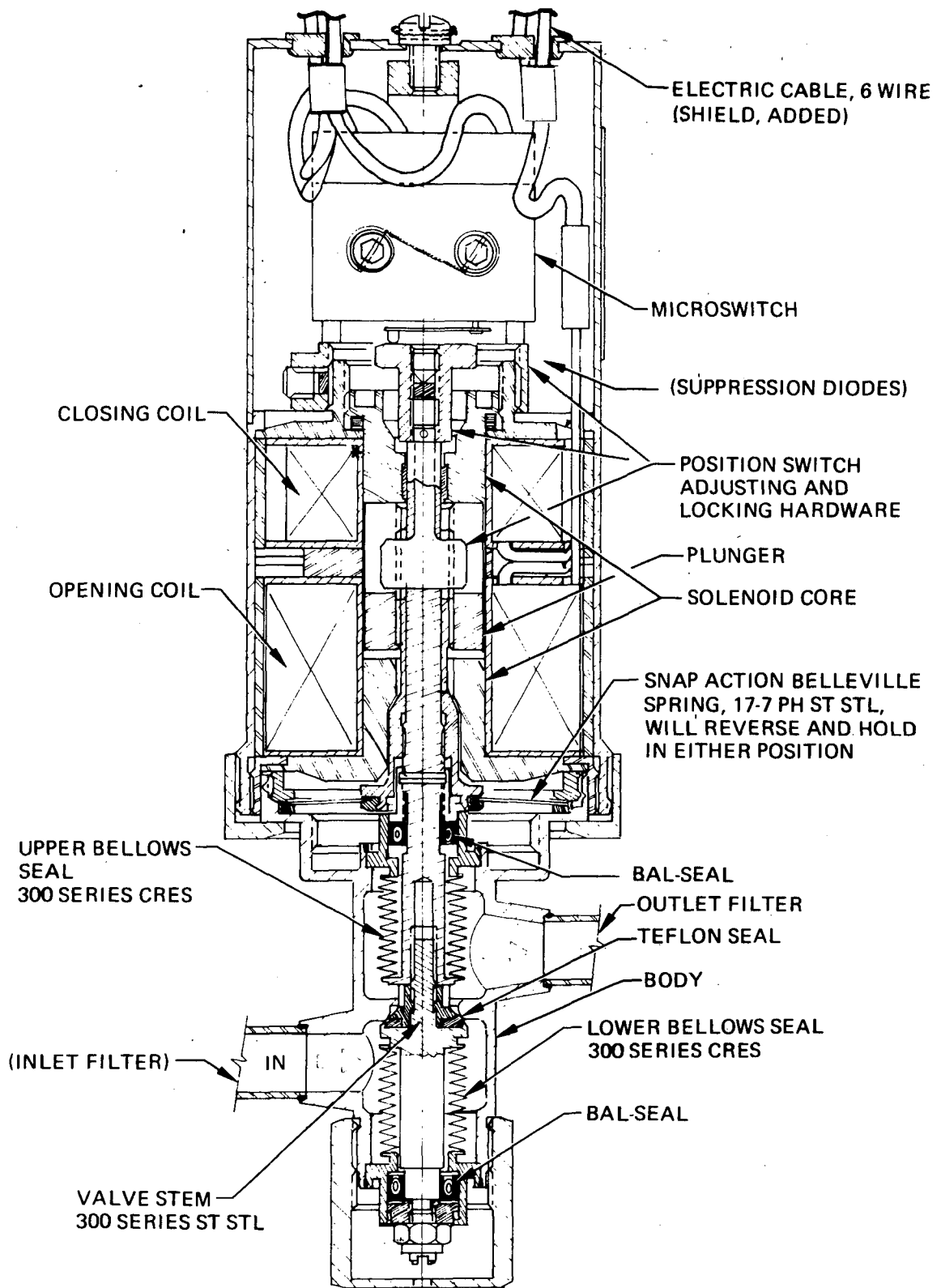


**Figure 5-20. QUALIFIED CONFIGURATION OF RECOMMENDED LATCHING VALVE
 CARLETON CONTROLS CORPORATION P/N 2217001-2**

The valve is actuated by a double-acting, flat-faced plunger solenoid. The solenoid plunger is threaded to the valve stem. Two coils are provided in a three-wire configuration with a common return. The magnetic circuit is arranged so that, when the opening coil is supplied with a voltage pulse, the principal flux path is across the opening air gap at one end of the plunger, creating a force sufficient to move the plunger to the open position, thus opening the valve seat and allowing flow. When a pulse is applied to the closing coil, the flux is principally across the closing air gap at the other end of the plunger and the valve closes. Latching is accomplished mechanically by a Belleville spring designed to be bistable, in the closed or open position, with the spring forces sized to control the pulse width and level required to open or close the valve. A microswitch assembly is provided to indicate whether the valve stem is in the open or closed position. The fluid containing portion of the valve has all external joints sealed by welding. The inlet and outlet ports are provided with titanium tubes for transition to titanium spacecraft plumbing in the qualified valve. The performance and electrical characteristics are described in Table 5-12, and the valve's environmental capability is given by Table 5-13.

**Table 5-13. ENVIRONMENTAL CAPABILITY OF CARLETON CONTROLS
P/N 2217001-2 LATCHING VALVE**

Environment	Planetary Explorer Requirement	Demonstrated Capability (Intelsat IV Qualifications)
Humidity	95% RH, 86°F assumed	95% RH, 86°F
Launch Acceleration	±9g along thrust axis ±3.9g along other axes	10.5g, 3 axes
Temperature	+40 to +122°F operating (estimated) +13 to +122°F non-operating (estimated)	-20 to +140°F -65 to +150°F
Random vibration	20-2000 Hz 0.09 G ² /Hz	20-2000 Hz 23.4 g RMS overall
Vacuum exposure	2 years in hard vacuum	8 year (goal) in orbit

5.3.4 Propellant Line Filter

The propellant filter selected for inclusion in the baseline design is the Vacco Valve Company PN S1-81847-1. The filter element consists of a stack of discs having chem-milled flow passages constructed to trap and hold contaminant particles. Vacco stacked-disc filters are used in RRC's Titan III-C Transtage RCS modules and in RRC's HPM and ERTS. The proposed filter, which is qualified for use in a classified satellite program, is essentially identical to the Vacco filter used by Hughes in the INTELSAT IV hydrazine system except that the body and tubing material is type 304L CRES instead of titanium and the element is approximately 10% shorter. Table 5-14 summarizes the filter design and performance.

Table 5-14. PROPELLANT LINE FILTER CHARACTERISTICS

Rated flow	0.025 lbm/sec N ₂ H ₄
ΔP (clean)	2.0 psi maximum
ΔP with 50 mg AC fine dust	5.0 psi maximum
ΔP estimated with 3.3 mg AC fine dust added	2.5 psi maximum
Proof pressure	4,000 psig
Burst pressure	6,680 psig
Rating	12μ absolute, 5μ nominal
Weight	0.38 lbm maximum
External leakage	1 x 10 ⁻⁷ sccs helium at 6,680 psig
Connections	1/4 inch 304L CRES tube stubs

5.3.5 Propellant Tank

A review of qualified propellant tankage indicates that only two existing propellant tanks can be considered as candidates for Planetary Explorer application. These are the Fansteel Advanced Structures Division P/N 4425039 IDCS tank and the Pressure Systems Incorporated P/N 80076 INTELSAT III tank. The INTELSAT III tank had disadvantages in volume/blowdown characteristics, porting, and mounting. The Fansteel IDCS tank has been selected as baseline for this study.

The three-port arrangement was designed to overcome some of the operational difficulties encountered with the use of more conventional two-port tanks when used for spacecraft spin-induced propellant orientation. The three-port tank allows simple, low-point draining of the propellant from the propulsion subsystem in its normal test or launch vehicle stacked position. This low-point fill and drain port, along with the gas pressure equalization line, interconnect each of the tanks. This arrangement allows the propellant to level itself in each pair of opposed tanks after fueling and pressurization through the common fill/drain line. This feature, not possible with the two-port horizontally oriented tank, prevents a large initial center of gravity offset and consequent vehicle perturbations induced during launch and spin-up. The location of the gas pressure equalization line 45 degrees above the tank equator permits propellant leveling with a fuel load in excess of half the tank capacity as indicated for this mission.

The tank is flight-qualified and available with 3/16-inch tube outlets (PN 4425034) and 1/4-inch tube outlets (PN 4425039). The configuration with the larger feed tubes was selected since 1/4-inch feed system plumbing is proposed to minimize system pressure drop and and eliminate the possibility of imbalance developing during propellant expulsion. Some of the pertinent tank specifications are summarized in Table 5-15.

Table 5-15. PROPELLANT TANK PARAMETERS

Supplier	Fansteel Advanced Structures Division
Part number	4425039
Design operating pressure, psig	400
Proof pressure, psig	670
Burst pressure, psig	900
Material	6Al-4V titanium alloy
Nominal wall thickness, inches	0.015
Volume, in. ³	497
Maximum weight, lbs	1.6
Diameter, inches	10.0

5.3.6 Instrumentation

Instrumentation recommendations are discussed in paragraph 4.1.5. Typical hardware is described here to permit definition of the complete propulsion systems. Some flexibility exists with regard to the location of the propulsion system/spacecraft interface. Pressure transducers, since they must be plumbed into the system, are considered a part of the propulsion system. In the case of temperature measurement, the interface may be defined to include the sensor and the signal conditioning equipment or only the sensor. The MR-50 engine, upon which the baseline system definition is based, uses the latter approach. A thermocouple is welded to the thrust chamber shell and the leads connected to the electrical connector-signal conditioners on the spacecraft side of the interface. This approach was also taken in the design studies reported herein. The instrumentation is discussed in more detail in the following sections. The latching valve position switches, considered a form of instrumentation, are an integral part of the isolation valve and are discussed in that section.

5.3.6.1 Pressure Transducers

The pressure transducer recommended is a unit manufactured by the Dynasciences Corporation. The unit is used by RRC on the Hydrazine Propulsion Module and ERTS Programs and has been qualified and is currently in production for the Apollo/LEM spacecraft. The unit contains its own signal conditioning.

The pressure transducer assembly is made by Dynasciences Corporation and is designed to the requirements of RRC Procurement Specification CS-0024 and RRC Source Control Drawing 24948.

The absolute pressure transducer features semiconductor gauges bonded to a machined diaphragm. The pressure transducer measures pressure from 0 to 500 psia. The sensing element incorporates semiconductor strain gauges bonded to a machined Ni Span C constant modulus steel diaphragm. The sensing element functions as an active arm of a Wheatstone bridge circuit. The sensing element output is fed into a differential amplifier of the integral signal conditioning electronics.

The integral cordwood electronic module provides isolation, regulation, and low gain amplification of 0- to 5-vdc output, using unregulated 28 ±8 vdc power.

The transducer has the following mechanical specifications:

Pressure range	0 to 500 psia
Proof pressure	1,000 psia with no shift out of error band
Burst pressure	10,000 psig with no internal or external leakage
Lowest resonant frequency	40,000 cps
63% rise time	0.5 millisecond maximum
Weight	5 ounces maximum

The transducer has the following environmental specifications:

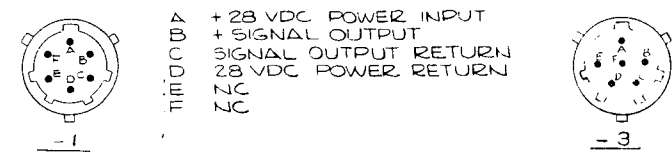
Temperature (storage and operation)	-65 to +250°F
Compensated temperature range	0 to 200°F
Sinusoidal vibration	30 g's peak to 2 kc
Random vibration	50 g's rms to 2 kc
Shock	1/2 sine wave, 100 g's peak 3-millisecond duration in each direction of three axes
Humidity	100% RH

The transducer has the following electrical specifications:

Input voltage	28 ± 8 vdc
Input current	10 milliamperes maximum
Regulation	±2 millivolts over above input voltage range
Output impedance	100 ohms maximum
Insulation resistance	100 megohms minimum at 100 vdc
Input-output isolation	100 megohms minimum at 100 vdc
Dielectric strength	Maximum leakage between circuits and case is 1.0 milliampere at 200 vac for 1 minute
Output ripple and noise	10 mv p-p maximum
Noise feedback	5 mv p-p maximum
Output capacitance	400 picofarads maximum
Overvoltage	Transients to 50 volts for 10 milliseconds at power input
Electromagnetic interference	Meets MIL-STD-826

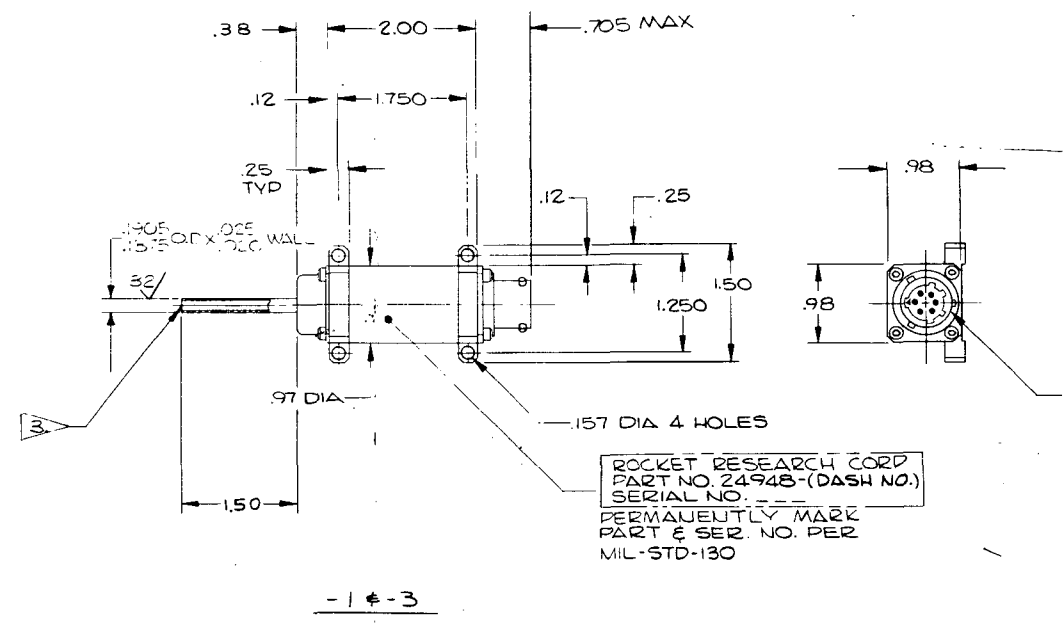
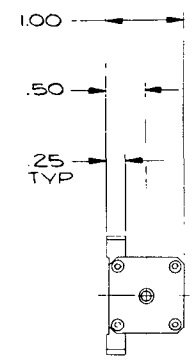
A drawing of the transducer, giving envelope dimensions, is shown in Figure 5-21.

1. INTERPRET DRAWING PER MIL-STD-100.
2. REMOVE ALL BURRS & SHARP EDGES.
3. PROTECT UNIT WITH DUST CAPS WHEN HANDLING, SHIPPING OR STORING.
4. THIS PART SHALL CONFORM TO THE REQUIREMENTS OF RRC-CS-0024.



PIN IDENTIFICATION

REVISIONS				
SYM	ZONE	DESCRIPTION	DATE	APPROVED
A		SEE DCN	1-18-67	4-16-67
B		SEE DCN	8/17/69	8/20/69
C		SEE DCN	8/20/69	7-31-69



-1 & -3

SOURCE CONTROL DRAWING

APPROVED SOURCES OF SUPPLY		
DASH NO.	VENDOR AND VENDOR'S PART NUMBER	APPLICATION
-1	WHITTAKER CORP. INSTRUMENT SYSTEMS DIV. 9601 CANOGA AVE. CHATSWORTH, CALIF. MODEL: 1025-0092	USE TO MONITOR PROPELLANT TANK PRESSURE ON THE HPM SYSTEM
-3	TO BE DETERMINED	USE TO MONITOR PROPELLANT TANK PRESSURE ON THE ERTS-AOS

ONLY THE ITEM(S) DESCRIBED ON THIS DRAWING WHEN PROCURED FROM THE VENDOR(S) LISTED HEREON IS APPROVED BY ROCKET RESEARCH CORPORATION, FOR USE IN THE APPLICATION SPECIFIED HEREON. A SUBSTITUTE ITEM SHALL NOT BE USED WITHOUT PRIOR TESTING AND APPROVAL BY ROCKET RESEARCH CORPORATION, OR BY THE GOVERNMENT PROCURING ACTIVITY.

SYM	CODE IDENT. NO.	PART OR IDENTIFYING NO.	QUANTITY	DESCRIPTION	MATERIAL	SPECIFICATION	UNIT WT	ZONE	ITEM NO.
				UNLESS OTHERWISE SPECIFIED DIMENSIONS ARE IN INCHES DECIMAL TOLERANCE .XX ± .03 .XXX ± .010 DO NOT SCALE DRAWING					
TREATMENT					LIST OF MATERIALS				
-3 1 1 26058 MRS-6B					ROCKET RESEARCH CORPORATION SEATTLE, WASHINGTON				
-1 1 1 25030 HPM					TITLE				
PART NEXT FINAL NEXT ASSY USED ON					TRANSducer, ABSOLUTE PRESSURE				
DASH NO. QTY REQ PER ASSY APPLICATION					CODE IDENT. NO. DWG NO. 21562 D 24948				
WORK CHARGE NO. 131004-2570					SCALE 1/1 RELEASE DATE 2-20-67 SHEET 1 OF 1				

Figure 5-21. TRANSDUCER ABSOLUTE PRESSURE

5.3.6.2 Temperature Measurement

A Chromel/Alumel thermocouple is tack-welded to the thrust chamber nozzle and the leads directed to the system electrical interface connector. The connector is provided with pins of the appropriate material. For propellant tank temperature measurement, the thermocouple (or thermistor) heat collector plate would be bonded to the tank surface near the outlet port and the leads directed to the spacecraft electrical connector. Signal conditioning equipment is assumed to be located on the spacecraft side of the interface. The weight of these elements is included in the thruster module and/or electrical cable allowance. Typical signal conditioning equipment might weigh in the order of 0.4 to 0.6 lbm and require approximately 0.14 watt for one channel.

5.3.7 Fill/Drain/Vent Valve

The fill valve assembly selected for the design definition studies of the Planetary Explorer Propulsion Subsystem is shown in Figure 5-22. The valve design was qualified by RRC on the Hydrazine Propulsion Module and ERTS Programs and has previously been used by the Jet Propulsion Laboratory on the Ranger Midcourse Propulsion System. Rocket Research Corporation has manufactured the valve in four different part numbers: 25030-9, 25030-19, 25030-29, and 25030-39. These valves differ only in the fill port size and/or the outlet tube stub size. The different sizes are used to prevent servicing errors.

The valve is manually operated and consists of a needle which is screwed into a valve body and seals against a sharp-edged seat in the valve body. The basic seat is metal-to-metal between the needle and the valve body. Redundant seals are obtained by use of a diametral O-ring seal on the needle and a bullnose O-ring seal on the fill fitting on the valve body. The valve mounts by use of a bulkhead type fitting on the valve body.

The valve has the following basic design characteristics:

Maximum operating pressure	3,600 psia
Proof pressure	5,400 psia
Minimum burst pressure	7,200 psia
Temperature range	150 to +165°F
Maximum allowable internal leakage	5 scc/hr GN ₂ at 3,600 psia
Maximum allowable external leakage	1 x 10 ⁻⁶ scc/hr He

The valve was subjected to the following qualification tests by RRC:

- a. Acceptance tests
 1. Proof pressure
 2. Internal leakage
 3. External leakage
 4. Temperature cycling, -100 to +165°F
 5. Operating break in
 6. Internal leakage
 7. External leakage
 8. Contamination check

- b. Mechanical shock
 - 1/2 sine wave shape to 30 g's peak for 8-ms duration three times in each direction of three orthogonal axes
- c. Internal and external leakage
- d. Acceleration
 - 11 g's for 5 minutes in each direction of each of three orthogonal axes
- e. Internal and external leakage
- f. Sinusoidal vibration in each of three orthogonal axes

5-14 cps	0.5 in. double amplitude
14-400 cps	5 g's peak
400-2000 cps	7.5 g's peak
- g. Random vibration in each of three orthogonal axes
 - 18.2 g's rms and 6.2 g's rms
- h. Leakage test
- i. Cycle life test – 280 open/close actuations with leakage measured every 28 cycles
- j. Temperature cycling from -150 to +150°F
- k. Burst test.

The fill valve met all qualification test requirements.

6.0 SYSTEM DEVELOPMENT

6.1 DEVELOPMENT TEST PLAN

The test plan for the hydrazine propulsion system is presented in the following paragraphs. Since the system is designed with a philosophy of using previously qualified components, no development tests are indicated. The areas of test include component and module acceptance tests and subsystem qualification.

Acceptance tests are designed to demonstrate that components or modules comply with specification requirements prior to initiation of qualification testing. The individual rocket engine assemblies (REA's) will be acceptance-fired prior to assembly into rocket engine modules (REM's) or into the system.

Qualification tests are conducted at the propulsion system level to demonstrate compliance to the specified flight requirements. Qualification at the system level is possible because of the large amount of previous development and qualification test history available on all components. Qualification testing will include environmental tests (vibration, shock, acceleration) and thermal vacuum tests followed by mission profile firings.

Propellant loading, off-loading, and system decontamination will be part of the GSE final functional and acceptance tests.

6.2 ACCEPTANCE TESTS

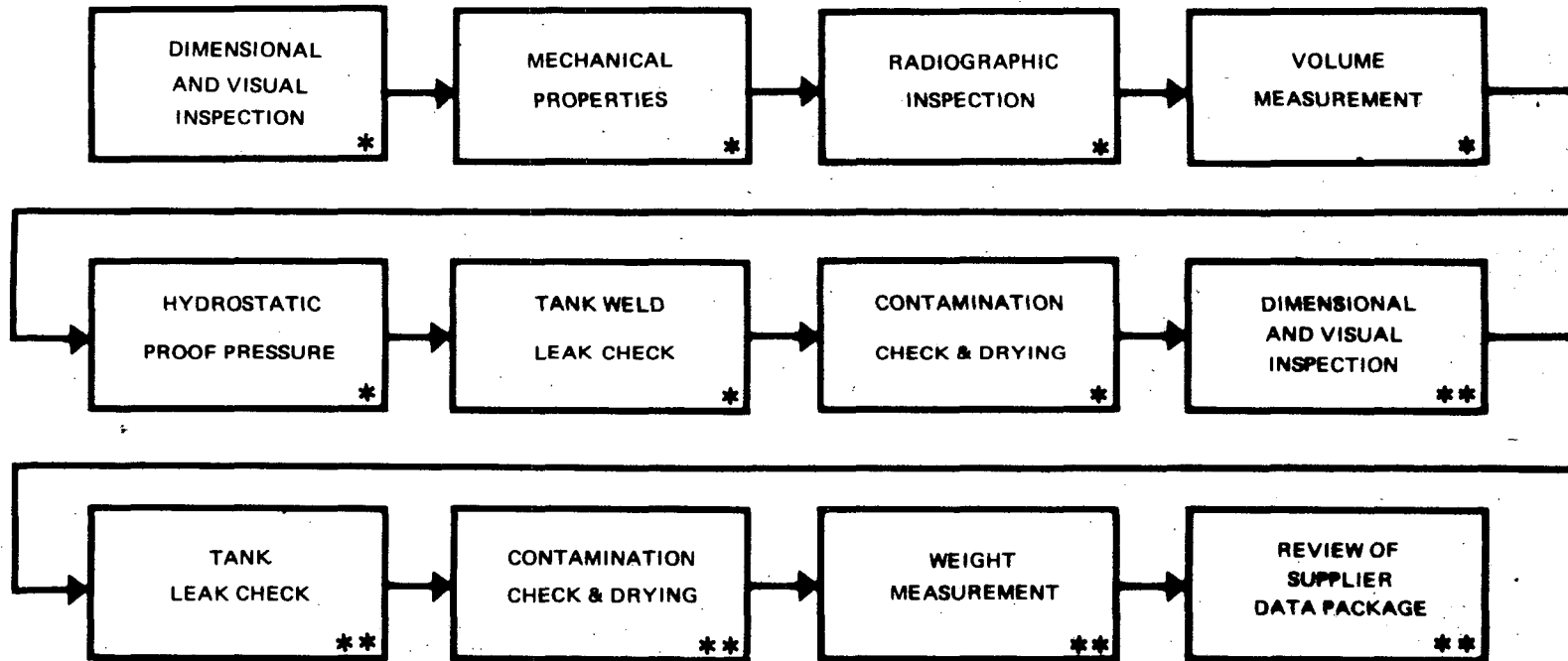
Acceptance tests will be conducted at the component, module, and system level to verify that the performance characteristics and structural integrity of each item conform to the applicable detail specification. Appropriate mechanical/electrical checkouts, witnessed by quality assurance personnel, will be conducted throughout the integration of components into the system. Complete subsystem mechanical and electrical tests will be conducted following completion of subsystem assembly.

6.2.1 Component Acceptance Tests

Acceptance tests will be performed at the supplier's facility, monitored by a propulsion system contractor (PSC) quality assurance representative, or at the PSC's facility, as indicated below. For all tests conducted at the supplier's facility, detailed test procedures will be generated, for the PSC and GSFC approval, in accordance with the requirements of the applicable specification. For tests conducted at the PSC's facility, documents will be prepared as required for customer approval to comply with the requirements of this plan.

6.2.1.1 Propellant Tank Assembly

Individual propellant tanks will undergo acceptance testing as presented in Figure 6-1. Following completion of these tests, the individual tanks are assembled into a module which undergoes additional testing (see Figure 6-9) prior to installation into the vehicle structure.



NOTE: AT LEAST TWO TANKS SHOULD BE BURST TESTED.
 * AT SUPPLIER'S FACILITY
 ** AT PROPULSION SUBSYSTEM CONTRACTOR'S FACILITY

Figure 6-1. PROPELLANT TANK ASSEMBLY – ACCEPTANCE TESTS

6.2.1.2 Filter

Filter acceptance tests will be conducted at the supplier's facility as indicated in Figure 6-2.

6.2.1.3 Fill and Drain Valves

The fill and drain valves are subjected to acceptance tests as shown in Figure 6-3. The critical requirements are leakage and contamination.

6.2.1.4 Pressure Transducer

The acceptance tests for the pressure transducer are presented in Figure 6-4.

6.2.1.5 Isolation (Latching) Valves

Acceptance tests for the latching valve are shown in Figure 6-5. A primary objective in placing acceptance vibration early in the sequence of tests is to verify leakage resistance and to expose any electrical defects in the valve (such as faulty solder joints). Contamination tests are performed prior to acceptance tests and after completion of all tests, just prior to shipment. A contamination test is also conducted at the propulsion system contractor's facility to verify that his tests have not contaminated the valve.

6.2.1.6 Thruster Control Valve

The thruster control valve tests, shown in Figure 6-6, are generally similar to those of the latching valve. The primary difference is the greater emphasis on functional characteristics (such as response, repeatability, and flow) for the thruster control valve compared to the latching valve.

6.2.1.7 Catalyst Acceptance Plan

The catalyst for the program should be purchased according to the applicable PSC's specification. The general flow plan for catalyst manufacture, product control, and acceptance is shown in Figure 6-7. All evidence of inspections and test by Shell Development Company will be reviewed prior to acceptance by the PSC quality assurance organization. The flow plan for acceptance of the catalyst is shown in Figure 6-7.

6.2.1.8 Thrust Chamber Assembly

The thrust chamber assembly acceptance tests are shown in Figure 6-8. Multiple basepoint firings and thermal vacuum testing are not recommended, since a thruster which has been qualified has presumably been shown to be insensitive to the various environments. Addition of these tests would result in a significant cost increase in the program without sufficient additional results to offset the cost. The initial vibration test is considered good practice as a screening measure against faulty mechanical or electrical assembly.

6.2.1.9 Propulsion System Acceptance

A flow block diagram showing the final assembly of the various components and modules into the complete system assembly on the vehicle structure is shown in Figure 6-9. The sequence of

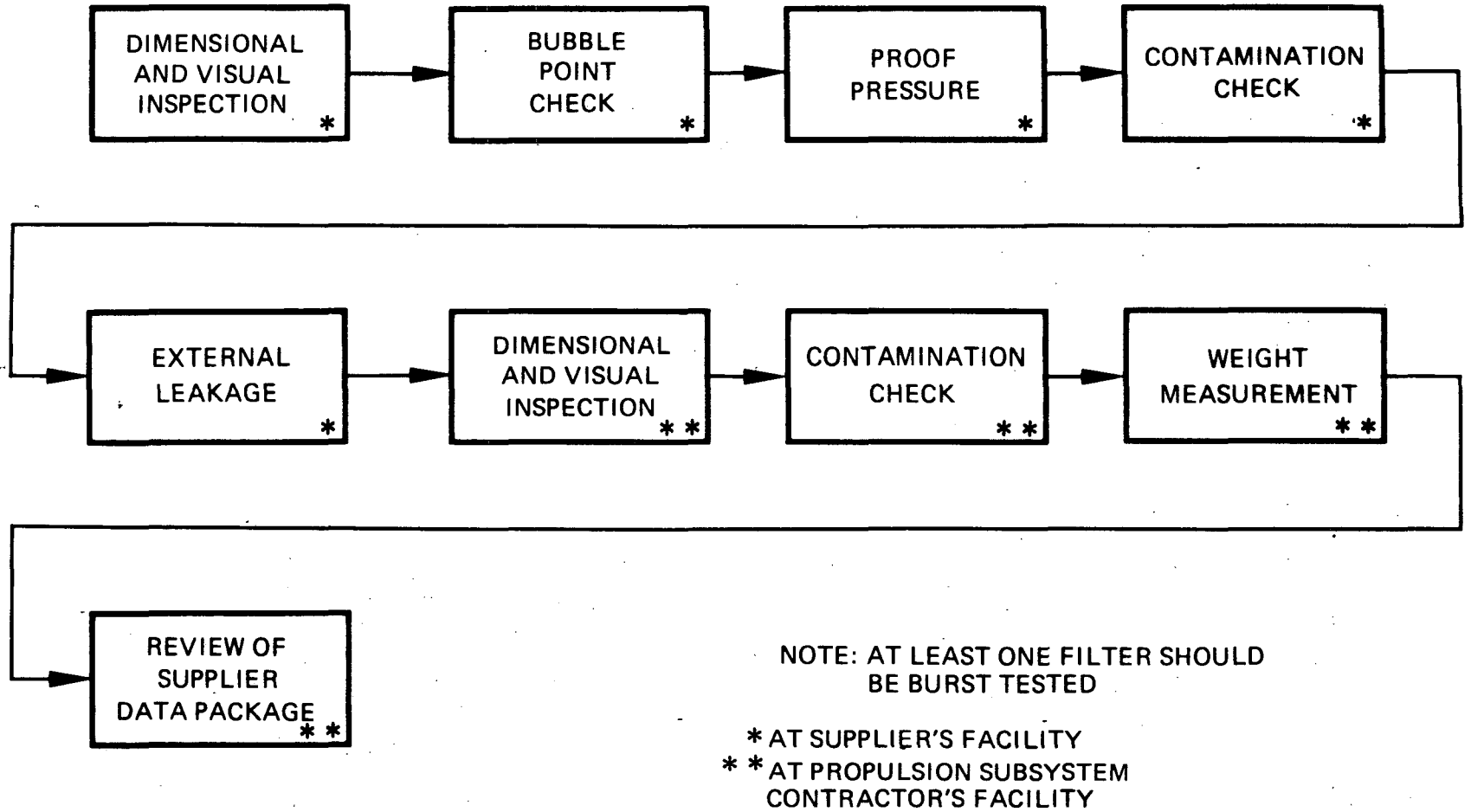


Figure 6-2. FILTER – ACCEPTANCE TEST

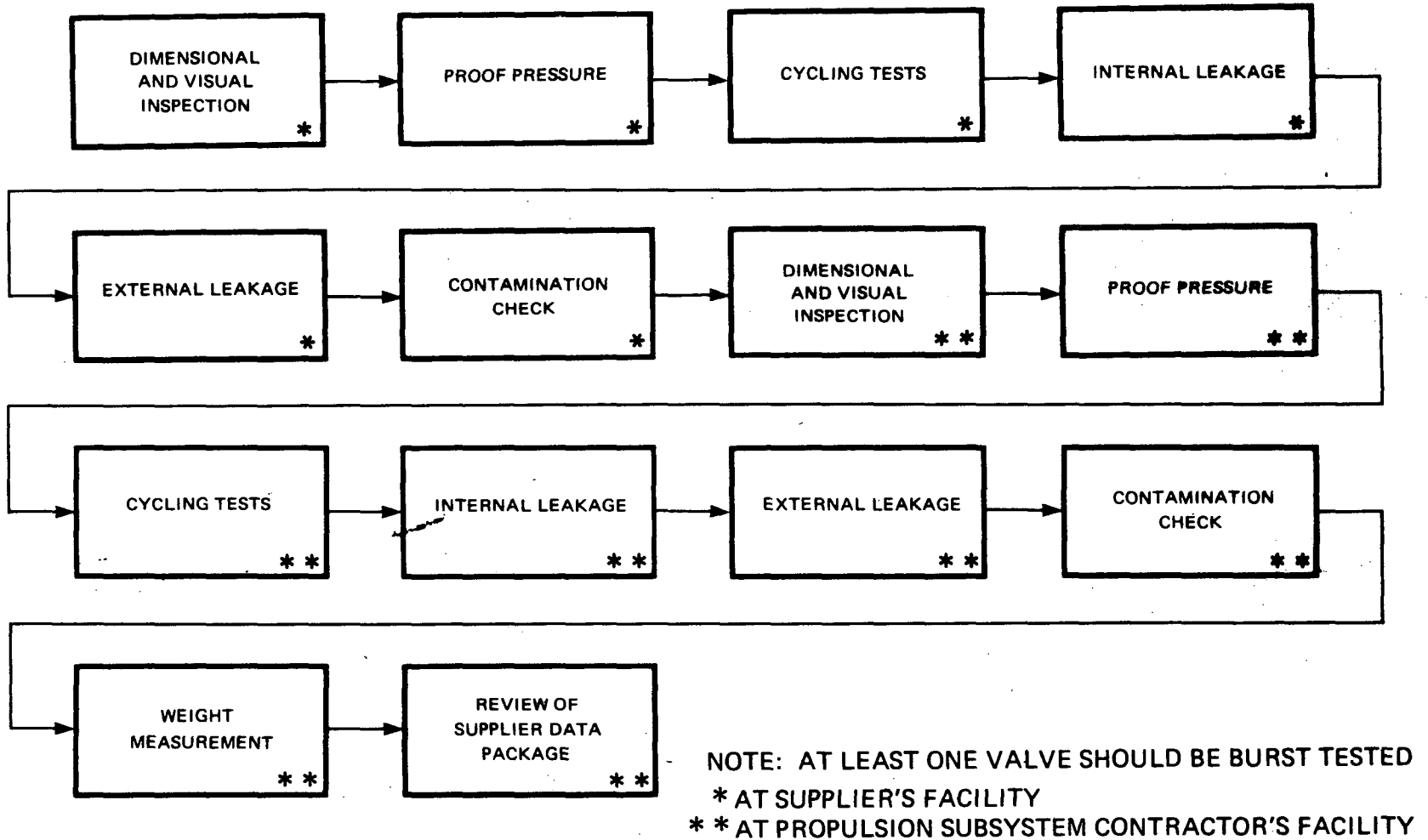
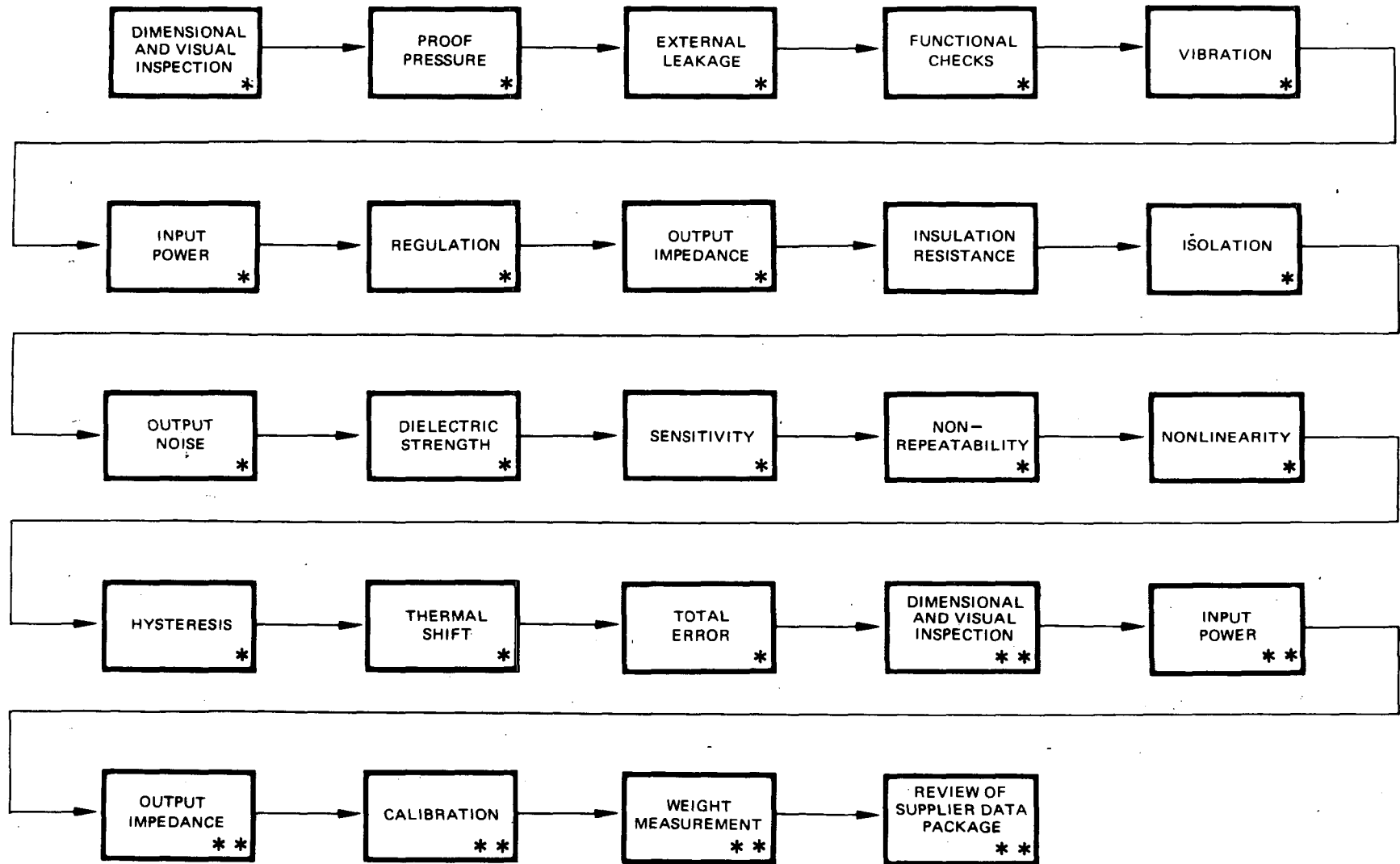
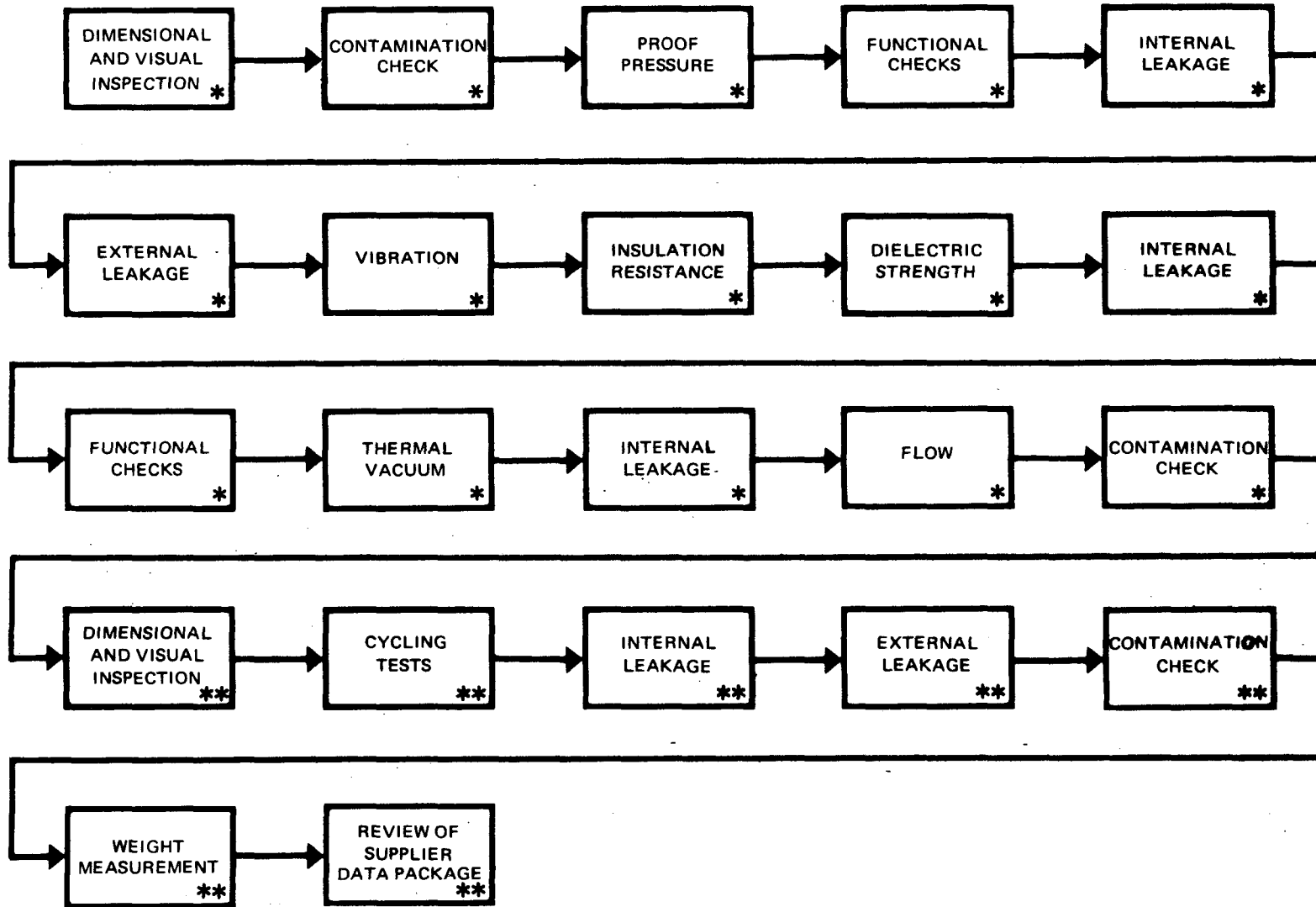


Figure 6-3. FILL AND DRAIN VALVES – ACCEPTANCE TESTS



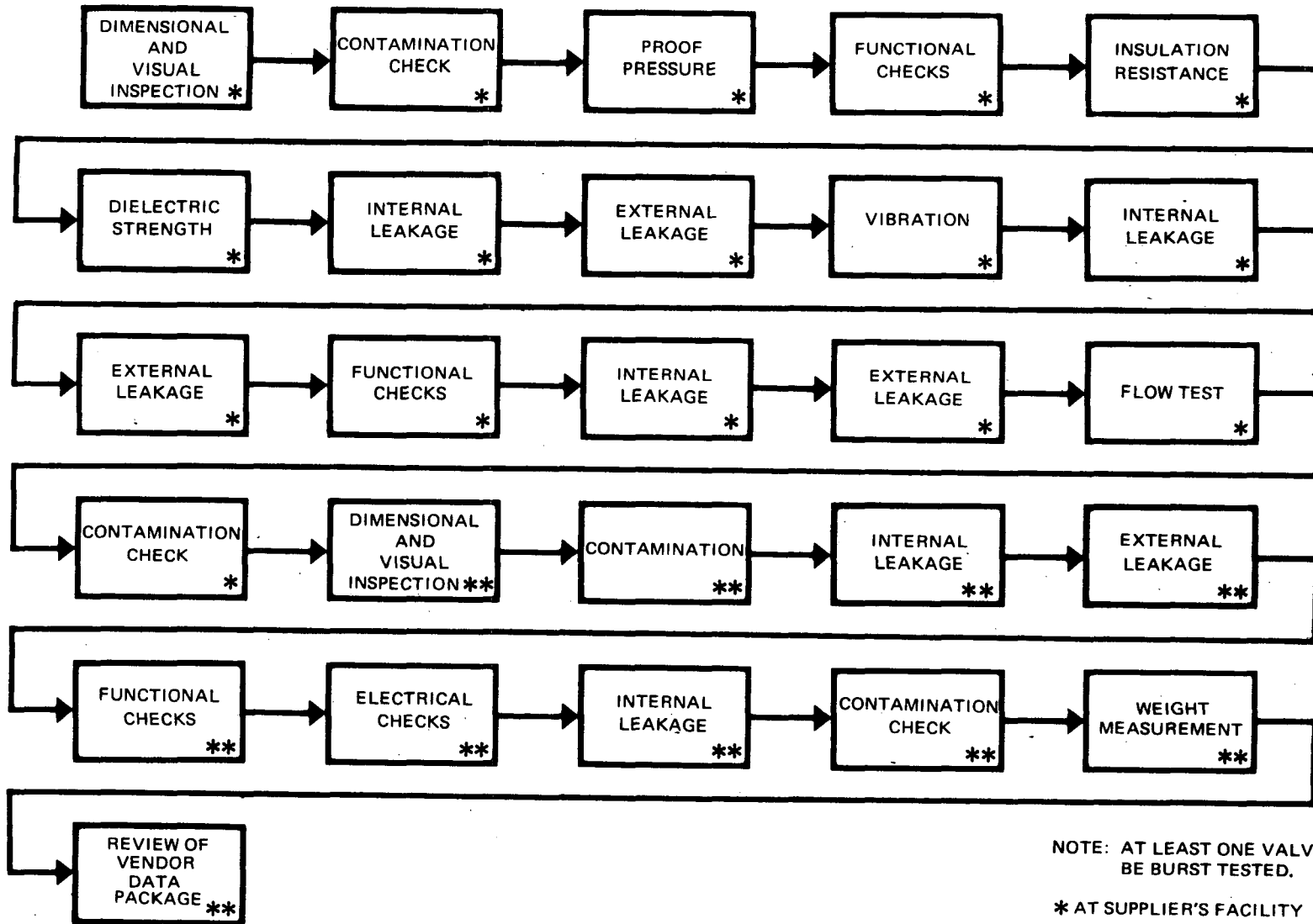
NOTE:
 AT LEAST ONE TRANSDUCER SHOULD BE BURST TESTED
 * AT SUPPLIER'S FACILITY
 ** AT PROPULSION SUBSYSTEM CONTRACTOR'S FACILITY

Figure 6-4. PRESSURE TRANSDUCER – ACCEPTANCE TESTS



* AT SUPPLIER'S FACILITY
 ** AT PROPULSION SUBSYSTEM CONTRACTOR'S FACILITY

Figure 6-5. ISOLATION (LATCHING) VALVE – ACCEPTANCE TESTS

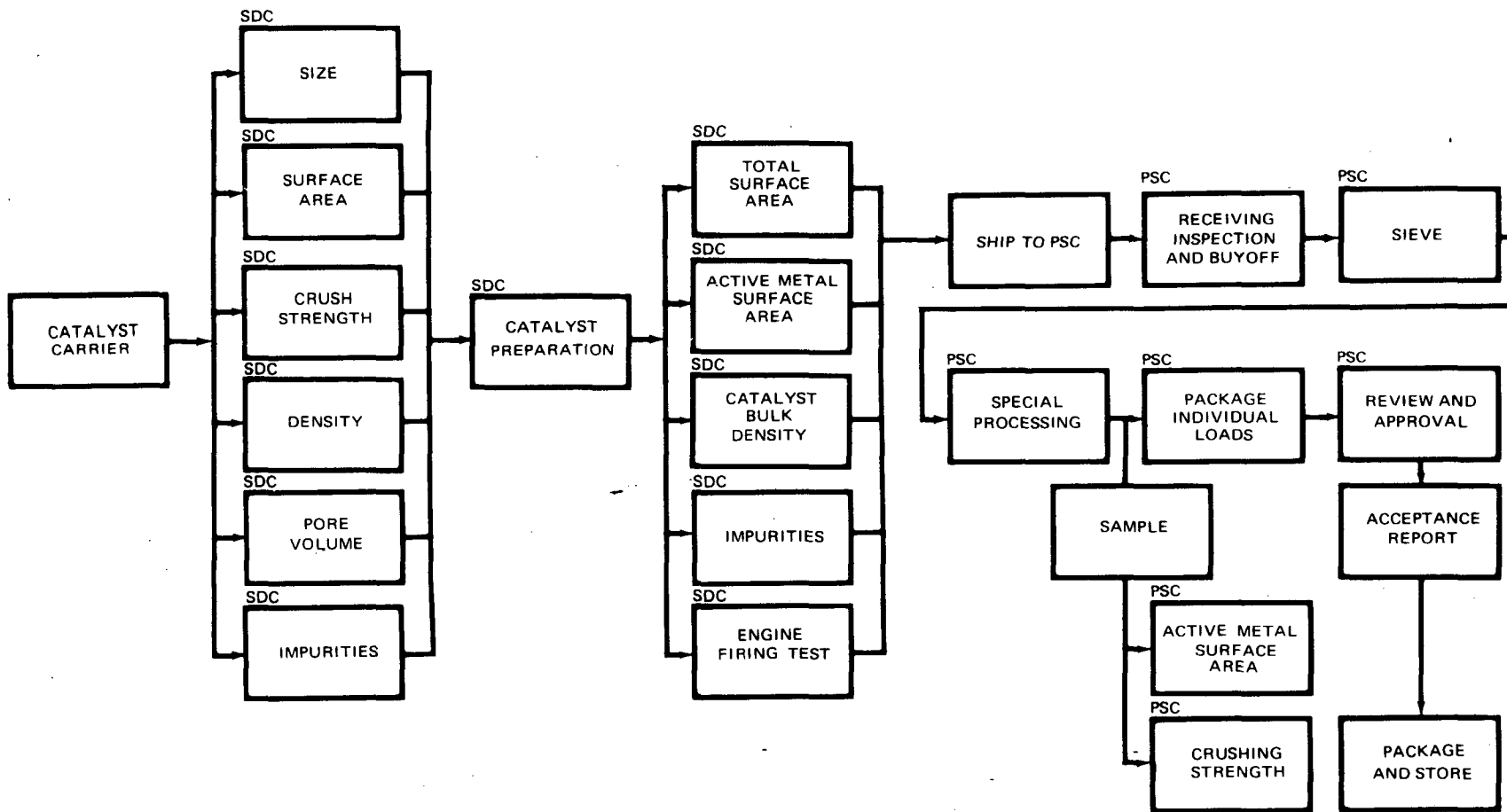


NOTE: AT LEAST ONE VALVE SHOULD BE BURST TESTED.

* AT SUPPLIER'S FACILITY

** AT PSC's FACILITY

Figure 6-6. THRUSTER CONTROL VALVE – ACCEPTANCE TESTS



NOTES:
SDC SHELL DEVELOPMENT COMPANY
PSC PROPULSION SYSTEM CONTRACTOR

Figure 6-7. CATALYST ACCEPTANCE FLOW PLAN

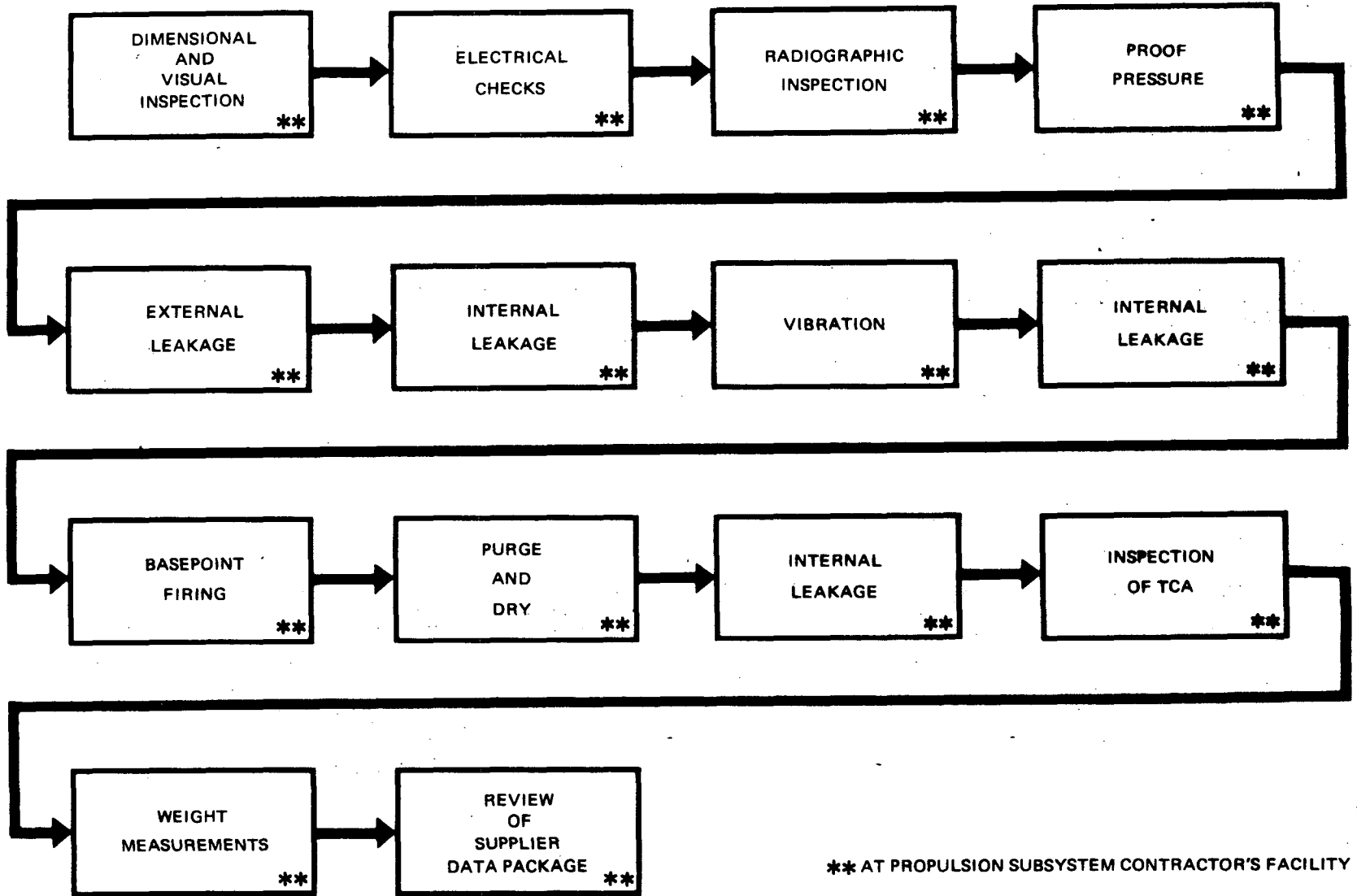


Figure 6-8. THRUSTER CHAMBER ASSEMBLY – ACCEPTANCE TESTS

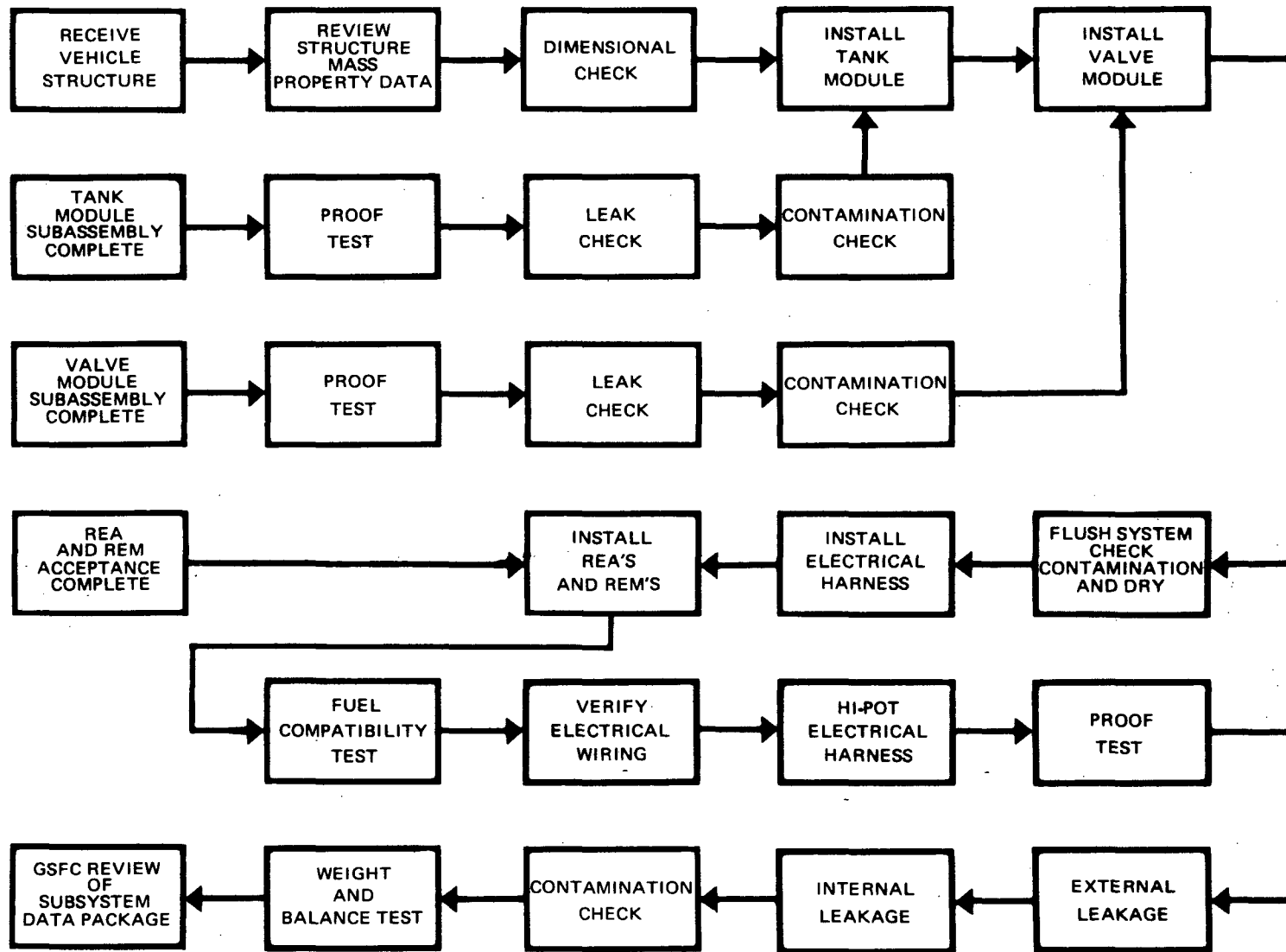


Figure 6-9. PROPULSION SUBSYSTEM – FINAL ASSEMBLY AND ACCEPTANCE TESTS

acceptance tests on the various modules and the final assembly is also presented. The various acceptance tests are scheduled to be performed in the most efficient manner to detect any problems as early as possible in the buildup sequence.

6.3 SYSTEM QUALIFICATION

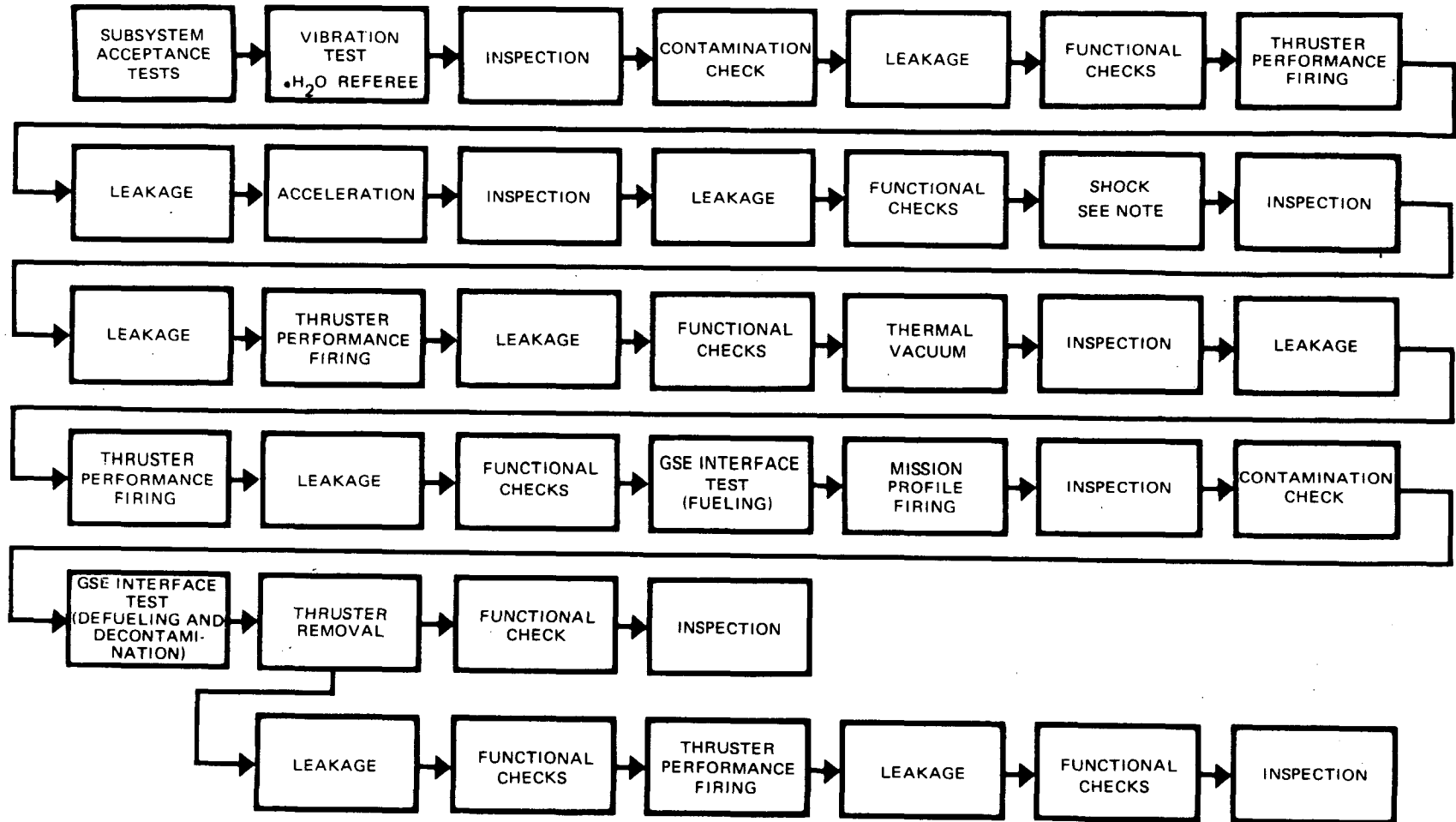
A flow block diagram of the system qualification tests is presented in Figure 6-10. The qualification system, as well as all flight systems will previously have been subjected to the component and system acceptance tests described in paragraph 6.2.

Following the environmental test, the system is prepared for mission profile firing tests by employing the flight GSE, thus providing assurance of correct GSE operation and procedures.

The mission profile tests are designed to verify capability of predicting system performance from known pressure and temperature data over the system blowdown range.

Following the mission profile test the GSE is again employed to check the defueling and decontamination procedures.

The thrusters are then removed and individually subjected to a final performance check in the acceptance test facility.



NOTE : THIS TEST IS BEST CONDUCTED BY PERFORMING A SPACECRAFT SEPARATION TEST AND CAN BE CONSIDERED A COMBINED SPACECRAFT SHOCK QUALIFICATION AND PROPULSION SUBSYSTEM QUALIFICATION TEST.

Figure 6-10. SUBSYSTEM QUALIFICATION TESTS

7.0 GROUND SUPPORT EQUIPMENT

Ground support equipment (GSE) required for the Planetary Explorer propulsion system is of two forms, mechanical and electrical. A discussion of the requirements for each type of GSE and descriptions of typical equipment are provided in the following paragraphs.

7.1 GSE REQUIREMENTS

The functional requirements for the mechanical and electrical GSE are presented in Tables 7-1 and 7-2 respectively. The philosophy employed is to completely separate the functions of the two items. For example, the mechanical GSE provides fluid handling capability and incorporates only its own electrical services. It is incapable of supplying an electrical signal to the spacecraft, hence enhancing safety during fueling or decontamination operations.

7.2 MECHANICAL GSE

A typical service cart to perform the mechanical GSE functions for a hydrazine propulsion system is that designed by RRC for the Radio Astronomy B Velocity Control Propulsion System (VCPS). This cart provides the capability to load, flush, and purge the system by use of hydrazine, isopropyl alcohol, water, helium, or nitrogen and to vacuum-dry the tankage, lines, and thrusters. The GSE is designed to ensure the safety and ease of handling necessary to protect the personnel and flight system during servicing operations.

Features of the cart and its operation are described in the following paragraphs.

7.2.1 Physical and Schematic Description

The mechanical GSE cart will perform all necessary mechanical service functions on the RAE-B VCPS. These functions consist of interfacing and contamination control, propellant loading, pressurizing, proof testing, propellant sampling, venting, propellant off-loading, draining, flush fluid loading and draining, purging, and vacuum drying. The VCPS valves may also be leak checked with the GSE cart.

The GSE cart will contain storage for, and control of, propellant (N_2H_4), flush fluids (H_2O and alcohol) and pressurant (GN_2). The GSE cart will also contain a vacuum pump (with cold trap), a catch basin for off-loaded fluids, a vapor scrubber for all vent gases and a water dilution system for the catch basin drain.

Provisions are also made for obtaining analysis sample of propellant from either the GSE cart or the VCPS into evacuated sample bottles.

An exterior view of the mechanical GSE cart is shown in Figure 7-1. The cart will be provided with drawers for storage of spare parts and operating manuals as well as storage for small tools and

Table 7-1. MECHANICAL GSE FUNCTIONAL REQUIREMENTS

1. Interface with fill and drain valves
2. Provide vacuum pumping capability for system evacuation prior to loading fuel
3. Provide accurate fuel loading capability
4. Provide pressurization with either GN₂ or G He
5. Provide draining capability
6. Provide catch tanks for drained liquids
7. Provide capability to flush system (decontamination) with isopropyl alcohol and distilled water
8. Provide capability to vacuum dry system
9. Provide capability to vacuum dry thrusters
10. Provide 5-micron filtration of all fluids delivered to the spacecraft
11. Provide scrubbing on all tank vents
12. Incorporate devices to prevent backflow of ambient air into tanks following venting operations
13. Provide pressure gauges on all pressurized parts of the GSE
14. Provide relief valves on all pressurized parts of the GSE
15. Incorporated tankage fabricated to ASME code
16. Provide compatible materials in all fluid systems
17. Incorporate a functional control layout
18. Operate safely in an explosive atmosphere
19. Operate successfully in 90% relative humidity
20. Designed for fork lifting and air transportation

Table 7-2. ELECTRICAL GSE FUNCTIONAL REQUIREMENTS

1. Operate on 115 vac, 60 Hz, single-phase input
2. Supply 27 ± 1.3 vdc to:
 - a. Thruster valves
 - b. Latching valves
 - c. Transducers
 - d. Heaters (if used)
 - e. Thermistors (if used)
3. Provide test points for all onboard electrical components
4. Interface onboard signals to external test equipment
5. Monitor output of onboard signals (singly selectable)
 - a. Valve response
 - b. Transducer
 - c. Thermocouples (if used)
 - d. Thermistors (if used)
6. Provide safety test modes for all components
7. Operate safely in an explosive atmosphere
8. Operate in 90% relative humidity

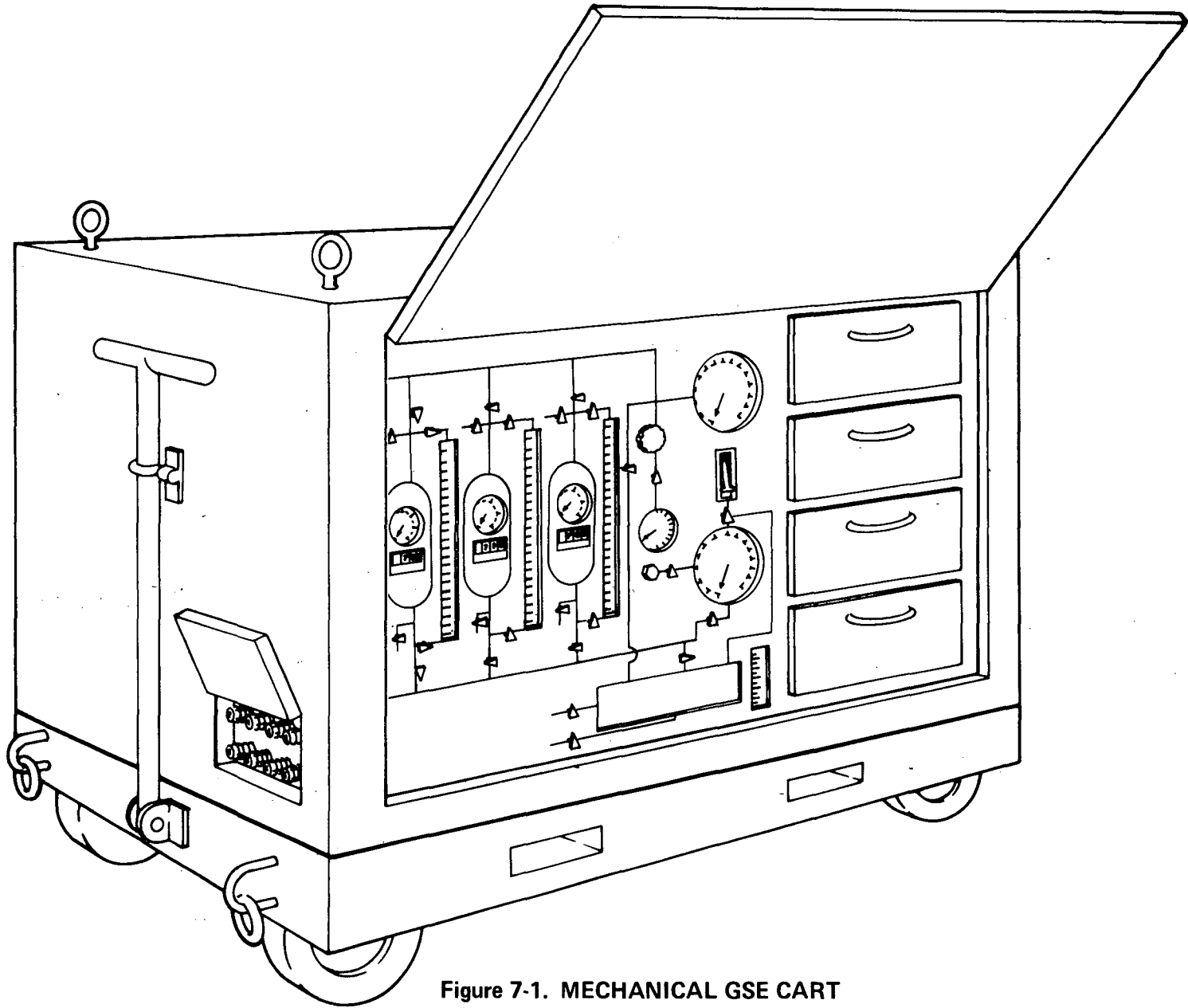


Figure 7-1. MECHANICAL GSE CART

miscellaneous test equipment. With the exterior doors closed and latched, the cart will be completely portable and air transportable.

Wheel locks for the casters and tie-down rings will be provided so that the cart may be shipped without the need for a separate shipping container. In addition, lifting eyes will be provided to facilitate sling-lifting the cart. Fork-lifting provision will be contained in the frame of the cart. A towing handle will be provided to facilitate movement of the cart by hand.

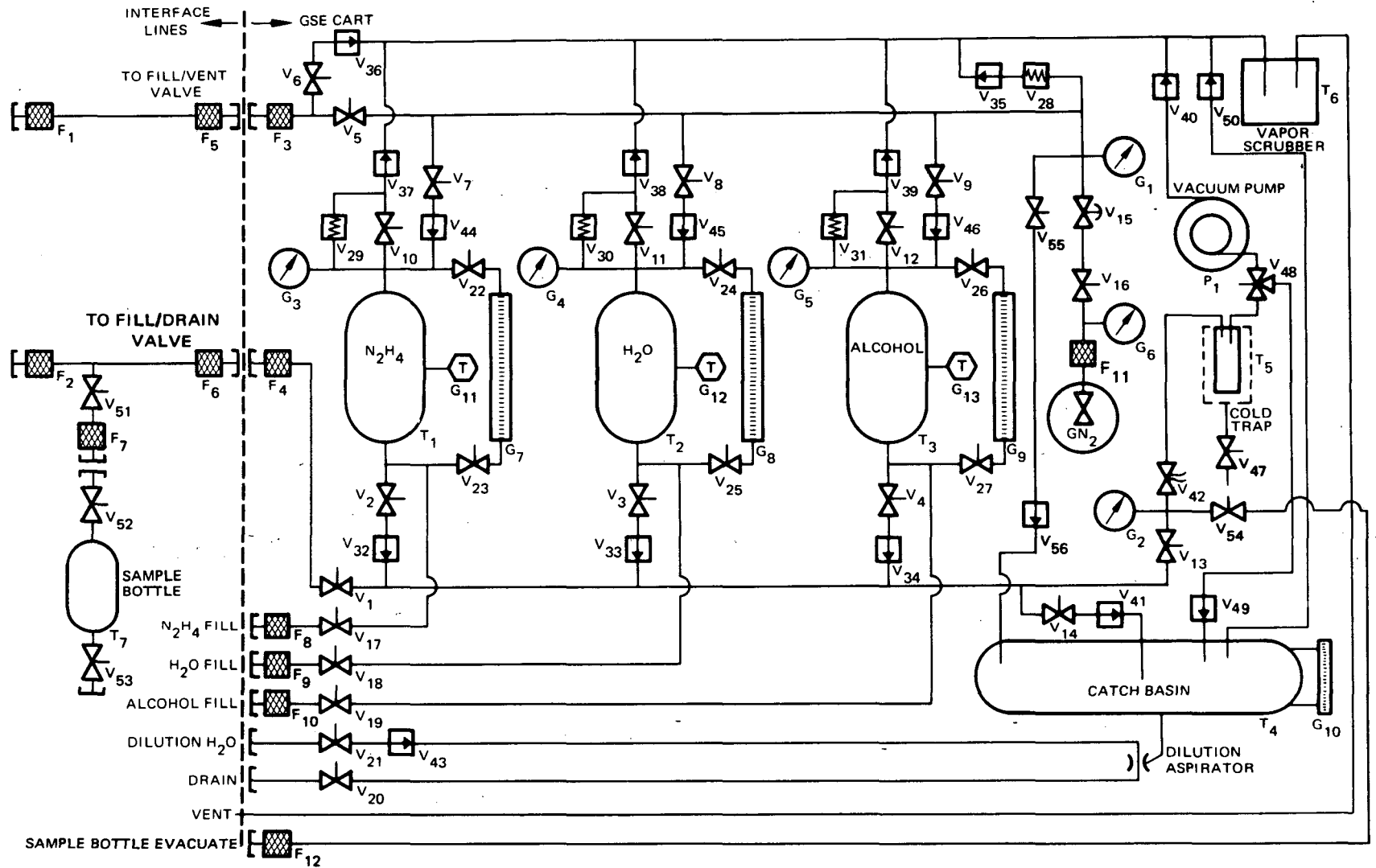
A schematic of the mechanical GSE cart is given in Figure 7-2. All pressure systems are protected by relief valves and all fluid systems are protected with check valves to prevent intermixing of the flush fluids with the propellant as well as preventing backflow from the vapor scrubber. All inlets are protected with 10μ absolute filters to maintain the internal cleanliness of the systems. Filters (10μ absolute) are provided at the service outlets of the cart as well as on both ends of the interface lines and at the sample outlet. All pressure systems are provided with visual pressure gauges for continuous monitoring of operations. All control valves will be manually operated and will be located, along with the pressure gauges, tank sight glasses, and tank temperature indicators on the front control panel. The catch basin drain is provided with a water dilution system to dilute all drained fluids to safe levels before they leave the cart.

The propellant supply tank and flush fluid supply tanks are provided with sight glasses for making quantity measurements. All sight glasses will be calibrated on a weight basis at standard conditions. Temperature sensors are provided on all supply tanks. Tables containing the necessary corrections to be made for temperature and weight of fluids contained in lines external to the VCPS will be provided in the GSE cart operating manual. The sight glass calibrations will be verified by actual weight measurements made on the VCPS before and after loading the VCPS from the GSE cart during subsystem qualification tests. The propellant tank will be sized to contain 50 lbm of N_2H_4 . The flush fluid tanks will each be sized to a volume equal to that of the propellant tank. The catch basin will be provided with a sight glass to indicate liquid level. The catch basin will be sized to a volume equal to the total volume of the three supply tanks.

The vacuum pump will be provided with an LN_2 cold trap immediately upstream of the pump inlet. The vacuum pump and cold trap will be protected by a 117 vac solenoid operated isolation valve which will be wired in parallel with the vacuum pump motor. In the event of inadvertent vacuum pump shutdown, due to power failure or operator error, the isolation valve will close, thereby preventing backstreaming from the pump into the GSE systems.

A water bath vapor scrubber is provided through which all vent gases are routed to prevent release of potentially toxic gases to the atmosphere. All vent lines into the vapor scrubber are protected against backflow by check valves.

The catch basin is provided with a GN_2 purge flow to carry all vapors from collected liquids through the vapor scrubber to prevent accumulations of toxic vapors.



-  CHECK VALVE
-  HAND VALVE
-  FILTER
-  SOLENOID VALVE
-  GAUGE
-  RELIEF VALVE
-  CAPPED FITTING
-  REGULATOR
-  SIGHT GLASS
-  TEMPERATURE SENSOR

Figure 7-2. MECHANICAL GSE SCHEMATIC

All control valves, pressure gauges, sight glasses, temperature indicators, and the pressure regulator will be mounted on the front control panel. The controls will be labeled to clearly indicate positions, function, and component designation number. The control panel will be marked with system flow schematics and the controls will be arranged in such a manner as to indicate the function and interrelation of all controls. The control panel layout is illustrated in Figure 7-3. A vacuum outlet is provided on the control panel to facilitate evacuation of the sample bottles during propellant analysis sampling.

The interfacing service lines will be size coded to the fill/vent and fill/drain valves to prevent incorrect connection with the VCPS. All lines within the GSE cart and the interfacing flex lines will be marked with color-coded labels to identify the fluids contained therein.

GN₂ supply is provided by a standard "K" bottle of GN₂ which is interfaced to the cart through a filter and is provided with a shutoff valve and a reference pressure gauge to indicate supply pressure. The "K" bottle itself is provided with a safety burst disc relief valve.

Measurement accuracies will be as follows: loaded propellant weight, $\pm 0.75\%$ using calibration tables in manual (0 to 50 lbm full scale, sight glasses graduated in 1 millimeter, resolution 0.5 millimeter); pressures, $\pm 0.25\%$ (0 to 300 psig for supply tank pressures, 1-psi graduation, 0.5-psi resolution); 0 to 500 psig for regulator outlet, 1-psi graduation, 0.5-psi resolution; 0 to 3,000 psig for GN₂ supply, 10-psi graduations, 5-psi resolution; 0 to 30 inches of mercury for vacuum gauge, 0.1-inch graduation, 0.05-inch resolution).

An operating manual will be provided with the mechanical GSE cart (10 copies delivered). The manual will contain detailed operating instructions for all operations to be performed with and/or on the mechanical GSE cart. The manual will be laid out as a detailed step-by-step procedure calling out which valves and controls are to be operated in which sequence to correctly perform each function. Instructions for the operation of the electrical GSE suitcase (see paragraph 7.1.3) will be called out in the mechanical GSE operating manual for those functions requiring the use of the electrical GSE. Complete instructions for each function will be provided; as an example, if it is desired to internally leak check the VCPS, the "VCPS Internal Leak Check" section of the operating manual will give complete step-by-step instructions for connecting the mechanical and electrical GSE to the VCPS, operating the GSE (both mechanical and electrical), securing the VCPS, disconnection of the GSE, and securing the GSE. The operating manual will also include sight-glass calibration tables, system schematics, block diagrams, component parts list with component part numbers, and a list of spare parts provided with the mechanical GSE. The operating manual will also contain instructions for securing the GSE for shipment.

A log book will be maintained with the GSE starting at the time of GSE assembly. This log will conform to paragraph 3.10 of NPC 250-1 and will contain a chronology of all inspection, testing, failures, repair, and maintenance of all components and spares of the mechanical GSE cart. All serialized components will be identified by serial number in all entries. The log book will be kept with the GSE at all times and will be delivered with the GSE.

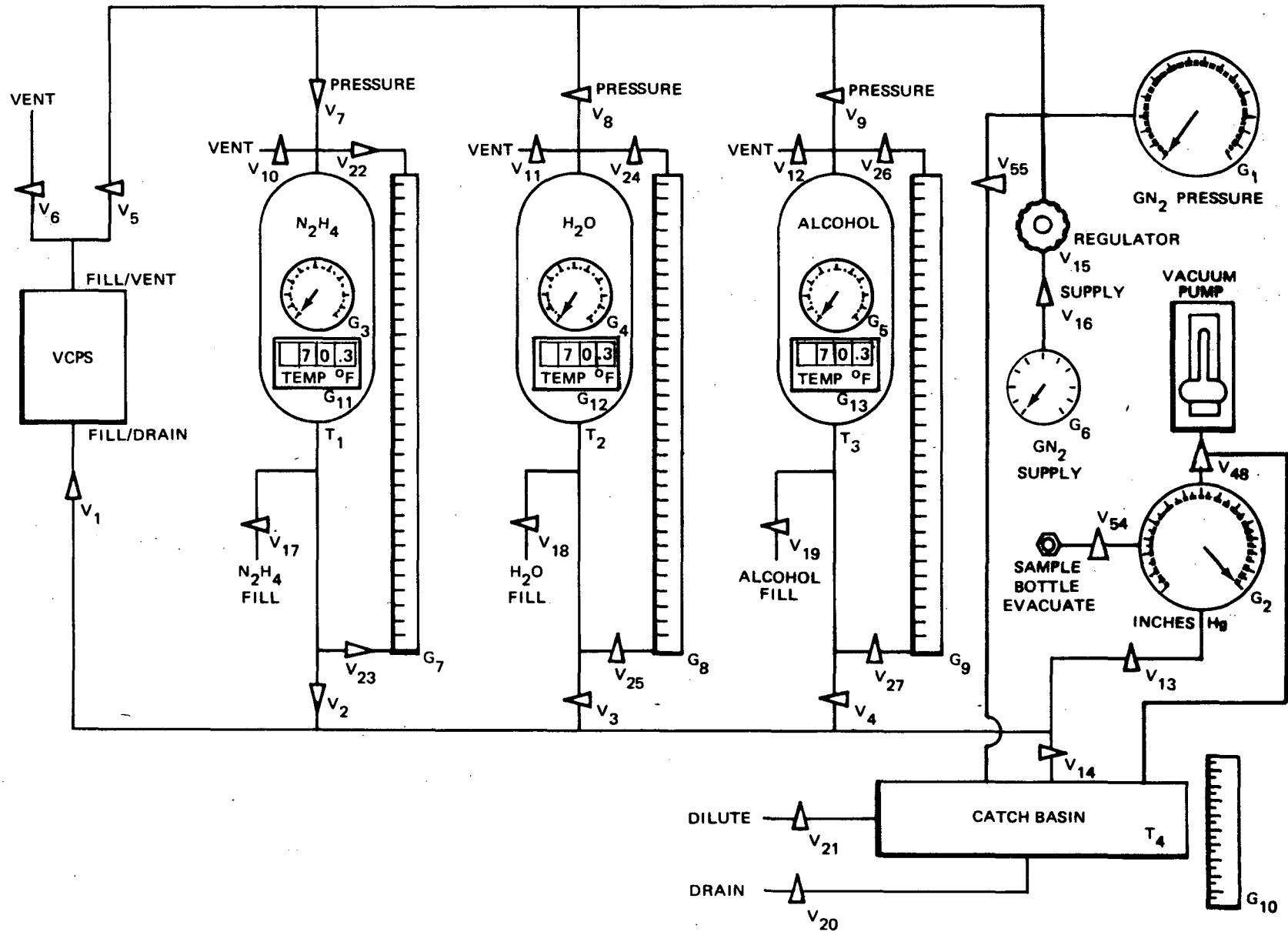


Figure 7-3. MECHANICAL GSE CONTROL PANEL

7.2.2 Mechanical GSE Functional Description

The following paragraphs describe the function performed by the mechanical GSE cart and are illustrated by schematic of the GSE systems in use for each of the functions described.

7.2.2.1 VCPS Evacuation

The GSE cart is interfaced to the VCPS through the fill/drain valve via the liquid interface line. The VCPS is then evacuated by use of the vacuum pump (through the cold trap) in the GSE. Vacuum pump exhaust vapors pass through the vapor scrubber before being overboarded. This procedure is used prior to loading the VCPS with propellant to ensure filling the dead ends in the system and is also used to dry the VCPS after the VCPS has been flushed during the decontamination procedure. The flow circuits in use in the GSE during VCPS evacuation are illustrated in Figure 7-4.

7.2.2.2 Sample Bottle Evacuation

A special fitting is provided on the front panel of the GSE for sample bottle evacuation (see Figure 7-3). The flow diagram for this procedure is shown in Figure 7-5. Two stainless steel sample bottles, with valves and fittings, will be provided with the GSE to enable samples to be taken of the propellant in the GSE prior to loading the VCPS and of the propellant in the VCPS after loading.

7.2.2.3 GSE Propellant Sampling

After the VCPS is evacuated (paragraph 7.2.2.1), the fill/drain valve is closed and V_2 is opened (V_{13} has been closed). This fills the GSE manifold and interface line with propellant. The sample bottle is then connected to the sample tap on the interface line and V_{51} and V_{52} are opened, filling the sample bottle. After V_{51} and V_{52} are closed, the sample bottle may be removed and the propellant extracted for chemical analysis to verify that the propellant meets the applicable specifications. The flow diagram for this operation is shown in Figure 7-6.

The propellant is analyzed to verify that it meets the requirements of MIL-P-26536B and RRC M&P-0015 which include:

	% by Weight
Hydrazine	97.5 minimum
Water	2.5 maximum
Ammonia	0.4 maximum
Analine	0.5 maximum
Total nonvolatiles	0.004 maximum

Rocket Research Corporation also performs a special "corrosivity" analysis to verify that the propellant has not been contaminated by CO_2 , which would lead to the formation of corrosive metal salt. This test does not give a quantitative measure of CO_2 content but does test for the presence of carbazic acid in the hydrazine through measurement of corrosivity rates. The test involves allowing the hydrazine to react with iron powder under controlled conditions and analyzing the resulting hydrazine. The iron content analysis is done quantitatively using a

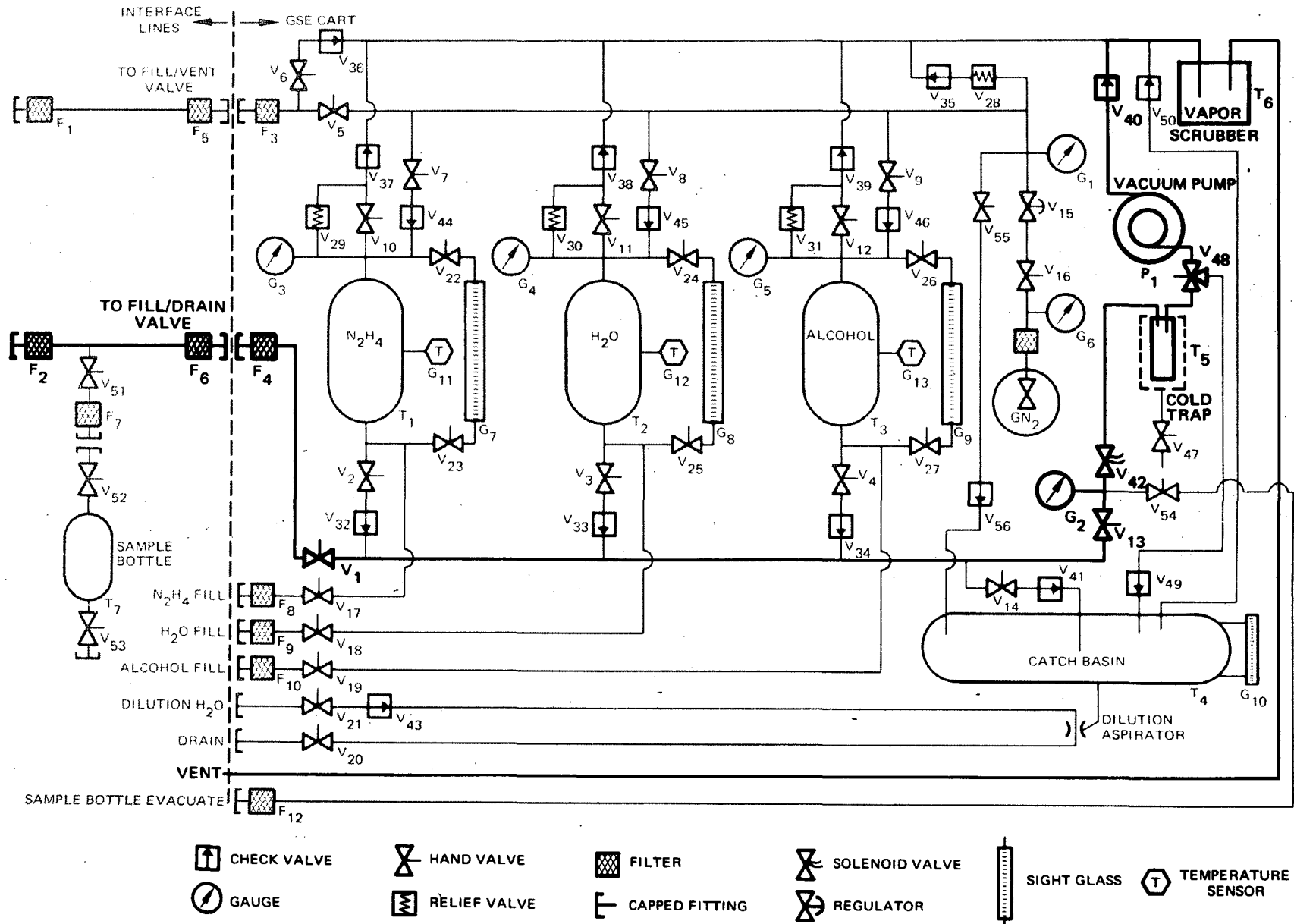


Figure 7-4. MECHANICAL GSE SCHEMATIC EVACUATION/VACUUM DRYING

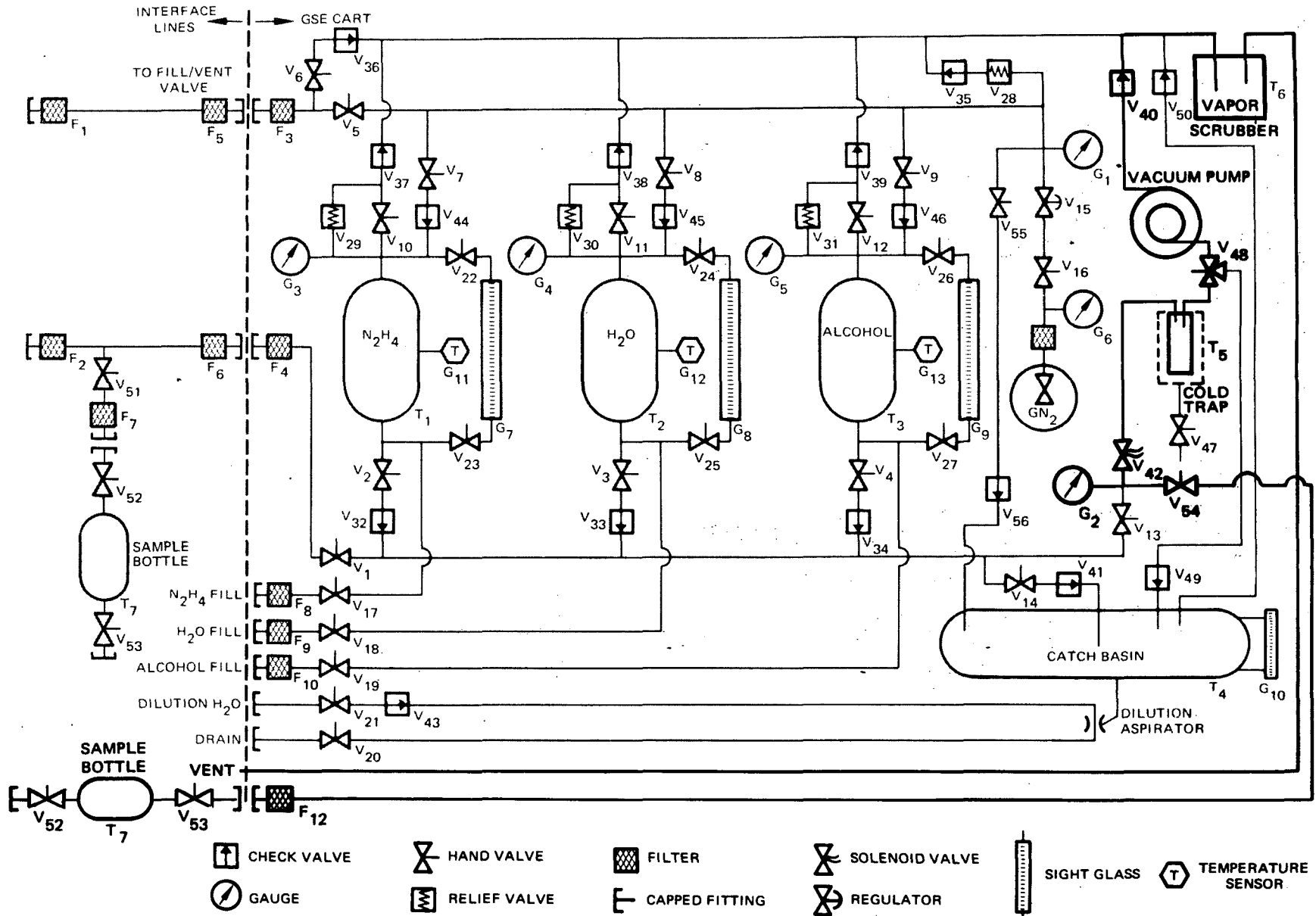


Figure 7-5. MECHANICAL GSE SCHEMATIC SAMPLE BOTTLE EVACUATION

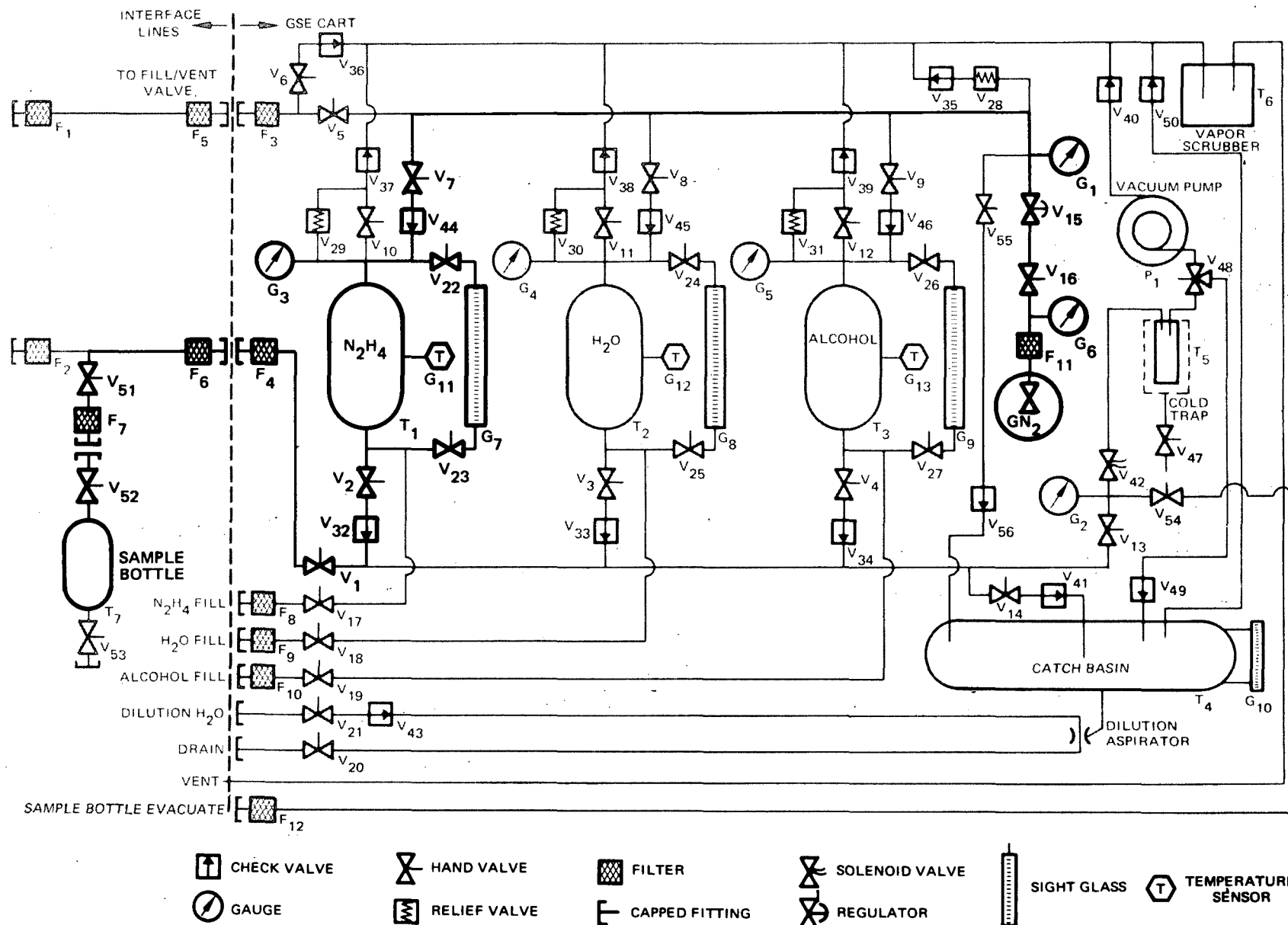


Figure 7-6. MECHANICAL GSE SCHEMATIC GSE N₂H₄ SAMPLE

spectrophotometric procedure. If large quantities of CO_2 are present in the hydrazine, iron will be detected in the hydrazine. The iron, which must be in the ferrous state, reacts with 2, 2' bipyridine to form a red-colored complex. The optical density of the solution is measured at $525 \text{ M}\mu$ and compared to a prepared calibration curve. Rocket Research Corporation has established through corrosivity tests that an iron content above 25 ppm by the above test is sufficient to reject the propellant because of excessive CO_2 content.

7.2.2.4 N_2H_4 Loading

After the sample has been taken (paragraph 7.2.2.3) the fill/drain valve is opened and the VCPS is vacuum filled until approximately 1 lbm of propellant has been transferred. This is to ensure that there are no pockets of gas trapped in dead ends in the VCPS. The propellant transfer is then temporarily stopped and the VCPS is backfilled with GN_2 through the fill/vent valve via the gas interface line. The remainder of the propellant load is then pressure transferred into the VCPS. The flow diagram for this function is shown in Figure 7-7. A calibrated amount of overload is transferred to enable a sample to be taken of the propellant in the VCPS. The weight of propellant transferred is measured by use of the calibrated sight glass on the propellant supply tank and the temperature sensor in the propellant supply tank. The necessary temperature correction tables for the sight glass will be contained in the operating manual.

7.2.2.5 VCPS Pressurization/Proof Testing

The flow diagram for pressurizing the VCPS is shown in Figure 7-8. As the GN_2 regulator and regulator output gauge both have a range of 0 to 500 psig, this connection may also be used for VCPS proof testing. The gauges on the supply tanks and the supply tank relief valves will have a range of 300 psig. The regulator output relief valve will be set at 500 psig.

7.2.2.6 VCPS N_2H_4 Sampling

As previously described, a sample bottle is evacuated and connected to the sample tap on the interface line. As the volume of the bottles has previously been calibrated and the correct amount of propellant has been overloaded into the VCPS, extraction of the analysis sample will bring the propellant load to the correct weight. The connection for this sample is shown in Figure 7-9.

7.2.2.7 N_2H_4 Off-Loading

In the event that through operator error the VCPS is overloaded, the excess propellant may be off-loaded back into the GSE supply tank and the quantity verified by use of the tank sight glass. The connections for this operation are shown in Figure 7-10. The interface line is connected to the N_2H_4 supply tank fill port, and the excess propellant is then returned to the supply tank.

To preclude the possibility of the N_2H_4 supply being contaminated with H_2O or alcohol through operator error, check valve V_{32} has been installed. This check valve prevents off-loading into the supply tank by reversing the loading flow path. Self-sealing, quick-disconnect fittings and filters on the interface lines and ports of the GSE prevent contamination of the propellant during this operation.

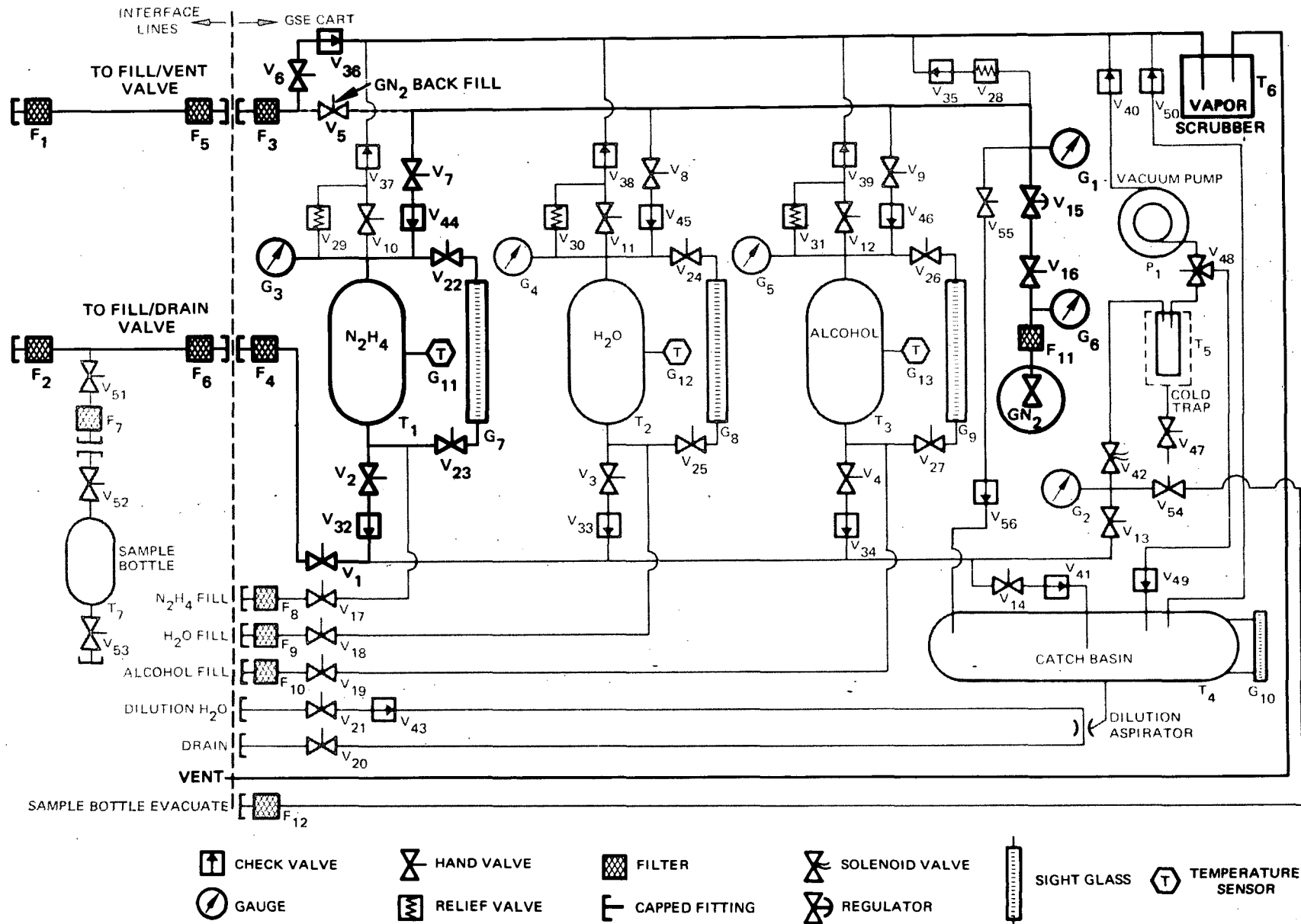


Figure 7-7. MECHANICAL GSE SCHEMATIC N_2H_4 LOADING

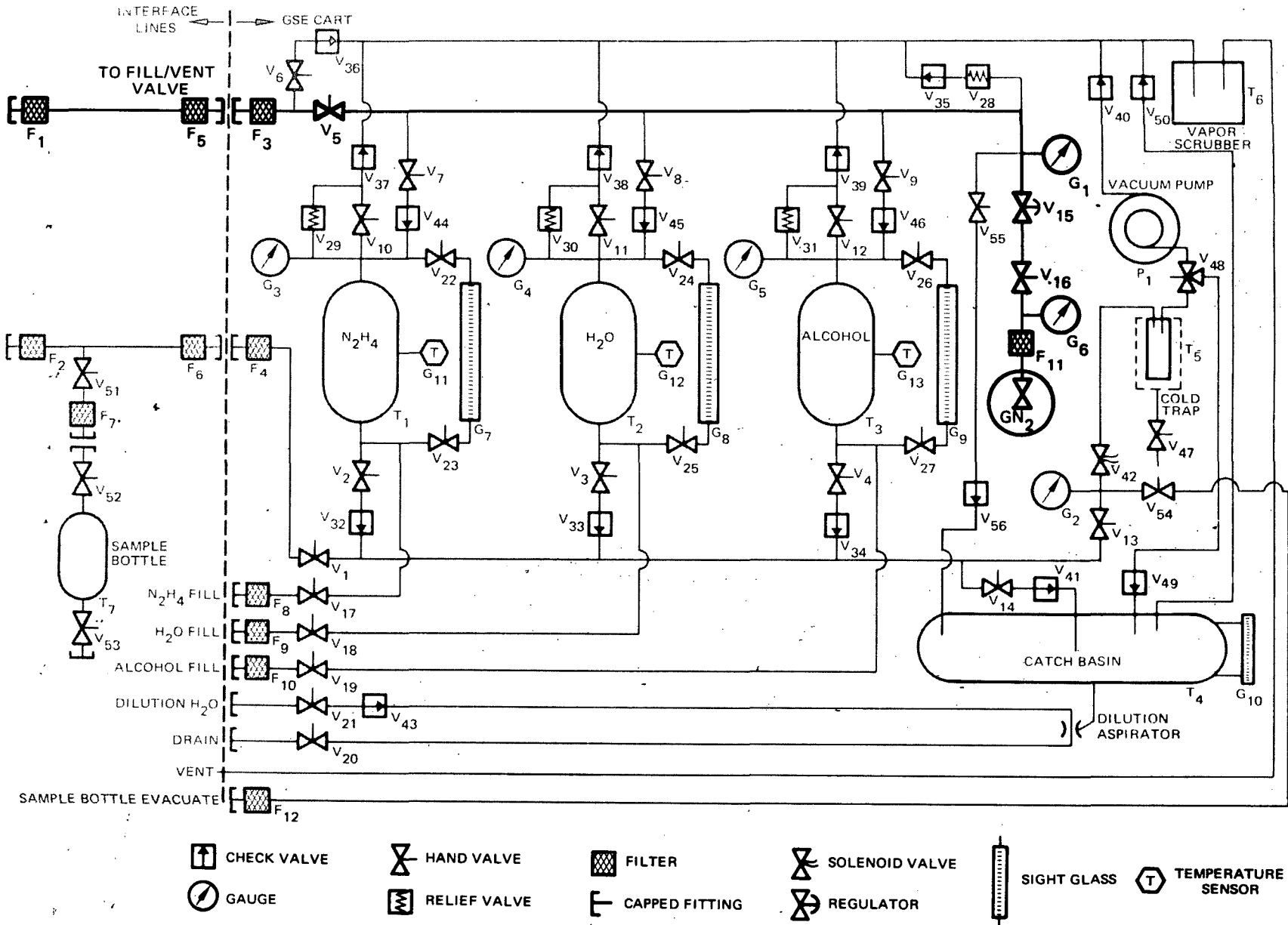
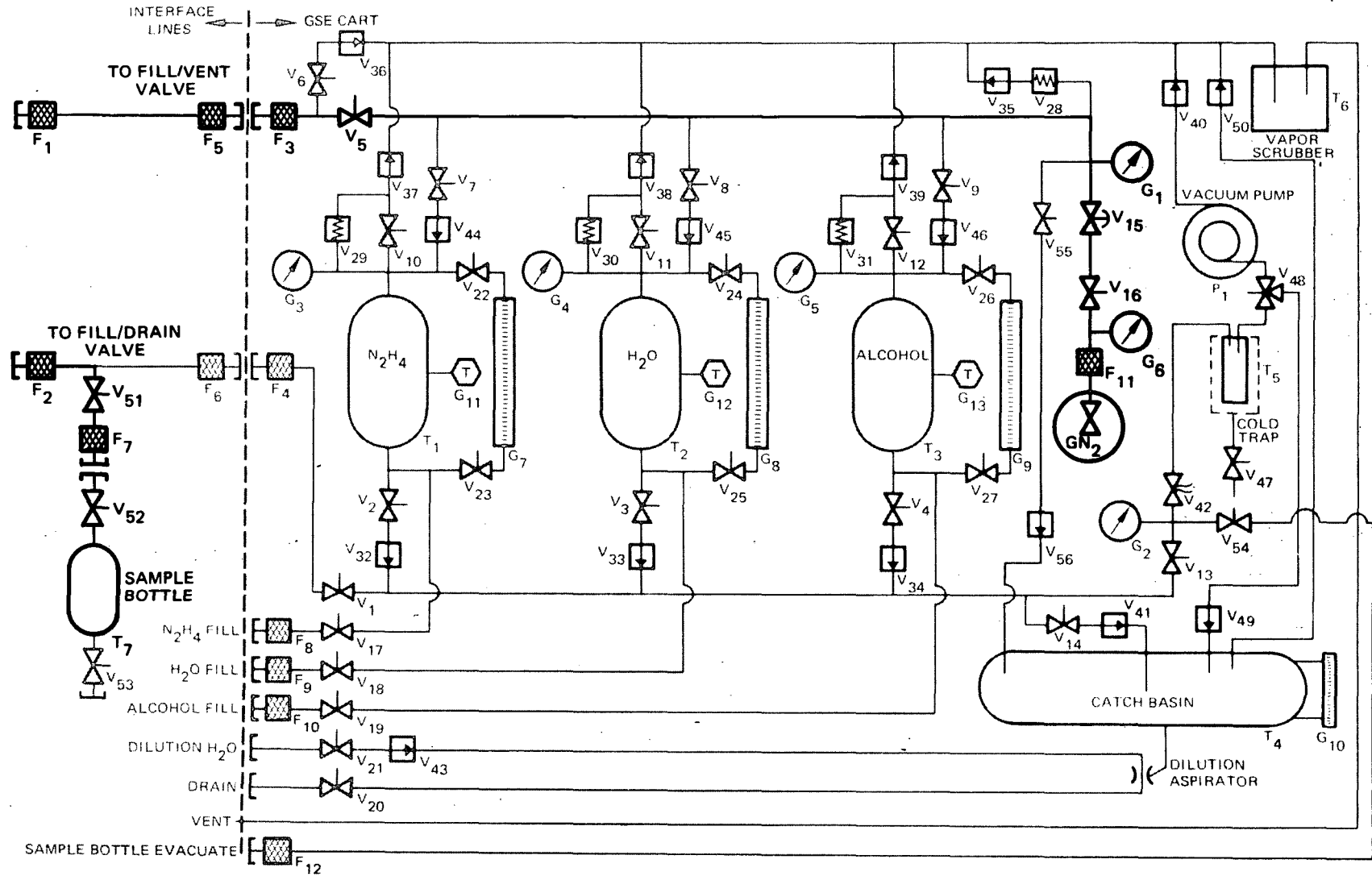


Figure 7-8. MECHANICAL GSE SCHEMATIC PRESSURIZING/PROOF TESTING



- | | | | | | | | | | | | |
|--|-------------|--|--------------|--|----------------|--|----------------|--|-------------|--|--------------------|
| | CHECK VALVE | | HAND VALVE | | FILTER | | SOLENOID VALVE | | SIGHT GLASS | | TEMPERATURE SENSOR |
| | GAUGE | | RELIEF VALVE | | CAPPED FITTING | | REGULATOR | | | | |

Figure 7-9. MECHANICAL GSE SCHEMATIC VCPS N_2H_4 SAMPLE

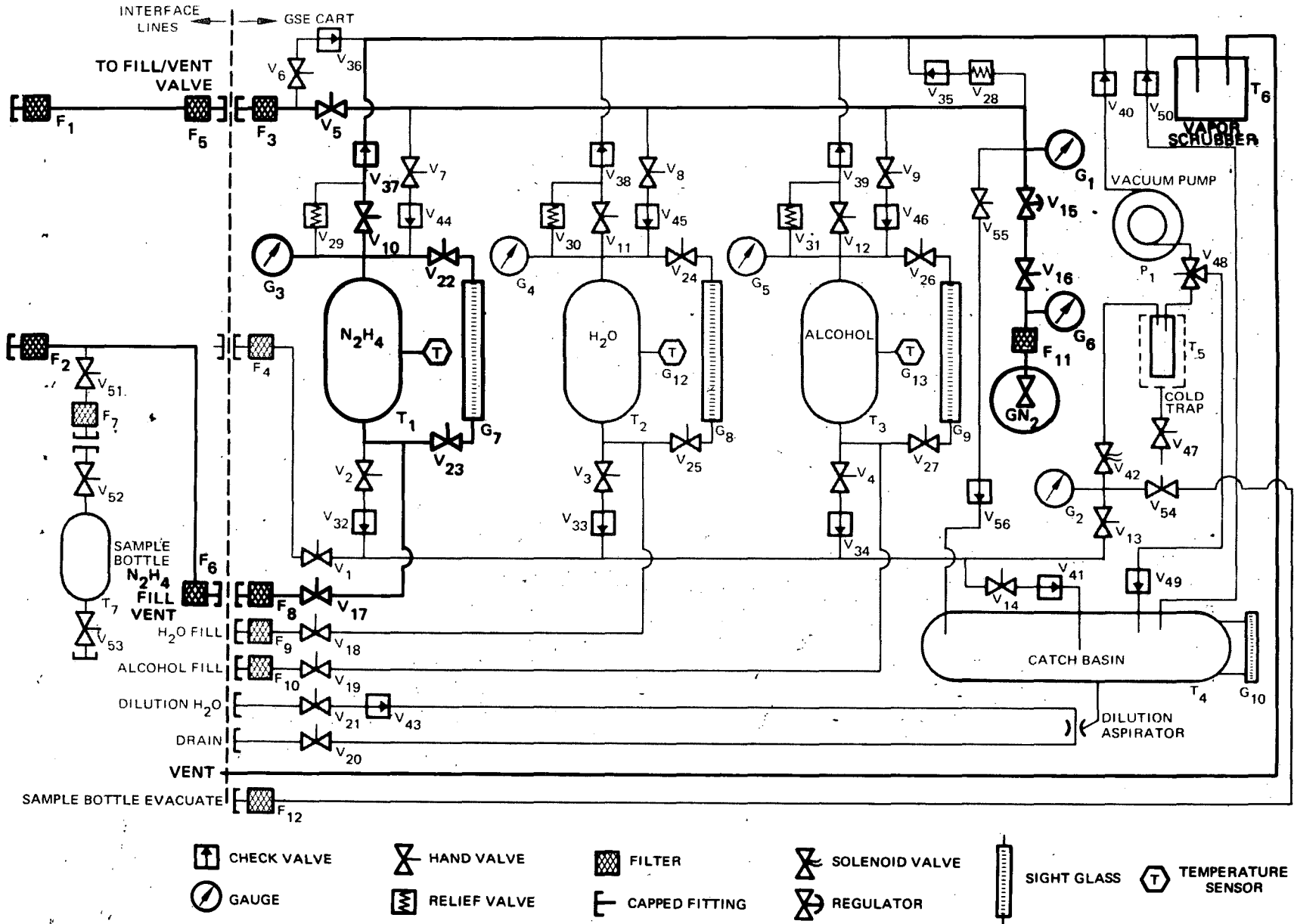


Figure 7-10. MECHANICAL GSE SCHEMATIC N₂H₄ OFF-LOADING

7.2.2.8 VCPS Venting

The flow diagram for venting the VCPS pressurant through the vapor scrubber in the GSE is shown in Figure 7-11.

7.2.2.9 VCPS Draining

Fluids contained in the VCPS are drained into the catch basin in the GSE. The connectors for this function are shown in Figure 7-12. The fluids are transferred under GN₂ pressure and the vapors from the catch basin are passed through the vapor scrubber before being vented.

7.2.2.10 VCPS Decontamination

The VCPS decontamination procedure consists of the following. The propellant is drained into the catch basin. The VCPS is then loaded with H₂O by use of the combination vacuum fill/pressure transfer technique as described for N₂H₄ loading. The H₂O absorbs the N₂H₄ and is then drained into the catch basin. The VCPS is then loaded with alcohol by use of the vacuum fill/pressure transfer technique. The alcohol absorbs the H₂O and is then drained into the catch basin. Contamination (particulate) samples of the alcohol are taken at the fill/drain valve and through the isolation valves. The above alcohol flush procedure is repeated until the particulate sample verifies that the VCPS is clean. The flow diagrams for H₂O loading and alcohol loading are given in Figures 7-13 and 7-14, respectively. At the completion of the above described flush and drain procedure, the VCPS is vacuum dried as described in paragraph 7.2.2.1.

7.2.2.11 VCPS Valve Leak Checks

Nozzle adapters and pipettes will be provided with the GSE to enable the VCPS valves to be leak checked. The pipettes are connected to the VCPS REA nozzles via the nozzle adapters. The VCPS is pressurized as described in paragraph 7.2.2.5. By use of the electrical GSE the primary valves are opened to leak check the secondary valves or the secondary valves are opened to leak check the primary valves. Although the VCPS valves will be leak checked with GN₂ by this procedure, the GN₂ minimum allowable leak rate of 3 scc/hr will be well within the specification leak rate of 4.5 scc/hr He. The GN₂ leak rates of the VCPS valves will be correlated with the He leak rates during VCPS qualification testing.

7.2.2.12 GSE Service Operation

7.2.2.12.1 Liquid Interface Line Decontamination

At the completion of VCPS loading operations, the GSE liquid interface line will be decontaminated and dried by use of the method described above for VCPS decontamination. This operation will be performed after the interface lines are demated from the VCPS and before the interface lines are demated from the GSE service ports for storage.

7.2.2.12.2 Cold Trap Drain and Flush

The LN₂ in the cold trap bucket will be drained through V₄₇. When the cold trap has warmed, the bypass valve, V₄₈ is opened and the cold trap is flushed with H₂O from the H₂O storage tank. The

MECHANICAL GSE SCHEMATIC VENTING

11041-28

7-18

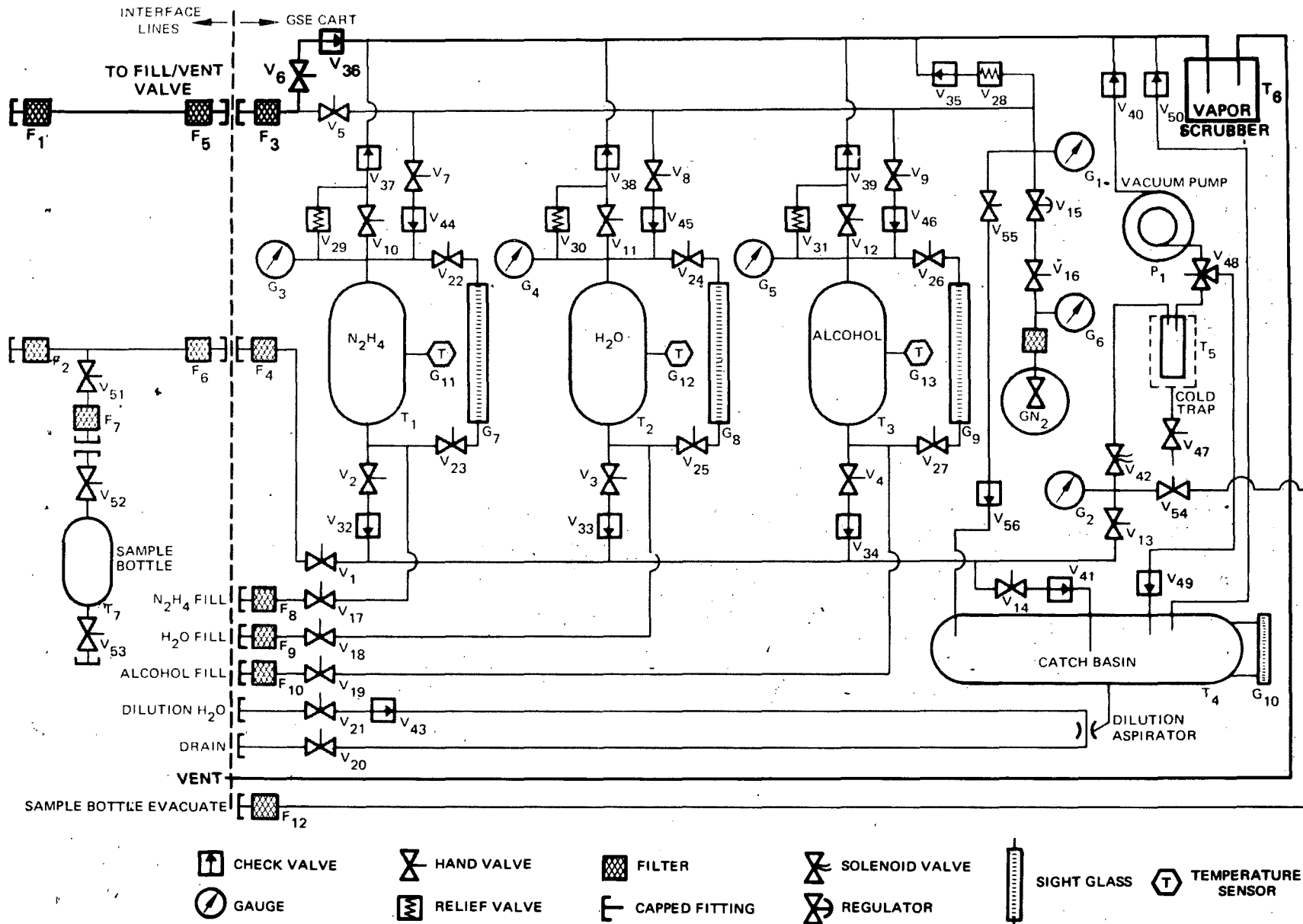


Figure 7-11. MECHANICAL GSE SCHEMATIC VENTING

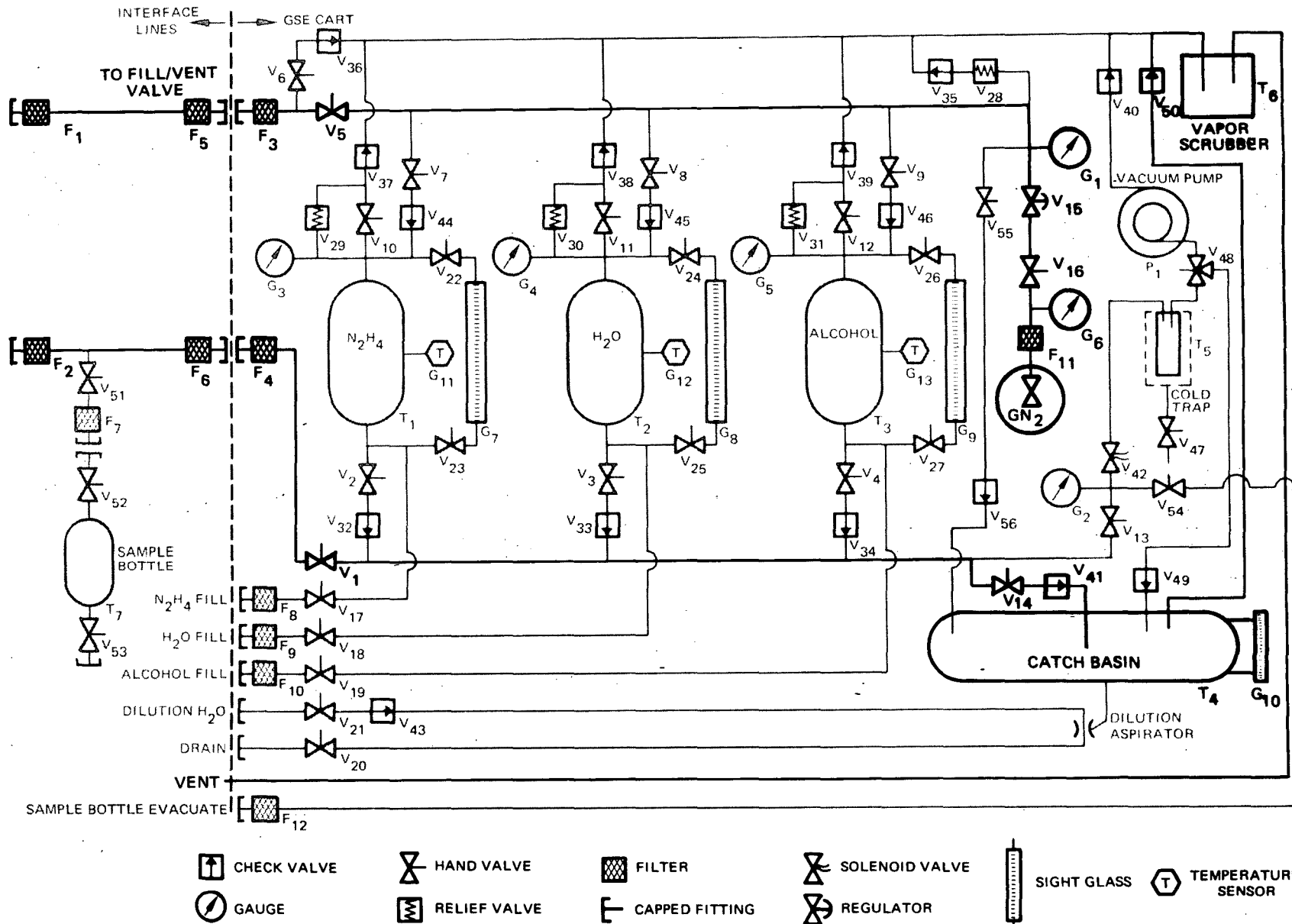


Figure 7-12. MECHANICAL GSE SCHEMATIC DRAINING

11041-30

7-20

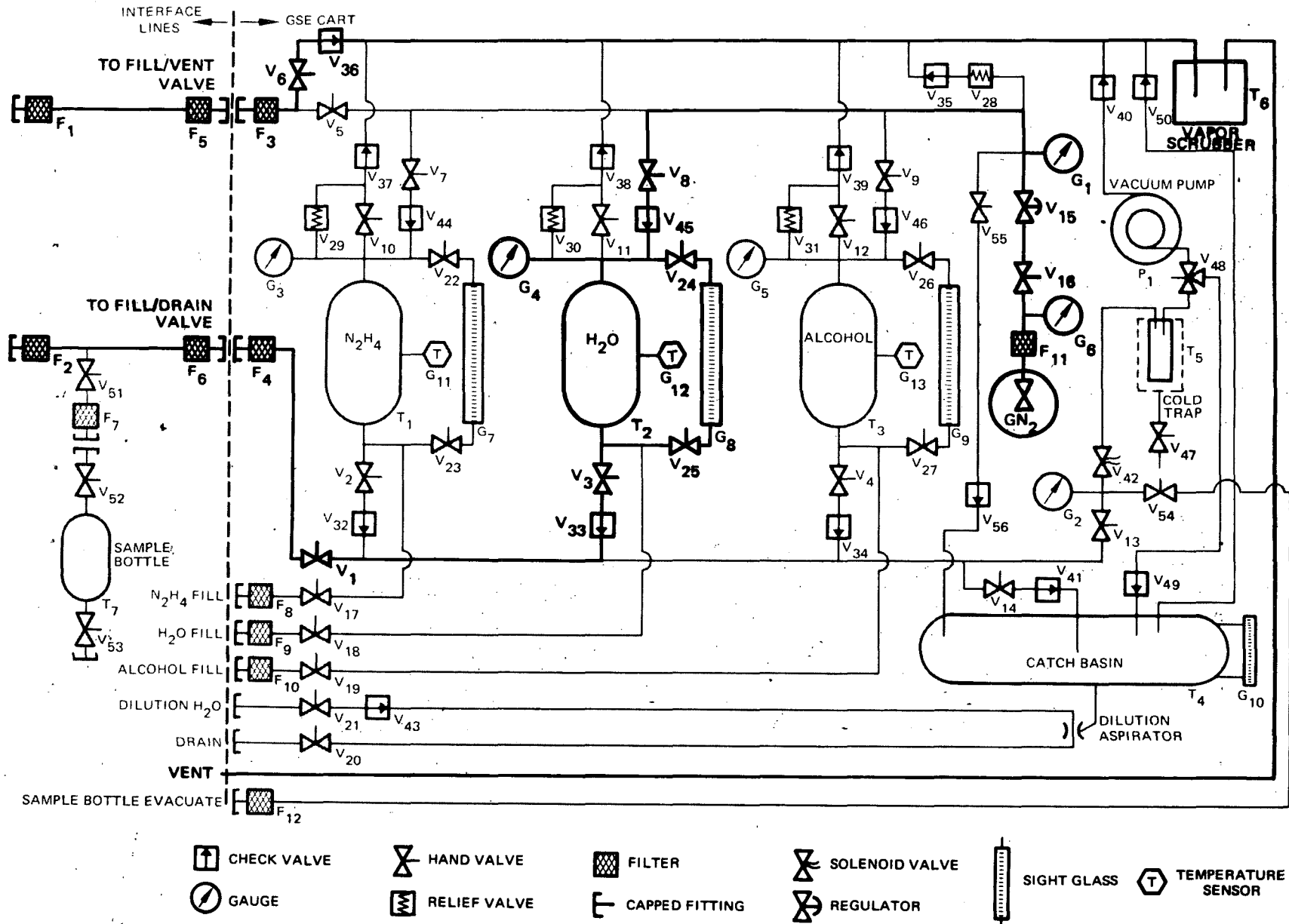


Figure 7-13. MECHANICAL GSE SCHEMATIC H₂O LOADING

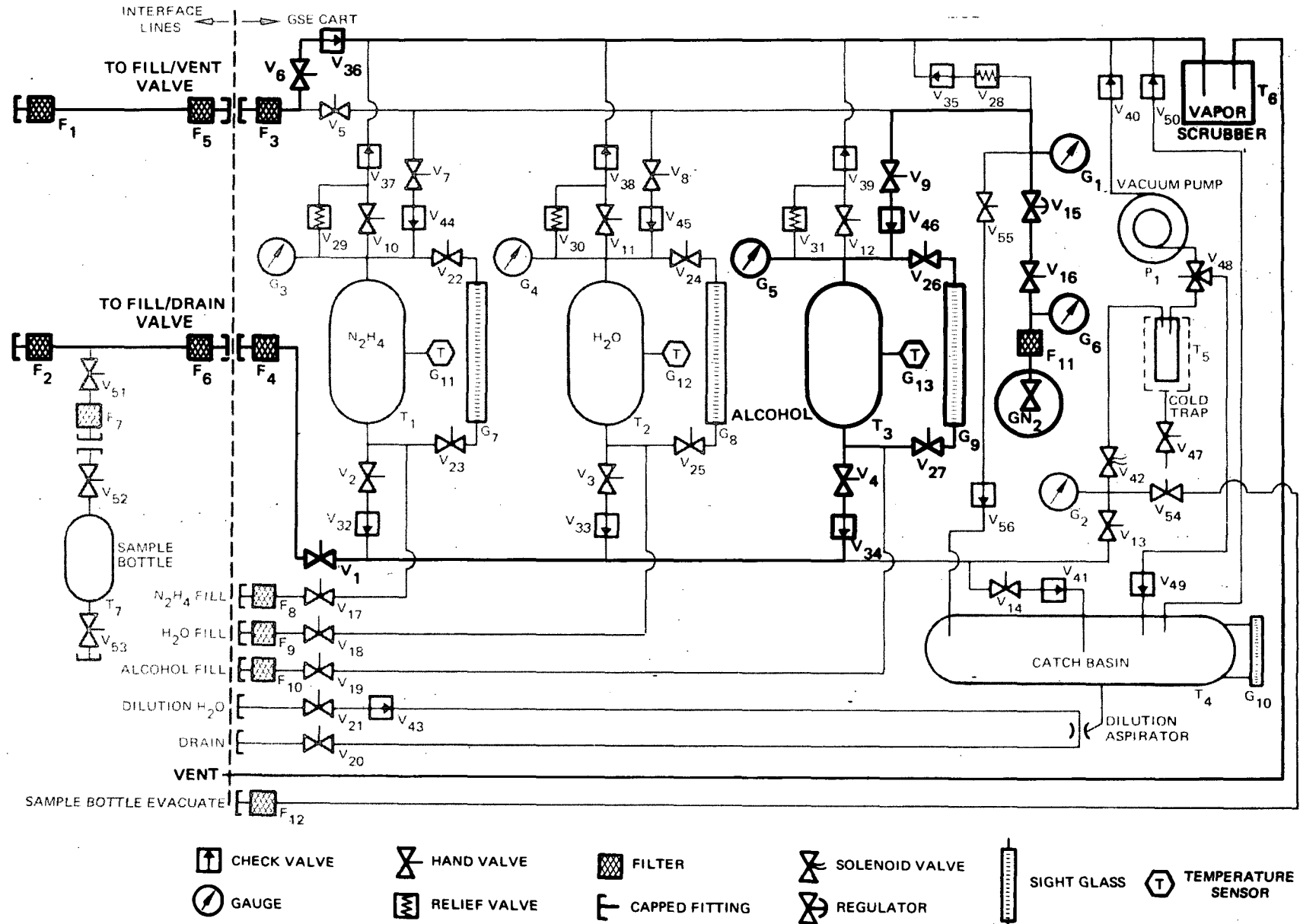


Figure 7-14. MECHANICAL GSE SCHEMATIC ALCOHOL LOADING

flush H_2O is dumped into the catch basin, the vapors passing through the vapor scrubber before being vented. Figure 7-15 shows the flow paths for this operation.

7.2.2.12.3 Catch Basin Drain and Purge

During catch basin draining the fluids contained in the catch basin are diluted to safe levels by the dilution aspirator by use of H_2O as the dilutant. The dilution aspirator is so connected that the catch basin cannot be drained unless the H_2O dilutant is flowing. The vapors contained in the catch basin are purged through the vapor scrubber with GN_2 before they are vented. The flow paths for these operations are shown in Figure 7-16.

7.2.2.12.4 Supply Tank Fill

N_2H_4 is transferred from the supply drum into the GSE N_2H_4 tank using the transfer system shown schematically in Figure 7-17. This transfer system will be provided with the GSE cart.

7.2.2.12.5 Other Operations

Other operations not listed here but necessary for GSE operation such as, but not limited to, securing the GSE for shipment and setup and checkout prior to use will be called out in detail in the operating manual.

7.2.3 Electrical GSE Design Description

The electrical GSE will be provided in a separate portable "suitcase." The electrical GSE will provide the functions of VCPS valve actuation, heater power and transducer power control with status indication as well as monitoring the output of the on-board pressure transducer and temperature sensors. An illustration of the electrical GSE is given in Figure 7-18.

An electrical schematic of the GSE is shown in Figure 7-19. The dc power supply output voltage will be variable over the range of 11 to 18 vdc to allow functional testing of the VCPS components at various input voltages. The power supply will be provided with a voltmeter to monitor output voltage level. However, the signal conditioning circuits for the thermistor temperature sensors (to GSFC's schematic) will be provided with zener diode voltage regulation at their power input terminals to ensure repeatable, accurate temperature indication from the thermistors. The variable voltage adjustment of the power supply will be a part of the power supply voltage regulator sensing circuit, therefore ensuring accurate regulation of the voltage level selected regardless of input line or load current variations.

Each control switch will be clearly labeled to indicate the VCPS component which it controls and will be provided with an indicator lamp to show VCPS component status. In addition, power to the primary valve control switches is routed through a key-operated arming switch and the primary valve switches will be provided with guard covers. These precautions are provided to prevent inadvertent thruster firings while enabling complete VCPS functional testing to be performed using the electrical GSE. Individual output monitoring meters will be provided for the on-board temperature sensors. A readout will be provided for monitoring the output of the on-board pressure transducer enabling accurate measurements of VCPS tank pressure to be made.

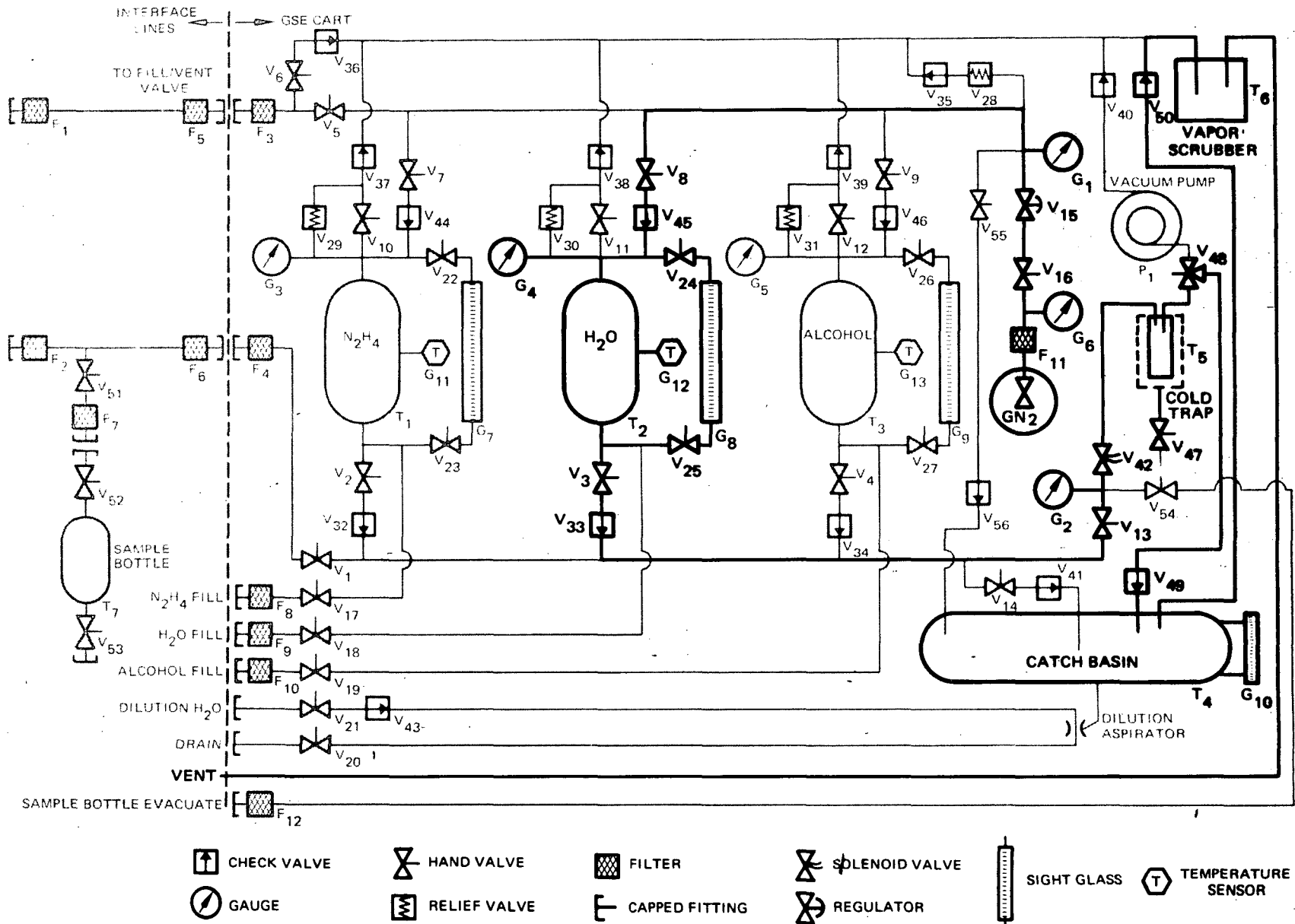


Figure 7-15. MECHANICAL GSE SCHEMATIC COLD TRAP FLUSHING

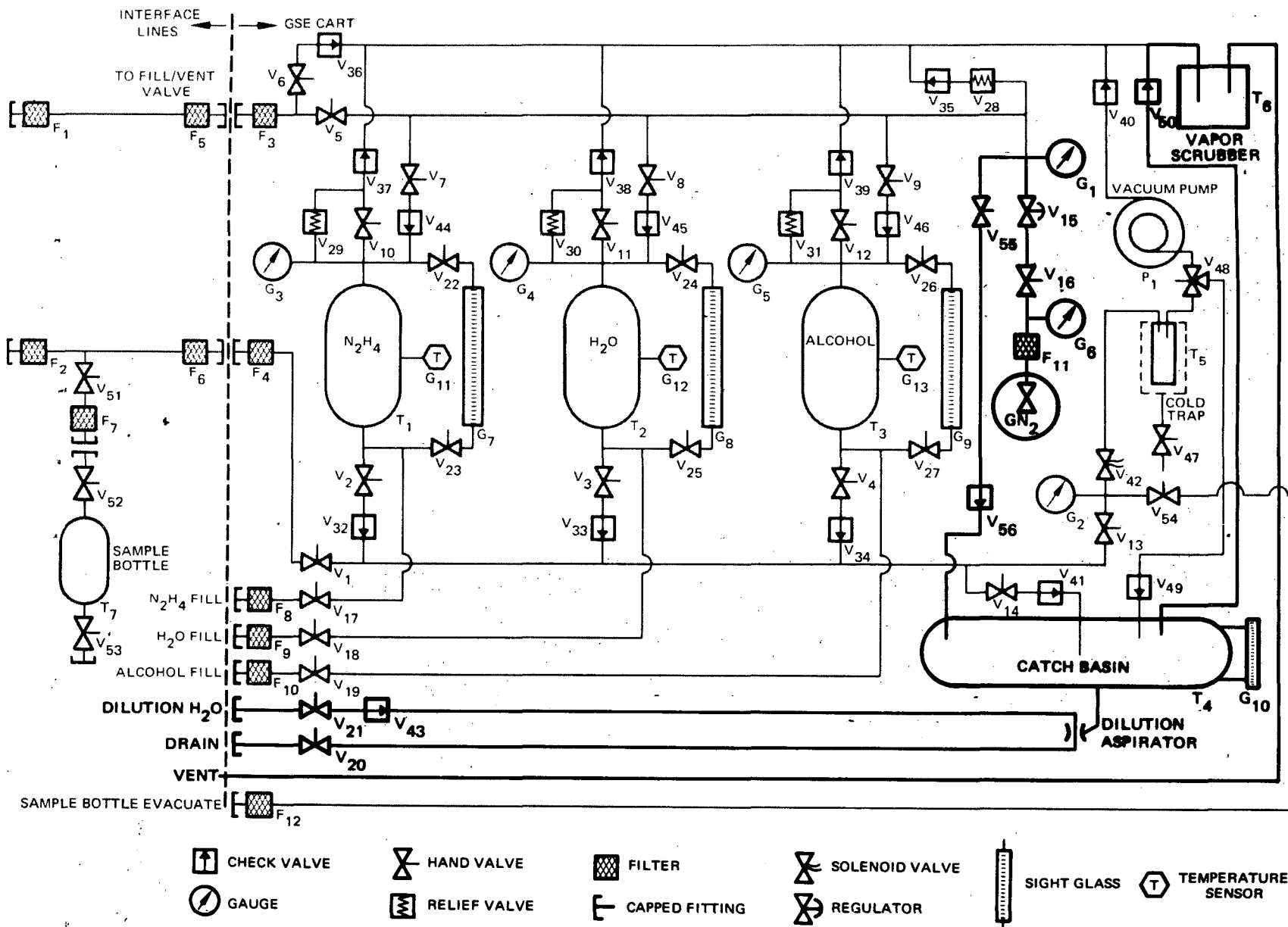


Figure 7-16. MECHANICAL GSE SCHEMATIC CATCH BASIN DRAIN AND PURGE

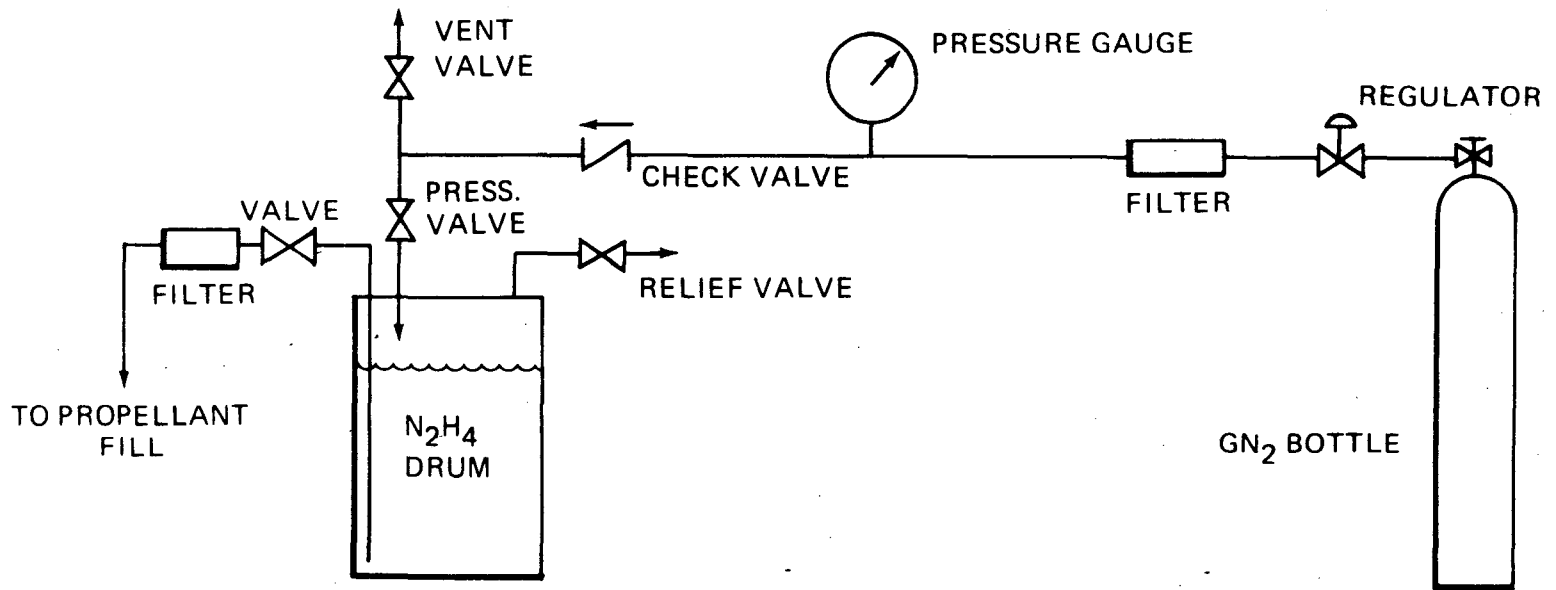


Figure 7-17. N_2H_4 TRANSFER SYSTEM

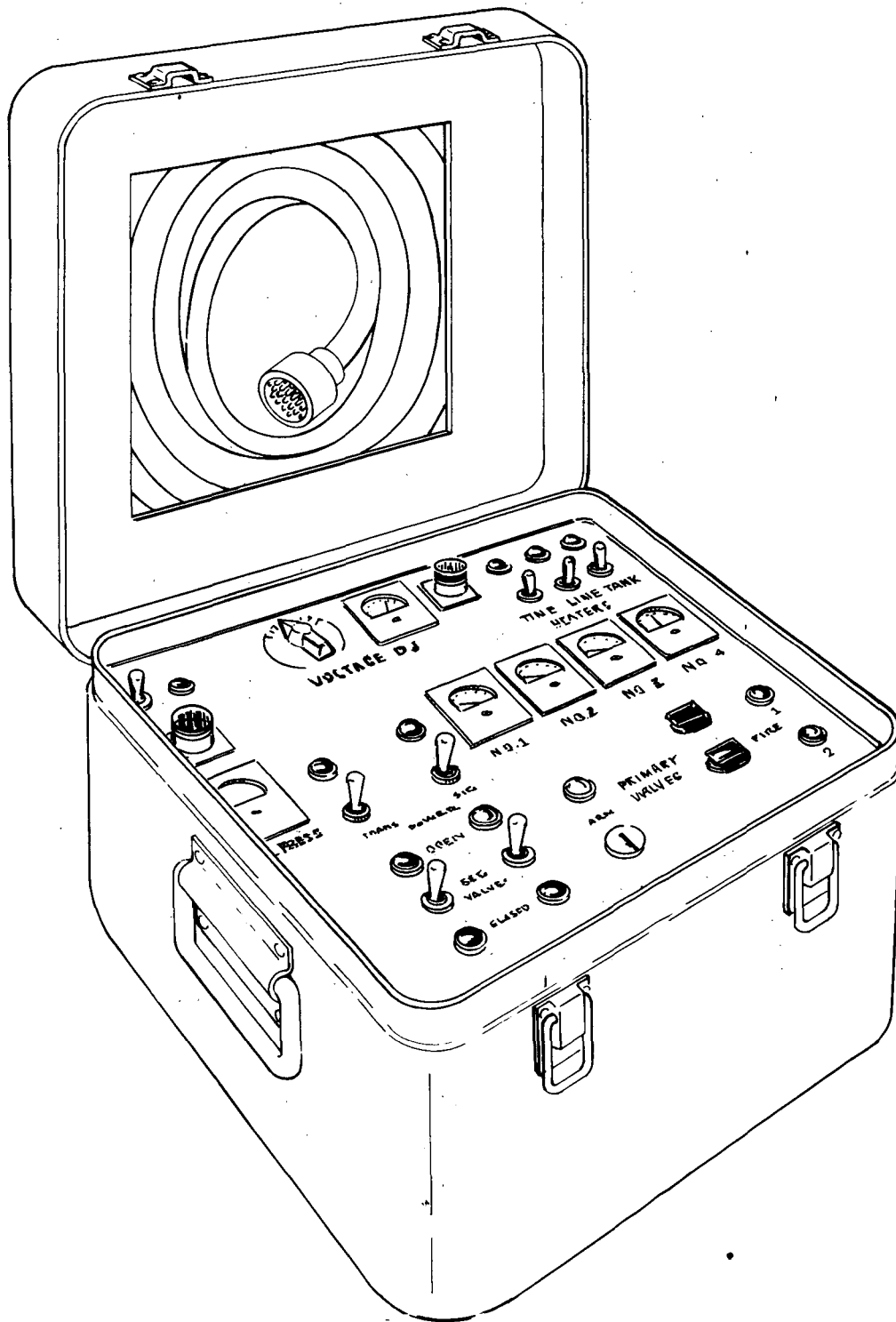


Figure 7-18. ELECTRICAL GSE

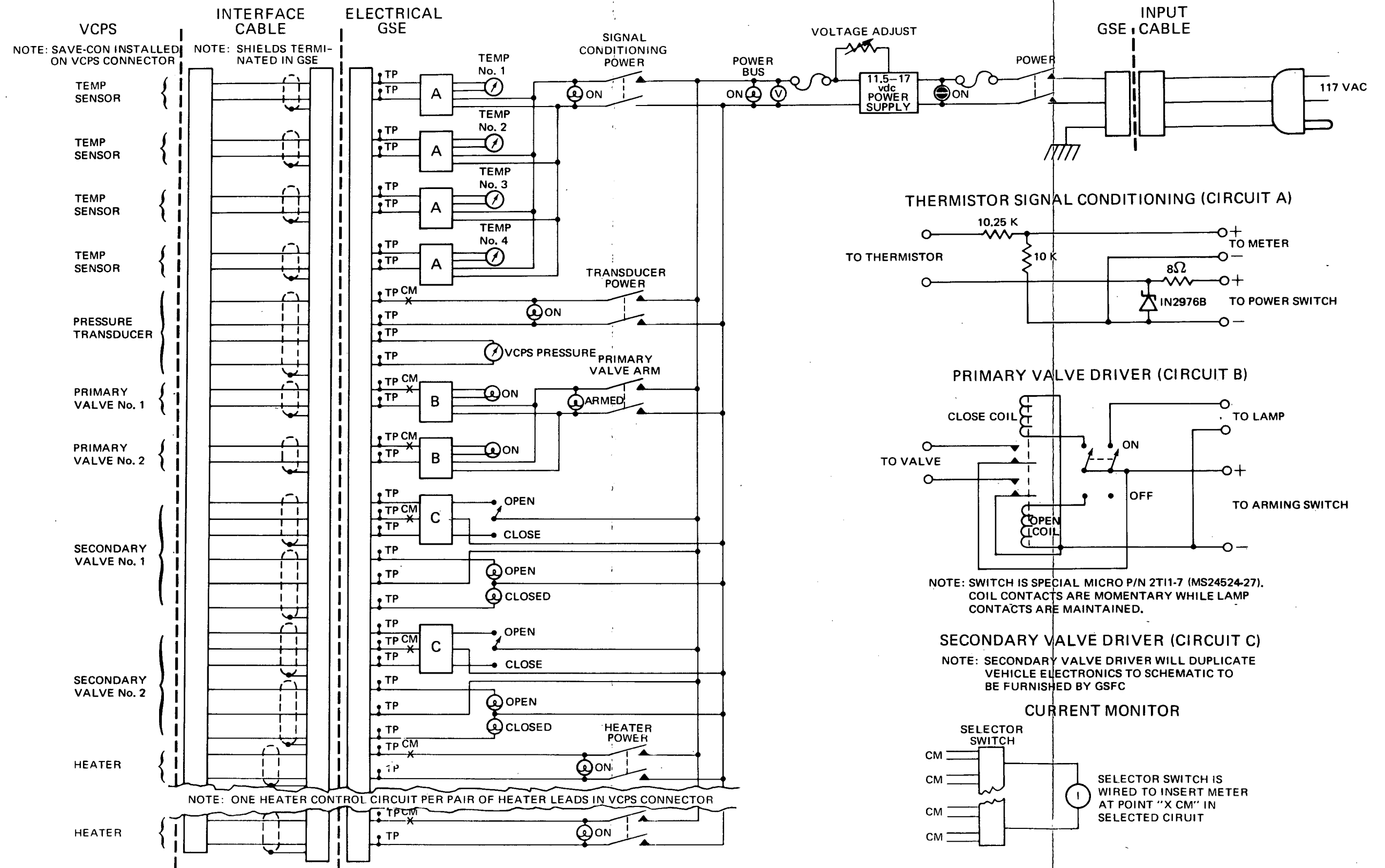


Figure 7-19. ELECTRICAL GSE SCHEMATIC

Power to the VCPS primary control valves will be controlled by latching relays to duplicate the flight vehicle control system. The relays selected will be the same components specified by GSFC for the flight vehicle control system. Control to the VCPS secondary valves will also duplicate the flight vehicle systems.

An ammeter and selector switch will be provided to enable current measurements to be made on the VCPS control valves (primary and secondary), VCPS heaters, and VCPS pressure transducer. The selector switch will be wired in such a manner as to measure the current flowing through the VCPS component only and not that current flowing through such GSE components as indicator lamps or control relays. In addition, test jacks will be provided to enable resistance measurements to be made on all VCPS components with an external ohmmeter.

All components selected for the electrical GSE will be ruggedized and sealed to enable operation of the GSE at the launch site. All components will be shock mounted within the GSE case. All internal wiring will be identified with wire numbers to facilitate circuit tracing should troubleshooting become necessary.

With the removable cover installed and latched, and employing the carrying handles as tie-downs, the GSE "suitcase" will serve as its own shipping container providing for ease of air transportation.

An operating manual will be provided with the electrical GSE (10 copies delivered). The manual will provide detailed operating instructions for all operations to be performed with and/or on the electrical GSE. In addition, for those operations which require that the electrical GSE be used in conjunction with the mechanical GSE, integrated instructions for the operation of both units in the correct sequence will be contained in the mechanical GSE manual (see paragraph 7.2.1). The manual will also include temperature sensor and pressure transducer output calibration data, GSE meter calibration data, GSE schematics and block diagrams, component parts lists with component part numbers, and a list of spare parts provided with the GSE. The manual will also include instructions for securing the GSE for shipment.

A log book will be maintained with the GSE starting at the time of GSE assembly. This log will conform to paragraph 3.10 of NPC 250-1 and will contain a chronology of all inspection, testing, failures, repair, and maintenance of all components and spares of the electrical GSE suitcase. All serialized components will be identified by serial number in all entries. The log book will be kept with the GSE at all times and will be delivered with the GSE.

8.0 SUMMARY AND CONCLUSIONS

8.1 COMPARISON OF SYSTEM SELECTION

The various analyses and comparisons developed in the preceding sections make the choice of the most suitable configuration straightforward. A qualitative summary of the various factors in the form of an advantages-disadvantages chart is presented in Table 8-1. As noted, the features which lead to significant differences between the configurations are in almost all cases those relating to vehicle dynamics.

8.1.1 Gimbaled Engines – Configurations A and E

Hardware concerns are, with one exception, minimal in that all the systems can be assembled from existing, qualified components with little compromise in weight or envelope. The one exception is the gimbal actuator for the two configurations using gimbaled thrusters. This component, while completely feasible and to some extent capable of being developed from existing parts, represents the most complex device required on any of the systems and hence the only hardware development risk.

The gimbaled configurations (A and E), in addition to presenting the only element of hardware development risk, are incapable of providing a velocity correction in any direction while maintaining sunline angles within the allowable ± 6 degree band. Because of the large axial movement of the center of gravity of the probe vehicle as a result of probe release and fuel consumption, gimbal angles of ± 13 to 15 degrees will be required to track the center of gravity. Deviations of the axis from perpendicularity with the sunline of the same amount must be allowed for if complete velocity control directional coverage is to be maintained. A relatively complex command system would also be required to implement this concept. In addition, flex lines or bellows are required in the fuel feed line degrading reliability. Since it is unable to meet one of the basic requirements and presents certain other elements of risk without distinguishing advantageous features, the gimbaled engine configurations, A and E, are not recommended for further consideration.

8.1.2 Tangential Doublets – Configuration C

Configuration C, tangential doublets, while possessing unique redundancy because of the use of each engine for every propulsive mode (velocity, attitude, and spin control), exhibits excessive instability during velocity control maneuvers. This is due to the large axial and/or radial displacement of the thrusters from the center of gravity. The differential forces due to dimensional alignment and engine variational errors acting over these large moment arms produce large torques which result in excessive disturbance of the vehicle attitude and spin rate. The magnitude of this problem is dramatically apparent from the data presented in Tables 2-2 and 2-3. At cruise conditions, a velocity increment of little more than 10 fps (out of a requirement for 354 fps) could be imparted to the spacecraft and still ensure that the allowable attitude drift was not exceeded. Increased spin rate stabilization is only partially effective because of pulse centroid repeatability the

Table 8-1. THRUSTER CONFIGURATIONS – SUMMARY COMPARISON

Configuration	Advantages	Disadvantages
A, Gimbaled	<ul style="list-style-type: none"> • Minimum number of engines (6) 	<ul style="list-style-type: none"> • Solar angles of 13–15° required for complete ΔV coverage (probe)* • High risk associated with actuator development • High command complexity
B, Radial pairs	<ul style="list-style-type: none"> • Minimum weight • Greatest stability during ΔV burns • Most stable after engine failure 	<ul style="list-style-type: none"> • Spin disturbance induced during attitude control • Low in reliability ranking
C, Tangential doublets	<ul style="list-style-type: none"> • Greatest redundancy—highest calculated reliability 	<ul style="list-style-type: none"> • Excessive instability during ΔV burns* • Excessive spin disturbance during ΔV burns* • Spin disturbance induced during attitude control • Highest weight • Maximum peak power • High command complexity • Widest range of engine duty cycles • Unstable in the event of engine failure
D-1, Rectangle—radial	<ul style="list-style-type: none"> • Low weight 	<ul style="list-style-type: none"> • Excessive instability during long ΔV burns (orbiter only)* • Suitability for probe dependent on minimum center of gravity shift • Highly unstable in the event of engine failure
D-2, Rectangle tangential	<ul style="list-style-type: none"> • Single duty cycle for ΔV engines 	<ul style="list-style-type: none"> • Excessive spin disturbance induced during ΔV* • Excessive attitude disturbance during long ΔV burns*
E, Alternate gimbaled	<ul style="list-style-type: none"> • More efficient attitude control than Configuration A 	<ul style="list-style-type: none"> • Solar angles of 13–15° required for complete ΔV coverage (probe)* • High risk associated with actuator development • High command complexity • Spin disturbance induced during attitude control

*Sufficient for concept rejection

effect of which deteriorates as spin rate is increased, partially offsetting the increased vehicle stability. Thruster impulse nonrepeatability acting over the large radial moment arms is also capable of inducing very large spin rate changes to the vehicle during velocity control thrusting. Although there is some flexibility in allowable spin rate, spin rate change during a ΔV maneuver alters the thruster pulse width, total impulse, and hence velocity increment in direct proportion to the change in spin rate due to the fixed firing sector control technique. While it may be possible to compensate for this effect by reducing the actual impulse imparted by review of the spacecraft spin rate data and applying successive vernier corrections, the magnitude of the problem is so gross as to require an unacceptable number of such vernier corrections. This instability is reflected in the system weight. Propellant is included for correcting the induced perturbations, making it the heaviest of the candidates considered. Command complexity and peak power is also highest because of the greater number of engines involved in a velocity control firing. This system also requires the widest range of engine duty cycles because of the very low and variable impulse bit requirements for the lower engines. This is not a problem in engine capability, but rather one of characterization. The MR-50 engine is capable of satisfactory operation at any of the duty cycles that may be called for. Because of the great emphasis on engine repeatability and the open-loop method of control, the engine should be thoroughly characterized in all its anticipated operating domains in order to enable predictable in-flight performance. This would require additional effort during system development. In addition, the engine repeatability errors will vary with duty cycle complicating the analysis and modeling required. The tangential doublets configuration is not recommended for further consideration.

8 1.3 Configuration D – Rectangle

The rectangle configuration suffers to some extent from the same problems as the tangential doublets configuration discussed previously. In the D-1 version, where the radial thrusters are used for ΔV maneuvers, the problems associated with spin axis torques and induced precession are present. In the D-2 version, where the tangential thrusters are used for ΔV maneuvers, spin disturbance problems are added. The tangential thrusters should be located near the plane of the mean center of gravity. Because of the discrete steps in center of gravity location due to retromotor fire or probe release, it is possible to locate the tangential thruster plane so that the center of gravity does not pass through their plane during the midcourse firing. When using the tangential thrusters for ΔV (D-2 configuration), either the lower or upper radial motor (but not both) will be required to cancel the torques induced by the offset of the tangential thruster plane from the instantaneous center of gravity. Because the center of gravity shift is axial, radial displacement of the ΔV engines is not a suitable solution. Of the two modes possible with the D configuration, the use of the radial thrusters for ΔV is clearly superior. Even this version, however, is excessively unstable for the orbiter spacecraft with its lower moment of inertia and particular center of gravity shift characteristics. This is not true for the probe spacecraft, however, because of its greater inherent stability and, in particular, the fact that the center of gravity shift during the critical first midcourse firing is essentially zero and occurs at the forward extremity of the center of gravity envelope. This permits location of the forward thruster very close to this center of gravity location. This requires that the aft engine deliver only a very small amount of the total impulse required and hence, even with its very large moment arm, it cannot induce large spin axis torques. This is a satisfactory

approach provided that should the spacecraft packaging and center of gravity shift characteristics do not change as the design evolves. This configuration could then become substantially less suitable. The rectangle configuration is not recommended for the orbiter spacecraft but could be considered further for use on the probe spacecraft.

8.1.4 Configuration B – Radial Pairs

The radial pairs configuration provides the best compromise and is the only configuration that can be considered for both the orbiter and probe missions. The close coupling of the radial ΔV thrusters with the center of gravity minimizes the contribution of mechanical alignment and thruster repeatability errors to disturbance torques leading to spin axis attitude or rate perturbations. With this configuration, it appears possible to accomplish the long duration first midcourse correction in a reasonable number of burn periods while ensuring that the vehicle attitude will not drift outside the prescribed limits or the spin rate be excessively perturbed. Following a calibration firing to enable programming out repeatable alignment errors, the remaining velocity correction for a maximum midcourse can be added in one additional firing period for the probe spacecraft. For the orbiter, because of its lower inherent stability, two separate firings with attitude/spin rate verification/correction in between would be required after the initial calibration. Corresponding numbers of discrete firing periods for the other configurations are on the order of 18 to 20. The lower sensitivity of the B configuration to error torques is reflected in the propellant weight required, making this the lightest of the candidate configurations. The use of the side-mounted tangential thrusters for attitude control could result in spin disturbance errors during attitude control. The propellant weight allowance for correcting these errors has been included in the total propellant weight allocation. In addition, attitude control maneuvers are typically of shorter duration than ΔV maneuver; hence the total effect of the perturbations is smaller and has less impact on overall system suitability. This, however, represents an area of disadvantage for this configuration. It is because of this propellant weight penalty that the D-1 configuration as used on the probe spacecraft, which does not suffer this penalty, is very close in total propellant and system weight. If the moment arm of configuration B attitude control thrusters must be reduced to reduce the severity of the plume impingement on the backside of the main probe as appears to be the case, the D-1 configuration may actually be lighter than the B configuration.

8.1.5 Selected Configuration

Configuration B, radial pairs, is selected as the only candidate suitable for the orbiter and probe missions. None of the other candidates is suitable for performing the orbiter mission satisfactorily and only one other configuration, D-1, is suitable for the probe mission. Further study should be limited to evaluation of configuration B or derivatives with possible consideration of configuration D-1 as an alternate for probe missions only. It should be noted that configurations B and D-1 use identical thruster modules and differ only in their location on the spacecraft.

Limitations must be placed on the operation of the propulsion system, and meeting of all goals and compliance with all areas of the specification is not possible. These are discussed throughout this report and summarized in the next paragraph.

8.2 LIMITATIONS ON SYSTEM OPERATION

The primary limitations on system operation are those brought about by the cumulative error torques during long velocity control firings. The approach taken has been to limit the size of a single maneuver to a value that provides assurance that the spacecraft attitude will not drift outside the allowable limits. These limits were initially defined as ± 6 precessional drift about the X (thrust) axis as specified and ± 1 -degree precessional drift about the Y (transverse) axis in order to maintain an average thrust direction within 0.5 degree of the initial direction. It was found that configuration B could meet these requirements provided that:

- a. A calibration maneuver could be performed that would enable programming of the engine thrusters so as to remove torques induced by fixed error sources
- b. The remaining velocity would be delivered in as many increments as required to meet the above conditions.

The calibration maneuver was found to be limited to approximately 22.7 m/sec for the probe and 11.1 m/sec for the orbiter. One (probe) to three (orbiter) separate maneuvers would be required to complete a maximum midcourse connection.

Consideration of engine failure during a long duration midcourse correction led to the conclusion that the individual maneuvers may be further reduced in duration and increased in number unless:

- a. Both primary and secondary thruster pairs are used, lessening the impact of a single-engine failure
- b. Spin rate is increased.

The criterion used was that the induced precessional drift about the X axis should not exceed 7 degrees. For the probe configuration, use of both primary and secondary thruster pairs was sufficient to limit the drift to require dividing a maximum midcourse maneuver (354 fps) into only two separate firing periods after the preliminary calibration run. The same result could be achieved with the orbiter only if spin rate was increased to 60 rpm after the calibration firing. This mode of operation was adopted as baseline.

Three other factors which may further limit the flexibility of operation are:

- a. Induced spin perturbations
- b. Total impulse predictability
- c. ΔV directional accuracy.

From the propulsion system standpoint, the primary effect of induced spin rate perturbations is to alter the total impulse delivered via the fixed sector firing control technique. The net effect then is an aggravation of total impulse nonpredictability. An adequate but complex method of circumventing the effects of impulse nonpredictability is to perform a vernier correction after each large maneuver. Use of an accelerometer for signaling engine cutoff can also be considered. Methods of improving impulse reproducibility, such as more precise engine matching through the use of cavitating venturis, should also be used. The cavitating venturi is effective only for relatively long duration (greater than 100 milliseconds) pulses.

From the material presented in paragraph 2.2.5, it is evident that the requirement for providing a directional accuracy of 0.5 degree will impose severe limitations on the system operation. This requirement should be reviewed in the light of attainable accuracies and alternate operating modes.

8.3 FUTURE WORK

With the primary objective of this study, that of identifying the most promising system accomplished, attention should turn to a detailed investigation of the operational modes and limitations of the recommended system. Primary areas of concern as identified by the study are largely those of vehicle dynamics as affected by various error sources, including the engine failure condition. Coupling of spin rate, attitude perturbations, and resolution errors with alignment and engine repeatability errors should be explored in detail. The practicality, method, and effectiveness of performing an in-flight calibration and reprogramming to compensate for fixed errors sources should be established.

9.0 NEW TECHNOLOGY

All key personnel working on this study were alerted to the requirement for identifying and reporting new technology. Because of the very nature of the study, however, namely the required maximum use of existing, qualified components and flight-proven techniques, conventional approaches were sought in order to prove the basic feasibility and minimize development risk. This goal was achieved because a propulsion system based entirely on developed, qualified hardware was defined. Consequently, no items of new technology were developed.

REFERENCES

1. Specification No. S-723-P-10, "Subsystem Specification, Midcourse Correction, Orbital Maneuver, Attitude Control, Spin (MICOMACS) Subsystem, Planetary Explorer Satellite
2. Parker-Hannifin, Document No. RPR5680048, September 28, 1970
3. Dynasciences Corporation, Document No. M1058, September 25, 1970
4. RADC-TR-67-307 (AD821988), July 1967
5. General Electric, Apollo Support Dept., Tech. Memo ASD-R-05-64-1, May 15, 1964
6. Goddard Space Flight Center, "Planetary Explorer Summary Phase A Report and Universal Bus Description," December 1970
7. Smith, W. W.; Nyberg, D. G.; Wilson, W. W.; and Hood, J. F., "Development and Design Aspects of a Five-Pound Thrust RCS Rocket Engine Model," Paper 70-654, AIAA 6th Propulsion Joint Specialist Conference, June 15-19, 1970
8. Bolz, C. W., "Iterative Solution of a Radiation Dominated Heat Balance," *J. Spacecraft and Rockets*, Vol. 8, No. 1, January 1971, pp. 79-80
9. Bolz, C. W., "REM-Mono Thermal Analysis Report," RRC 68-R-148R1, April 10, 1970, Rocket Research Corporation, Redmond, Washington
10. Sparrow, E. M. and Cess, R. D., "Radiation Heat Transfer," Brooks/Cole, Belmont, California, pp. 164 ff
11. Ishimoto, T. and Bevans, J. T., "Temperature Variance in Spacecraft Thermal Analysis," *J. Spacecraft and Rockets*, Vol. 5, No. 11, November 1968, pp 1372-1376
12. Etheridge, F. G. and Boudreaux, R. A., "Attitude Control Rocket Exhaust Plume Effects," AIAA Paper No. 69-574
13. Martinkovic, P. J., "Bipropellant Attitude-Control Rocket (ACR) Plume Contamination Investigation," AFRPL-TR-69-251
14. Martinkovic, P. J., "Monopropellant Exhaust Contamination Investigation," AFRPL-TR-69-72

15. Hill, Jacques, A. F. and Draper, James S., "Analytical Approximation for the Flow from a Nozzle into a Vacuum, *J. Spacecraft and Rockets*, Vol. 3, No. 10, October 1966, pp 1552 ff
16. Piesik, E. T.; Koppang, R. R.; and Simkin, D. J., "Rocket Exhaust Impingement on a Flat Plate at High Vacuum, *J. Spacecraft and Rockets*, Vol. 3, No. 11, November 1966, pp 1650 ff
17. Maddox, A. R., Impingement of Underexpanded Plumes on Adjacent Surfaces, *J. Spacecraft and Rockets*, Vol. 5, No. 6, June 1968, pp 718 ff

A-2

APPENDIX A
CONCEPT SURVEY

1.0 INTRODUCTION

A preliminary screening of thruster arrangements for the spin stabilized Planetary Explorer Spacecraft is necessary in order to provide a workable scope and permit a more detailed evaluation of the most promising candidate approaches. The results of this screening are summarized below.

Requirements for three basic propulsion functions exist:

- a. Velocity control
- b. Attitude control
- c. Spin control

Midcourse correction, orbital maneuvers, and retargeting for probe release all involve alternation of the spacecraft velocity vector and are classified as velocity control. Capability for dumping unused midcourse propellant for orbital missions must also be considered. It is a ground rule of the study that an alternate or backup mode be available for accomplishing the various propulsive functions. Control commands are to be issued from ground stations on the basis of telemetered data regarding spacecraft velocity, attitude, and rates.

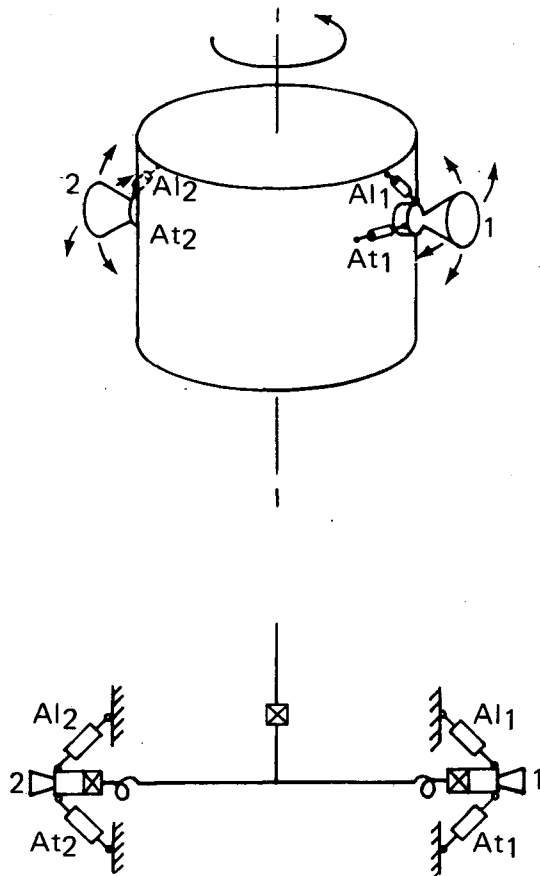
2.0 CANDIDATE APPROACHES

Review of the propulsive functions indicates that the velocity control requirement for a spinning spacecraft which undergoes fairly large center of gravity excursions is the most demanding. Attitude and spin control are accomplished by application of control torques in a plane parallel or normal to the spin axis as required. The basic concept will require velocity (and attitude) control thrusters pulsed in synchronism with spacecraft spin and some mechanism for aligning the net thrust vector with the spacecraft center of gravity and the direction of the required impulse.

A gross survey of thrust vector center of gravity alignment techniques is listed in Table A-1. Figures A-1 through A-6 further illustrate the various approaches defined. A tabulation of the engines used for each propulsive function in both primary and degraded modes along with a list of advantages and disadvantages is also provided. A simplified schematic is also shown. The propellant feed portion of the schematic is omitted, since it is assumed somewhat independent of the thruster configuration and arrangement.

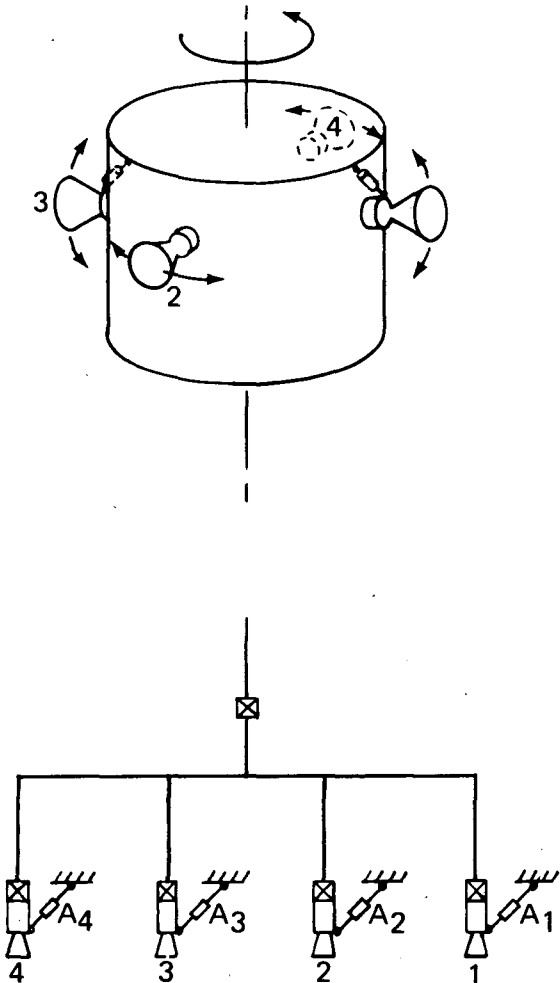
2.1 MOVABLE ENGINES

In the movable engine category, the gimballed engine provides an interesting approach. By use of fully gimballed engines 180 degrees apart in a plane normal to the spin axis, all propulsive functions can be accomplished with a system using only two thrusters (see Figure A-1). Degraded mode redundancy (noncouples) is provided for attitude and spin control. Engine position actuators are, of course, required.



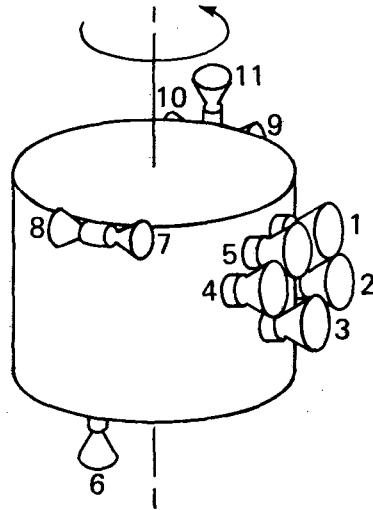
<u>Function</u>	<u>Primary</u>	<u>Secondary</u>
Velocity	1, Al ₁ , At ₁	2, Al ₂ , At ₂
Attitude	1, 2, Al ₁ , Al ₂	1, Al ₁ or 2, Al ₂
Spin	1, 2, At ₁ , At ₂	1, At ₁ or 2, At ₂
Advantages:	All propulsion functions accomplished with degraded mode (nonpure couples) backup with two-engine system Small, out of plane ΔV can be provided without reorienting spacecraft	
Disadvantages:	Actuator critical to system operation Complicates feed system (flex lines) Inefficient in attitude and spin functions unless large gimbal angles used	

Figure A-1. CONCEPT NO. 1 – GIMBALED ENGINES



<u>Function</u>	<u>Primary</u>	<u>Secondary</u>
Velocity	1, A1 + spin or 2, A2 + A++	3, A3 + spin
Attitude	1, 3, A1, A3	1, A1 or 3, A3-
Spin	2, 4, A2, A4	2, A2 or 4, A4
Advantages:	Four engine systems Out of plane ΔV could be provided without spacecraft reorientation	
Disadvantages:	Actuators critical to system operation Complicates feed system (flex lines) Inefficient in attitude and spin functions unless large swivel angles used	

Figure A-2. CONCEPT NO. 2 – SWIVELED ENGINES



<u>Function</u>	<u>Primary</u>	<u>Secondary</u>
Velocity	1, 2, 3, 4, 5	Any 4 of 1-5
Attitude	6, 11	6 or 11
Spin	8, 9	8 or 9
	7, 10	7 or 10

Advantages: Velocity control engine out capability
Small disturbance torques

Disadvantages: Large number of engines
Cannot group engines into similar modules
Engines not deployed—for functional redundancy
High peak power

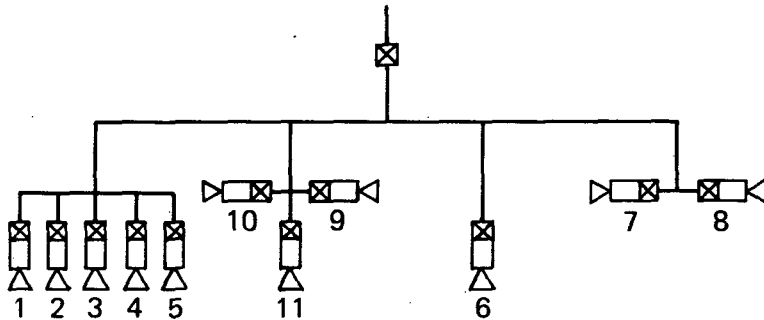
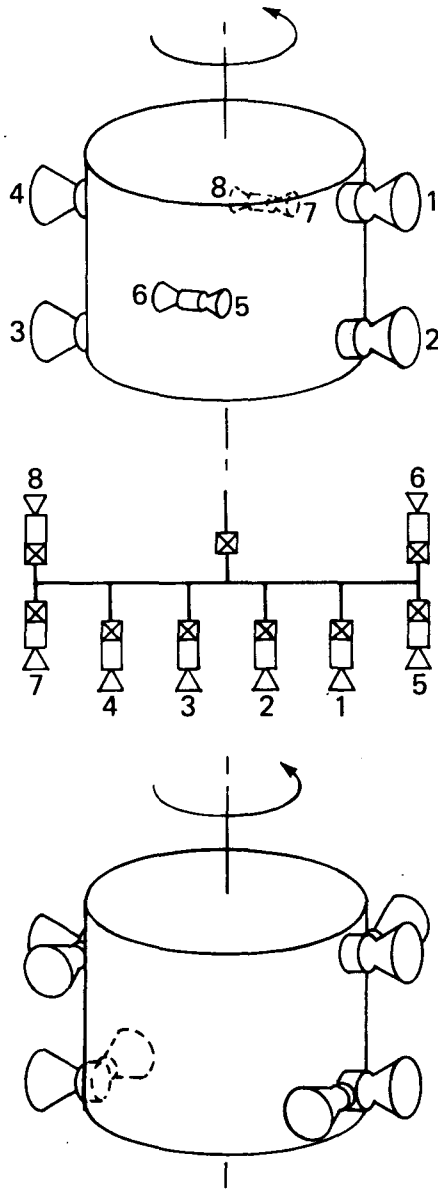
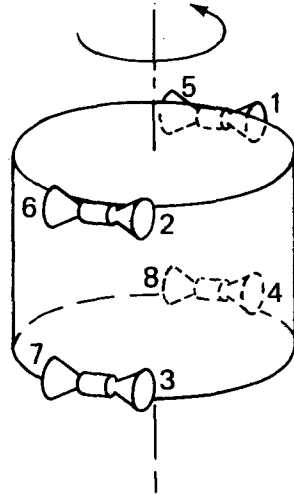


Figure A-3. CONCEPT NO. 3 – 5-ENGINE CONCEPT



<u>Function</u>	<u>Primary</u>	<u>Secondary</u>	<u>Other</u>
Velocity	1, 2	3, 4	1, 3 or 2, 4 or 1, 5, 7, etc.
Attitude	1, 3	2, 4	1 or 2, or 3 or 4
Spin	6, 7 5, 8	6 or 7 5 or 8	
Advantages:	Lower peak power 3 engines less than Config 1 Provides redundant couples for attitude control		
Disadvantages:	Possible impingement of roll exhaust on solar cells		
ALTERNATE:	Concept No. 4A		
Advantages:	Engines grouped into identical modules		
Disadvantages:	(Compared to above)		
	Canted spin nozzles increase spin propellant		
	Degraded spin mode (1 engine) may induce more precession than above		

Figure A-4. CONCEPT NO. 4 - LINEAR ARRAY



<u>Function</u>	<u>Primary</u>	<u>Secondary</u>	<u>Other</u>
Velocity	1,2,7,8	3,4,5,6	
Attitude	1-2,7-8	5-6,3-4	1, 8; 4, 5; 2, 7; 3, 6
Spin	1, 6 2, 5	4 3	6 5
Advantages:	Full redundancy for all functions Engines modularized		
Disadvantages:	High peak power		

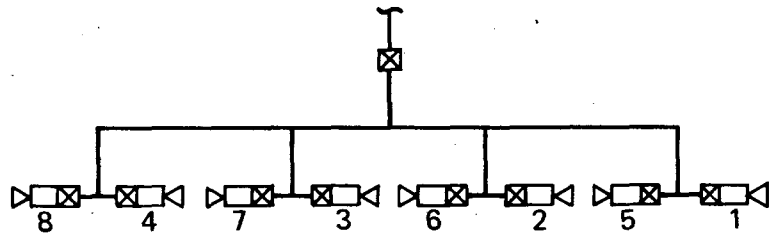
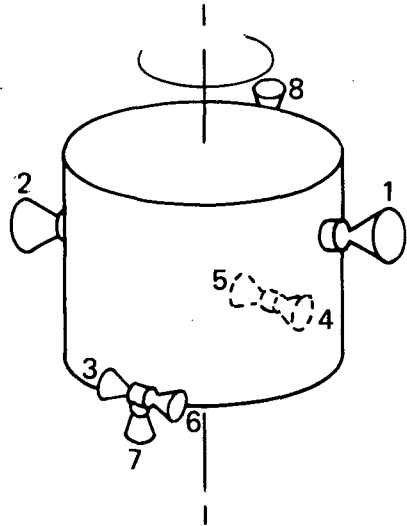


Figure A-5. CONCEPT NO. 5 – TANGENTIAL DOUBLETS

**CONCEPT NO. 6
AREA ARRAY UTILIZING SPIN THRUSTERS**



<u>Function</u>	<u>Primary</u>	<u>Secondary</u>
Velocity	1, 4, 6	2, 3, 5
Attitude	7, 8	7 or 8
Spin	3, 4	3 or 4
	5, 6	5 or 6

Advantages: Less engines than Config 1 (8 vs 11)

Disadvantages: Cannot modularize engines (have single radial & axial, tangential and triad)

Concept No. 6A

Alternate: Delete 7 & 8

Velocity	1, 4, 6	2, 3, 5
Attitude	1, 3, 5	2, 4, 6 or 1 or 2, or 4, 6 or 3, 5
Spin	3, 4	3 or 4
	5, 6	5 or 6

Advantage: Fewer engines (6)

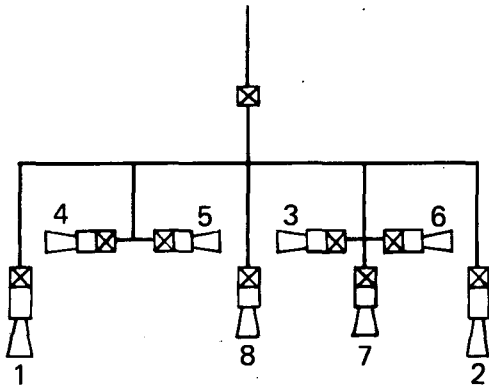


Figure A-6. CONCEPT NO. 6 – AREA ARRAY UTILIZING SPIN THRUSTERS

Table A-1
THRUST VECTOR/CENTER OF GRAVITY ALIGNMENT
FOR VELOCITY CONTROL

Movable Engine(s)	Engine Array
Gimbal	Area array
Swivel	Linear array & ACS
Translate	
	Center of Gravity Control
Jet Deflection	Gimbaled mass
Gimbal nozzle	Propellant positioning
Swivel nozzle	
Jet vanes	
Nozzle injection	
Nozzle deformation	

Various arrangements of swiveled (one-plane) engines are possible. Swiveling simplifies the engine pivot and propellant line problems; these, however, are of more concern for larger bipropellant engines. Only one actuator per engine is required, since movement is restricted to a single plane. In order to meet the guideline of pure precessional and roll control torques in the primary mode and to allow for degraded mode redundancy, a system of four engines spaced 90 degrees apart near the spacecraft equator could be considered (Figure A-2). This approach requires four engines and, like the fully gimbaled concept, four actuators.

2.2 JET DEFLECTION

Jet deflection is ruled out as a practical approach for engines of the size required.

2.3 ENGINE ARRAY

Various arrangements of fixed engines, when used with appropriate pulse widths and duty cycles, can be used to provide a net effective thrust vector in the envelope of the engine mounting area. The configurations vary regarding how redundancy is incorporated and how the velocity control functions are integrated with the engines used for attitude and spin control.

At one end of the spectrum is the GSFC five-engine concept. The number of engines is somewhat arbitrary, however, in that any number in excess of three may be used to bound an area which when projected intercepts the center of gravity. Five or more engines can be used to provide some form of redundancy or engine-out capability (Figure A-3). A distinguishing feature of this approach is that the primary attitude and spin control functions are not accomplished with the thrusters used for velocity control. This is not to say, however, that the attitude and spin perturbations induced by the velocity control engine(s) firing will not or cannot be taken out by proper programming of the engine firing schedule and individual engine duty cycles. This basic concept may be referred to as an "area array."

An alternate concept has been termed the "linear array." This approach recognizes the fact that spacecraft center of gravity excursions are largely axial and hence the velocity control engines can be located longitudinally along the spacecraft. The simple application of this approach employs thrusters at the upper and lower extremities of center of gravity travel. Additional provisions have to be made for attitude and spin control.

It is apparent that, by an increase in the separation between the engines, the capability for torquing the spin axis and hence for providing attitude control is developed. This eliminates the need for separate attitude control thrusters as shown in Figure A-4. Separate spin control thrusters are still, however, required.

Further modularization of the thruster packages can be accomplished by incorporation of one roll-control engine with each radial engine. This approach simplifies installation and plumbing and has the advantage of using four identical two-engine modules. The roll thrusters can also provide additional backup for attitude and, conceivably, velocity control. This concept is also shown in Figure A-4.

Another approach to combining the thrusters is to use opposed pairs of tangentially mounted "bow tie" modules at the upper and lower extremities of the spacecraft. In this way velocity control is provided by an area array of four thrusters firing in one direction. The four thrusters pointing in the opposite direction provide a backup.

Full, nondegraded redundancy exists for both the attitude and spin control engines with additional degraded modes also available. This concept, referred to as "tangential doublets," is illustrated in Figure A-5.

A combination of the above approaches consists of a single radial thruster in conjunction with two "bow tie" modules, straddling the spacecraft center of gravity. Precessional torques for attitude orientation can be provided by the engines on opposite sides of the spacecraft or by separate precessional thrusters (see Figure A-6).

2.4 CENTER-OF-GRAVITY CONTROL

Although propellant tank configuration and location to minimize center-of-gravity excursion as fuel is being consumed should be considered, use of center-of-gravity control as a primary alignment technique does not appear promising for this application.

2.5 ALTERNATE ATTITUDE/SPIN CONTROL ARRANGEMENT

A guideline used in the preceding survey was that the attitude- and spin-control functions be accomplished with pure torque couples in the primary mode. In the degraded or malfunction mode it was considered satisfactory to use noncouples for these functions. It was determined subsequently from consideration of induced perturbations that pure couples would be required for both primary and degraded mode attitude control and that noncouples could be tolerated for spin control in either mode. This makes possible an asymmetrical attitude/spin control thruster grouping

of four thrusters arranged in two tangential "bow tie" modules at the upper and lower extremities of the spacecraft and the same circumferential position. This arrangement can be combined with any of the velocity control configurations, most logically those that do not have inherent attitude- and/or spin-control capability in themselves, such as the "linear array," the five-engine concept, and the axial plane swiveled engine:

APPENDIX B
FAILURE MODES ANALYSIS

1.0 FAILURE MODE/EFFECTS ANALYSIS

A preliminary FMEA has been conducted at the component/piece part level. The results of this analysis are presented in Appendix B.

Criticality has been estimated by the following criteria:

- I *Critical* – Catastrophic to mission equipment, mission abort, or severe degradation to mission performance, or death or severe injury to personnel
- II *Major* – Loss of 50% of mission function, performance, or availability or time-loss injury to personnel
- III *Minor* – Essential mission functions performable but with decreased capability or availability; “no time-loss” injury to personnel

Although probabilities of failure modes have not been assigned, a review of the reliability analysis indicates that fair allocation of component failure rates to the modes would show that I or II ratings would have a very low probability of occurrence.

FAILURE MODE, EFFECTS, AND CRITICALITY ANALYSIS

INDEX NO. 1

COMPONENT/PART NAME Propellant Tank Assembly

PART NUMBER

FUNCTION: Contains Propellant and Pressurant

FAILURE MODE	POSSIBLE CAUSES	EFFECTS ON THE SYSTEM	PREVENTIVE DESIGN FEATURES AND CONTROL MEASURES	CRITICALITY	PROBABILITY
(1) Rupture	(a) Flaw in forging (b) Stresses due to launch environment (c) Inadequate process control during fabrication	(1) Propellant depletion and loss of thrust	(a) Forgings processed per procurement control specification. All fabrication processes controlled per vendor specifications. All tanks proof tested as part of acceptance. (b) Tank designed for adequate safety factor at operating pressure and temperature. (c) Tank subjected to qualification testing for slosh, vibration, and acceleration environments. Tanks burst as part of qualification to verify design adequacy.	I	
(2) Weld Joint Leakage or Failure	(a) Inadequate or defective weld (b) Stresses due to launch environment (c) Inadequate process control during fabrication	(2) Pressurant depletion and thrust below specified limits	(a) Welding process stringently controlled by vendor specifications. (b) All weld joints X-rayed and dye penetrant inspected. (c) All tanks subjected to proof and leakage tests as part of acceptance.	I	

FAILURE MODE, EFFECTS, AND CRITICALITY ANALYSIS

INDEX NO. 3

COMPONENT/PART Lines and Fittings

FUNCTION: Supply Propellant to Thrusters and Pressurant to Propellant Tank

FAILURE MODE	POSSIBLE CAUSES	EFFECTS ON THE SYSTEM	PREVENTIVE DESIGN FEATURES AND CONTROL MEASURES	CRITICALITY	PROBABILITY
<p>(1) Propellant or Pressurization Line Rupture</p> <p>(2) Leakage</p>	<p>(a) Flaw in material</p> <p>(b) Stresses due to launch environment</p> <p>(a) Inadequate or faulty braze joint or flaws in material</p>	<p>(1) Propellant depletion and loss of thrust</p> <p>(2) Propellant and/or pressurant leakage and thrust limits out of specification</p>	<p>(a) Materials controlled by procurement specification. Structural integrity verified during system prequalification and qualification tests.</p> <p>Tubing designed for 6,000 psia minimum burst pressure. All lines leak checked with nitrogen as part of acceptance test.</p> <p>(b) Same as (a)</p> <p>(a) All brazing operations controlled by specification detailing brazing procedures, process controls, and post braze joint inspection requirements.</p> <p>All braze joints proof and leak checked. Same as (a) above</p>	<p>I</p> <p>I to III</p>	

FAILURE MODE, EFFECTS, AND CRITICALITY ANALYSIS

INDEX NO. 4

COMPONENT/PART Propellant Filter

NAME

PART NUMBER

FUNCTION: Propellant filtration downstream of tanks

FAILURE MODE	POSSIBLE CAUSES	EFFECTS ON THE SYSTEM	PREVENTIVE DESIGN FEATURES AND CONTROL MEASURES	CRITICALITY	PROBABILITY
(1) Rupture of Filter Housing	(a) Flaw in material	(1) Propellant depletion and loss of thrust	(a) Filter subjected to proof and leak tests as part of acceptance and to qualification level environment as part of system qualification.	I	
	(b) Stresses due to launch environment		(b) Same as (a)		
(2) Weld Leakage or Failure	(a) Inadequate or defective weld	(2) Propellant depletion and loss of thrust	(a) All filters proof and leak tested as part of acceptance. Weld joint X-ray and dye penetrant inspected.	I to III	
(3) Increase in Pressure Drop Across Filter	(a) Upstream system contamination	(3) Slow propellant feed to thrusters	(a) All system parts cleaned per contamination control specification, RRC-PS-0025, Level 250. Propellant and pressurant loading should be conducted with 10-micron filters	III	
(4) Filter Element damaged or collapses; contamination particles pass through	(a) Deterioration due to launch environment or installed in damaged condition	(4) Contamination of downstream system	(a) Control measures per 3 (a) and 2 (a) above.	II	
	(b) Inadequate design to withstand surge flow upon valve actuations		(b) Special tests must be conducted with filter during valve tests to verify design adequacy, especially if upstream explosive-actuated valves are to be used.		

B-5

FAILURE MODE, EFFECTS, AND CRITICALITY ANALYSIS

INDEX NO. 5

COMPONENT/PART Pressure Transducer

FUNCTION: Inflight Telemetry Readout of Propellant Tank Pressure

NAME

PART NUMBER

FAILURE MODE	POSSIBLE CAUSES	EFFECTS ON THE SYSTEM	PREVENTIVE DESIGN FEATURES AND CONTROL MEASURES	CRITI-CALITY	PROB-ABILITY
(1) Rupture of Case	(a) Flaw in material and/or stress due to launch environment.	(1) Propellant or pressurant depletion and loss of thrust.	(a) Proof and leak tests conducted as part of acceptance test. Case designed for 5,000 psia pressure. Transducer previously qualified to substantially more severe launch environments for other programs.	I	
(2) Fails to provide signal or inadequate signal	(a) Electrical component breakdown or drift (b) Sensitive to EMI	(2) Impairs system performance analysis.	(a) All electrical components subjected to screening and burn-in tests. (b) EMI adequacy verified during EMI test program.	III	
(3) Internal leakage	(a) Diaphragm failure	(3) Loss of output. Impairs system performance analysis.	(a) Functional tests conducted as part of acceptance to verify diaphragm adequacy. Same as note above	III*	
(4) Generates EMI	(a) Improper shielding or circuit design	(4) Interference with surrounding electrical components.	(a) EMI protection verified during EMI test program *NOTE: The P _t is considered redundant with certain system operational parameters that may be used as backup to the P _t .	III	

B-6

FAILURE MODE, EFFECTS, AND CRITICALITY ANALYSIS

INDEX NO. 6

COMPONENT/PART Latching Valve

NAME

PART NUMBER

FUNCTION: Close/open propellant flow to TCV/thruster assemblies

FAILURE MODE	POSSIBLE CAUSES	EFFECTS ON THE SYSTEM	PREVENTIVE DESIGN FEATURES AND CONTROL MEASURES	CRITICALITY	PROBABILITY
<p>(1) Failure to open or failing partly open</p>	<p>(a) Short or open in coil or connector</p> <p>(b) Contamination between moving and mating parts</p> <p>(c) Misadjustment and eccentricity of moving and mating parts</p> <p>(d) Failure of Belleville latching spring</p>	<p>(1) Upstream latching valves in parallel redundancy--probability of not opening at least one is negligible.</p> <p>Failure to open one of downstream latching valves would shut off half of propulsion subsystem.</p> <p>*Propulsion subsystem is redundant. Valve failure can be critical only if the other side has already failed.</p>	<p>(a) Electrical continuity and resistance checks, 100% screening and burn-in tests and pull-in/drop-out voltage tests are in the acceptance tests at vendor and RRC.</p> <p>(b) Stringent clean controls imposed at all fabrication and handling steps. GN₂ purging and vacuum drying procedures to minimize probability of foreign particles remaining with the valve apply at both vendor and RRC. All valves are pressure-drop tested and particle counts are made at vendor. Filter provided upstream of the valves.</p> <p>(c) All mechanical elements of the valve are designed and built to maximum operating stresses and requirements. The springs and poppets used on valves have never failed in RRC experience. Valves are vibration tested on REA to required levels. All valves subjected to rigid acceptance tests.</p> <p>(d) Same as (c)</p>	<p>I to III*</p>	

B-7

FAILURE MODE, EFFECTS, AND CRITICALITY ANALYSIS

INDEX NO. 6

COMPONENT/PART Latching Valve (Continued)
NAME

PART NUMBER

FUNCTION: Close/open propellant flow to TCV/thruster assemblies

FAILURE MODE	POSSIBLE CAUSES	EFFECTS ON THE SYSTEM	PREVENTIVE DESIGN FEATURES AND CONTROL MEASURES	CRITI- CALITY	PROB- ABILITY
(2) Failure to close completely (leakage)	(a) Contamination between valve poppet and seat, or damage to those parts. (b) Misalignment and eccentricity of poppet and seat (c) Failure of Belleville latching spring	(2) Leakage past latching valve would be a problem only if a TCV had a major closure failure. Both failures would deplete the propellant and possibly cause uncontrollable parasitic propulsion functions.	(a) Same as 1-(b) (b) Same as 1-(c) (c) Same as 1-(c)	I to III*	
(3) Failure to close from open position	(a) Short or open in coil or connector circuit (b) Failure of Belleville latching spring	(3) Same as 2	(a) Same as 1-(a) (b) Same as 1-(c)	I to III*	
(4) Failure of microswitch	(a) Short or open in switch or connector circuits	(4) Loss of information to ground control re valve position	(a) Switch qualified for mission requirements. Screening inspection and electrical requirements are included in part and valve acceptance tests at vendors and RRC.	III	
(5) Rupture and external leakage	(a) Same as for TCV or fill valves	(5) Same as for TCV or fill valves *Propulsion subsystem is redundant. Valve failure can be critical only if multiple closure failures occur.	(a) Same as for TCV or fill valves	I	

B-8

Failure Mode, Effects, and Criticality Analysis

INDEX NO. 7

COMPONENT/PART NAME Torque Motor Hard Seat Propellant Valve (TCV)
(Series Redundant Configuration)

PART NUMBER

FUNCTION: Controls flow of propellant into thruster

FAILURE MODE	POSSIBLE CAUSES	EFFECTS ON THE SYSTEM	PREVENTIVE DESIGN FEATURES AND CONTROL MEASURES	CRITICALITY	PROBABILITY
(1) Failure to close or internal leakage	<p>(a) Structural failure of the armature, flexure tube, flapper, poppets or seats, or combination of the above, due to material defects, weld failures, or environmental stresses.</p> <p>(b) Misalignment or damage to the poppet and seat due to improper installation, high temperatures, contamination, severe vibration, or wear.</p> <p>(c) Spring force of flexure tube/flapper assembly changed as a result of fatigue or high temperature exposure.</p> <p>(d) Chips, burrs, and other contamination causing binding or any moving part of holding the poppet off the teflon seat.</p>	<p>(1) Poppet will not seat which will cause continuous propellant flow past the seat</p> <p>*NOTE: Minor on a system basis with redundancy in all functions. **NOTE: Full redundancy is available in thruster capability in ΔV, AC, and Spin. Latching valve may be used for closing off failed branch.</p>	<p>(a) Each propellant valve assembly contains a series redundant torque motor assembly, and poppet-seat assembly. About 85 percent of all valve failures are due to inability to close on demand (internal leakage). This redundant feature will help eliminate these failure modes.**</p> <p>(b) Screening, electrical continuity, proof pressure, internal leak, calibration, and burn-in tests are part of the acceptance tests conducted. The valves tested to substantially higher vibrational requirements as part of the qualification program.</p> <p>Welding processes are stringently controlled per vendor specifications. Mechanical elements of the valve are designed with adequate strength safety factors.</p> <p>(c) Same as (b).</p> <p>(d) Stringent cleanliness controls have been imposed on the manufacturer in handling and fabrication processes to minimize the probability of foreign material remaining within the valve. Valve contains integral inlet filter. Filter in line upstream of valve.</p>	II* to III	

B-9

FAILURE MODE, EFFECTS, AND CRITICALITY ANALYSIS

INDEX NO. 7

COMPONENT/PART Torque Motor Hard Seat Propellant Valve (TCV)
(Series Redundant Configuration) (Continued)

NAME

PART NUMBER

FUNCTION: Controls flow of propellant into the thruster

FAILURE MODE	POSSIBLE CAUSES	EFFECTS ON THE SYSTEM	PREVENTIVE DESIGN FEATURES AND CONTROL MEASURES	CRITI-CALITY	PROB-ABILITY
(2) Failure to open or partially opens	(a) Electrical failure due to shorted or open connections or coils (b) Poppets bound in retainers due to excessive contaminants or galling as a result of alignment or exposure to a vacuum. Foreign material wedged between the solenoid assembly and the armature causing restricted movement. Poor spring characteristics could impede the flapper movement.	(2) Insufficient flow from the valve assembly to provide required thrust levels. Two opportunities exist for each failure cause due to the series redundant actuating mechanism configuration. Only 11 percent of all valve failures are expected to occur in this failure mode. The result is the loss of one thruster.	(a) Materials are selected to be compatible with propellant and environments. Electrical continuity checks, screening, and burn-in tests are a portion of the acceptance tests to be performed.** (b) Same as 1 (d)	1*	
(3) Rupture or excessive external leakage	(a) Defective weld, porous material or otherwise defective, or environmental stresses or hard starts.	(3) Loss of all propellant and thus loss of all thrusters. * See previous note ** See previous note.	(a) Welding tolerances and techniques that have proven successful on other programs have been specified. Proof pressure acceptance tests are required. Material processes and controls have been implemented.	1*	

B-10

FAILURE MODE, EFFECTS, AND CRITICALITY ANALYSIS

INDEX NO. 7

COMPONENT/PART NAME Torque Motor Hard Seat Propellant Valve (TCV)
 (Series Redundant Configuration) (Continued)

PART NUMBER _____

FUNCTION: Controls flow of propellant into the thruster

FAILURE MODE	POSSIBLE CAUSES	EFFECTS ON THE SYSTEM	PREVENTIVE DESIGN FEATURES AND CONTROL MEASURES	CRITICALITY	PROBABILITY
(4) Premature opening	(a) Electromagnetic interference	(4) Loss of spacecraft control and premature propellant depletion.	(a) Valve case has been grounded to the spacecraft. Shielded leads are being used. Note: Redundancy available in all functions**.	I*	
(5) Premature closing	(a) Open or shorted circuit, or poor electrical connections, due to vibration, moisture, manufacturing, or handling problems	(5) Loss of one thruster.	(a) Preflight electrical checks. Same as 4 (a). The valve tested to substantially higher vibrational requirements than required as part of the qualification program.	I*	
(6) Large pressure drop	(a) Contamination in the flow passage	(6) A high change in pressure at the outlet could result in out-of-specification thrust levels and response.	(a) All valves are pressure drop acceptance tested and particle counts are made at the vendor prior to shipping. Flow calibration tests are made prior to assembly into the final units. Same as 1 (d).	II*	
(7) Slow closing response	(a) Decreased poppet spring and/or flexure/flapper spring rates as a result of fatigue or high thermal exposure. (b) Contamination causing added friction between moving mechanical elements	(7) Excessive flow through the valve after the electrical closing command is given. The result would be undesirable thrusts, probably requiring corrective maneuvers. *See previous note **See previous note.	(a) The series redundant internal components will help preclude this mode of failure. Note: Redundancy available in all functions. ** (b) Valve acceptance tests include particle counts and flush tests to reduce acceptance of a contaminated valve. Same as 1 (d).	II*	

B-11

FAILURE MODE, EFFECTS, AND CRITICALITY ANALYSIS

INDEX NO. 8

COMPONENT/PART Thrust Chamber Assembly (Continued)

FUNCTION: Provide thrust

FAILURE MODE	POSSIBLE CAUSES	EFFECTS ON THE SYSTEM	PREVENTIVE DESIGN FEATURES AND CONTROL MEASURES	CRITI CALITY	PROB ABILITY
<p>(4) Reduced catalyst activity or poisoning of catalyst</p>	<p>(a) Catalyst unprotected during storage life.</p> <p>(b) Sulpher poisoning or high ammonia concentration in catalyst bed.</p> <p>(c) Grain growth and iridium evaporation loss</p>	<p>(4) Excessive ignition delay times and possible erratic thruster operation.</p>	<p>(a) Cover maintained over thrusters during storage. Catalyst stored in a clean glass or polyethylene container, not handled with bare hands. The propellant is controlled for impurities by RRC-M&P-0015, Rev. B. Catalyst housing cleaned per RRC-M&P-0005 and materials selected for vaporization characteristics. Acceptable carriers are delineated in RRC MS 0110.*</p> <p>(b) Purged with hot GN₂ after any testing. During operation in a vacuum environment the vacuum will remove residual hydrazine decomposition products from the catalyst bed.</p> <p>(c) Propellant dissolved salt content is controlled by RRC-M&P-0015. The catalyst beds are purged with hot gaseous nitrogen after testing of all flight hardware. I_r evaporation is a very slow process and not an important degradation mechanism except on long-term space missions with a hot insulated thrust chamber.</p> <p>*See previous note.</p>	<p>I to II*</p>	

Failure Mode, Effects, and Criticality Analysis

INDEX NO. 8

COMPONENT/PART NAME Thrust Chamber Assembly (Continued)

PART NUMBER

FUNCTION: Provide thrust

FAILURE MODE	POSSIBLE CAUSES	EFFECTS ON THE SYSTEM	PREVENTIVE DESIGN FEATURES AND CONTROL MEASURES	CRITICALITY	PROBABILITY
(5) Increased catalyst bed pressure drop	(a) Compacting of catalyst bed (b) Breakup of catalyst during vibration (c) Loading too fine catalyst mesh size (d) Breakup or plugging of catalyst from chlorine salts in propellant.	(5) Reduced thrust and possible erratic reactor operation	(a) Reactor bed loading is low to minimize or eliminate compacting during firing. Development tests conducted to verify catalyst bed configuration.* (b) Qualification tests to verify vibration environment compatibility. Other RRC reactors have been successfully subjected to much higher vibration environments (40 g's rms) with no catalyst breakup. (c) Catalyst size controlled by screening prior to loading. (d) Propellant specification controls dissolved salts.	II to III*	
(6) Catalyst loss from chamber	(a) Damaged bed plate screen or structural failure of bed plate, or dislocation of bed plate during launch environment, or improperly packed chamber.	(6) Erratic thruster operation and loss of thrust	(a) Bed plate screen designed for high temperature environment. Same material used in all other RRC thruster designs. Bed plate designed for adequate safety margins at temperature. Qualification testing to verify adequacy of bed plate. Same design successfully used on other thruster of same size.* Acceptance testing eliminates marginal performance.	II to III*	
(7) Rupture of chamber	(a) Flaw in material or stresses from thermal and pressure cycling.	(7) Loss of thrust	(a) All material ultrasonically tested for flaws. Chamber stress adequacy verified during development and qualification testing. Chamber subjected to proof and leak tests as part of acceptance.*	I to III*	
(8) Failure of weld joint	(a) Inadequate or defective weld joint or stresses due to launch environment.	(8) Loss of thrust	(a) Weld joint designed for adequate strength safety margins. Weld quality controlled per process specification. All welds subjected to dye penetrant inspection. Structural integrity verified by qualification testing. All reactors proof and leak tested.*	I to III*	
(9) Change in nozzle contour	(a) Thermal stresses (b) Erosion of material	(9) Thrust falls out of specified limits, or thrust misalignment out of specification	(a) Nozzle material selected and design is calculated to have adequate safety margins under operating environment.* (b) Material integrity verified during development testing. *See previous note	II to III*	

APPENDIX C

POWER REDUCTION CONCEPTS

1.0 INTRODUCTION

The propellant valves consume a relatively large proportion of available spacecraft power. Since total power is limited, any power allocated to the propulsion system is unavailable for other equipment. For this reason, several approaches were investigated to reduce power consumed by the propulsion system. These approaches break down into two basic types, specifically:

- a. Direct reduction of total current
- b. Reduction of the percentage of time that current is applied

The effect, if any, on the spacecraft control system (number of commands) was investigated, as well as any effects on valve performance. Reliability effects are discussed in a qualitative manner where a particular approach could have an adverse effect on reliability.

The three basic approaches considered involve one or more of the following:

- a. Modifications to existing valves (internal)
- b. Use of an external driver circuit or electrical control method
- c. Use of a different valve concept

Various methods of implementing these approaches are described in the following paragraphs.

2.0 INTERNAL MODIFICATIONS TO EXISTING VALVES

Internal coil modifications (some in combination with external commands) may be employed to reduce power. In the following discussions, it is assumed that the opening and closing force margins of a modified valve are to be maintained equal to that of the existing valve. The appropriate relationships governing the effects of changes in parameters are shown by the following proportionability relationships:

$$L \propto N^2 \quad (1)$$

$$F \propto (NI)^2 \text{ or } \left(\frac{N}{R}\right)^2 \left(\text{for constant force } N = \frac{N_o I_o}{I}\right) \quad (2)$$

$$t_c = L/R \propto N^2/R \quad (3)$$

or, considering equation (2), to maintain constant force:

$$t_c \text{ Modified Coil} = t_c \text{ Original Coil} \frac{R_{\text{Modified}}}{R_{\text{Original}}} \quad (4)$$

and

$$P = 1/2 LI^2 \text{ (for constant force, P is constant)} \quad (5)$$

where

- F = Solenoid force
- N = Number of coil turns
- I = Coil current
- L = Coil inductance
- P = Stored energy in coil
- R = Coil resistance
- t_c = Coil time constant

The first case considered is that of increased coil resistance to reduce power. If power is arbitrarily reduced to 25% of the baseline value (while maintaining force margins), R coil is increased by a factor of 4. Thus,

$$\begin{aligned} F &= \text{const.} = F_o \\ t_c &= 4 t_{co} \\ P &= \text{const.} = P_o \end{aligned}$$

(subscript o designates initial values)

The time constant has increased by a factor of 4. This has an adverse effect on opening response (directly) and on response repeatability from valve to valve due to differences between valves in pull-in current and the slower rise rate of current in the modified coil. As an example of this effect, the following two valves, designed to have the same force characteristics, should be considered:

	Baseline	Modified
$I_{\text{max.}}$	1.0 amp	0.25 amp
Number of turns	N	4N
Resistance	R	4R
Time constant, t_c	0.01	0.04
Pull-in current	$0.25 I_{\text{max.}} \pm 10\%$	$0.25 I_{\text{max.}} \pm 10\%$

Given these conditions, the time to reach minimum and maximum pull-in current was calculated from

$$t = -t_c \left(\ln \left(1 - \frac{I_{\text{pull-in}}}{I_{\text{max.}}} \right) \right)$$

for each case and the time difference computed. These values are presented below.

	Baseline	Modified
Time to cross pull-in current band, milliseconds	0.667	2.77

Thus, the potential effect on response repeatability due to valve-to-valve pull-in differences is seen to be inversely proportional to the amount of power applied, in this case resulting in a factor of 4 difference. This may also be seen directly from the equation, since the ratio $I_{\text{pull-in}}/I_{\text{maximum}}$ is the same for both cases; thus, the variation in t_c is the controlling parameter. Similarly, the increase in time constant will result in slower valve closing time (and poorer repeatability). It should be noted that, since the ground rule is that force margins are to be maintained, dropout current is reduced by a factor of $R_{\text{Orig.}}/R_{\text{Mod.}}$. This can cause potential problems if the dropout current of the original design is near the point where circuit current leakage can hold the valve open. Reducing the normal power under these conditions would produce a valve with an unacceptable failure mode; that is, leakage current could hold the valve open. Thus, this method can only be used where the above restriction does not apply (or the amount of power reduction permitted without violating dropout requirements may not be as great as desired). In addition, physical limitations in the existing design may preclude the required number of coil turns within the available envelope.

Alternate methods were considered using multiple coils whereby the dropout problem is resolved by reduction of coil force output once the valve is in the open position so that dropout current is not reduced. The opening coil is sized to maintain opening force margin and time constant.

Coil time constant can be held equal to or less than that in the baseline valve only if power increases or is equal to the baseline (if force margins are to be maintained) since, as shown previously,

$$F_a \propto \frac{N^2}{R}$$

$$t_c \propto \frac{N^2}{R}$$

For example, if R is doubled and N is increased by a factor $\sqrt{2}$, t_c will remain constant; but F would be cut in half. If it is also assumed that peak power should not rise above the baseline value, then the original coil parameters N and R represent design values for the pull-in coil of a two-coil valve.

If the dropout current of the valve is to remain constant, then the holding coil requires the same number of turns as the main coil. Assuming that minimum holding current must have a margin over dropout current of the order of 50%, the resistance ratio, $R_{\text{nom}}/R_{\text{holding}}$ is given by

$$\frac{R_{\text{nom}}}{R_{\text{holding}}} = \frac{1.5 I_{\text{drop-out}}}{I_{\text{nominal}}} = \beta$$

Since the coil must have the same number of turns, the wire diameter must decrease to increase the resistance per turn. The holding coil volume will then be on the order of $1/\sqrt{\beta}$ times that of the main coil if wound to the same diameters. Thus, a holding coil of 10 times the resistance will have a volume of $\sqrt{10}$ times that of the main coil which may present problems in the attempt to modify an existing valve to accept the holding coil.

3.0 EXTERNAL METHODS OF POWER REDUCTION

One obvious method of reducing power to the valve is to pulse-modulate the applied voltage. Knowing the time constant of the coil, the dropout current, and the system minimum voltage and taking into account the effect of any back voltage suppression in the driver circuit, a minimum off-time could be computed which would ensure that the valve would not drop out. This time would be of the order of 2 to 3 milliseconds. If the nominal on-time were 20 milliseconds, this is equivalent to a 25 to 30% reduction in power. The means of mechanizing this approach lies in the sectoring device. One sector is equivalent to 4 to 5 milliseconds. Thus, by proper choice of the back voltage suppression, dropout could be prevented during this time span. The sequence would then be to have voltage on for three sectors and off for one. Also, the total number of sectors fired per pulse must be divisible by 4 so that the coil current at pulse end is the same for each different type of firing (different sector widths) so that pulse centroid will not be affected.

The difficulties of employing this method are:

- a. Mechanization of the pulsing circuit within the vehicle guidance system.
- b. Additional complexity in the engine test program, since the same pulsing circuitry must be employed to obtain valid centroid data.
- c. Possibility of the valve dropping out during the "off" sector if spin rate is lower than normal.

Alternate approaches involve modifications to the vehicle driver circuit to produce particular desired effects on valve operation. A typical circuit representing one of the approaches that may be

taken is shown in Figure C-1. (Reference: NAVWEPS Report 8118). This particular circuit was designed to speed up the opening and closing time of a solenoid valve and, in the process, results in low power during the holding portion of the pulse. Not all the components are necessarily required for application to the Planetary Explorer mission; for example, the two zener diodes are included to suppress a 1- to 2-volt pulse that occurred in the off signal of the particular command circuit employed. The basic operating principle of the circuit is to apply a 28-volt positive signal to one side of the coil which decays exponentially to the holding current level. Rapid opening of the valve is ensured by simultaneously applying a short duration pulse of -20 volts to the opposite side of the coil; thus providing a total of 48 volts.

Operation of the circuit is as follows. The input signal of Q1 turns on transistors Q2 and Q4. As Q2 is turned on, the voltage drops at point 1 in the circuit. Since the capacitor C1 is initially uncharged, the current surge through resistor R1 lowers the voltage applied to Q3, turning it full on (thus applying 28 volts to the valve). As capacitor C is charged, the voltage applied at Q3 approaches a steady-state value achieved by the steady-state current flow through the 20K base resistor producing a small drop across R1. Q3 thus remains partially on, limiting the holding current flow through the coil. The negative pulse is achieved as Q4 is turned on. Capacitors C1 and C2 control and shape the voltage applied to Q5 and hence shape its output. As Q5 is turned on, the positively charged side of C3 is essentially connected to ground. The negative side is connected to the low side of the coil. Diode D1 turns off when the opposite polarity pulse appears across it; thus the voltage initially across the coil is +28 and -20 volts for a total of 48 volts.

If it is not desired to speed up the valve opening response, the upper portion of the circuit alone may be employed. However, this approach would require careful design of the circuitry to ensure that the voltage remained high long enough to ensure opening the valve. Parasitic power loss in the circuit (without the fast opening feature) is on the order of one-third the desired valve dropout current and is additive directly to it.

Rocket Research Corporation has developed a proprietary power reduction circuit which is applicable to the Planetary Explorer vehicle. This circuit has the following advantageous characteristics:

- a. No capacitors are required for its operation.
- b. The power is not reduced until sufficient force has developed to ensure valve opening.
- c. In the event of an inadvertent power supply undervoltage, the power reduction portion of the circuit is not operative, thus ensuring that the valve will not close when power is reduced to the holding level.

As an alternate to the circuits described above which operate automatically from the "on" command signal, two separate commands may be employed to reduce power. For example, a transistor, biased on by the initial command signal, may be inserted in series with the coil and the transistor shunted with a resistor capable of producing the required power reduction. A second guidance command delivered three or four sectors after the "on" command could be employed to

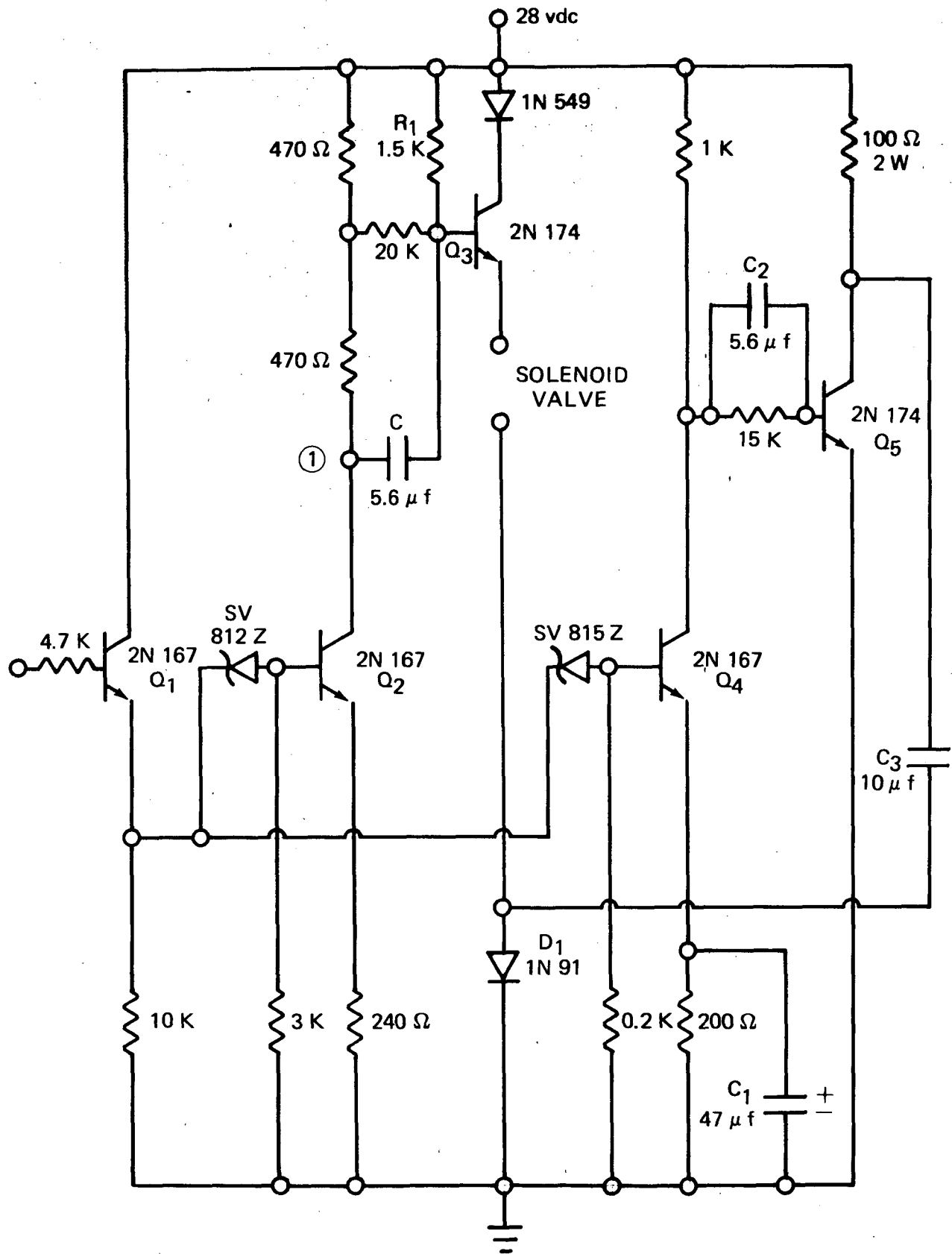


Figure C-1. VALVE DRIVER CIRCUIT

switch the transistor off, thus reducing the power. As an alternate, the resistor could be left out and the transistor biased partially closed by the command signal as employed in the first circuit described above. These approaches add complexity to both the guidance system and the driver circuit instead of limiting the changes to the driver circuit only. Also, a command-controlled power turndown with the full on-time derived from a given number of sectors has a unique failure mode. If, for example, a spin thruster was leaking or failed open and went undetected for a long enough period, the time to traverse a fixed number of sectors decreases (if spin rate is increasing) and a point is ultimately reached where the full power to holding power commands will be so close together as to prevent the valves from opening. The number of sectors at full power can be increased, of course, to the point where a very gross change in spin rate would be required to cause failure to open. This approach, however, introduces a problem in that, for anything more than about four to five sectors at full power, the change to holding power occurs at some point above minimum impulse bit. This then will introduce a step change in pulse centroid location from minimum impulse bit pulses to longer firings. From the above analysis, it was concluded that the automatic power reduction circuit is the better approach since it operates on essentially a fixed time base which is independent of spin rate.

4.0 POWER REDUCTION (ALTERNATIVE VALVE CONCEPT)

A latching valve may be considered as a means of reducing power since power is applied for short periods only to open or close the valve, with the latching mechanism holding the valve in the last commanded position. Latching valves are normally employed where long time periods occur between actuations and are not typically employed for pulse-mode operation. The power reduction achievable by this approach is, however, substantial. For example, at 12 rpm and assuming operation for high efficiency (98%), the pulse width of 555 milliseconds. If 15 milliseconds are allotted both to open and close the valve, total power consumed per pulse is only 5.4% of that normally consumed.

The primary disadvantage of the latching valve for this application is the fact that the valve can fail open if, for example, the coil became shorted. The latching valve in the feed system would then have to be closed to prevent total loss of propellant. With a normal valve, the same failure would result in the valve going to the closed position. Thus, the remaining thrusters connected to that half of the feed circuit could still be used.

5.0 SUMMARY

As a result of the above discussions it appears that the driver circuit (automatic power reduction) approach (which reduces power by 70 to 75%) is the most desirable for the Planetary Explorer mission for the following reasons:

- a. Coil modifications alone do not produce valves with acceptable repeatability.
- b. Commanded power changes require increased guidance system complexity and introduce undesired failure modes.
- c. Use of a latching valve introduces a bad potential failure mode (fail open).

APPENDIX D

DYNAMICS ANALYSIS – FORMULAE DERIVATIONS

1.0 CONSTRUCTION OF THE \mathbf{T} MATRIX

The contributions to the time independent \mathbf{T} matrix may be constructed by expanding the vector cross product definition of \mathbf{T} . In particular,

$$\mathbf{T} / \begin{matrix} \text{time} \\ \text{indep} \end{matrix} \equiv \frac{1}{F} \{ \vec{R} \times \vec{F} - \vec{R}_O \times \vec{F}_O \} \quad (\text{D1-1})$$

where:

$$\vec{R} = \hat{i}(X_O - X_1 + X_2) + \hat{j}(Y_O - Y_1 + Y_2) + \hat{k}(Z_O - Z_1 + Z_2) \quad (\text{D1-2})$$

$$\vec{F} = F \left\{ \hat{i} \left(-1 + \frac{\Delta F}{F} \right) + \hat{j} \delta + \hat{k} \delta \right\} \quad (\text{D1-3})$$

$$\vec{R}_O = \hat{i} X_O + \hat{j} Y_O + \hat{k} Z_O \quad (\text{D1-4})$$

$$\vec{F}_O = -\hat{i} F \quad (\text{D1-5})$$

In general, the unit vectors \hat{i} , \hat{j} , and \hat{k} , which correspond to the X, Y, and Z axes, respectively, combine in the operation of the cross product, as follows:

$$\begin{array}{lll} \hat{i} \times \hat{i} = 0 & \hat{j} \times \hat{i} = -\hat{k} & \hat{k} \times \hat{i} = \hat{j} \\ \hat{i} \times \hat{j} = \hat{k} & \hat{j} \times \hat{j} = 0 & \hat{k} \times \hat{j} = -\hat{i} \\ \hat{i} \times \hat{k} = -\hat{j} & \hat{j} \times \hat{k} = \hat{i} & \hat{k} \times \hat{k} = 0 \end{array} \quad (\text{D1-6})$$

Therefore, neglecting second order effects,

$$\vec{R} \times \vec{F} = F \begin{bmatrix} \hat{i}(\delta Y_O - \delta Z_O) \\ \hat{j} \left([-Z_O + Z_1 - Z_2] + \frac{\Delta F}{F} Z_O - \delta X_O \right) \\ \hat{k} \left([Y_O - Y_1 + Y_2] - \frac{\Delta F}{F} Y_O + \delta X_O \right) \end{bmatrix} \quad (\text{D1-7})$$

$$\vec{R}_O \times \vec{F}_O = F \begin{bmatrix} \hat{i}(0) \\ \hat{j}(-Z_O) \\ \hat{k}(Y_O) \end{bmatrix} \quad (\text{D1-8})$$

Substituting D1-8 and D1-7 into D1-1 the time independent torque arm matrix is expressed as follows:

$$\mathbf{T}/\text{time indep} = \begin{bmatrix} \hat{i} (\delta Y_o - \delta Z_o) \\ \hat{j} \left([Z_1 - Z_2] + \frac{\Delta F}{F} Z_o - \delta X_o \right) \\ \hat{k} \left([-Y_1 + Y_2] - \frac{\Delta F}{F} Y_o + \delta X_o \right) \end{bmatrix} \quad (\text{D1-9})$$

2.0 DEVELOPMENT OF THE $\overline{\mathbf{T}}$ MATRIX

The $\overline{\mathbf{T}}$ matrix is developed to describe the total effect of two sets of motors firing simultaneously, where it is assumed that one set of motors is displaced above the spacecraft center of gravity by a distance $Z_o(U)$ and the other set below the center of gravity by a distance $Z_o(L)$. The $\overline{\mathbf{T}}$ matrix is intended for use during the ΔV firing regime of the mission. As a consequence, the upper and lower set of motors must fire for a total period of time to produce the required impulse, and the firing schedule for the upper set must be biased with respect to the lower set so that no net torque about the Y axis is produced (see Figure 2-1 for coordinate system definition).

These criteria can be expressed as follows:

$$F_o(U) t(U) + F_o(L) t(L) = I_o (\Delta V) \quad (\text{D2-1})$$

$$F_o(U) t(U) Z_o(U) = F_o(L) t(L) Z_o(L) \quad (\text{D2-2})$$

The uncertainty torque impulse (torque times time) for the upper and lower motors produced during a firing are as follows:

$$\text{upper } T(U) = F_o(U) \overline{\mathbf{T}}(U) t(U) \quad (\text{D2-3a})$$

$$\text{lower } T(L) = F_o(L) \overline{\mathbf{T}}(L) t(L) \quad (\text{D2-3b})$$

The total disturbance torque impulse produced by the upper and lower sets of motors is:

$$T(U) + T(L) = F_o (\overline{\mathbf{T}}(U) t(U) + \overline{\mathbf{T}}(L) t(L)) \quad (\text{D2-4})$$

In the above equations,

$F_o(U) = F_o(L) = F_o =$ motor set total thrust

$t(U, L) =$ upper or lower motor set firing period

$I_o (\Delta V) =$ total impulse required

From equation D2-2 it can be determined that:

$$t(L) = \frac{Z_o(U)}{Z_o(L)} t(U) \quad (D2-5)$$

Substituting D2-5 into D2-4 the following result is obtained:

$$T(U) + T(L) = F_o t(U) \left(\bar{T}(U) + \frac{Z_o(U)}{Z_o(L)} \bar{T}(L) \right) \quad (D2-6)$$

In order to express $F_o t(U)$ in terms of $I_o(\Delta V)$ equation D2-1 can be used as follows:

$$F_o(U) t(U) + F_o(U) t(U) \frac{F_o(L) t(L)}{F_o(U) t(U)} = I_o(\Delta V)$$

or

$$F_o(U) t(U) \left[1 + \frac{t(L)}{t(U)} \right] = I_o(\Delta V) \quad (D2-7)$$

and from equation D2-2,

$$\frac{t(L)}{t(U)} = \frac{Z_o(U)}{Z_o(L)} \quad (D2-8)$$

Substituting D2-8 into D2-7 solving for the following expression is obtained:

$$F_o(U) t(U) = \frac{I_o(\Delta V)}{1 + \frac{Z_o(U)}{Z_o(L)}} \quad (D2-9)$$

Returning to equation D2-6 and substituting D2-9 the defining equation for \bar{T} is obtained:

$$T(U) + T(L) = \frac{I_o(\Delta V) \left(\bar{T}(U) + \frac{Z_o(U)}{Z_o(L)} \bar{T}(L) \right)}{1 + \frac{Z_o(U)}{Z_o(L)}} \quad (D2-10)$$

From equation D2-10 it is convenient to extract the following expression, which is contained in computations of $\Delta V_{\max i}$:

$$\bar{T} \equiv \frac{T(U) + \frac{Z_o(U)}{Z_o(L)} T(L)}{1 + \frac{Z_o(U)}{Z_o(L)}} \quad (D2-11)$$

3.0 DEVELOPMENT OF THE $\Delta V_{\max i}$ FORMULAE

3.1 $\Delta V_{\max X}$, $\Delta V_{\max Y}$

A torque applied in a given inertial direction at right angles to the spin axis of a rotating body will cause the average orientation of the spin axis to decline away from its original position in a steady fashion. Uncertainty torques would be expected to produce this effect during the preprogrammed ΔV maneuvers required for midcourse trajectory correction and late mission velocity changes.

Combining equations D2-10 and D2-11 in Section 2.0, it is clearly possible to express the total uncertainty torque produced by the upper and lower engine sets as follows:

$$T(TOT) = T(U) + T(L) = I_o(\Delta V) \bar{T} \quad (D3-1a)$$

Broken down by components the relationship is:

$$\begin{aligned} T_i(TOT) &= T_i(U) + T_i(L) = I_o(\Delta V) \bar{T}_i \\ &= M \Delta V \bar{T}_i \end{aligned} \quad (D3-1b)$$

where:

M = Mass of the spacecraft

ΔV = Velocity change that will result from an impulse input of $I_o(\Delta V)$

Clearly the magnitude of the torque impulse is proportional to the size of the velocity increment produced.

An angle of declination, a , will result from an applied torque as described by the following relationship:

$$a = \left(\frac{1}{0.017453} \right) \frac{T}{I_Z \Omega_Z} \quad (D3-2a)$$

Where a is expressed in degrees and other units are as follows:

$$\begin{aligned} T &= \text{lbf-ft-sec} \\ I_Z &= \text{Slug-ft}^2 \\ \Omega_Z &= \text{Radians/second} \end{aligned} \quad (\text{D3-2b})$$

Substituting $I_O(\Delta V) \bar{T}$ for T and solving for T , the following result is obtained:

$$I_O(\Delta V) \bar{T} = (0.017453) a(\Delta V) I_Z \Omega_Z \quad (\text{D3-3})$$

Implicit in equation D3-3 is the fact that declination $a(\Delta V)$ is caused by torque impulse $I_O(\Delta V) \bar{T}$.

The desire to describe the maximum preprogrammed velocity impulse allowed by the prescribed limits of declination of the spacecraft spin axis can be achieved by observing that

$$\frac{a(\Delta V)}{a(\Delta V_{\max i})} = \frac{\Delta V}{\Delta V_{\max i}} \quad (\text{D3-4a})$$

or, solving for $\Delta V_{\max i}$,

$$\Delta V_{\max i} = \frac{a(\Delta V_{\max i})}{a(\Delta V)} \Delta V \quad (\text{D3-4b})$$

Substituting the relationship D3-2a for $a(\Delta V)$ and renaming $a(\Delta V_{\max i})$ as a_{ji} , the following result is obtained:

$$\Delta V_{\max i} = (0.017453) \Delta V a_{ji} \frac{I_Z \Omega_Z}{I_O(\Delta V) \bar{T}_i} \quad (\text{D3-5})$$

Equation D3-5 above is identical to equation 2-9a in the body of the text considering that $M_Z \equiv I_Z \Omega_Z$.

3.2 $\Delta V_{\max Z}$

A torque applied about the spin axis of a rotating body will change the spin rate. The basic equation for this phenomenon is as follows:

$$I_Z \frac{d\Omega_Z}{dt} = \text{torque about } Z \quad (\text{D3-6})$$

The change in Ω_Z , $\Delta\Omega_Z$, produced by a steady applied torque is therefore:

$$\Delta\Omega_Z = \frac{T}{I_Z} \quad (\text{D3-7})$$

where:

- T = Torque impulse delivered
- I_Z = Z axis moment of inertia

The relationship between the values of $\Delta\Omega_Z$ produced for different values of velocity increment induced by cross coupling uncertainty torques during a velocity change maneuver is as follows:

$$\frac{\Delta\Omega_Z (\Delta V_{\max Z})}{\Delta\Omega_Z (\Delta V)} = \frac{\Delta V_{\max Z}}{\Delta V} \quad (D3-8)$$

where ΔV is the velocity increment produced by an amount of impulse, I_0 , and $\Delta V_{\max Z}$ is the amount of ΔV that can be delivered without exceeding $\Delta\Omega_Z(\Delta V_{\max Z})$, which by definition is the value of the maximum allowed spin rate perturbation.

Using equation D3-8 to solve for $\Delta V_{\max Z}$ and substituting D3-7 for $\Delta\Omega_Z(\Delta V)$ and $I_0(\Delta V) \bar{T}_Z$ for T, the following expression results:

$$\Delta V_{\max Z} = \Delta V \frac{\Delta\Omega_Z I_Z}{I_0(\Delta V) \bar{T}_Z} \quad (D3-9)$$

which is equation 2-9b in the main text.

4.0 CALIBRATION FACTORS C_X, C_Y, C_Z

To account for motor performance dispersions that are off normal, calibration factors are defined to provide a quantitative technique of predicting the increases in $\Delta V_{\max i}$ that can be achieved by correcting the motor firing schedules to compensate for fixed uncertainty torques. In practice this is achieved by conducting a calibration firing of the ΔV motor assembly prior to the first segment of the midcourse or other ΔV maneuver. This firing might be conducted on the ground in a space-environment simulator or in space.

The calibration factors are defined to provide a parameter of relationship between the $\Delta V_{\max i}$ (CAL) and $\Delta V_{\max i}$ (UNCAL), which are the maximum allowed values of uncorrected velocity change in the calibrated or uncalibrated conditions respectively. A calibration factor value of unity would by definition imply that all (100%) uncertainty torques were fixed and could be calibrated out and that the SCADS and rotation rate measurement systems were perfectly accurate. If such a situation were possible, one calibration maneuver would provide enough data to allow elimination of all uncertainty torque effects, thereby allowing an after calibration ΔV maneuver of unlimited length.

Consistent with what has been discussed above, the calibration factor is defined as follows:

$$\Delta V_{\max i}(\text{CAL}) = \frac{\Delta V_{\max i}(\text{UNCAL})}{1 - C_i} \quad (\text{D4-1})$$

where:

- $\Delta V_{\max i}(\text{CAL})$ = Potential ΔV_{\max} limit that could be reached after calibration.
- $\Delta V_{\max i}(\text{UNCAL})$ = ΔV_{\max} limit that would be allowed prior to calibration of torques about the i^{th} axis, if measurement errors are neglected.
- C_i = Calibration factor for torques about the i^{th} axis.

Figure D-1 graphically depicts the calibrated and uncalibrated motor firing schedule effect on maximum allowed velocity increment. In the figure the steeper line starting at the origin reflects the analytical technique used to compute $\Delta V_{\max i}(\text{UNCAL})$. The line starts at the origin rather than at the intersection of the error band and the vertical axis, because the measurement error limitation on ΔV_{\max} was ignored for the calibration.

The second line represents an upper limiting situation for the calculated values of $\Delta V_{\max}(\text{CAL})$. The rudimentary equations for $\Delta V_{\max}(\text{CAL})$ and $\Delta V_{\max}(\text{UNCAL})$ are as follows:

$$\Delta V_{\max}(\text{UNCAL}) = \frac{\theta_A}{\left(\frac{\Delta\theta}{\Delta V}\right)\Big|_{\text{all}}} \quad (\text{D4-2a})$$

$$\Delta V_{\max}(\text{CAL}) = \frac{\theta_A - \theta_M}{\left(\frac{\Delta\theta}{\Delta V}\right)\Big|_{\text{var}}} \quad (\text{D4-2b})$$

where:

- θ_A = Maximum allowed value of dispersion due to uncertainty torques.
- θ_M = Maximum before-plus-after maneuver attitude or spin rate dispersion.
- $\left(\frac{\Delta\theta}{\Delta V}\right)\Big|_{\text{all}}$ = Rate of change of attitude or spin rate with velocity change, as caused by both fixed and variable uncertainty torques.
- $\left(\frac{\Delta\theta}{\Delta V}\right)\Big|_{\text{var}}$ = Rate of change of the dispersion parameter with velocity, as caused by only variable uncertainty torques.

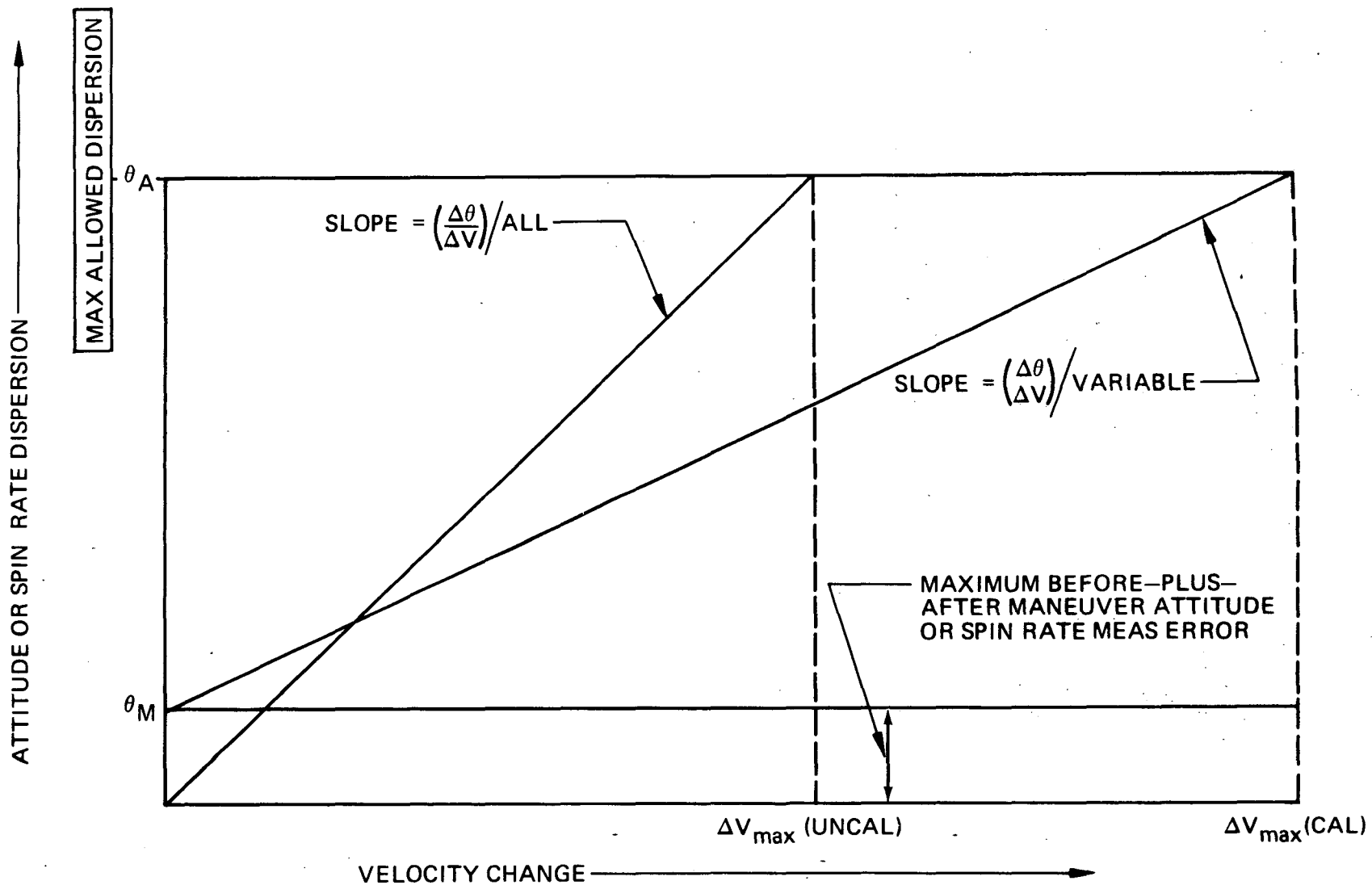


Figure D-1 UNCALIBRATED AND CALIBRATED MOTOR FIRING SCHEDULE STATUS EFFECT ON ALLOWED VELOCITY INCREMENT

Values of the individually identifiable dispersion parameters, which contribute to θ_A are defined below.

$$\theta_A = \theta_F + \theta_V + \theta_M \quad (D4-3)$$

where:

θ_F = Dispersion angle produced during a ΔV maneuver by fixed uncertainty torques

θ_V = Dispersion angle produced during a ΔV maneuver by variable uncertainty torques

The relationship between $(\Delta\theta/\Delta V)|_{\text{var, all}}$, all and θ_F and θ_V may be expressed as a simple proportionality as follows:

$$\left(\frac{\Delta\theta}{\Delta V}\right)|_{\text{var, all}} = K_{V, A}(\theta_V, \theta_F + \theta_V) \quad (D4-4)$$

Using equations D4-1, D4-2, and D4-4 the ratio between $\Delta V_{\text{max}}(\text{UNCAL})$ and $\Delta V_{\text{max}}(\text{CAL})$ can be constructed as follows:

$$\frac{\Delta V_{\text{max}}(\text{UNCAL})}{\Delta V_{\text{max}}(\text{CAL})} = \frac{\theta_V}{\theta_A - \theta_M} = 1 - C \quad (D4-5)$$

Solving for C the following relationship is derived:

$$C = \frac{\theta_A - \theta_M - \theta_V}{\theta_A - \theta_M} \quad (D4-6)$$

In order to provide a conservative estimate of the calibration factor, the measurement error numerical effect in the denominator was neglected with respect to the numerical effect of θ_A . Consequently, the final form of the calibration factors used in the main text is as shown below.

$$C = \frac{\theta_A - \theta_M - \theta_V}{\theta_A} \quad (D4-7)$$

5.0 TOTAL PROPULSIVE AND TORQUE IMPULSE FORMULAE

The computation of the total impulse required for velocity correction or attitude and spin control must reflect both nominal and cross coupling effects. In particular, the list of significant factors is as follows:

- a. Nominal requirements
- b. Self-coupling effects
- c. Cross-coupling effects

Nominal requirements are determined by the mission and the characteristics of the spacecraft such as mass, moments of inertia, spin rate, and size. Cross- or self-coupling effects are determined by the configuration, placement accuracy, firing direction accuracy, and motor performance repeatability of the mounted propulsion system. Cross- and self-coupling torques must be annulled to achieve the desired maneuver accuracy. Therefore, fuel to compensate for coupling torques and forces must be loaded into the spacecraft.

In general, a set of numbers, $F_B(A)$, were defined to permit bookkeeping of the coupling factors. The factor $F_B(A)$ is defined as follows:

$$F_B(A) = \text{Fraction of an affect, A, that cross couples into B and produces the effect, } B_A.$$

Therefore,

$$B_A = AF_B(A) \quad (D5-1)$$

In general the aggregate effect on B is the sum of the nominal required value plus the coupling contributions. This is written as follows:

$$B(\text{TOT}) = B + B_A + B_B + B_C + \text{etc.} \quad (D5-2)$$

The term B_B is the self-coupling effect, which is found to be significant, if the uncertainty in motor thrust level or delivered impulse size is a significant fraction of the nominal thrust level or impulse bit size.

In general the functions are velocity change, attitude control, and spin control. Nominal levels for each function are established by the spacecraft design team. Figure D-2 presents a matrix of the cross coupling factors.

In general the torque cross-coupling factors are broken down into X-, Y-, and Z-axis components of the total. In particular

$$F_{AC}(AC) \rightarrow F_X(AC) \text{ and } F_Y(AC) \quad (D5-3a)$$

$$F_{AC}(\text{spin}) \rightarrow F_X(\text{spin}) \text{ and } F_Y(\text{spin}) \quad (D5-3b)$$

The given nominal values for propulsive impulse and torque impulse may be defined as follows:

$$\begin{aligned} \text{Propulsive impulse} &\equiv I_O (\Delta V) \\ \text{Attitude torque impulse} &\equiv T_O (AC) \\ \text{Spin torque impulse} &\equiv T_O (\text{spin}) \end{aligned}$$

<div style="text-align: center;">SOURCE</div> <div style="text-align: center;">AFFECT</div>	VELOCITY CORRECTION	ATTITUDE CONTROL	SPIN CONTROL
VELOCITY CORRECTION	$f_{\Delta V(\Delta V)}$	$f_{\Delta V(AC)}$	$f_{spin(\Delta V)}$
ATTITUDE CONTROL	$f_{AC(\Delta V)}$	$f_{AC(AC)}$	$f_{AC(spin)}$
SPIN CONTROL	$f_{spin(\Delta V)}$	$f_{spin(AC)}$	$f_{spin(spin)}$

Figure D-2 CROSS AND SELF-COUPLING FACTORS

From what has been discussed above, the values of total impulse relate to the nominal values, as follows:

$$I_{TOT}(\Delta V) = I_o(\Delta V) + F_{\Delta V}(\Delta V) I_o(\Delta V) + F_{\Delta V}(AC) T_o(AC) + F_{\Delta V}(spin) T_o(spin) \quad (D5-4a)$$

$$T_{TOT}(AC) = F_{AC}(\Delta V) I_o(\Delta V) + T_o(AC) + F_{AC}(AC) T_o(AC) + F_{AC}(spin) T_o(spin) \quad (D5-4b)$$

$$T_{TOT}(spin) = F_{spin}(\Delta V) I_o(\Delta V) + F_{spin}(AC) T_o(AC) + T_o(spin) + F_{spin}(spin) T_o(spin) \quad (D5-4c)$$

The specific values of the cross-coupling factors are given in the next section.

6.0 CROSS AND SELF COUPLING FACTORS

6.1 VELOCITY CORRECTION SELF COUPLING

When a set of radially firing motors are programmed to thrust in a given direction, the delivered impulse will be off nominal in the X, Y, and Z directions, as discussed below. The nominal direction of firing is assumed to be along minus X, which is fixed in space. The Y and Z axes are orthogonal to the X axis, and the Z axis is the spin axis.

The principal contributor to self coupling parallel to the nominal direction of firing is the engine output performance variation factor $\Delta F/F$ which is of the order of 5%. Along the perpendicular axes, the significant factor is the misalignment of the thrust vector which by assumption is 0.1 degree = 0.0017453 radian. Because the off-nominal thrust component is proportional to the sine of the dispersion angle, i.e., $\sin 0.1$ degree, the off-axis effect is insignificant compared to the parallel effect. Therefore the conclusion is made that

$$F_{\Delta V}(\Delta V) = \frac{\Delta F}{F} \quad (D6-1)$$

6.2 ΔV IMPULSE COUPLING INTO ATTITUDE AND SPIN TORQUE IMPULSE

With the spacecraft ΔV motors facing in the minus X direction, a ΔV firing will produce a cross-coupling torque about the X, Y, or Z axis proportional to \bar{T}_X , \bar{T}_Y , or \bar{T}_Z respectively. In particular the cross-coupling torque impulses about X, Y, and Z are as follows:

$$T_{AC-X}(\Delta V) = I_o(\Delta V) \bar{T}_X \quad (D6-2a)$$

$$T_{AC-Y}(\Delta V) = I_o(\Delta V) \bar{T}_Y \quad (D6-2b)$$

$$T_{spin}(\Delta V) = I_o(\Delta V) \bar{T}_Z \quad (D6-2c)$$

In the equation for $T_{TOT}(AC)$, the orthogonal effects along X and Y are combined as follows:

$$T_{AC}(\Delta V) = I_o(\Delta V) \sqrt{\bar{T}_X^2 + (1 - C_Y)^2 \bar{T}_Y^2} \quad (D6-3)$$

where:

$T_{AC}(\Delta V)$ = Total torque impulse about orthogonal axes due to ΔV impulse cross coupling.

The multiplying factor $(1 - CY)$ is introduced in front of \bar{T}_Y to reflect the fact that a rescheduling of ΔV firing motors will reduce the magnitude of the Y axis torque according to the value of CY .

6.3 ATTITUDE CONTROL TORQUE CROSS COUPLING

By assumption, the attitude control motors always fire to produce a nominal torque about the Y axis.

The self-coupling factor, $F_{AC}(AC)$, can be broken down into components about the X and Y axes. Consequently, the self-coupling torque impulse of attitude control back into attitude control is as follows:

$$T_{AC}(AC) = T_o(AC) \sqrt{F_X^2(AC) + F_Y^2(AC)} \quad (D6-4)$$

An attitude control thruster assembly will in general be made up of two sets of motors, i.e., an upper and lower set. The uncertainty torques will in general be a fraction of the nominal torque according to the ratio of the appropriate uncertainty torque arm matrix element to the overall nominal torque arm length.

As discussed in the main body of the text the \mathbf{T}' matrix elements apply to attitude control maneuver situations. These elements are therefore used here. The coupling factors are as follows:

$$F_{AC-X}(AC) = \frac{\sum_m \mathbf{T}'_{X,m}}{\sum_m Z_{o,m}} = \frac{\sum_m \mathbf{T}'_{X,m}}{Z_o(U) + Z_o(L)} \quad (D6-5a)$$

$$F_{AC-Y}(AC) = \frac{\sum_m \mathbf{T}'_{Y,m}}{\sum_m Z_{o,m}} = \frac{\sum_m \mathbf{T}'_{Y,m}}{Z_o(U) + Z_o(L)} \quad (D6-5b)$$

By similar arguments the equation for the cross coupling of attitude control into spin are as follows:

$$T_{spin}(AC) = T_o(AC) F_{spin}(AC) \quad (D6-6)$$

$$F_{spin}(AC) = \frac{\sum_m \mathbf{T}'_{Z,m}}{\sum_m Z_{o,m}} \quad (D6-7)$$

The cross coupling of attitude control into velocity correction is similar to the cross coupling into spin or altitude control. If it is assumed that one motor exceeds the nominal thrust level by the factor $\Delta F/F$ and the other by the same factor except with the opposite sign, the total mismatch between upper and lower motors will be:

$$\Delta I = \frac{\Delta F}{F} (I_o(U) + I_o(L)) \quad (D6-4)$$

and the total nominal torque impulse will be:

$$T_o(AC) = I_o(U) Z_o(U) + I_o(L) Z_o(L) \quad (D6-5)$$

where:

$$\begin{aligned} I_o(U, L) &= \text{Propulsive impulse of the upper and lower motors, respectively.} \\ Z_o(U, L) &= \text{Z axis displacement of the upper and lower motors, respectively.} \end{aligned}$$

Because both the upper and lower motors fire for the same period of time,

$$I_o(U) = I_o(L) = I_o$$

and consequently the ratio of the total propulsive impulse mismatch to the total nominal torque is:

$$\frac{\Delta I}{T_o} = \frac{2 \frac{\Delta F}{F} I_o}{I_o [Z_o(U) + Z_o(L)]} = \frac{2 \frac{\Delta F}{F}}{Z_o(U) + Z_o(L)} \quad (D6-7)$$

6.4 SPIN CONTROL CROSS COUPLING

The coupling of spin back into itself is related to the spin control uncertainty torque factors T'' in a similar fashion to the coupling of attitude control into itself. In the case of spin the nominal torque arm is Y_o , which is the same for all Planetary Explorer spacecraft. By similarity with the already-described development for attitude control, therefore,

$$F_{\text{spin (spin)}} = \frac{\sum_m T''_{Z, m}}{\sum_m Y_{o, m}} \quad (D6-8)$$

An identical argument based upon the ratio of the X and Y axis uncertainty torque values to the nominal spin torque values provides the basis for the cross coupling of spin into attitude control, as follows:

$$F_{AC(\text{spin})} = \frac{\sum_m T''_{X, Y, m}}{\sum_m Y_{o, m}} \quad (D6-9)$$

where again there are separable X and Y components, which are to be combined in the root-sum-square fashion.

The coupling of spin into a spacecraft velocity increment is noteworthy. Because the spin motor is assumed to fire in a schedule that is symmetrical about the spin axis, all velocity increments except those parallel to the Z axis are cancelled. The cross coupling of spin into ΔV is therefore along the spin axis and is proportional to the thruster misalignment angle, δ .

$$F_{\Delta V}(\text{spin}) = \frac{\delta}{Y_0} \quad (\text{D6-10})$$

7.0 SINGLE ENGINE OUT TORQUE EQUATION

If a single engine of a set of two fails to fire in a velocity-correction maneuver, the other engine in the set could be expected to continue to fire for the duration of the intended firing cycle, thereby producing a continuous torque (positive or negative) about the Y axis. To determine the degree of precession of the spin axis that such an occurrence would produce, it is necessary to calculate the torque impulse of one motor firing in an unbalanced fashion. In general the following relationships may be written:

$$I_0 = I_0(U) + I_0(L) \quad (\text{D7-1})$$

$$I_0(U) Z_0(U) = I_0(L) Z_0(L) = T(\text{EF}) \quad (\text{D7-2})$$

where:

- I_0 = Total impulse to be delivered by both engines together.
- $I_0(U, L)$ = Impulse delivered by the upper or lower engine.
- $T(\text{EF})$ = Effective unbalanced torque impulse of one engine.

Using equation D7-2, $I_0(U)$ and $I_0(L)$ may be solved in terms of $T(\text{EF})$. In particular:

$$I_0(U, L) = \frac{T(\text{EF})}{Z_0(U, L)} \quad (\text{D7-3})$$

Substituting D7-3 into D7-1, finding a common denominator for the resulting terms involving $T(\text{EF})$, the following result may be determined for $T(\text{EF})$:

$$T(\text{EF}) = \frac{Z_0(U) Z_0(L)}{Z_0(U) + Z_0(L)} \quad (\text{D7-4})$$